C-C bond forming catalysis with Alkaline Earth acetylides

Lomas, Sarah

Award date:
2013

Awarding institution:
University of Bath

C-C bond forming catalysis with Alkaline Earth acetylides

Sarah Lomas

Degree of Doctor of Philosophy

University of Bath
Department of Chemistry
September 2012

Supervisor: Professor Mike Hill

Copyright declaration

Restrictions

September 2012

Acknowledgements

I would like to thank Professor Mike Hill, rest of the Hill group at The University of Bath for making my time and studies in Bath an enjoyable experience.

Abstract

After spending so many years in the shadow of magnesium chemistry the chemical abilities of the heavier alkaline earth metals, calcium, strontium and barium are beginning to emerge. This thesis is concerned with the development of a catalytic reactivity for the heavier alkaline earth metals. By taking inspiration from lanthanide metal catalysis, this thesis will begin by describing the hydroamination and hydrophosphination of unsaturated molecules catalysed by lanthanide and group 2 metals before extending this work to the group 2 catalysed hydroacetylation of terminal acetylenes (chapter 2), and the insertion of unsaturated bonds of carbodiimides (chapter 4), and organic isocyanates (chapter 5) into the polarised M-C bonds of group 2 acetylides. The third chapter of this thesis will describe the observation of the first acetylide coupling with a group 2 metal complex and extension of this reactivity to a catalytic process.

Chapter 1 of this thesis provides an introduction to alkaline earth and lanthanide chemistry, specifically relating to organometallic reactivity, as well as a description of the use of group 2 complexes in molecular catalysis.

The second chapter of this thesis discusses the different orientations observed from the co-ordination of both non-donor- and donor-functionalised terminal acetylenes within dimeric β-diketiminato calcium acetylide complexes. Although simple non-donor-functionalised acetylenes are found to co-ordinate with a conventional symmetric orientation, the introduction of donor-functionalised acetylene ligands provides a notable contrast. In comparison to the symmetric complexes, the asymmetric complexes experience a reduction in the bond angle between the group 2 metal and the bridging acetylide unit. This co-ordination is proposed to exert a shift in electron density within the C≡C triple bond as the acetylide unit within the asymmetric complex is pulled closer to the metal center.

Chapter 3 further investigates the consequences of these interactions between the two bridging acetylide units which may be coupled together to produce cumulated butatriene molecules. A variety of stoichiometric and catalytic systems are described and the

reactivity is proposed to occur via the intermediacy of unobserved dimeric calcium butatriendiyl complexes.

The fourth chapter of this thesis explores the formation of propargyl amidinate complexes following the insertion of a symmetric carbodiimide into a group 2 metal acetylide. Results indicate the amidinate structure to be dependent upon the carbodiimide employed following the observation of both mono- and bis-insertion. This reactivity is also extended to a catalytic regime for the formation of propargyl amidines, which is observed to take place via the formation of dimeric amidinate complexes featuring terminal and bridging ligands.

Chapter 5 attempts to extend the catalytic reactivity described in chapter 4 to the synthesis of propargyl amides through insertion reactions of calcium acetylides and organic isocyanates. Although stoichiometric insertion to form a series of calcium propargyl amidate complexes is found to be facile, no catalytic reactivity is observed. This latter observation is reasoned to be due to lower acidity of the terminal alkyne substrate and consequent inability to effect protonolysis of the amidate intermediates.

Abbreviations

THF = Tetrahydrofuran

D_8-tol = Deuterated Toluene

C_6D_6 = Deuterated benzene

cat = catalyst

M = metal

Ae = Alkaline earth metal

Ln = Lanthanide metal

L = Ligand

dipp = 2,6-di-*iso*-propylphenyl

BIAN = bis(imino)acenaphthene

NMR = nuclear magnetic resonance

ppm = parts *per* million

s = singlet

d = doublet

t = triplet

m = multipet

br = broad

T = temperature

R = alkyl or aryl substituent

Ar = Aromatic hydrocarbon substituent

Cp = cyclopentadienyl

Cp^* = 1,2,3,4,5-pentamethylcyclopentadienyl

^{i}Pr = *iso*-propyl

cy = cyclohexyl

Me = methyl

Et = ethyl

Ph = phenyl

^{t}Bu = *tert*-butyl

OMe = methoxy

OPh = phenoxy

X = halide

Compounds

Ligands

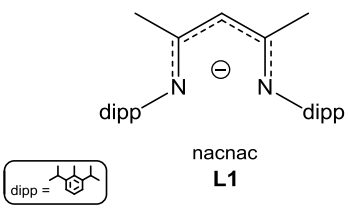

nacnac
L1

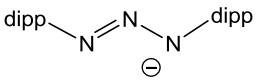

L2

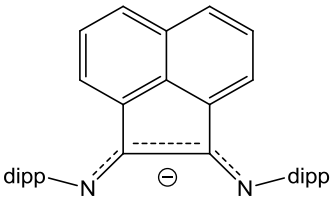

L3

Group 2 metal complexes

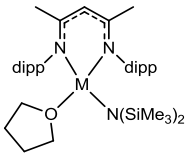

M = Ca **C1**
Sr **C2**

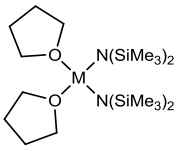

M = Ca **C3**
Sr **C4**
Ba **C5**

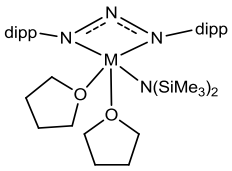

M = Ca **C6**
Sr **C7**

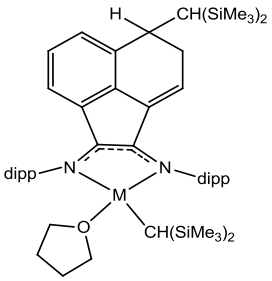

M = Ca **C8**
Sr **C9**

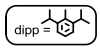

Acetylenes

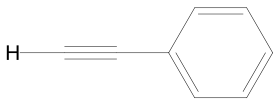

a Phenyl acetylene

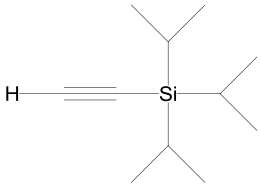

b Tri-*iso*-propylsilyl acetylene

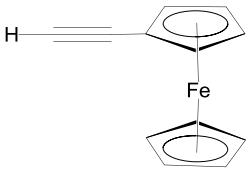

c Ethynyl ferrocene

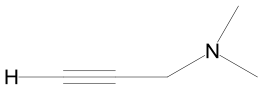

d 3-dimethylamino-1-propyne

e Methyl Propargyl ether

f Phenyl Propargyl ether

Carbodiimides and isocyanate

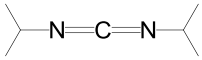

g N,N'-di-*iso*-propylcarbodiimide

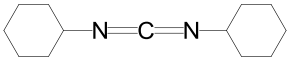

h 1,3-dicyclohexylcarbodiimide

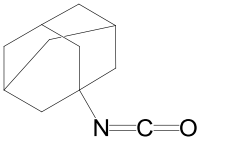

i 1-adamantyl isocyanate

Group 2 acetylides

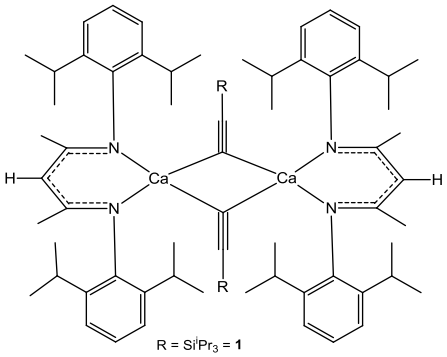

R = Si^iPr_3 = **1**
$(C_5H_4)Fe(C_5H_5)$ = **2**
CH_2NMe_2 = 3
CH_2OMe = **4**
CH_2OPh = **5**

Acetylide coupling

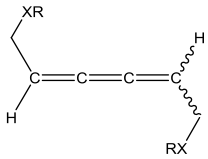

XR = NMe_2 **6**
OMe **7**
OPh **8**

Amidinates

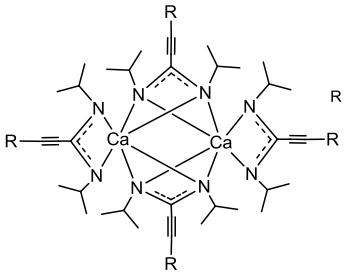

R = C_6H_5 **18**
Si^iPr_3 **12**
$CH_2N(CH_3)_2$ **24**
CH_2OCH_3 **30**
CH_2OPh **36**

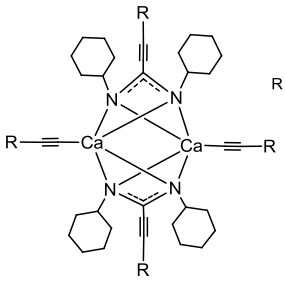

R = C_6H_5 **19**
Si^iPr_3 **13**
$CH_2N(CH_3)_2$ **25**
CH_2OCH_3 **31**
CH_2OPh **37**

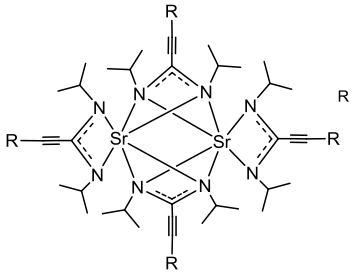

R = C_6H_5 **20**
Si^iPr_3 **14**
$CH_2N(CH_3)_2$ **26**
CH_2OCH_3 **32**
CH_2OPh **38**

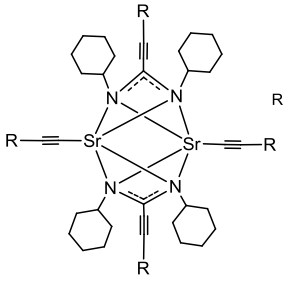

R = C_6H_5 **21**
Si^iPr_3 **15**
$CH_2N(CH_3)_2$ **27**
CH_2OCH_3 **33**
CH_2OPh **39**

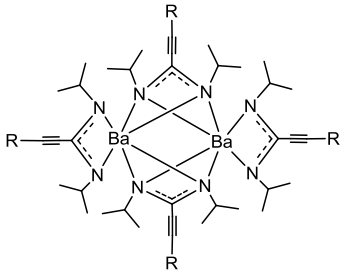

R = C_6H_5 **22**
Si^iPr_3 **16**
$CH_2N(CH_3)_2$ **28**
CH_2OCH_3 **34**
CH_2OPh **40**

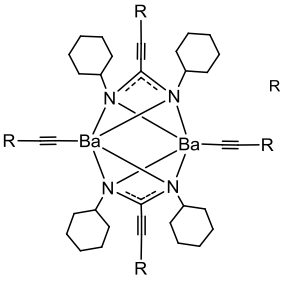

R = C_6H_5 **23**
Si^iPr_3 **17**
$CH_2N(CH_3)_2$ **29**
CH_2OCH_3 **35**
CH_2OPh **41**

Amidates

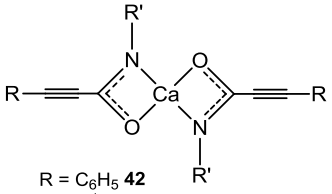

R = C_6H_5 **42**
Si^iPr_3 **45**
CH_2NMe_2 **48**
CH_2OCH_3 **51**
CH_2OPh **54**
R' = 1-adamantyl

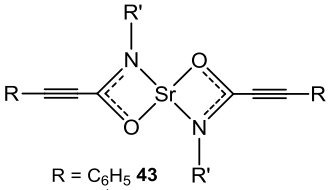

R = C_6H_5 **43**
Si^iPr_3 **46**
CH_2NMe_2 **49**
CH_2OCH_3 **52**
CH_2OPh **55**
R' = 1-adamantyl

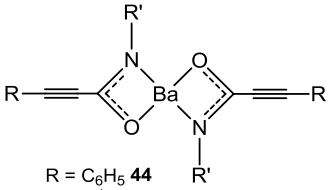

R = C_6H_5 **44**
Si^iPr_3 **47**
CH_2NMe_2 **45**
CH_2OCH_3 **53**
CH_2OPh **56**
R' = 1-adamantyl

Contents

Chapter 2

Chapter 3

Chapter 4

Chapter 5

Chapter 6

Chapter 7

Chapter 8

Appendix

Chapter 1

1.0 Introduction

Taking inspiration from the lanthanide chemistry this thesis aims to explore and develop the chemistry of the alkaline earth metals, and centres around the hydroacetylation of terminal acetylenes. The insertion of carbodiimides and an organic isocyanate will ensure the respective formation of the amidinate and amidate intermediate complexes, scheme 1.

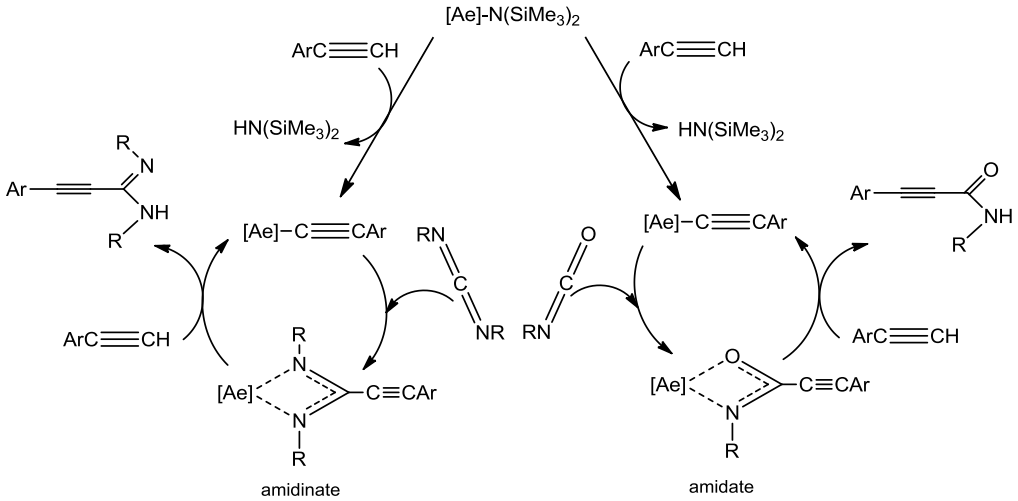

Scheme 1: Proposed catalytic hydroacetylation

The inclusion of acetylenes containing electron donating atoms such as oxygen and nitrogen, has initiated the first reported carbon-carbon coupling with the alkaline earth metal complexes. In order to provide a perspective on the recent advances in catalytic applications of the group 2 metals, both chemical and economical comparisons with the well-established lanthanide metals need to be addressed.

1.1 The heavier group 2 (alkaline earth) metals

Despite being inexpensive and existing in high natural abundance, catalytic applications of the heavier group 2 alkaline earth metals remain in their infancy. Although significant developments have been made with magnesium, most notably by the widespread use of Grignard reagents in both organic and inorganic chemistry, organometallic complexes of the heavier alkaline earth metals, calcium, strontium and barium have effectively been ignored.

1.1.1 Electronic structure

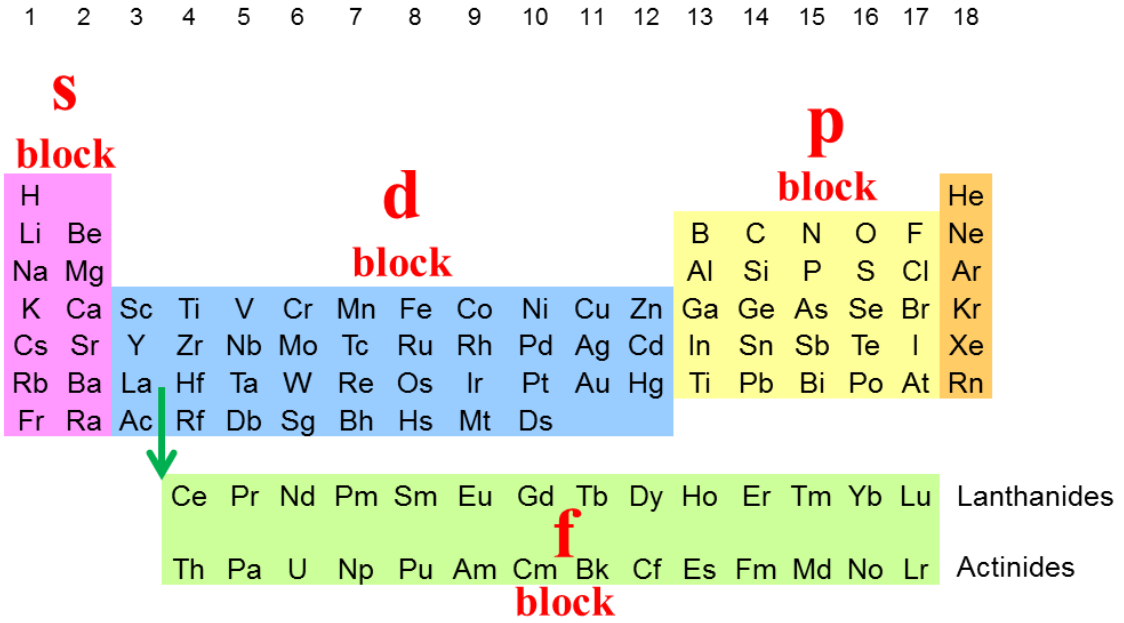

Figure 1: Periodic table.

The group 2 elements are found in the *s*-block of the periodic table and consist of a full outer *ns* valence electron configuration, figure 1. As the group is descended, the atomic radii increase as a result of the shells becoming progressively further away from the nucleus, consequently reducing both ionisation energies and electronegativity, table 1.

Group 2 metals	Atomic Number	Electronic Configuration	Atomic Radius Å	Ionic Radius Å (M^{2+})	Ionisation Energies KJ/mol			Electronegativity (Pauling scale)
					1st	2nd	3rd	
Beryllium	4	$[He]2s^2$	1.13	0.34	899.5	1757.1	14848.7	1.57
Magnesium	12	$[Ne]3s^2$	1.60	0.78	737.7	1450.7	7732.7	1.31
Calcium	20	$[Ar]4s^2$	1.97	1.06	589.8	1145.4	4912.4	1.00
Strontium	35	$[Kr]5s^2$	2.15	1.27	549.5	1064.2	4138	0.95
Barium	56	$[Xe]6s^2$	2.17	1.43	502.9	965.2	3600	0.89

Table 1: Atomic and ionic properties of the heavier group 2 alkaline earth metals.

Due to their electronic configuration, the loss of the two electrons from the outer *ns* sub-shell gives rise to a closed shell configuration. This, therefore, explains why the first and second ionisation energies are considerably less than that of the third ionisation energy.

Unlike transition metals that are able to change from one oxidation state to another, group 2 elements are thus restricted to a single 2+ oxidation state and their complexes are not affected by crystal field effects. The electropositive nature of the metals also results in highly ionic bonding and labile coordination chemistry. This lability is amplified as the group is descended due to the increasing radii and decreasing charge densities of the M^{2+} ions.

1.1.2 Chemical uses and applications

Although group 2 metals are non-toxic and found in high natural abundance where they are used in a variety of chemical, biological, agricultural, construction and technological applications, their catalytic abilities have yet to be fully explored. The following is a brief account of some of the uses and applications of the heavier alkaline earth metals magnesium, calcium, strontium and barium.

1.1.2.1 Magnesium

Magnesium is a very useful element and is the most widely used group 2 metal while being the 8^{th} most abundant element in the Earth's crust. It is used in agriculture in fertilisers while it is able to form alloys with both aluminium and zinc and can be used in the Kroll process for the manufacture of titanium. Magnesium can be found in furnace linings in which iron, steel, glass and cement are produced.

Due to its low atomic number, pure magnesium is stronger and lighter than aluminium and so is used in the manufacture of car body parts and engines. This low weight is also an attractive property for the electronics industry with magnesium being used in small devices such as mobile phones, laptops and cameras.

While present in many food additives as salts, magnesium is essential to all living cells as it is capable of manipulating biological polyphosphate compounds such as ATP, DNA and RNA. Magnesium is also a necessity in the successful function of some enzymes.

In contrast to the lack of synthetic work of the heavier group 2 metals, calcium, strontium and barium, magnesium boasts one of the most long-standing and well-known organometallic classes of compounds, namely Grignard reagents formed when magnesium reacts with alkyl- or aryl- halides.

1.1.2.2 Calcium

Calcium is the 5th most abundant element in the Earth's crust, and can also be mainly found in bones, teeth and shells; calcium is, thus, an essential metal in living organisms.

Calcium intake is thus very important when ensuring a healthy diet. Rickets and poor blood-clotting along with osteoporosis in menopausal women may result from a long term calcium deficiency while overretention can lead to hypercalcemia impairing the function of the kidneys and decreasing the absorption of other minerals. Vitamin D can be added to calcium supplements to aid in the conversion of the hormone in the body that induces the synthesis of the intestinal proteins that are responsible for the calcium absorption.

Being so reactive, calcium is ored from its mineral limestone, $CaCO_3$. On heating, the limestone produces quicklime, CaO, and slaked lime, $Ca(OH)_2$. Slaked lime is widely used in the construction industry for making mortar and plaster while being an inexpensive base material in the chemical industry.

1.1.2.3 Strontium

Biologically strontium is similar to calcium where it is the 16th most abundant element in the Earth's crust. Strontium can form a number of salts that have a wide range of applications, from being used to combat against sensitive teeth when it is found in toothpaste as $SrCl_2$ to being used in the manufacture of fireworks as the carbonate, $SrCO_3$, when it produces a red colour due to its distinctive atomic emission.

Pure strontium forms a 90 - 10 % alloy with aluminium with an eutectic composition that is used for the modification of aluminium-silicon casting alloys.

1.1.2.4 Barium

Barium is the 14th most abundant element in the Earth's crust. Biologically barium can be used to help control the nervous system. Although a low dose of barium can act as a low toxicity muscle stimulant, a high dose can be dangerous with the risk of cardiac irregularities as well as weakness and anxiety to conditions as serious as paralysis.

As an oxide, BaO, it is used to coat electrodes. In an electronic vacuum tube such as those found in cathode ray televisions, barium can be employed as a scavenger removing all final traces of oxygen and other gases. In mechanical industries barium can form an alloy with nickel where it can be found in automobile ignitions.

1.1.3 Grignard reaction

A Grignard reagent, formulated as R-Mg-X (where X = halide and R = alkyl or aryl group), was discovered by the French chemist Francios Auguste Victor Grignard, [1] who for his efforts, was awarded the joint recipitant of the 1912 Nobel prize. Although the initiation step is slow the Grignard reagent is prepared during a single electron transfer when a halogenoalkane is added to a suspension of magnesium in ether, scheme 2.

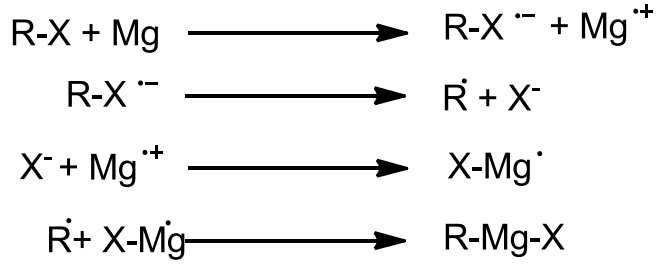

Scheme 2: Formation of Grignard reagents via free radical intermediates.

The Grignard reaction is particularly important for the stoichiometric formation of C-C bonds during coupling reactions as well as the formation of other C-heteroatom bonds such as C-P, C-Sn, C-Si and C-B. Alkyl Grignard reagents will react with water and carbon dioxide to produce alkanes and carboxylic acids respectively, while alcohols can be prepared through reactions with carbonyl-containing compounds, scheme 3.

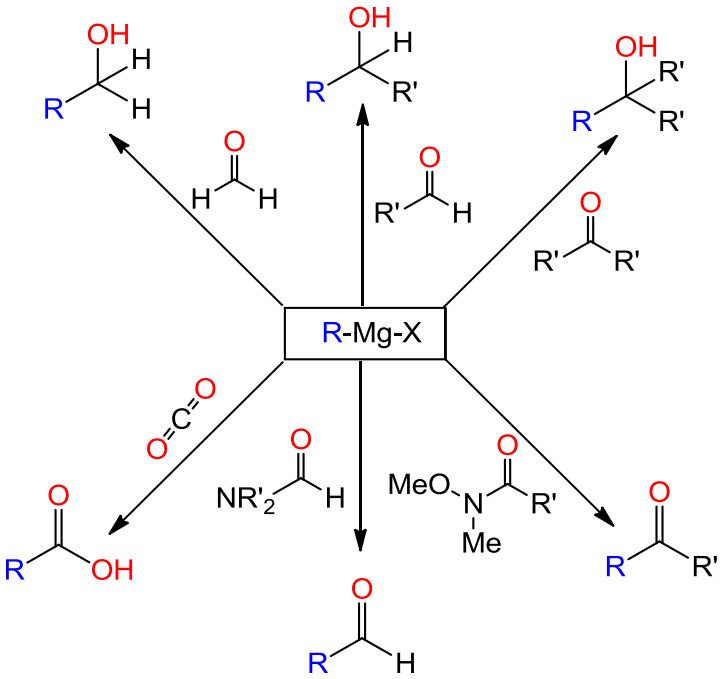

Scheme 3: Reactions involving Grignard reagents.

Such organometallic chemical reactions occur as a result of the polarity of the Grignard reagent. With the C of the alkyl or aryl group in the C-Mg bond being more electronegative than the Mg, the electron pair within the bond is pulled towards the carbon, therefore resulting in a polar C-Mg bond, figure 2. As a result of this charge distribution the Grignard reagent acts as a nucleophile with the δ^- attacking for example, the electrophilic carbon of the carbonyl compound. A major disadvantage presented by the Grignard reagents is that they have to be prepared in anhydrous solvents as this charge distribution results in the complex readily reacting with protic solvents, such as water or with compounds containing acidic protons such as alcohols or amines.

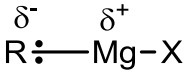

Partial negative charge as bonding electrons are attracted to the more electronegative C of the R group

Partial positive charge as bonding electrons shift to the more electronegative C of the R group

Figure 2: Charge distribution determines the polarity of the compound.

1.1.4 Schlenk equilibrium

The Schlenk equilibrium discovered and named after the German chemist Wilhelm Schlenk was found to occur in solutions of Grignard reagents, equation 1.

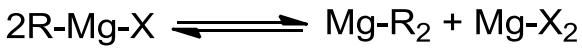

Equation 1: The Schlenk equilibrium.

Equation 1 shows the re-distribution of 2 equivalents of the alkyl- or aryl- magnesium halide compounds via oligomeric or polymeric species to 1 equivalent of the dialkyl- or diaryl- magnesium compound and to 1 equivalent of the magnesium salt.

The equilibrium can be difficult to control with factors such as solvent and temperature, the identity of the substituents and the presence of impurities affecting the position of the equilibrium. The size and charge density of the metal ion also affects the behaviour of the equilibrium as the larger the metal, the higher its tendency to redistribute. Hence as group 2 is descended the larger ions become increasingly susceptible towards the redistribution process and it becomes more difficult to control their co-ordination geometry.

1.1.4.1 Controlling the Schlenk equilibrium

Controlling the position of the Schlenk equilibrium can prove quite difficult when considering the overall stability and size of the group 2 metal complexes. Some influence over the coordinative stability of the complexes can be maintained by variation of the charge, size and denticity of the ligands within the metal complex. Group 2 metals form cations with a +2 charge and are stabilised by ligands possessing a negative charge, figure 3. The kinetic stability of the group 2 organometallic and coordination compounds decrease as the group descends as the larger cations demand larger, more sterically demanding ligands to ensure their stability. Hence the chemistry and stability of these complexes are governed by both electrostatic and steric factors.

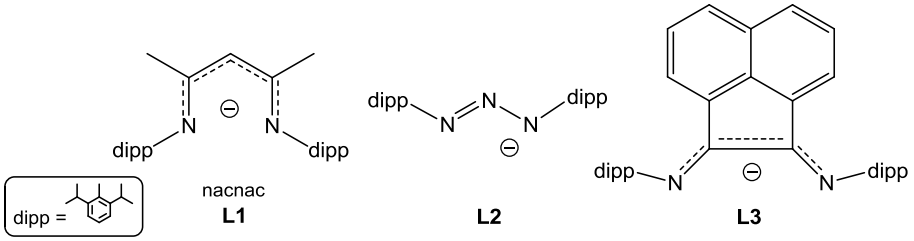

Figure 3: Ligands suitable for controlling the Schlenk equilibrium of the group 2 metals.

As the size of the metal cation increases, the steric protection provided by larger ligands is required to maintain their coordinative stability. Consequently, the metal centre becomes crowded as the ligands themselves become more bulky. Although being surrounded by a large bulky ligand inevitably increases the kinetic stability of the metal cation, the ability to carry out further well-defined reactions or catalysis becomes increasingly more challenging. Increasing the denticity of the ligands also increases the stability of the metal cations. However, this can also lead to over-crowding of the metal centre inhibiting any further reactions. A major challenge, therefore, in seeking to elaborate useful reaction chemistry for these elements is the delicate balance between a useful level of stability and complete unreactivity.

The polymerisation of lactides led to the development of new stabilising ligands for the heavier group 2 catalysts that not only ensured the efficient polymerisation reaction but also possesed a biocompatible and biodegradable nature. Although polylactides are of great potential importance in industrial and biological materials, full control over the polymerisation reaction by limiting the number of side reactions and the removal of the embedded metal had proven more difficult. Chisholm developed suitable catalysts with the biocompatible calcium at the centre [2] with a variety of bulky ligands capable of ensuring the overall stability of the catalytic complex, figure 4.

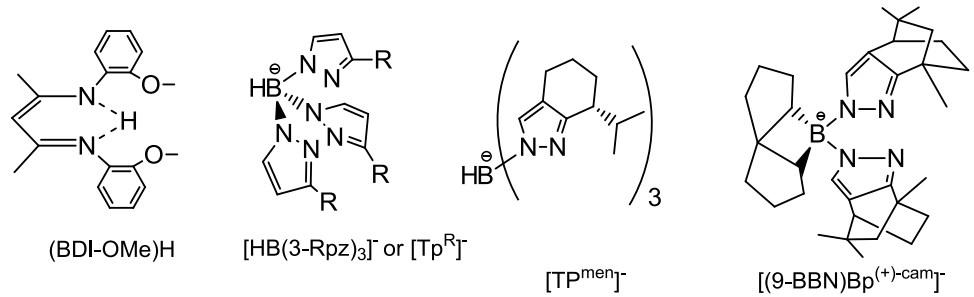

Figure 4: Ligands for the stabilisation of calcium complexes. [2]

Gibson and co-workers prepared both zinc and magnesium complexes with a range of stabilising amidinate and triazenide ligands. [3] Compared to the β-diketiminato ligand **L1**, the triazenide ligands were proposed to increase the complexes catalytic stability.

Findings in the Hill group, for example, have shown the heteroleptic β-diketiminato calcium catalytic complex **C1**, stabilised by the β-diketiminato ligand **L1**, serves as a

useful and reliable stable prototype reagent with which to explore calcium amide reactivity in a variety of catalytic reactions. [4a, 5a, 6, 7a, 8-11]

Schlenk-type re-distribution, however, was found to inhibit the applicability of analogous strontium and barium complexes making them unstable to solution equilibration and limiting their catalytic suitability. In a bid to overcome these problems Hill and co-workers looked towards the development of alternative ligands that not only stabilised the heavier alkaline earth metal centre but allowed for controlled catalysis. Although the diketiminate ligand **L1**, was shown to be a suitable reagent for many reactions, it was also found to re-distribute to its inactive homoleptic derivative, scheme 4. The re-distribution has been shown to be supressed by using a triazene ligand **L2**, or a large BIAN ligand. The ligands and heavier alkaline earth complexes are shown in figure 5.

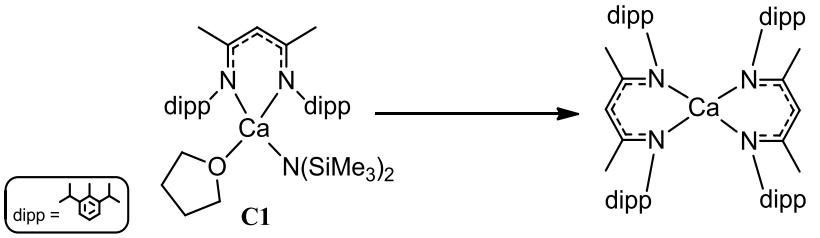

*Scheme 4: Re-distribution of the heteroleptic β-diketiminato calcium amide **C1**, to the inactive homoleptic derivative.*

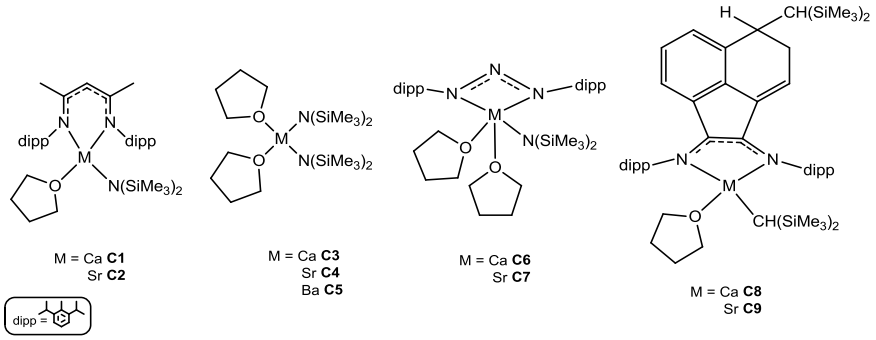

Figure 5: Heteroleptic and homoleptic heavier alkaline earth complexes.

1.2 The lanthanide (rare earth) metals

Inspiration for the work discussed in this thesis is provided by analogous chemistry reported for the lanthanide metals. This thesis therefore aims to explore the similar chemical behaviour and traits between the lanthanide and heavier group 2 metals.

Being extremely reactive in their native states, like group 2 metals, the lanthanide metals are found as minerals in the Earth's crust. Despite being somewhat abundant, the lanthanides are also known as the rare earth metals due to the long and monotonous processes involved in the purification of the elements from their oxides in the years leading up to 1945. Although ion-exchange and solvent extraction methods have enabled the purification processes to become more atom- and cost-efficient, they are still deemed as "rare earth" metals. A rare earth metal's abundance in the Earth's crust, however, can be put into context by comparing them with more familiar elements, table 2.

Element	Symbol	Atomic Number	Abundance in the Earth's crust	Occurrence
Oxygen	O	8	1st 46 %	Practically everywhere
Calcium	Ca	20	5th 5 %	Minerals of chalk, limestone, gypsum and anhydrite
Sodium	Na	11	6th 2.3 %	Minerals of salt, halite, soda and zeolite
Magnesium	Mg	12	8th 2 %	Minerals of dolomite, magnesite, olivine and talc.
Barium	Ba	56	14th 340 ppm	Mineral barite – crystallised barium sulfate
Strontium	Sr	38	16th 360 ppm	sulphate mineral celestite ($SrSO_4$) and carbonate strontianite ($SrCO_3$)
Copper	Cu	29	26th 50 ppm	Minerals of chalcopyrite, bornite, covellite and cuprite
Cerium	Ce	58	27th 60 ppm	Minerals of allanite, monazite, bastnaesite and zircon
Neodymium	Nd	60	28th 33 ppm	Ores of monazite sand, bastnaesite and Misch metal
Nitrogen	N	7	31st 25 ppm	Minerals of saltpetre, Chile saltpetre and sal ammoniac
Thulium	Tm	69	58th 0.45 ppm	Minerals of monazite
Gold	Au	79	82nd 0.0031 ppm	In its native state

Table 2: Relative elemental abundance in the Earth's crust.

The lanthanide metals are also referred to as 4*f* elements due to their position in the periodic table. Like the group 2 metals, the lanthanide metals are only able to form a single oxidation state, in this case 3+ rather than 2+ formed by group 2 metals. They form trivalent compounds with largely ionic bonding with O- and N- donor ligands, figure 6. Variations in the chemistry of the lanthanides is largely determined by changes in their ionic radii, which unlike the group 2 metals decrease with increasing atomic number. This decrease across the lanthanide period is termed the lanthanide contraction and is a result of the core-like nature and poor screening ability of the 4*f* valence orbitals.

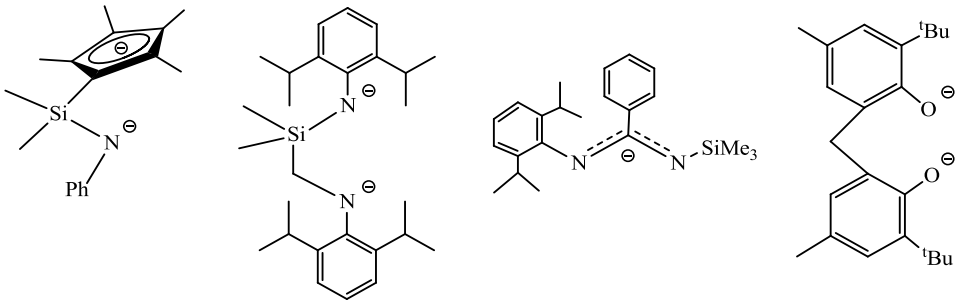

Figure 6: Some ligands found in lanthanide metal complexes.

1.2.1 The lanthanide contraction

The general electronic configuration of the lanthanide metals is [Xe] $6s^2$ $4f^n$ where the value of *n* determines the metal. Unlike group 2 metals, the lanthanide elements are found in the same period with each successive metal possessing one more electron in the 4*f* subshell than the previous metal. As a result of this the number of subshells remain constant throughout the lanthanide series indicated by the small decrease in the atomic radii resulting from the increasing the effective nuclear charge, $Z_{eff,}$ across the series. The 'lanthanide contraction' is a result of the addition of these new electrons. The inner *s* electrons reduce the attraction exerted by the nucleus on the outer *f* electrons with shielding effects decreasing in the order, $s > p > d > f$. As the 4*f* subshell is filled, there is an incremental decrease in ionic radii of the lanthanide cations with increasing Z_{eff} across the series. As the orbitals contract, their distance from the nucleus decreases, allowing the nucleus to have a greater attraction towards the outer electron. This is also indicated by the increase in the 3rd ionisation energies as the period proceeds, table 3.

Lanthanide metals	Atomic Number	Electronic Configuration	Atomic Radius Å	Ionic Radius Å (M^{3+})	Ionisation Energies KJ/mol			Electronegativity (Pauling scale)
					1st	2nd	3rd	
Cerium	58	$[Xe]4f^{1}5d^{1}6s^{2}$	1.825	1.01	527	1047	1949	1.12
Praseodymium	59	$[Xe]4f^{3}6s^{2}$	1.828	0.99	523	1018	2086	1.13
Neodymium	60	$[Xe]4f^{4}6s^{2}$	1.821	0.983	529	1035	2130	1.14
Promethium	61	$[Xe]4f^{5}6s^{2}$	1.81	0.97	536	1052	2150	1.13
Samarium	62	$[Xe]4f^{6}6s^{2}$	1.802	0.958	543	1068	2260	1.17
Europium	63	$[Xe]4f^{7}6s^{2}$	2.042	0.947	546	1085	2404	1.2
Gadolinium	64	$[Xe]4f^{7}5d^{1}6s^{2}$	1.802	0.938	593	1167	1990	1.2
Terbium	65	$[Xe]4f^{9}6s^{2}$	1.782	0.923	564	1112	2114	1.2
Dysprosium	66	$[Xe]4f^{10}6s^{2}$	1.773	0.912	572	1126	2200	1.22
Holmium	67	$[Xe]4f^{11}6s^{2}$	1.766	0.901	581	1139	2204	1.23
Erbium	68	$[Xe]4f^{12}6s^{2}$	1.757	0.89	589	1151	2194	1.24
Thulium	69	$[Xe]4f^{13}6s^{2}$	1.746	0.88	597	1163	2285	1.25
Ytterbium	70	$[Xe]4f^{14}6s^{2}$	1.94	0.868	603	1176	2415	1.1
Lutetium	71	$[Xe]4f^{14}5d^{1}6s^{2}$	1.734	0.861	523	1340	2033	1.27

Table 3: Atomic and ionic properties of the lanthanide rare Earth metals.

1.3 Comparisons between the group 2 and lanthanide metals

The heavier group 2 metals exhibit properties and characteristics superficially similar to those of the lanthanide 4*f* metals. Both species possess large atomic radii and readily form large electropositive cations. However, while descending group 2 increases the atomic radii, the lanthanide metals undergo 'lanthanide contraction' in which the atomic radii decreases as the period proceeds. Unlike transition metals capable of forming a number of oxidation states, both the heavier group 2 metals and the *4f* elements are only able to form single oxidation states of +2 and +3 respectively.

Consideration of the ionic radii of the two sets of metals allows for comparisons in their size. Although calcium is the smallest of the heavier alkaline earth metals covered in this thesis and has an ionic radius of 1.06 Å, this is still 0.05 Å larger than the largest true lanthanide 3+ ion, cerium 1.01 Å, table 4. The heaviest members, strontium and barium possess considerably larger 2+ ions due to their closed shell [Kr] and [Xe]

configurations. As a result the group 2 cations show a considerably lower charge density and a much wider range of polarisabilities than the smaller trivalent *4f*-elements.

Despite the resultant lability of both sets of (M^{2+}, Ln^{3+}) cations the co-ordination environments of both series may be controlled to a certain extent by the co-ordination of kinetically stabilising ligands. As described previously, the coordination environment of the heavier alkaline earth metal cations may be usefully stabilised by a single anionic ligand. Most notable, for example, throughout this thesis is the β-diketiminate ligand **L1** while the 4*f* lanthanide metal cations are stabilised by di-anionic ligands as in the half-sandwich yttrium alkyl complex, figure 7. In both cases, however, a single more reactive amide or alkyl anion remains bonded to the metal available for further reactivity.

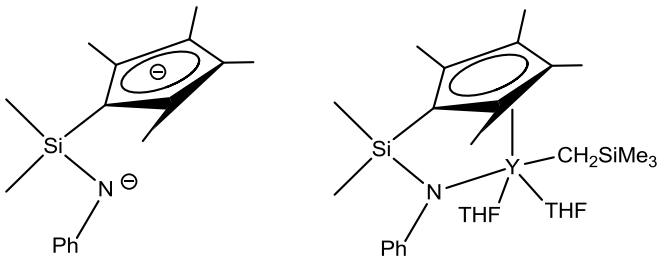

Figure 7: Anionic ligands stabilising lanthanide metal cations.

While the use of bulky cyclopentadienyl ligands was successfully developed for the stabilisation of lanthanide metal complexes, [4d] transferring the idea to the heavier alkaline earth metals complexes proved more difficult due to the lower charge density of the metals and attention turned to alternative ligand sets. The bidentate β-diketiminato ligands are of particular interest in the stabilisation of the main group elements and in lanthanide and transition metal catalytic complexes. The size of the ligands and the bulky substituents at the nitrogen atoms has been of significant interest over recent years. [12]

Group 2 metals	Atomic Number	Electronic Configuration	Atomic Radius Å	IonicRradius Å (M^{2+})
Calcium	20	$[Ar]4s^2$	1.97	1.06
Strontium	35	$[Kr]5s^2$	2.15	1.27
Barium	56	$[Xe]6s^2$	2.17	1.43

(a) Atomic and ionic properties of the heavier group 2 metals.

Lanthanide metal	Atomic Number	Atomic Electronic Configuration	Ln^{3+} Electron Configuration	Atomic Radius Å	Ionic Radius Å (Ln^{3+})
Cerium	58	$[Xe]4f^15d^16s^2$	$[Xe]4f^1$	1.825	1.01
Praseodymium	59	$[Xe]4f^36s^2$	$[Xe]4f^2$	1.828	0.99
Neodymium	60	$[Xe]4f^46s^2$	$[Xe]4f^3$	1.821	0.983
Promethium	61	$[Xe]4f^56s^2$	$[Xe]4f^4$	1.81	0.97
Samarium	62	$[Xe]4f^66s^2$	$[Xe]4f^5$	1.802	0.958
Europium	63	$[Xe]4f^76s^2$	$[Xe]4f^6$	2.042	0.947
Gadolinium	64	$[Xe]4f^75d^16s^2$	$[Xe]4f^7$	1.802	0.938
Terbium	65	$[Xe]4f^96s^2$	$[Xe]4f^8$	1.782	0.923
Dysprosium	66	$[Xe]4f^{10}6s^2$	$[Xe]4f^9$	1.773	0.912
Holmium	67	$[Xe]4f^{11}6s^2$	$[Xe]4f^{10}$	1.766	0.901
Erbium	68	$[Xe]4f^{12}6s^2$	$[Xe]4f^{11}$	1.757	0.89
Thulium	69	$[Xe]4f^{13}6s^2$	$[Xe]4f^{12}$	1.746	0.88
Ytterbium	70	$[Xe]4f^{14}6s^2$	$[Xe]4f^{13}$	1.94	0.868
Lutetium	71	$[Xe]4f^{14}5d^16s^2$	$[Xe]4f^{14}$	1.734	0.861

(b) Atomic and ionic properties of the4f lanthanide metals.

Table 4: Atomic and ionic properties of (a) heavier group 2 and (b) 4f lanthanide metals.

1.3.1 σ-bond metathesis and olefin insertion

Reaction of both the lanthanide and group 2 metal complexes with small molecules may occur by σ-bond metathesis and olefin insertion. σ-bond metathesis involves the substitution of a σ-bond of the metal complex with a σ-bond of another incoming molecule while the oxidation state remains constant, scheme 5. This ligand exchange mechanism may occur via the four-centre transition state and is common with the early transition metals and allows for the activation of small molecules at redox inactive metal centres.

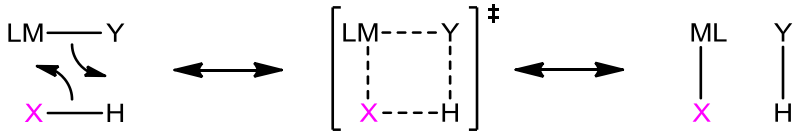

Scheme 5: Mechanism of σ-bond metathesis.

The regiochemistry of the products formed during the insertion of unsymmetric olefins with both lanthanide and group 2 metal complexes is determined by the Markovnikov addition rule. The products either form via a Markovnikov or an anti-Markovnikov addition, scheme 6. Generally when in the presence of a Bronsted or Lewis acid the Markovnikov product is favoured. The determination of the product also depends on the substituents on the unsaturated carbon bond. For a Markovnikov addition of H-X where X=NR_2, the H attaches to the carbon of the double bond that is bonded to more H's while the X attaches to the more substituted carbon. For the anti-Markovnikov addition, the hydrogen bonds to the more substituted carbon while, the X bonds to the less substituted carbon.

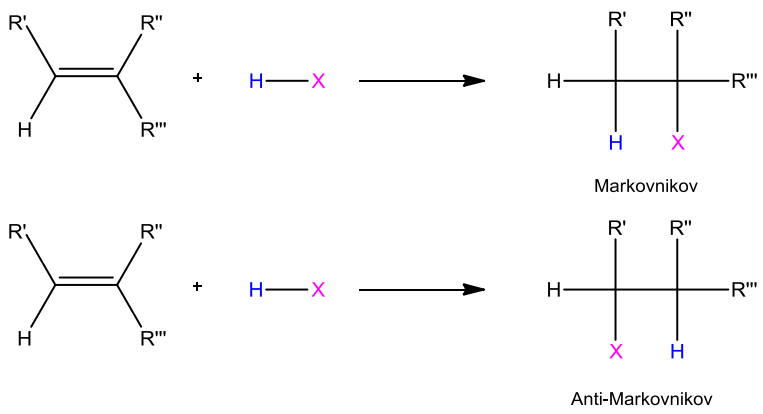

Scheme 6: Olefin insertion via Markovnikov and anti-Markovnikov addition.

1.4 Organolanthanide-based catalysis

Organolanthanide compounds L_2LnR have been employed in many catalytic reactions involving the heterofunctionalisation of unsaturated C-C bonds including hydroamination, hydrophosphination and hydroacetylation (scheme 7).

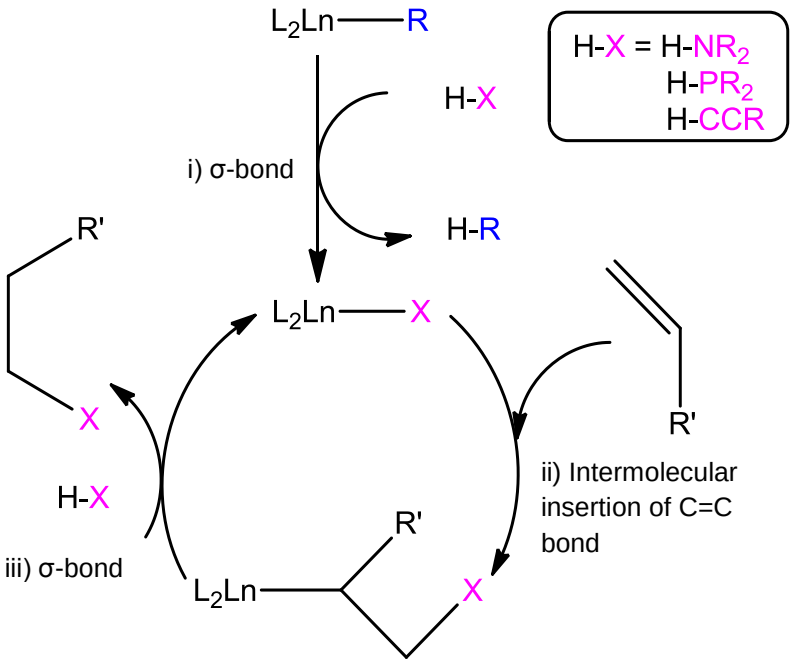

Scheme 7: Organolanthanide-based catalytic cycle for the hetero functionalisation of an unsaturated C-C bond.

The first step of this catalytic cycle requires a ligand exchange between the organolanthanide complex and the incoming amine, phosphine or acetylene molecule through a σ-bond metathesis reaction. The insertion of an unsaturated bond in the second step proceeds via Markovnikov insertion. The unsaturated bond can either be found on the incoming olefin or, in the case of intramolecular insertion, on the already co-ordinated organolanthanide complex resulting in a cyclisation reaction. A further σ-bond metathesis enables the liberation of the free product.

Hou et al. [13] reported the reaction of diethylamine with a stabilising half-sandwich yttrium metal complex scheme 8. σ-bond metathesis is shown to occur between the amine and the CH_2SiMe_3 group on the organolanthanide metal before the insertion of the *iso*-propyl carbodiimide.

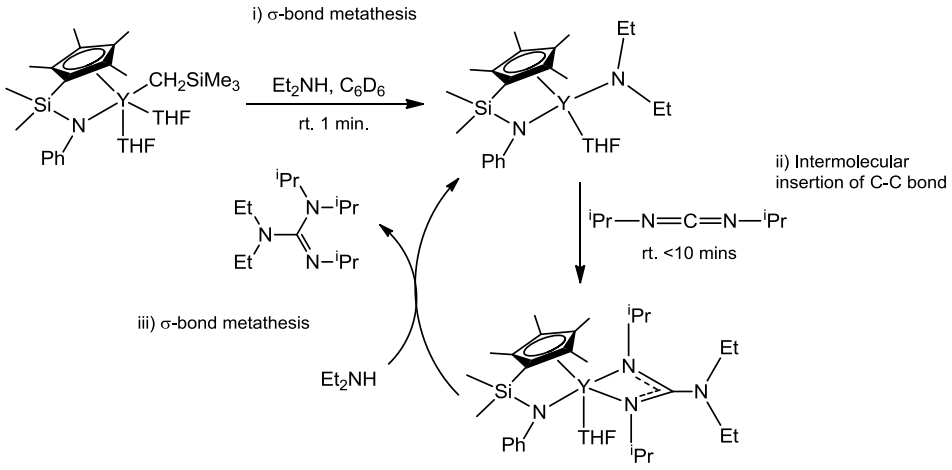

Scheme 8: Organolanthanide catalysis with σ-bond metathesis and Markovnikov insertion. [13]

Following the catalysis outlined for organolanthanide complexes involving σ-bond metathesis and Markovnikov insertion, the catalytic system was employed for analogous reactions of the alkaline earth metal complexes.

1.5 Alkaline earth metal amide catalysis

Similarities in the reactivity between the heavier alkaline earth metals and the lanthanide metals were initially highlighted by Harder [4c] in which a calcium complex, stabilised by a benzylic α-Me_3Si-substituent, initiates the insertion of a C=C double bond in the polymerisation of styrene.

Prior to the report of Westerhausen [14a] in 1991, compounds of the bis(trimethylsilyl)amide ligand of the heavier alkaline earth metals calcium, strontium and barium remained unknown, in contrast to the lighter alkaline earth metals beryllium and magnesium. The beryllium derivative was isolated with a monomeric structure following the metathesis reaction of $BeCl_2.O(C_2H_5)_2$ and sodium bis(trimethylsilyl) amide [14b] scheme 9.

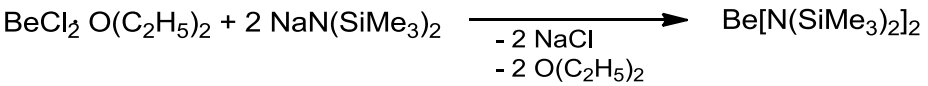

Scheme 9: Metathesis reaction for the formation of beryllium bis(trimethylsilyl) amide. [14b]

Westerhausen reported the first isolation and characterisation of the heavier alkaline earth metal bis(trimethylsilyl) amides via a transmetalation reaction of the elements with the tin derivative. [14a] Westerhausen prepared the reaction in different solvents, 1,2-dimethoxyethane (DME) and tetrahydrofuran (THF). Both reactions resulted in two of the ether molecules co-ordinating to the metal atom increasing the co-ordination number of the complexes to 6 and 4 respectively, scheme 10.

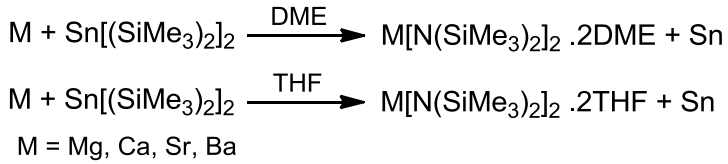

Scheme 10: Transmetallation with the co-ordination of 2 DME or 2 THF molecules in the monomeric complexes. [14a]

Although removal of these coordinated ether molecules resulted in decomposition of the compounds, the reaction was also shown to occur in non-complexing solvents toluene and benzene by the formation of dimeric alkaline-earth-metal diamides, scheme 11.

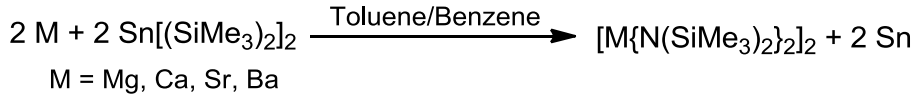

Scheme 11: Transmetallation with non-co-ordinating toluene and benzene molecules in the dimeric complexes. [14a]

The synthesis of homoleptic heavier alkaline earth metal complexes, [Ae{$N(SiMe_3)_2$}$_2$], is a well-established process. However, displacing one of the hexamethyldisilazide groups, {$N(SiMe_3)_2$}, with another ligand to yield the heteroleptic species was reported by Chisholm in 2003 [4e] as a one-pot synthesis to yield the heteroleptic β-diketiminato calcium amide, **C1**. Following the synthesis of the heteroleptic calcium amide, **C1**, Hill and co-workers strived to synthesise the strontium and barium derivatives [4a] employing the synthetic procedure reported by Chisholm. Although all three reactions yielded colourless crystalline products, the strontium and barium derivatives were found to have re-distributed to the more stable homoleptic moieties, scheme 12.

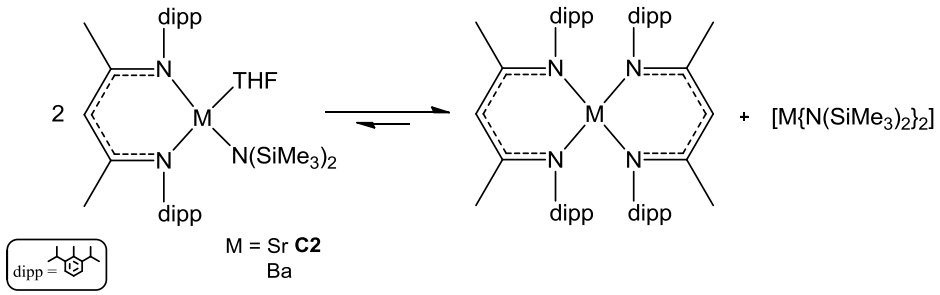

Scheme 12: Re-distribution of the heteroleptic strontium and barium β-diketiminato amide complexes to the more stable, inactive homoleptic derivative. [4a]

After numerous unsuccessful attempts to obtain the strontium and barium derivatives it was assumed the increased atomic size of the strontium and barium favoured the formation of homoleptic over the heteroleptic complexes. However during the course of the work discussed in this thesis limited success in the isolation of the strontium derivative has been achieved. Obtained as a white powder and characterised by ^{1}H NMR as the heteroleptic derivative, **C2**, its use within this thesis is therefore restricted to chapter 3. Interestingly, following a 'slow cooling of a hot hexane solution' Hill had earlier successfully isolated large platelet crystals of the barium derivative. [4a] Like the calcium complex, the barium complex was found to exist as a monomer despite the large size of the barium dication.

The hetero-functionalisation of unsaturated C-C bonds by hydroamination (H-N), hydrophosphination (H-P) and hydroacetylation (H-C) is the most atom and cost efficient process of generating new C-N, C-P and C-C bonds respectively (scheme 13). This thesis will explore the hydroacetylation via σ-bond metathesis between a terminal acetylene and the alkaline earth metal derivatives (chapter 2) before the insertion of unsaturated C-C bonds of both carbodiimides (chapter 4) and isocyanate (chapter 5).

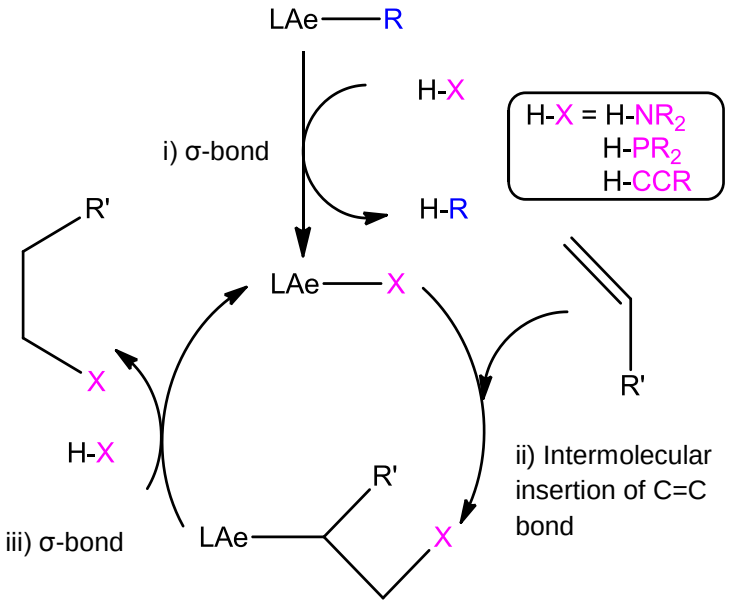

Scheme 13: Alkaline earth metal based catalytic cycle for the hetero-functionalisation of an unsaturated C-C bond.

1.6 Hydroamination

Hydroamination, the addition of an N-H bond across an unsaturated C-C bond to yield a new amine derivative proceed via either a Markovnikov or anti-Markovnikov insertion reaction, scheme 14.

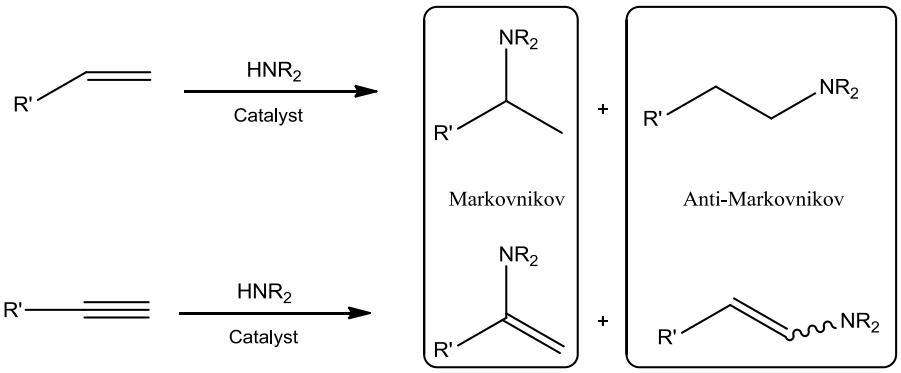

Scheme 14: Hydroamination of unsaturated C=C and C≡C bonds.

Although lanthanide half-sandwich complexes are proven efficient catalysts [15c] for hydroamination [15d] and hydrophosphination [15e] they are more expensive and less accessible than the homoleptic lanthanide bis(trimethylsilyl) amides, $[Ln\{N(SiMe_3)_2\}_3]$ where Ln = Y, lanthanide. This therefore increases the desirability of the lanthanide complexes. In 1989 Marks and co-workers [15a] reported a highly regiospecific organolanthanide-catalysed hydroamination/cyclisation of amino olefins, scheme 15.

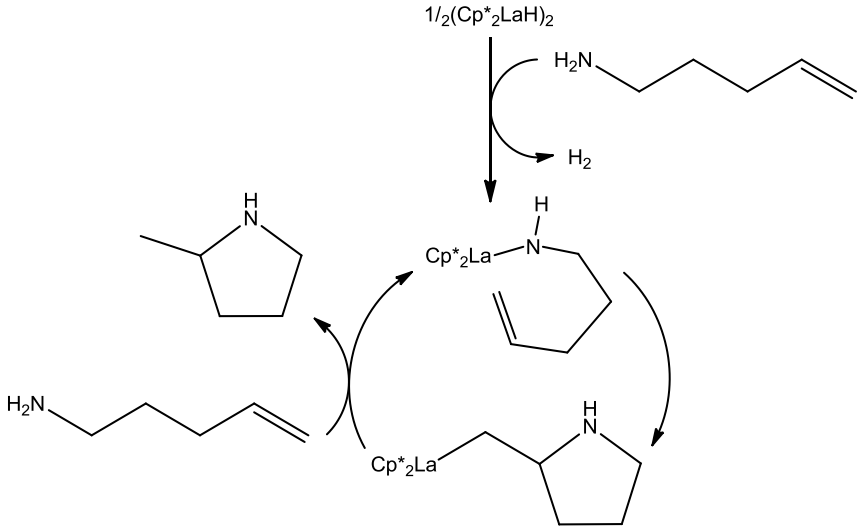

Scheme 15: Organolanthanide hydroamination/cyclisation catalysis of amino olefins. [15a]

After considering the catalysis reported with the metallocenes, $[(C_5Me_5)_2LnR]$, where R = $N(SiMe_3)_2$, $CH(SiMe_3)_2$, Roesky et al. [15b] developed Marks' work by reporting homoleptic lanthanide amides as suitable catalysts for stoichiometric hydroamination. Comparing the catalytic activity in the hydroamination/cyclisation of aminoalkynes with organolanthanide complexes, $[Y\{N(SiMe_3)_2\}_3]$, (*1a)* and $[La\{N(SiMe_3)_2\}_3]$, (*1b*) with the metallocene $[(C_5Me_5)_2YCH(SiMe_3)_2]$ *(2)*. Roesky deduced the superior catalytic ability of the metallocene over the lanthanide amido complexes by the increased yield obtained despite the lower temperature, table 5.

Entry	Substrate	Product	Catalyst	N_t [h^{-1}]	Yield [%] NMR scale
1	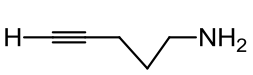		*2* [(a)]	3.3	quant.
2			*1a*	0.3	71
3			*1b*	-	-
4	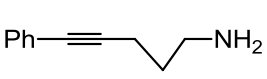	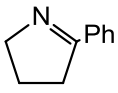	*2* [(a)]	8.6	quant.
5			*1a*	0.1	75
6			*1b*	0.09	quant.
7		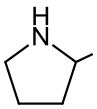	*2* [(a)]	0.5	quant.
8			*1a*	-	-
9			*1b*	-	-

[(a)] *reaction at 21 °C*

N_t [h^{-1}] = turn over per hour

Table 5: Hydroamination/cyclisation with 3-5 mol % catalyst in d_8 toluene at 60 °C. [15b]

The cleavage of the $SiMe_3$ groups on the organolanthanide complexes by protonation with the substrate enables the catalysis. However, Roesky proposed that increasing the protonation potential of the organolanthanide complex by adding further $SiMe_3$ groups decreases the overall catalytic rate.

Employing chemical similarities between the lanthanide metals and the heavier alkaline earth metals, calcium, strontium and barium, Hill and co-workers used the β-diketiminato calcium amide, **C1**, for aminoalkene intramolecular hydroamination catalysis [10a] with a variety of primary amines and found the amine to co-ordinated to the calcium metal centre via the displacement of a THF molecule, [4a] scheme 16. However, limitations with the catalytic reaction were observed with the irreversible re-distribution to the inactive homoleptic species.

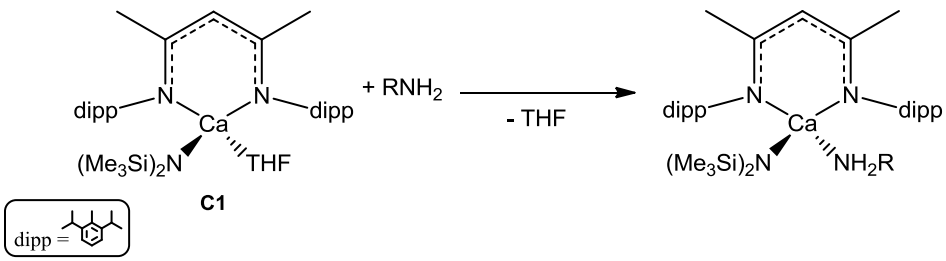

Scheme 16: Stoichiometric co-ordination of a primary amine via the displacement of a THF molecule. [4a]

Similar Schlenk-like re-distribution was also observed during the addition of benzylamine to **C1** with variable temperature NMR confirming the formation of a dynamic equilibrium, [6] scheme 17, with high temperatures favouring the starting materials.

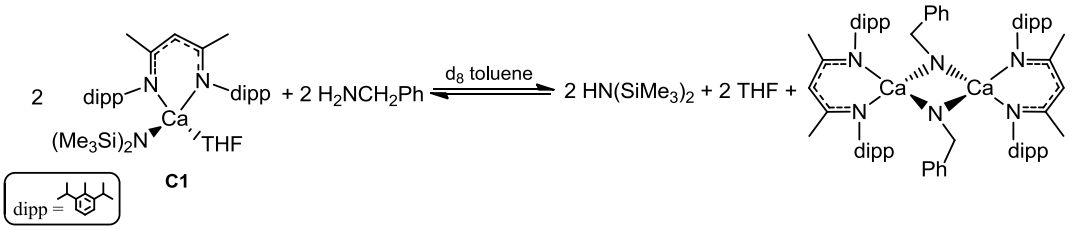

*Scheme 17: Dynamic equilibrium with the hydroamination of **C1** and benzylamine.* [6]

In 2005 Hill and co-workers reported the importance of the stabilising ligand **L1** on the alkaline earth catalytic complex **C1** during the hydroamination of aminoalkenes [5a] table 6. The absence of this ligand in the homoleptic calcium

bis(bis(trimethylsilyl)amide) **C3** resulted in protonolysis of the bis(trimethylsilyl) amide ligand, thus preventing the hydroamination.

Aminoalkene	Product	T/^{o}C	t/h	Conv. %
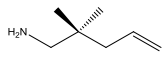		0.25	25	>99[a]
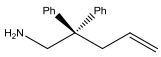		0.25	25	>99[a]
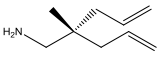	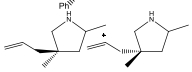	0.25	25	>99[a]
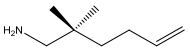		6	60	89[b]

[a] *10 mol % catalytic loading*
[b] *20 mol % catalytic loading*

Table 6: Hydroamination catalysis of aminoalkenes with β-diketiminato calcium amide, ***C1****, conversion determined by* ^{1}*H NMR spectroscopy.* [5a]

1.7 Hydrophosphination

Similar to hydroamination, the formation of new phosphine derivatives from the addition of a P-H bond across an unsaturated C-C bond may proceed by either a Markovnikov or anti-Markovnikov reaction, scheme 18.

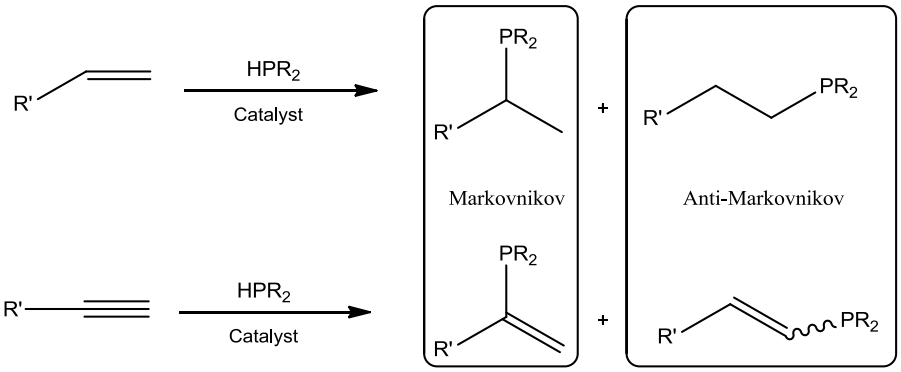

Scheme 18: Hydrophosphination of unsaturated C=C and C≡C bonds.

Marks et al. reported the catalytic intramolecular hydrophosphination/cyclisation of a phosphine and an unsaturated organic substrate with lanthanocene catalysts, $Cp^{*}_{2}LnX$ (where X = H, $CH(SiMe_3)_2$ and Ln = La, Sm, Y, Lu) [15d] scheme 19, with σ-bond metathesis of the Ln-C bond and the insertion of the unsaturated bond.

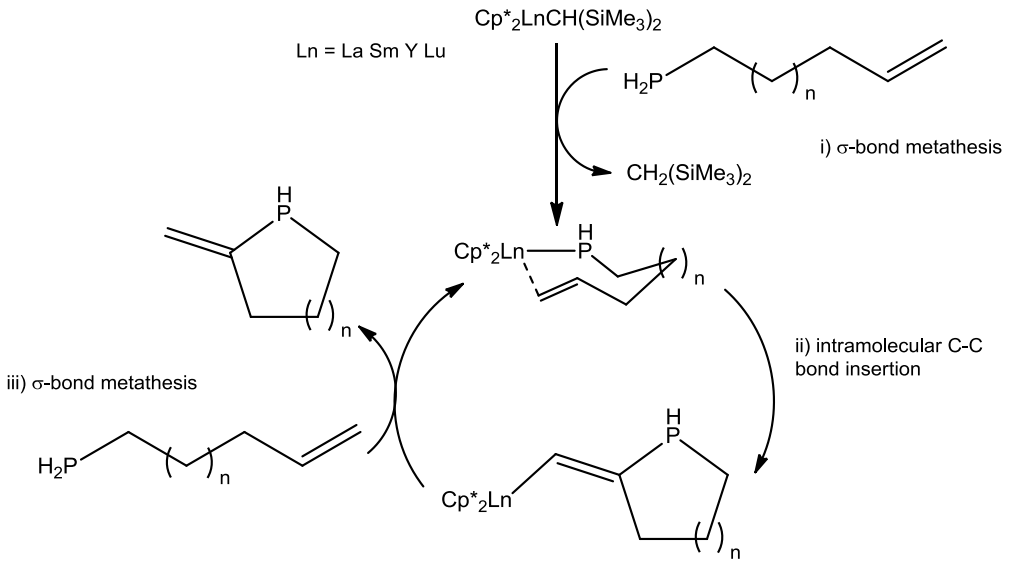

Scheme 19: Lanthanide catalytic intramolecular hydrophosphination/cyclisation. [15d]

Hill and co-workers extended their work to intermolecular hydrophosphination with the heavier alkaline earth metal catalysts. [7a] The highly efficient catalysis was conducted with a variety of unsaturated substrates at 10 mol % catalytic loading of **C1**, table 7. The compounds obtained where characterised by ^{1}H and ^{31}P NMR and were found to have undergone anti-Markovnikov addition of the H-P bond across the less hindered C=C double bond of the substrate. The reaction was also found to be dependent upon the steric demands of the phosphine with the reaction progress being reduced with increased steric bulk.

Although completion is achieved with the homoleptic **C3** derivative, it required a further 16 hours in comparison with the reaction of the heteroleptic **C1** derivative. Hill reported the importance of the β-diketiminato ligand **L1** for ensuring solubility whilst maintaining a high catalytic concentration throughout the reaction. Absence of the ligand on **C3** resulted in the formation of the insoluble homoleptic calcium phosphide $[Ca(PPh_2)_2(S)_x]_y$ (where S = THF, $HPPh_2$) thus decreasing the catalyst concentration.

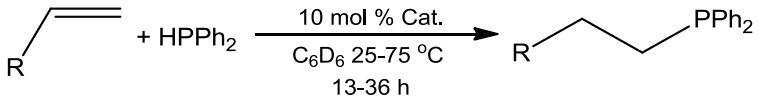

Substrate	Product	T/°C	t/h	Conv. %
[a] Styrene	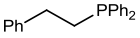	75	20	95
[b] Stryrene	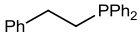	75	36	92
[a] Isoprene	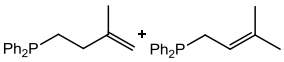	25	24	95
[a] 1,3-cyclohexadiene	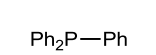	75	24	78
[a] Diphenylacetylene	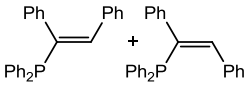	75	13	94[c]

*[a] cat. β-diketiminato calcium amide, **C1***
*[b] cat. calcium bis(bis(trimethylsilyl)amide) **C3***
[c] 20 mol %

Table 7: Calcium-mediated intermolecular hydrophosphination of alkenes. [7a]

Despite this, Hill and co-workers successfully isolated and characterised the homoleptic phosphide derivatives with the heavier alkaline earth metal homoleptic complexes **C3-5** [16] equation 2.

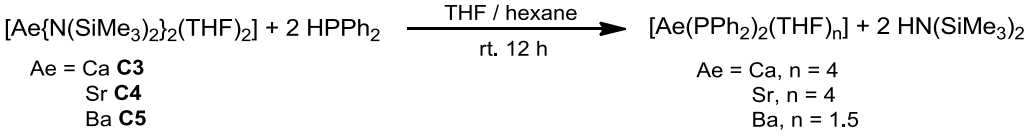

*Equation 2: Homoleptic phosphide derivatives from the homoleptic calcium, strontium and barium bis(bis(trimethylsilyl)amides) **C3-5**.* [16]

1.8 Alkaline earth based acetylides

Further to hydroamination and hydrophosphination of amines and phosphines respectively, the stoichiometric addition of a terminal acetylenes to lanthanide alkyl catalyst, $Cp^*_2LnCH(SiMe_3)_2$ (where Ln = Ce, La), produces dimeric acetylides $[Cp^*_2LnC{\equiv}CR]_2$, a number of which have been characterised by X-ray crystallography.

In a bid to further understand σ-bonded heavier alkaline earth acetylides Hanusa and co-workers [17a] looked towards preventing Schlenk-type redistribution of the complex with the aid of a bulky ligand on the catalyst and reaction of a terminal acetylene with

$(Cp^{4i})Ca[N(SiMe_3)_2](THF)$ where Cp^{4i} = $^{i}Pr_4C_5H$. [17b] In order to achieve a direct comparison between the lanthanide and the alkaline earth acetylide derivatives Hanusa adopted the reaction process of the lanthanide derivatives $Cp^{*}_2Ln[N(SiMe_3)_2]$ [17a] to the reaction of the alkaline earth moieties.

Ruhlandt-Senge and co-workers also addressed the synthesis of alkaline earth σ-bonded complexes and reported a series of calcium, strontium and barium complexes. [18] Reacting the homoleptic alkaline earth catalytic complex with [18]crown-6 yielded $[M([18]crown-6)(CCSiPh_3)_2]$, M = Ca, Sr, Ba, equation 3. The products themselves were extremely air- and moisture-sensitive and must be stored under an inert atmosphere.

$$[M\{N(SiMe_3)_2\}_2(THF)] + 2HCCSiPh_3 + [18]crown\text{-}6 \longrightarrow [M([18]crown\text{-}6)(CCSiPh_3)_2] + 2HN(SiMe_3)_2$$

M = Ca, Sr, Ba

Equation 3: Formation of alkaline earth acetylides. [18]

In 2004 Hill and co-workers carried out reaction of the heteroleptic β-diketiminato calcium amide, **C1**, with a series of terminal acetylenes resulting in the isolation and characterisation of unsolvated dimeric acetylides, scheme 20. [8] The acetylide forms following the deprotonation of the terminal acetylene and the formation of $HN(SiMe_3)_2$. The products are stable under an inert atmosphere but readily liberate the free acetylene when exposed to atmosphere.

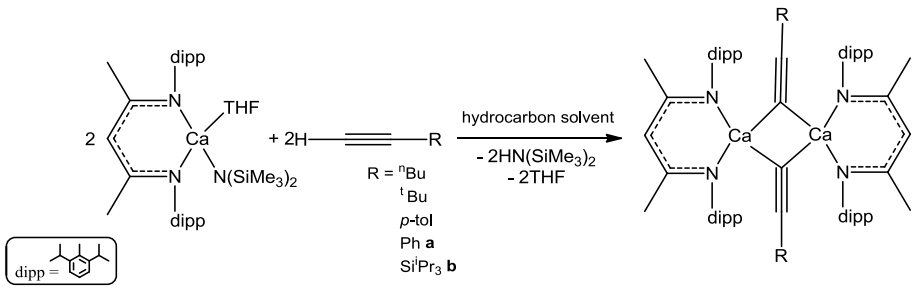

*Scheme 20: Formation of dimeric acetylide with **C1** and a terminal acetylene.* [8]

Interestingly reaction of trisopropylsilyl acetylene, **b**, not only produced a dimeric acetylide with an apparent π-interaction and three-centre-two-electron bond, but also a monomeric acetylide species with a single σ-bond, [19] scheme 21. Both derivatives were found to exist in equilbirum.

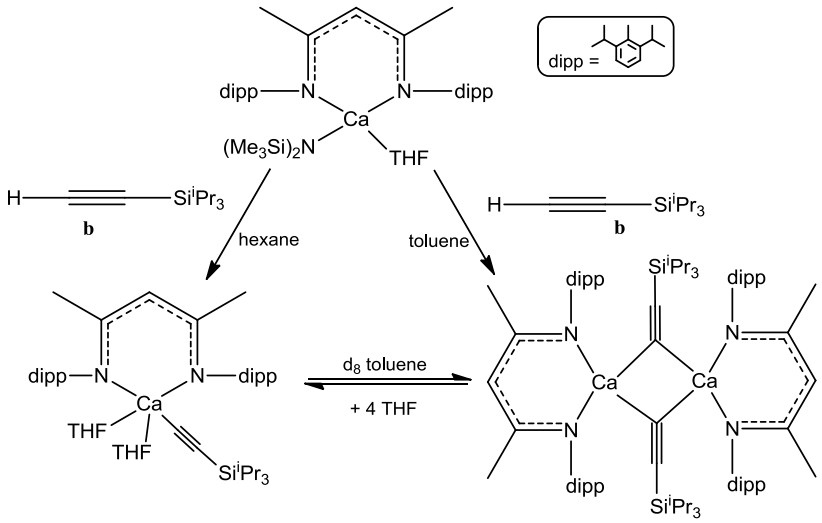

Scheme 21: Both monomeric and dimeric moieties exist in equilibrium. [19]

1.9 Acetylene-based C-C catalytic coupling

Of relevance to the work described in chapter 3 of this thesis, Yamazaki reported the catalytic dimerisation of ^{t}butylacetylene with dihydridocarbonyl tris(triphenylphosphine)ruthenium by heating at 100 ^{o}C in benzene for several hours. [20] A total of five products with a fractional ratio of 6:1:1:4:88 were observed, figure 8, with the isomeric vinylacetylenes *i*, *ii* and *iii* being assigned from I.R. and NMR spectra. The isomeric butatrienes *iv* and *v* were assigned from ^{1}H NMR spectra following distillation in the ratio 1.25:1 for *v*:*iv*.

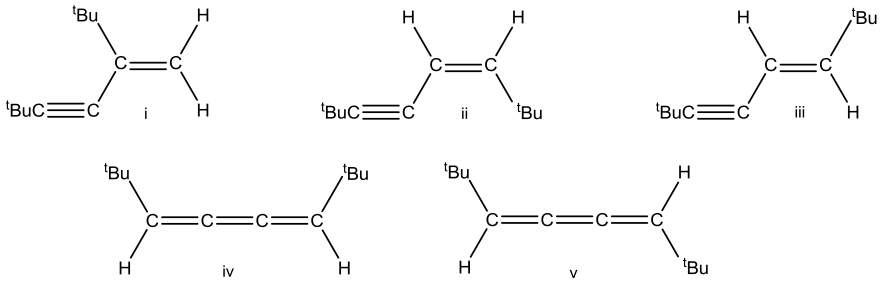

Figure 8: Isomers from the Ru-catalysed dimerisation of ^{t}butylacetylene. [20]

The coupling of two acetylide units to produce a butatriene derivative has previously been catalysed by transition and lanthanide metal complexes. However isolation of the butatriene derivative has proven to be more of a challenge due to its low thermodynamic stability and high tendency to isomerise to its more stable enyne form, scheme 22. [21a]

The low thermodynamic stabilities of the C-C coupled butatriene derivatives were found to impede their isolation and characterisation.

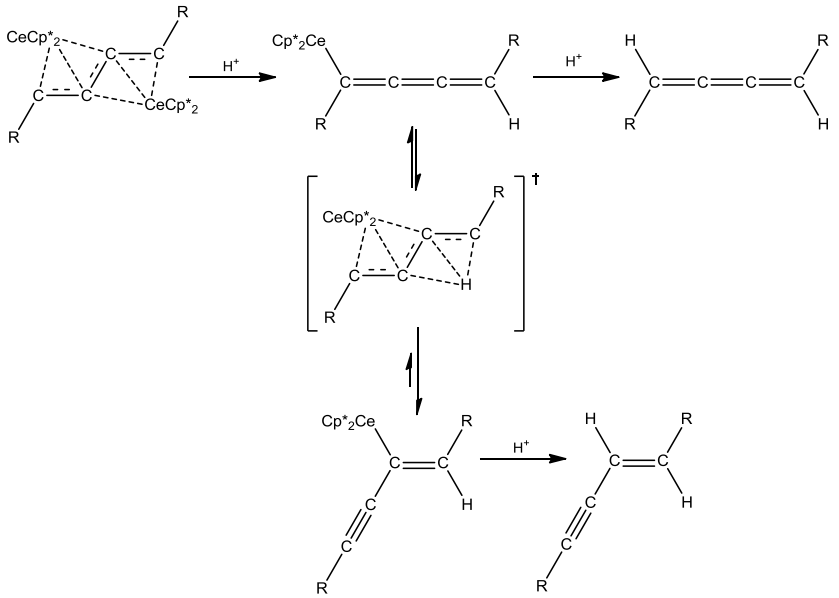

Scheme 22: Cerium-catalysed coupling and butatriene isomerisation to the more thermodynamically stable enyne form. [21a]

Wakatsuki et al. [22a] calculated the relative energies of the butatriene structure and its more stable enyne form, observing a significant difference between the two energies, (17.3 Kcal mol^{-1}), figure 9. This energy difference between the structures illustrates the higher stability of the thermodynamically favourable enyne structure over the unfavourable butatriene complex and why its isolation has proven difficult.

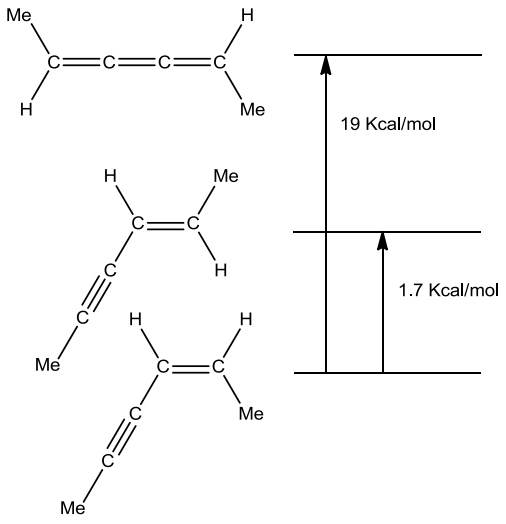

Figure 9: Relative energies of three isomers. Geometries and energies were calculated by the ab initio LCAO-MO-SCF method with a DZV basis set. [22a]

1.9.1 Transition metal based C-C coupling

The catalytic regio- and stereoselective dimerisation of terminal acetylenes has been successfully reported with transition metal (titanium, palladium and ruthenium) complexes possessing a large, bulky, electron donating polydentate nitrogen ligand (tris(pyrazolyl)borate), (TP) or a polypodal phosphorus ligand ($P(CH_2CH_2PPh_2)_3$(PP_3) or a pentamethylcyclopentadienyl ligand. The nature of the acetylene is important during these coupling reactions. The simple acetylene, phenyl acetylene, catalysed by [$Ru(Cl)(PPh_3)_2$)(TP)], coupled to produce *(E)*-1,4-diphenylbut-1-ene-3-yne while the more bulky acetylenes, (trimethylsilyl)acetylene and *tert*-butylacetylene coupled to yield the *Z* isomer, [23a] scheme 23.

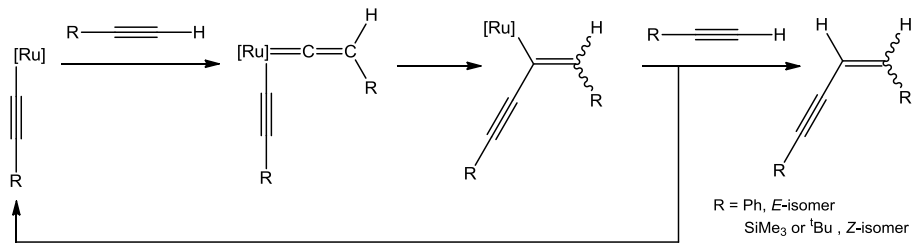

Scheme 23: Coupling of simple and bulky acetylenes with ruthenium metal catalyst, [$Ru(Cl)(PPh_3)_2$)(TP)]. [23a]

The acetylene coupling can proceed via head-to-tail coupling as observed with titanium and palladium catalysts forming 2,4-disubstituted (branched) enynes [22b, c] or by head-to-head coupling with palladium and rhodium complexes to form *(E)*-1,4-disubstituted enynes [22d, e] by the oxidative addition of terminal acetylene, insertion of a second acetylene molecule and finally reductive elimination. [22f]

During the homogeneous catalytic dimerisation of terminal acetylenes with the ruthenium hydride complexes $C_5Me_5Ru(L)H_3$ (where L = PPh_3 (*i*), PCy_3 (*ii*) and PMe_3 (*iii*)), Yi and co-workers [24] obtained the rare thermodynamically unstable $PhCH_2CH{=}C{=}C{=}CHCH_2Ph$ (*vii*) as well as the more stable cis- and trans- 1,4-disubstituted (*iv*) and (*v*) and 1,3-disubstituted enynes (*vi*), scheme 24. The nature of the ligand proved to be an important factor in the overall product selectivity, table 8.

Although (*vi*) was not obtained in entries 1, 6 and 11 of table 8, the selectivity of (*iv*) and (*v*) was significantly influenced by the ligand on the catalyst while entry 6 shows (*iv*) as the predominant product over (v) with 90:10 ratio. This ratio was overturned in entry 11 with (*v*) being the predominant product at 90:10. Formation of the unstable cumulene (vii) was identified in the ^{1}H NMR with the vinyl proton resonance signal at 6.03 ppm while the quaternary carbon was observed at 210.1 ppm in the ^{13}C NMR spectrum.

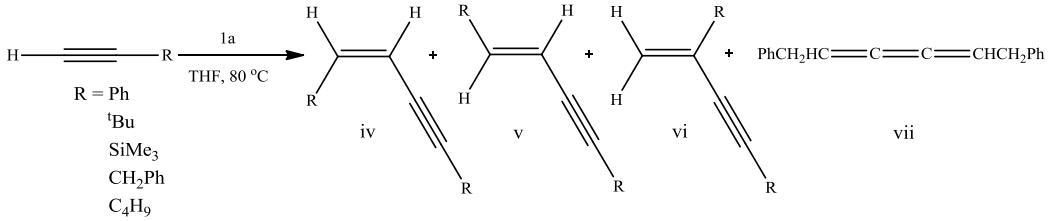

Scheme 24: Homogeneous catalytic dimerisation of terminal acetylenes. [24]

Entry	Substrate	Catalyst $C_5Me_5Ru(L)H_3$	Product ratio 2:3:4	% yield
1	HC≡CPh	i	67:33:0	85
2	HC≡CC$(CH_3)_3$	i	5[a]:95	91
3	HC≡CSiMe_3	i	2[b]:98	100
4	HC≡CCH_2Ph	i	0:27:73	80
5	HC≡CC_4H_9	i	0:37:63	88
6	HC≡CPh	ii	90:10:0	86
7	HC≡CC$(CH_3)_3$	ii	17:35:48	17
8	HC≡CSiMe_3	ii	5[b]:95	58
9	HC≡CCH_2Ph	ii	>95 of (*5*)	93
10	HC≡CC_4H_9	ii	<5[b]>95	14
11	HC≡CPh	iii	10:90:0	82
12	HC≡CC$(CH_3)_3$	iii	33:39:12[b]	87
13	HC≡CSiMe_3	iii	10:28:62	83
14	HC≡CCH_2Ph	iii	14:62:24	78
15	HC≡CC_4H_9	iii	24:26:50	79

i (L = PPh_3) ii (L = PCy_3) iii (L = PMe_3)
[a]Combined ratios of (iv) and (v).
[b]16 % of (vii)

Table 8: Product selectivity depending upon the ligand employed. [24]

In 1991 Wakatsuki et al. [22a] reported the high yield and stereoselectivity of *(Z)*-1,4-di-*tert*-butylbutatriene, (*Z*)-dbb, by the dimerisation of *tert*-butylacetylene with the ruthenium complex [Ru(Cod)(Cot)], (Cod = 1,5-cyclooctadiene, Cot = cyclooctatriene). Although the complex does not affect the overall catalytic activity, the activity can be greatly enhanced by the addition of phosphines. The stereoselectivity towards the formation of *(Z)*-dbb is increased by the large, bulky environment surrounding the ruthenium metal centre. Wataksuki carried out the reactions in benzene at 100 ^{o}C with at least 3 mol ratio of a tertiary phosphine to 1 mole of ruthenium with the catalytic activity increasing in the order $P(OPh)_3 < PPh_3 < P^iPr_3 < P^nBu_3$ while the selectivity increases in the order $P(OPh)_3 < P^nBu_3 < PPh_3 < P^iPr_3$. The reactions were also carried out with $[Ru(CO)(PPh_3)_3H_2]$ with Wataksuki observing the best results with 3 molar excess P^iPr_3 for 96 % *(Z)*-dbb selectivity with *ca*. 90 catalytic turnovers per ruthenium for 48 hours at 50 ^{o}C.

In 2000 Ohmura and co-workers reported the regio- and stereoselective dimerisation of terminal acetylenes with iridium catalysis. [25] The reaction produced a mixture of linear *(E)*- and *(Z)*- enynes. The rate and stereochemistry of the reaction was dependent upon the acetylene and the phosphine ligand on the iridium metal catalyst and increased with the presence of the base triethylamine.

In 1965 Nakamura [26a] reported the stabilisation of unstable organic compounds such as cyclobutadiene with an organo-cobalt metal complex and diphenyl acetylene via the formation of a stable organometallic tetraphenylcyclobutadiene cobalt π-complex, while unsubstituted butatriene compounds were shown to be stabilised by an iron carbonyl complex, $C_4H_4Fe_2(CO)_5$. [26b] Following the successful isolation of the butatriene iron carbonyl complex, Nakamura went on to investigate the corresponding iron complex of hexapentaene by the dehalogenation of dihalobutyne and an analogous dehalogenation of dihalohexadiyne with zinc powder in the presence of tri-iron dodecacarbonyl, equation 4.

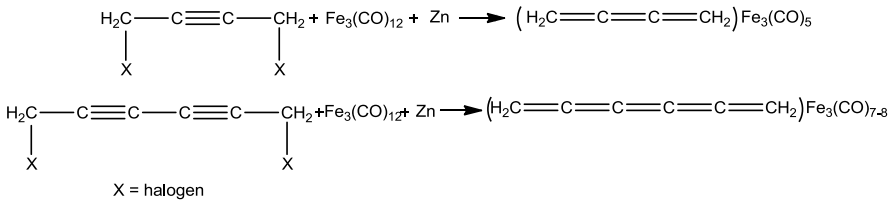

Equation 4: Formation of the butatriene-iron-pentacarbonyl complex and the hexapentaene tri-iron dodecacarbonyl complex. [26a]

Although the unsubstituted hexapentaene was obtained at a significantly low yield of 1.2 % it was its thermal and air stability that presented the most interesting property. The formation of unsubstituted butatriene reported in 1954 by Schubert et al. [26c] was found to be stable at very low temperatures under a nitrogen atmosphere and was found to have a higher stability than that of the unsubstituted hexapentaene. Nakamura also reported how the formation of a π-complex by co-ordination to the iron metal complex in a η^2-π-co-ordination mode, figure 10, increased the stability for temperatures above 250 ^{o}C while its crystals were found to be air stable.

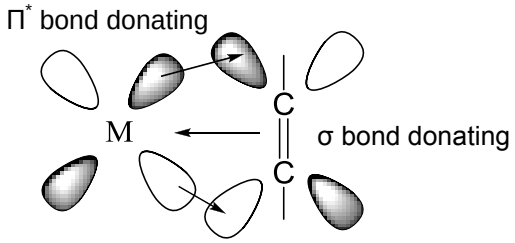

Figure 10: η^2-π-co-ordination mode.

Maas et al [27a] reported new crystalline π-complexes (scheme 25 A-D) in 1983 with the interaction of four butatriene derivatives with chlorotris(triphenylphosphine)rhodium, Wilkinson's catalyst. [27b] While complexes (B-D) were prepared under mild conditions, (A) required a reflux in benzene for several hours. All of the compounds (A-D) were isolated via chromatography in reasonable yields and found to be air-stable over a short period of time and slightly oxygen-sensitive when in solution. The co-ordination mode of the butatriene ligand on the rhrodium metal catalyst was determined by an X-ray crystal structure. The cumulene ligands co-ordinate to the transition metals with one of three modes a carbene, a η^1-alkyl (cumulenyl) or a η^2-olefin.

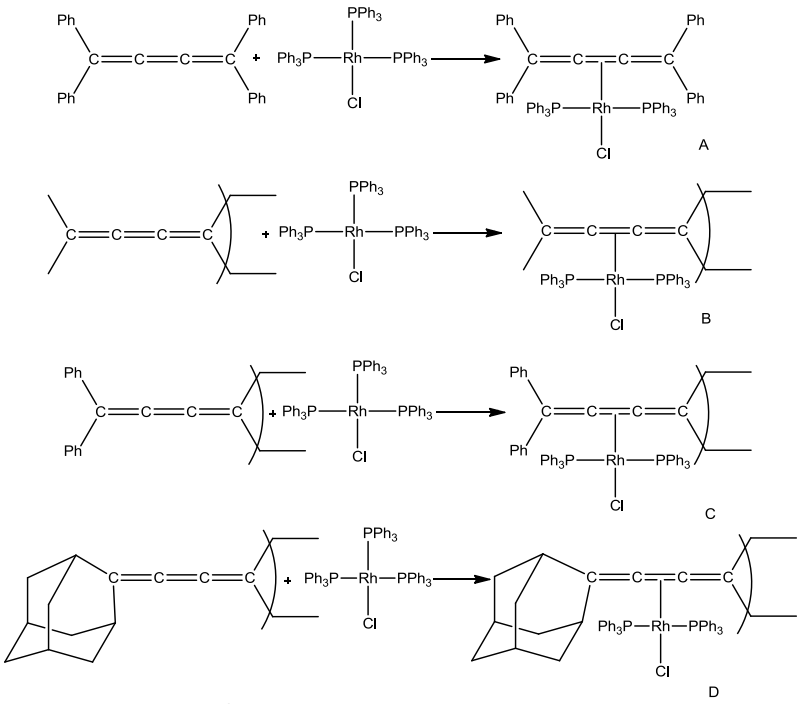

Scheme 25: Synthesis of η^2-butatriene complexes with Wilkinson's catalyst. [27b]

Suzuki and co-workers continued the work with rhodium and in 2003 reported the isomerisation of an η^2-π-co-ordinated butatriene on a rhodium metal, [28] scheme 26.

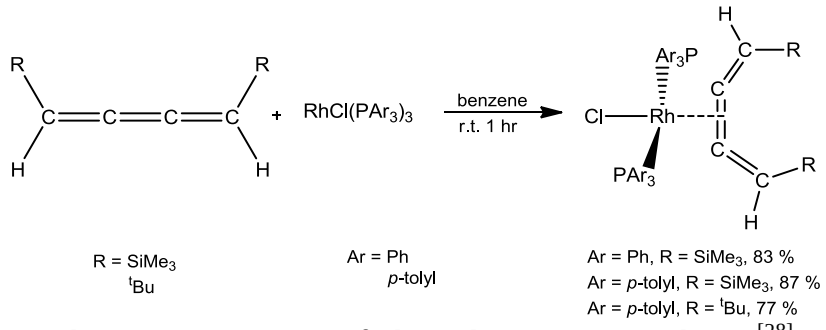

Scheme 26: Formation of Rh-(Z)-butatriene complexes. [28]

Schafer et al. [29] studied the co-ordination of terminal acetylenes to alkynyl(vinylidene)rhodium(I) complexes, *trans*-[Rh(C≡CR)(=C=CHR)(P^iPr_3)$_2$], with CO migratory insertion giving rise to the stereoselective formation of the butenynyl compounds with the catalytic dimerisation of the terminal acetylene.

The overall instability of the cumulene complexes and their high tendencies to re-distribute or decompose has limited their characterisation. However, in 2007 Akkerman et al. [30a] synthesised a more stable 1,1,4,4-tetrafluorobutatriene by co-ordination to Vaska's complex, [Ir(CO)(PPh_3)$_2$Cl] [30b] scheme 27. The formation of this 2,3-η^2-triene

complex and the rhodium derivative increased the stability allowing further reactions to be carried out as well as the identification and characterisation of the crystal structure.

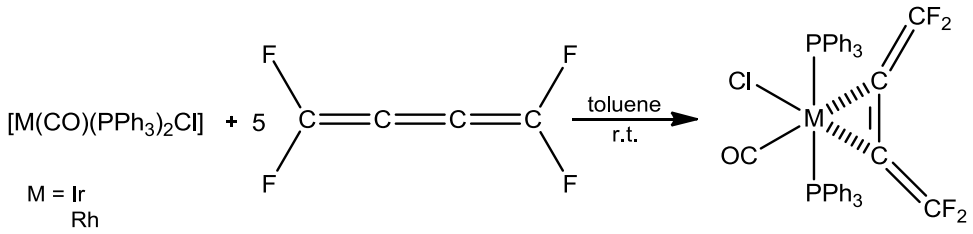

Scheme 27: Co-ordination of the cumulene to Vaska's complex and its rhodium analogue increases the overall stability as a 2,3-η^2-triene complex. [30a]

Following the interest in organometallic vinylidene ligands [M=C=CHR], Bruneau et al. [23a] looked at their catalytic implications. The vinylidene-metal complexes have been prepared by the deoxygenation of acyl-metals with $(CF_3SO_2)_2O$, [23d] deprotonation of metal carbynes [23e, f] and the rearrangement of alkylidene metallacyclobutane [23g] as well as the addition of electrophiles [23h, i] such as alkyl groups [23j, k] to the β-C of the alkynyl ligand. The most efficient route of forming the vinylidene-metal complexes is by the activation of a terminal alkyne to an initial η^2-co-ordinated alkyne intermediate before either a 1,2-hydrogen migration over the C≡C bond or by the oxidative addition of the ligands C-H bond to the metal. The nature of the co-ordination of the vinylidene ligand on the metal depends on the position of the metal in the periodic table. The ligand acts as a nucleophile with the early transition metals and an electrophile with the late transition metals.

Bruneau was able to show the nucleophilic reaction of titanium vinylidene on a stoichiometric scale by the efficient synthesis of tetra-substituted allenes from ketones and 1,1-disubstituted allenes, [23a] scheme 28. However the reaction was not successfully repeated on a catalytic scale due to the formation of stable Ti-O bonds.

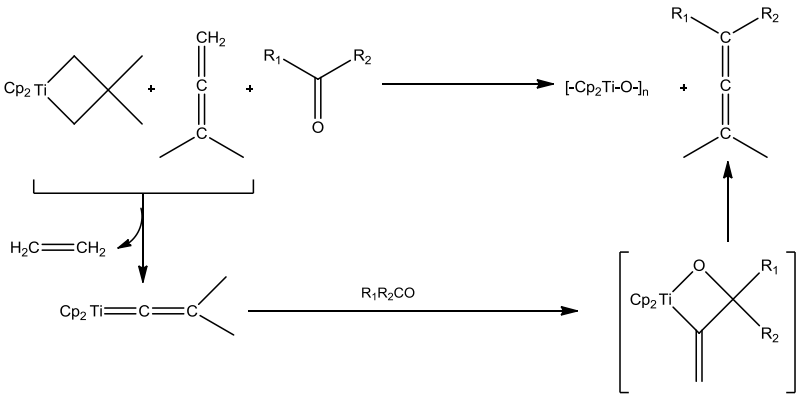

Scheme 28: Stoichiometric nucleophilic addition with titanium vinylidene. [23a]

The electrophilic α-C centres of the vinylidene complexes were shown to react with non-sterically hindered nucleophiles producing functionalised metal carbene complexes, scheme 29.

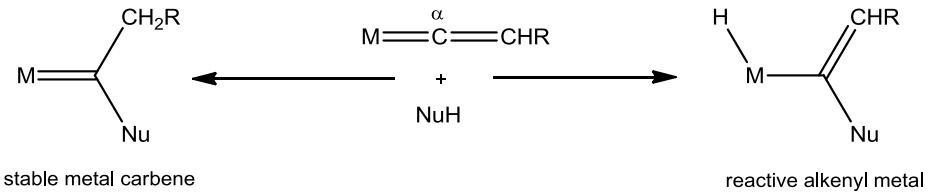

Scheme 29: Formation of functionalised metal carbene complexes. [23a]

They also form C-C bonds by the intramolecular interactions of the vinylidene and the 2-electron alkynyl ligand, an important step in the dimerisation of the alkynes to enynes or butatrienes depending on the nature of the ligand. The polymerisation via metathesis is achieved by [2+2] interaction of the M=C bond and the unsaturated C=C bond, scheme 30.

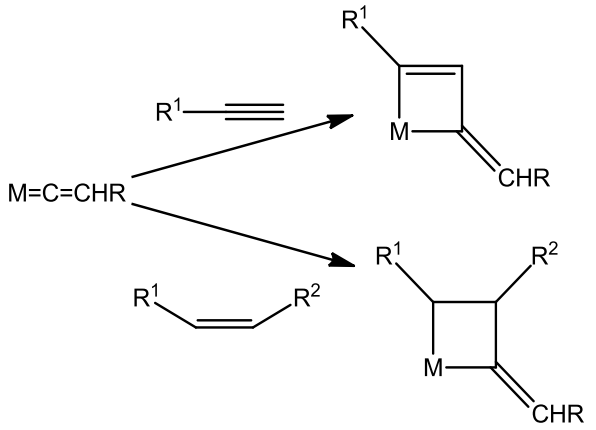

Scheme 30: Initiating the polymerisation by the [2+2] interaction of M=C bond with C=C bond. [23a]

Following the formation of zirconium metallacycles by Suzuki, [28] Burlakov et al [31] looked at the reduction of 1,4-dichlorobut-2-yne with a titanocene complex [$Cp_2Ti(\eta^2$-$Me_3SiC_2SiMe_3$] to produce a 1,2,3-butatriene derivative, scheme 31.

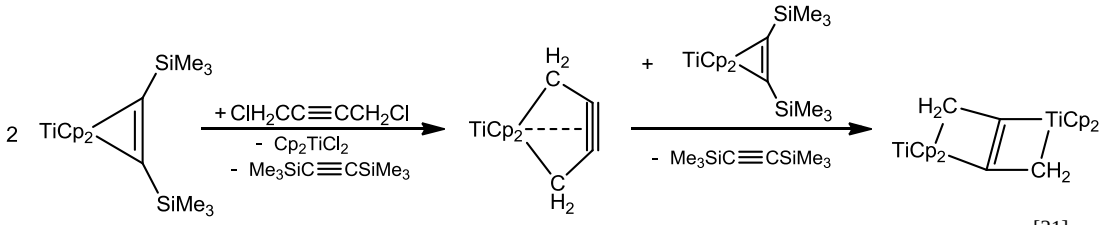

Scheme 31: Reduction of 1,4-dichlorobut-2-yne with titanium metal complex. [31]

The X-ray crystal structure indicated two bent titanocenes bridged by a symmetrical "zig-zag" C-4 ligand, scheme 32.

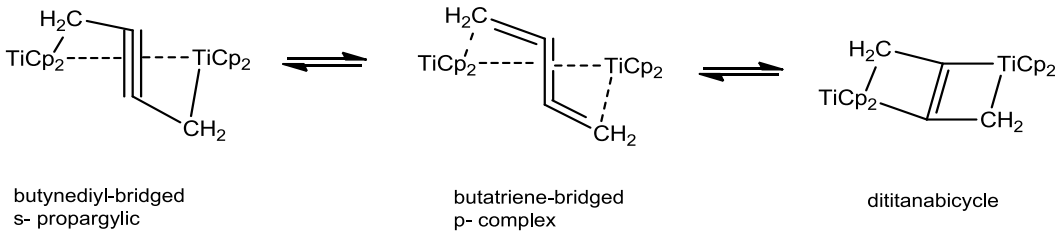

Scheme 32: Symmetrical 'zig-zag' structure of the di-titana-bicycle. [31]

Pollack et al [32] reported the formation of a crystalline polymer from 1,1,4,4-bis(pentamethylene)butatriene by thermally induced 1,4 free-radical polymerisation. However, spectroscopic studies of this butatriene complex have been hindered due to it being prone to undergo spontaneous polymerisation in both the presence and absence of oxygen.

In 1985 Landon et al. [23b] reported the first catalytic process for the polymerisation of phenylacetylene by the photolysis of $W(CO)_6$, generating the vinylidene complex [$W(CO)_5$(=C=CHPh)], the active precursor for the polymerisation and the photochemical displacement of a carbonyl (CO) ligand, scheme 33.

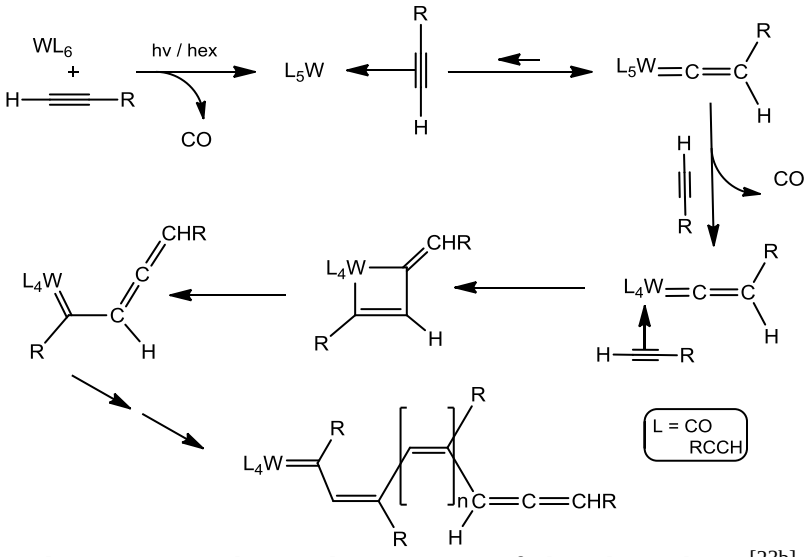

Scheme 33: Catalytic polymerisation of phenylacetylene. [23b]

1.9.2 C-C coupling with lanthanide metal complexes

Organolanthanide based C-C coupling of terminal acetylenes, which occurrs via the intermediacy of lanthanide acetylides, was initially achieved by Heeres [33] through reaction of the lanthanide complex $Cp^*_2LnCH(SiMe_3)_2$ with RC≡CH where Ln = Y, La or Ce. The regio-selectivity of the coupling reaction at the yttrium metal centre was found to be dependent upon the substituents on the acetylene. The highest selectivity towards the head-to-tail dimerised 2,4-disubstituted 1-buten-3-yne complex was obtained for the alkyl groups ^{n}Pr and ^{t}Bu while phenyl acetylene **a** and tri-*iso*-propylsilyl acetylene, **b**, were found to be less selective with the production of the two isomers 2,4-disubstituted 1-buten-3-yne and 1,4-disubstituted 1-buten-3-yne. Both lanthanum and cerium displayed lower regio-selectivity than yttrium, with the identity of the final products determined by the acetylene, scheme 34.

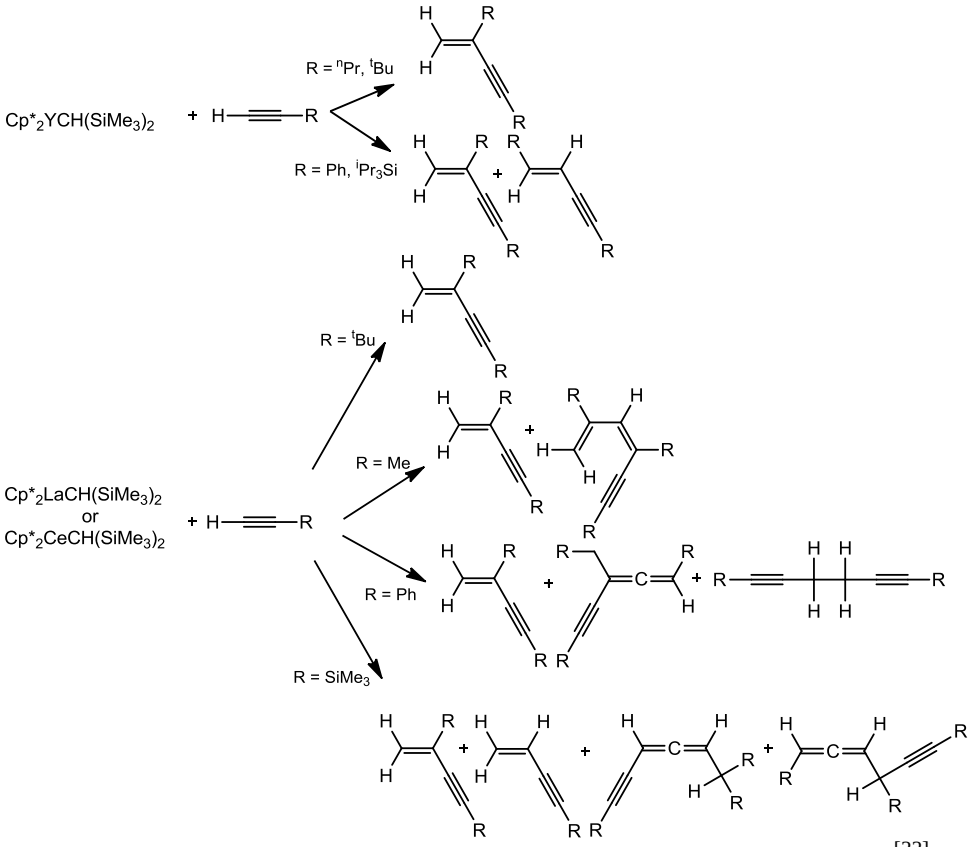

Scheme 34: Regio-selectivity of the lanthanide acetylide coupling. [33]

The first examples of oxidative coupling of terminal acetylenes with lanthanide metals, [34a, c] equation 5, forming a butadiyne dianion and trivalent metals are clearly related to those of titanium that form a butadiyne tetra-anion and tetravalent titanium [34d] equation 6.

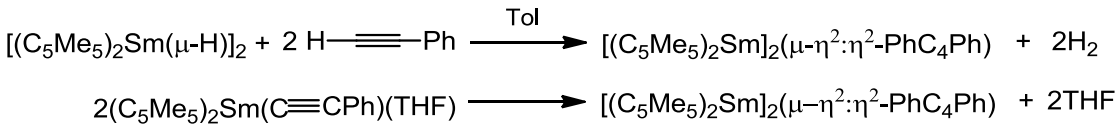

Equation 5: First examples of lanthanide-mediated coupling of alkynide ligands identified by crystallographic and NMR data. [34a]

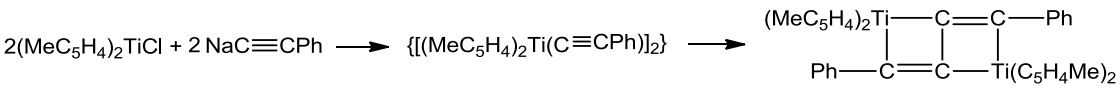

Equation 6: Titanium complex is related to its lanthanide derivative. [34d]

Although the mechanism for the reactions involving samarium and titanium metals were proposed to occur via reduction, coupling, electron transfer and 'internal reduction and oxidation', it was proposed by Evans et al. [34a-c] that steric effects are as important as thermodynamics as it is these steric constraints that enable the product to re-distribute.

Evans et al. [34a] reported the first organolanthanide coupling of two phenylethynyl ligands with a samarium metal catalyst $Cp^*_2Sm[CH(SiMe_3)_2]$. The reaction was thought to proceed via the formation of a dinuclear samarium μ-C bridged acetylide complex equation 7.

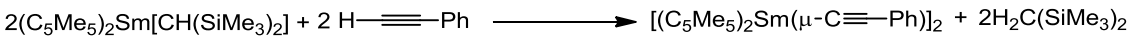

Equation 7: Proposed mechanism for acetylene co-ordination. [34a]

However a subsequent X-ray crystal structure clearly showed the re-distribution of the C≡C triple bonds forming three new C=C double bonds of the butatriendiyl complex. It was suggested that this behaviour resulted from the steric constraints about the samarium centre, equation 8.

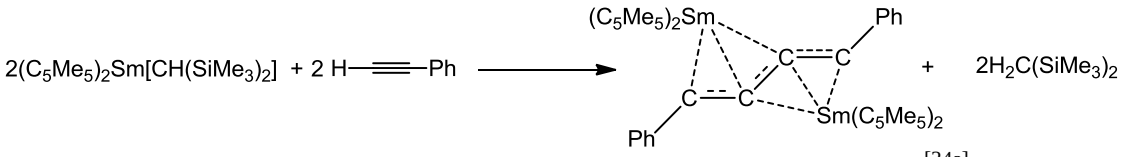

Equation 8: Actual mechanism for acetylene co-ordination. [34a]

In 1991 Heeres and co-workers [21b] identified acetylides $[Cp^*_2CeC{\equiv}CR]_n$ where R = Me, or ^{t}Bu. However, it was not until 1993 that a more convincing understanding of the coupling mechanism was achieved. [21a] The evidence suggested the reactions proceed by the initial formation of the lanthanide acetylide before the temperature dependant coupling and rearrangement. The final products from the protonation of this coupled acetylide are determined by the thermodynamics of the reaction, equation 9. As previously stated, the desired butatriene structure is not thermodynamically favourable and re-distributes to the more stable enyne forms.

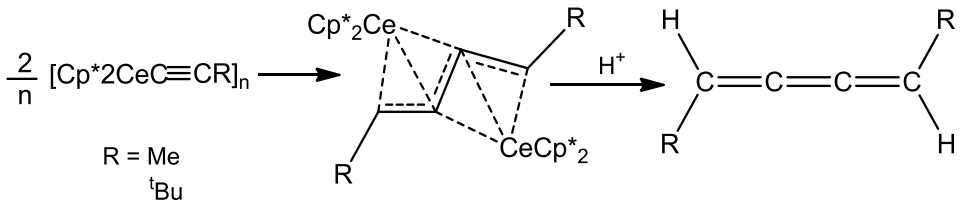

Equation 9: The acetylides re-arrange and couple together before protonation to the butatriene complex. [21a]

In 1993 Evans and co-workers extended their work on acetylide coupling by reporting the successful coupling with cerium and neodymium metal catalysts, [35] hence proving

the coupling is not restricted to samarium metal catalysts. Heeres et al. reported the formation of a cerium metal acetylide complex $[Cp^*_2CeC{\equiv}CR]_n$ where R = Me, ^{t}Bu with a bridging RC_4R moiety, [33] scheme 35. A reversible carbon-carbon coupling within the acetylide complex was found to occur with the early lanthanide derivatives at ambient temperature. The size of the metal was found to have a significant effect on the overall reaction. The acetylide intermediate complex of the smaller samarium metal, $[Cp^*_2SmC{\equiv}CR]_n$ was not observed despite the isolation of the carbon-carbon coupled product, $[Cp^*_2Sm]_2(\mu\text{-}\eta^2{:}\eta^2PhC_4Ph)$.

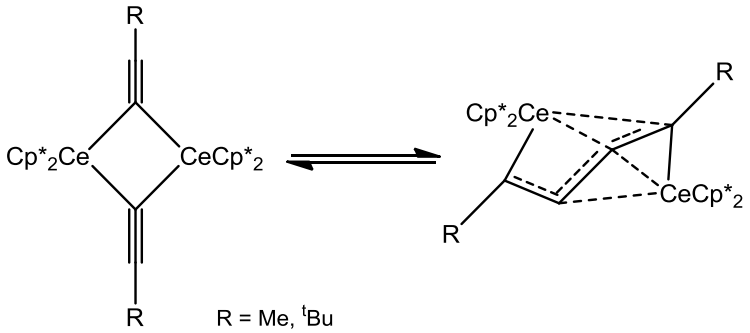

Scheme 35: Cerium metal acetylides couple to give a bridging RC_4R complex. [33]

Berg et al. [36] explored the coupling reaction by the replacement of the established two Cp^* ligands by a single deprotonated macrocycle 4,13-diaza-18-crown-6 ligand, DAC, in the yttrium metal complex $(DAC)Y(CH_2SiMe_3)$. The DAC ligand was found to be sterically equivalent to the two Cp^*, however the electronic structure was considerably different with the DAC ligand able to donate electrons to the metal centre giving the complex more flexibility. The results indicated that changing the ligand on the metal catalyst had an overall effect on the coupled butatriene complex with the more flexible DAC ligand resulting in the formation of the *(Z)*-butatriene unit and the Cp^* system favouring the *(E)*- isomer.

Although ligand coupling reactions by reductive elimination is an important process in transition metal-based catalysis, it is not the case in organolanthanide chemistry. For simple reductive elimination to be successful the complexes need to have access to 2-electron-redox couples. However this was not observed for bimetallic complexes of $[(C_5R_5)_2Ln](\mu\text{-}R')(\mu\text{-}R'')[Ln(C_5R_5)_2]$ where R = H, Me and R', R'' = alkyl, aryl, hydride, halide and pseudohalide ligands, due to the coupling being electrostatically

inhibited by the partial negative charge on the R groups as it co-ordinates to the electropositive lanthanide metal.

Marks et al. [37] proposed that the coupling of acetylenes was not restricted to those metals that change oxidation states as the reaction may proceed via an insertive pathway. Although those metals that undergo a ±1 oxidation change are not as common while further oxidation change of ±2 are not as well documented. Following analysis of ^{1}H NMR data Marks challenged the isomerisation proposed by Evans [34a] and the use of the redox-active lanthanide metal centre with the addition of phenylacetylene to $Cp^*_2LaCHTMS_2$ (equation 10). NMR and X-ray data showed the product to be a dimeric C-C coupled structure that does not require the involvement of the redox-active lanthanide proposed by Evans.

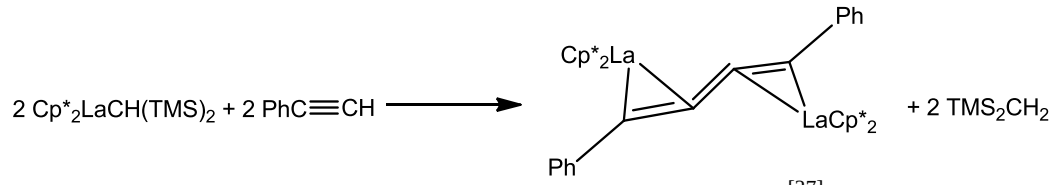

Equation 10: Insertive acetylene coupling. [37]

1.10 Carbodiimide insertion chemistry

Zhou and co-workers [38a] prepared a series of novel dianionic diguanidinate binuclear and polynuclear lanthanide complexes by carbodiimide insertion to a bifunctional amido lanthanide complex producing a new monomeric complex with two guanidinate linkages, [38b] scheme 36.

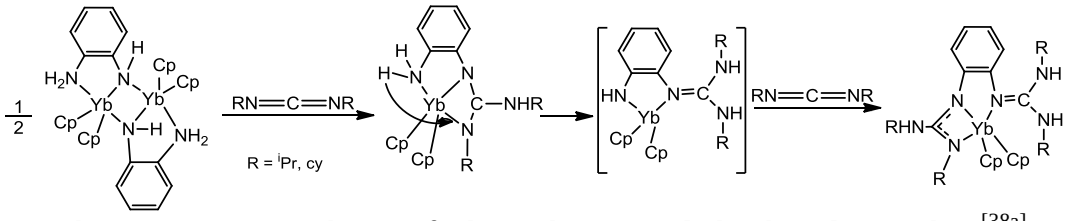

Scheme 36: Diguanaylation of a heterolpetic amido lanthanide complex. [38a]

Zhou proposed that the symmetrically bridging ligands would allow the addition of two different carbodiimide molecules, scheme 37. [38a]

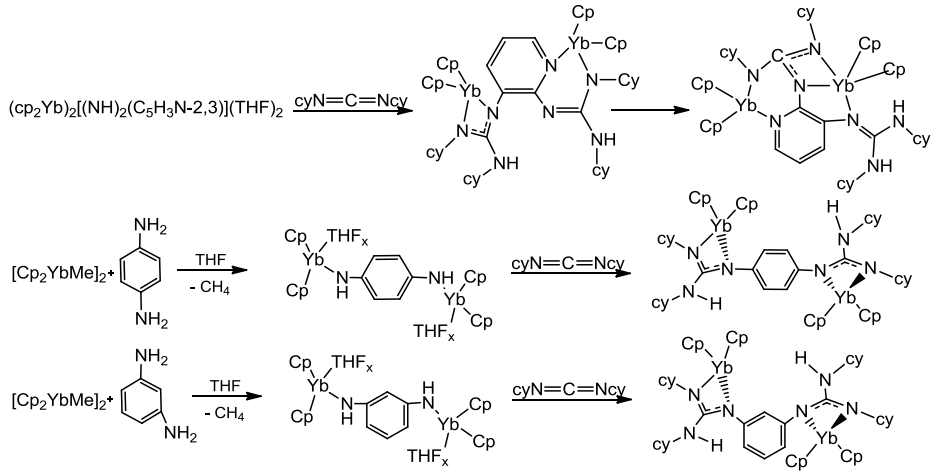

Scheme 37: Insertion of carbodiimide molecules to Yb complex with different amido bridging units. [38a]

Zhang et al. [39] studied the insertion of a carbodiimide to anthranilontrile and the effects of the substituents on the organolanthanide amide, $Cp_2LnN^iPr(THF)$. The intermolecular nucleophilic addition/cyclisation of the anthranilontrile reported by Zhang was found to significantly reduce the harsh conditions required for the reaction to proceed due to the presence of the Lewis acid moiety on the organolanthanide complex. In 2010 Zhang reported the first anionic bis(trimethylsilyl)amide lanthanide complex. [40] The Ln-C σ-bond of the complex was shown to be more reactive than the Ln-N bond, scheme 38.

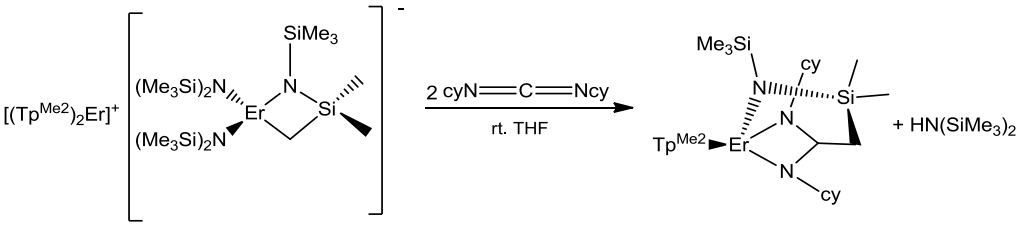

Scheme 38: Carbodiimide inserts into the more active Er-C bond rather than the Er-N bond. [40]

Lee and co-workers studied the formation of lanthanide (II) bis(amidinate) complexes [41] by chelating four membered metallacyclic rings (MNCM) with the sterically bulky 2,6-diisopropylphenyl substituted $[PhC(NSiMe_3)(NC_6H_3{}^iPr_2\text{-}2,6)]^-$ ligand. The MNCM ring was formed by the nucleophilic addition of C≡N groups of benzonitrile and the migration of the $SiMe_3$ group. Addition of a carbodiimide to samarium bis(amidinate) resulted in the co-ordination and formation of a mononuclear, mixed-ligand tri(amidinate) complex. [42]

Shen and co-workers extended their work to the activation and transformation of a carbodiimide with the Ln-O group of $Ln(OAr)_3(THF)_2$ where Ln = lanthanide, yttrium. [43] Results indicated that large bulky substituents on the aryloxide afforded the co-ordinated carbodiimide product while smaller substituents did not, scheme 39.

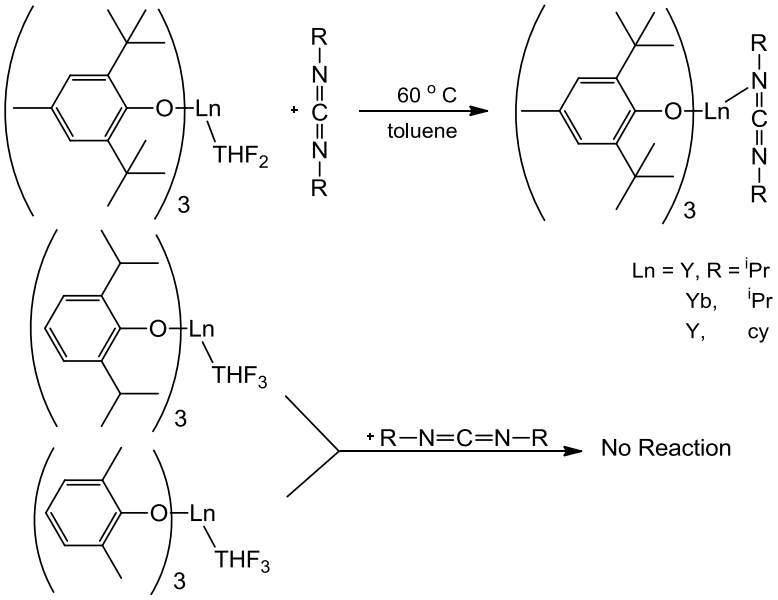

Scheme 39: Reaction of $Ln(ArO)_3(THF)_3$ with a carbodiimide. Large bulky (OAr) groups produce the product while no reaction is observed for the smaller (OAr) substituents. [43]

As pre-catalysts in organic synthesis divalent lanthanide complexes have been proven efficient reagents at single-electron transfer. This therefore led to Shen and co-workers [**44**] adopting these complexes to employ as catalysts in the addition of both N-H and C-H bonds to a carbodiimide. The divalent formula is given as $LnL_2(THF)_n$ where L = $N(SiMe_3)_2$, n = 3; L = MeC_5H_4, n = 2; L = ArO, Ar = [2,6-(^{t}Bu)$_2$-4-MeC_6H_2], n = 2. The lanthanide reactivity is found to increase Yb<Eu<Sm. Comparisons between the divalent complex to the trivalent lanthanide amide complex found the divalent complex to be the most reactive.

Although carbodiimides efficiently insert into primary aliphatic amines during guanalation, [45b] secondary and aromatic amines do not. However under catalytic conditions lithium bis(trimethylsilyl)amide $LiN(SiMe_3)_2$, will catalyse the intermolecular hydroamination of aromatic amines and carbodiimides [45c] while the yttrium alkyl complex $\{Me_2Si(C_5Me_4)(NR)\}Y(CH_2SiMe_3)(THF)_n$ will catalyse the guanylation of secondary and aromatic amines. [45d] Wang and co-workers [45a] reported

the efficient guanylation of both secondary and aromatic amines and the formation of propiolamidines with terminal acetylenes by employing the lanthanocene amido complex [ethylenebis(η^5-indenyl)][bis(trimethylsilyl)amido] lanthanide (III) complexes (EBI)LnN($SiMe_3$)$_2$, Ln = Y, Sm, Yb with σ-bond metathesis to produce the amido intermediate complexes before the insertion of the carbodiimide to the guanidinate and amidinate species, scheme 40.

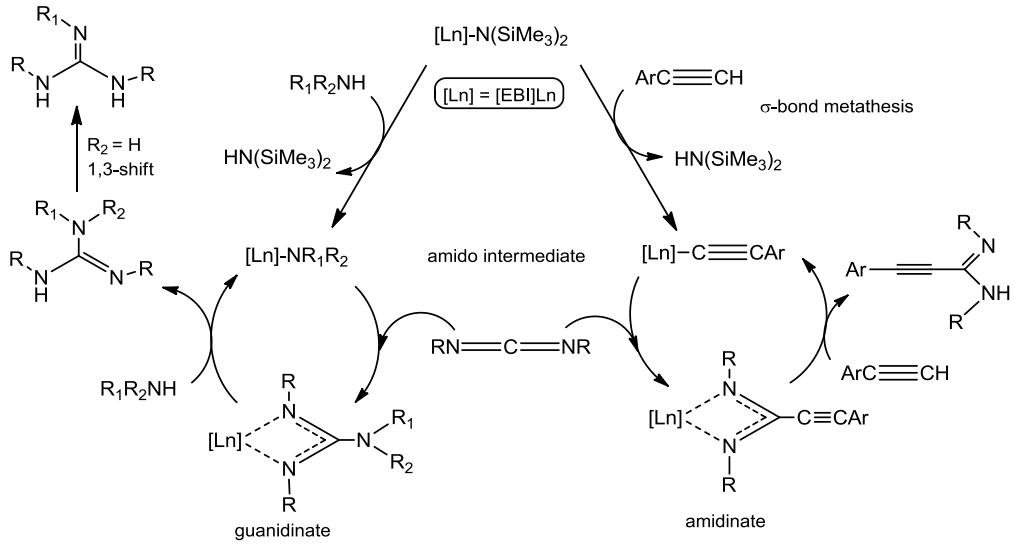

Scheme 40: Catalytic guanylation of N-H and C-H bonds to a carbodiimide with [ethylenebis(η^5-indenyl)][bis(trimethylsilyl)amido] lanthanide (III) complexes (EBI)LnN($SiMe_3$)$_2$. [45a]

In 2005 Harder et al. reported two synthetic routes for the formation of both homoleptic calcium and strontium bis(guanidinate) complexes. [46] The most efficient synthetic route follows the direct addition of the carbodiimide to the homoleptic [Ae{N($SiMe_3$)$_2$}$_2$] while the indirect approach involves adding the carbodiimide to the potassium hexatrimethylsilyl amide followed by the addition of the metal iodide, scheme 41.

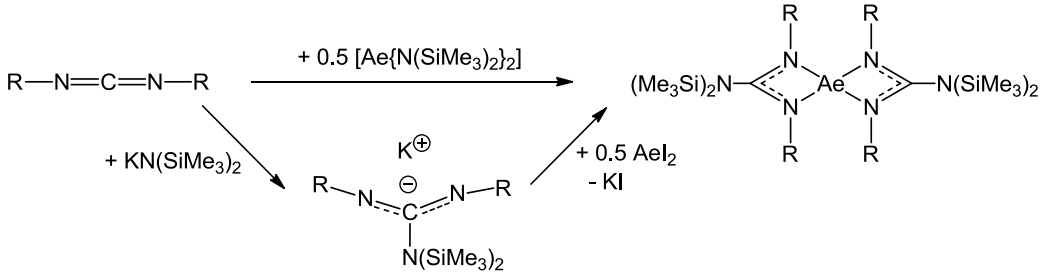

Scheme 41: Direct and indirect diguanylation of a carbodiimide with an alkaline earth metal catalyst. [46]

1.10.1 Catalytic carbodiimide insertion chemistry: guanylation

$ZnEt_2$, $MgBu_2$ and ^nBuLi are efficient at the guanylation of a range of primary and secondary aromatic and heterocycle amines regardless of the substituents on the aromatic. Aluminium compounds, $AlMe_3$ reported by Zhang and co-workers [47] were found to be active for the guanylation of primary amines while Richeson et al. [48] reported a less efficient titanium-imido complex $[\{(Me_3N)C(N^iPr)_2\}_2Ti{=}N(2,6\text{-}Me_2C_6H_4)]$ from the guanylation of aromatic and heterocyclic amines with a lithium hexamethyldisilazide

Hou and co-workers [13] reported the catalytic addition of a number of primary, secondary and aromatic amines to a half-sandwich lanthanide alkyl guanidinate complex. The reaction was not affected by the electron-withdrawing or –donating substituents on the aromatic ring with each reaction producing a free guanidine complex at more than 96 % yield, table 9.

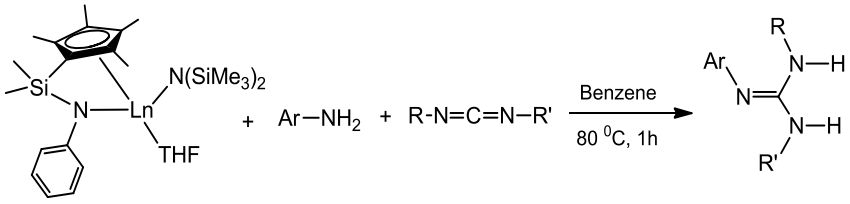

Ar	R	R’	Yield %
Br	^{i}Pr	^{i}Pr	>99
I	^{i}Pr	^{i}Pr	>99
NC	cy	cy	96
	^{i}Pr	^{i}Pr	>99
Cl	^{i}Pr	^{i}Pr	>99
F	^{i}Pr	^{i}Pr	>99
OMe	^{i}Pr	^{i}Pr	>99
	Et	^{t}Bu	96

Table 9 Catalytic addition of various primary anilines to carbodiimide. [13]

The addition was found to be selective with regards to the reactivity between the primary and secondary amines. Since the primary amines are more reactive than the secondary amines, the addition was found to favour the primary amine leaving the secondary moiety unaffected. However further addition occurred at the secondary amine resulting in a diguanidinate complex, scheme 42, while reaction with a teriary amine subsequent yields a triguanidinate complex.

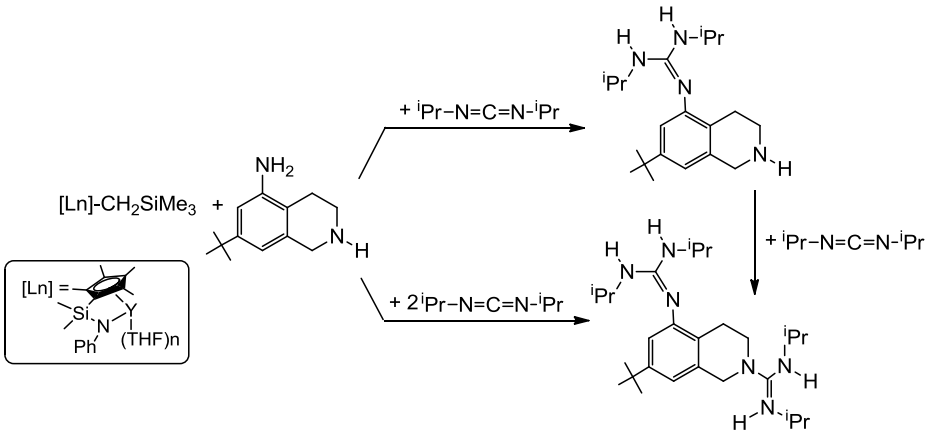

Scheme 42: Stepwise catalytic addition of 1,2,3,4-tetrahydro-5-amino isoquinodine to a half-sandwich yttrium metal guanidinate complex. [13]

In 2009 Shen and co-workers [49] reported amine addition to a carbodiimide with the ytterbium triflate complex $Yb(OTf)_3$. Being the smallest of the lanthanides, Yb is shown to be the most active. Shen employed the catalyst to the addition of primary and aromatic amines. Although electron-withdrawing –donating groups did not affect the reaction, the size and increasing sterics of the substituents on the aromatic amines decreased the activity.

Guanylation of carbodiimides with $Zn(OTf)_2$ [50] and a copper iodide complex [51] scheme 43, have been reported as a one-pot synthesis by Zhang and Xi respectively while Mashima and co-workers [52] reporting the diguanylation of a homoleptic titanium tetrakis(amide) complex.

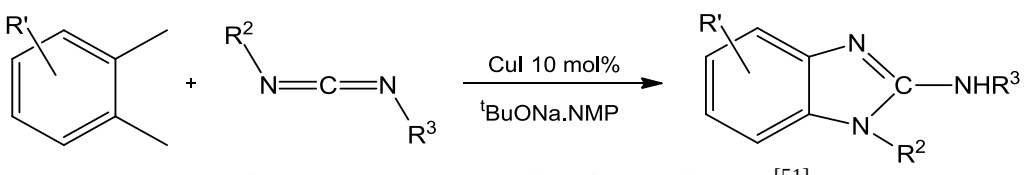

Scheme 43: Copper catalysed guanylation. [51]

Hill and co-workers [9, 10] employed the heteroleptic β-diketiminate calcium amide for the catalytic and stoichiometric guanylation of a carbodiimide resulting in both the β-diketiminate ligand and the guanidinate ligand co-ordinating to the calcium metal, scheme 44. The presence of the β-diketiminate ligand ensured the stability of the complex towards Schlenk-type redistribution.

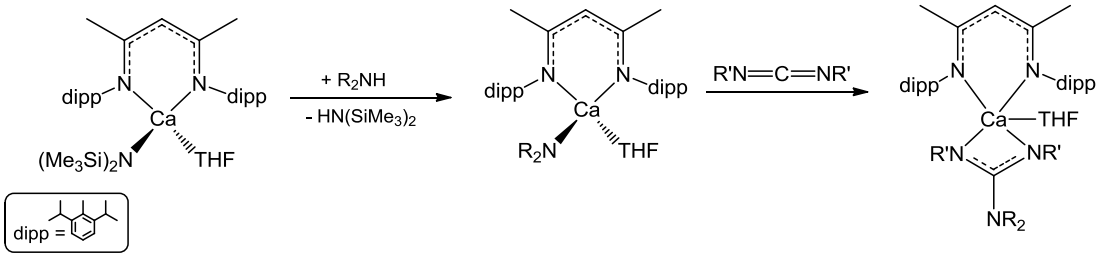

Scheme 44: Synthesis of heteroleptic calcium amide and its reaction with 1,3-carbodiimides. [9]

Hill carried out the work with a series of amines and 1,3-carbodiimides. [9] The catalytic results indicated the reaction to be dependent upon the sterics of the amine and carbodiimide with bulky *tert*-butyl groups on the carbodiimide preventing the co-ordination to the calcium metal with a 0 % conversion even at elevated temperatures of 80 ^{o}C, whereas the smaller, less demanding *iso*-propyl and cyclohexyl groups produced more than 95 % conversion at 25 ^{o}C. The increased steric demands of the amine crowded the calcium metal and prevented co-ordination.

1.10.2 Catalytic carbodiimide insertion chemistry: phosphoguanylation

The catalytic activity in the addition of a phosphine to a carbodiimide is determined by the size of the lanthanide metal employed. While the large lanthanide metals produce high catalytic yields, the lanthanide contraction across the lanthanide period not only reduces the size of the metal but also the final catalytic yield. Hou and co-workers reported the addition of diphenylphosphine to a variety of lanthanide catalysts [13] and found the larger lanthanide ion, La, to be the most productive with a yield of more than 99 % of the phosphoguanidinate whilst the smallest ion, Sc, only yielded 15 %, table 10.

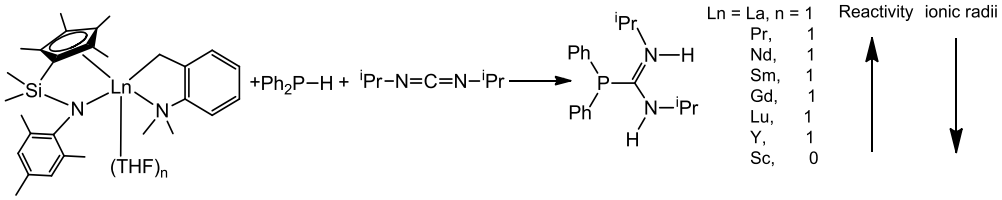

Cat Ln	Ionic radius	Time/h	Yield %
Sc	0.745	1	15
Y	0.900	1	86
Lu	0.861	1	50
Gd	0.938	1	65
Sm	0.958	1	69
Nd	0.983	1	93
Pr	0.990	0.5	94
La	1.032	1	>99

Table 10: Catalytic addition of diphenylphosphine to a 3 mol% lanthanide o-dimethylaminobenzyl alkyl phosphoguanidinate complex at 80 ^{o}C. [13]

Hill and co-workers continued their work on group 2 metals with phosphoguanylation catalysis with the heteroleptic β-diketiminate calcium amide **C1** and the homoleptic calcium, strontium and barium bis(bis(trimethylsilyl)amides) **C3-5** on both catalytic and stoichiometric scales. Following the successful results with the heteroleptic β-diketiminate calcium amide **C1**, Hill expanded the work to the homoleptic calcium, strontium and barium bis(bis(trimethylsilyl)amides) **C3-5** with a range of phosphines and carbodiimides, scheme 45. ^{1}H and ^{31}P NMR spectroscopy were employed to deduce the phosphoguanidinate yield, table 11, with the phosphine initiating the catalysis. [11]

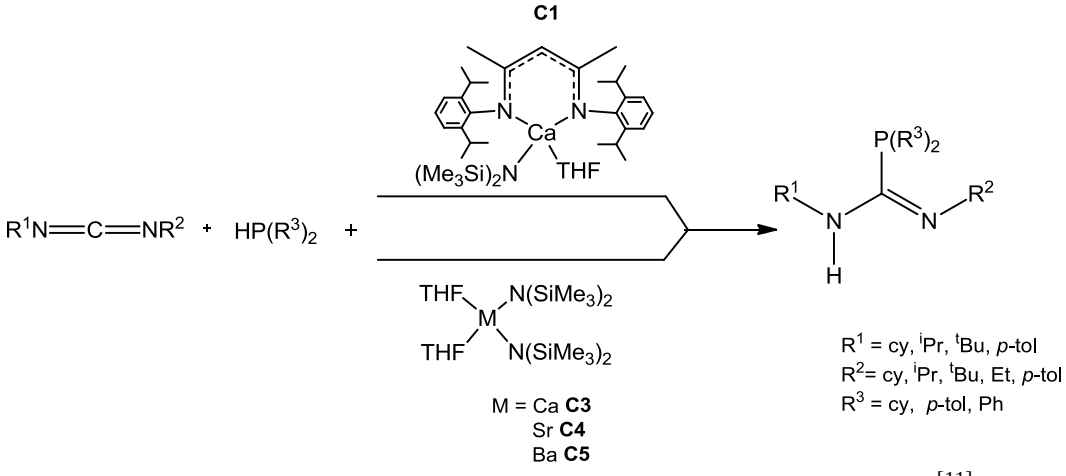

Scheme 45: Intermolecular hydrophosphination of carbodiimide. [11]

entry	R^1	R^2	R^3	Cat	mol %	T (^oC)	t (h)	% yield
1	cy	cy	Ph	**C1**	1.5	25	28	85
2	cy	cy	Ph	**C3**	3	25	4	>95
3	cy	cy	Ph	**C4**	2	25	0.5	>99
4	cy	cy	Ph	**C5**	2	25	0.5	>95
5	^{i}Pr	^{i}Pr	^{i}Pr	**C1**	1.5	25	6	>99
6	^{i}Pr	^{i}Pr	^{i}Pr	**C4**	2	25	0.5	>99
7	^{t}Bu	^{t}Bu	Ph	**C4**	5	60	16	0
8	^{t}Bu	Et	Ph	**C4**	2	25	0.25	>95
9	*p*-tol	*p*-tol	*Ph*	**C4**	2	25	12	68
10	^{i}Pr	^{i}Pr	*p*-tol	**C4**	10	25	0.25	>95
11	^{i}Pr	^{i}Pr	cy	**C4**	5	60	16	0

Table 11: Intermolecular hydrophosphination of carbodiimide. [11]

The results suggested the homoleptic species *(entries 2-4)* to be more productive than the heteroleptic derivate *(entry 1)* with an increased conversion of 10 %. While reducing the steric hinderance exerted by the larger cy R groups, *(entry 1)* with the smaller ^{i}Pr groups, *(entry 5)* was found to reduce the reaction time of the heteroleptic **C1** derviate by 22 hours.

1.10.3 Catalytic carbodiimide insertion chemistry: amidination

Following the catalytic insertion of a carbodiimide forming a guanidinate species, Zhang and co-workers [53] employed the same principles in the formation of a propiolamidinate complex. Employing a half-sandwich lanthanide complex Zhang formed the acetylide intermediate from the addition of a terminal acetylene before introducing the carbodiimide. An excess of the terminal acetylene went on to yield the free amidine species, scheme 46 Zhang reported this process to be successful for a variety of terminal acetylenes and carbodiimides with the ligand on the lanthanide catalyst ensuring the overall stability of the complex and preventing the amidinate's tendency towards hydrolysis.

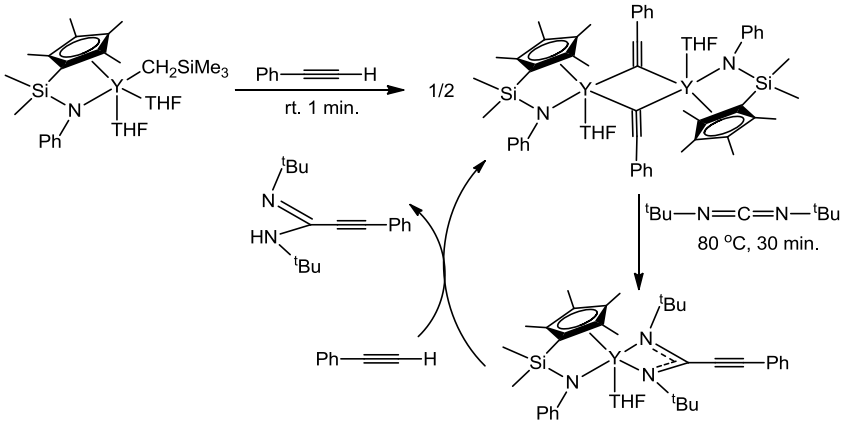

Scheme 46: Catalytic cycle for the insertion of a carbodiimide with a lanthanide metal catalyst. [53]

Hou and co-workers [13] reported the catalytic addition with a half-sandwich yttrium alkyl complex. Although the free amidine was not observed from the addition of a further phenyl acetylene equivalent in d_8-toluene at room temperature, increasing the temperature to 80 ^{o}C resulted in the liberation of the free amidine and regeneration of the acetylide, scheme 47. The reaction was found to be successful for a range of terminal acetylenes producing yields of more than 90 % irrespective of the presence or location of electron-donating or –withdrawing substituents on the phenyl ring of the aromatic acetylenes.

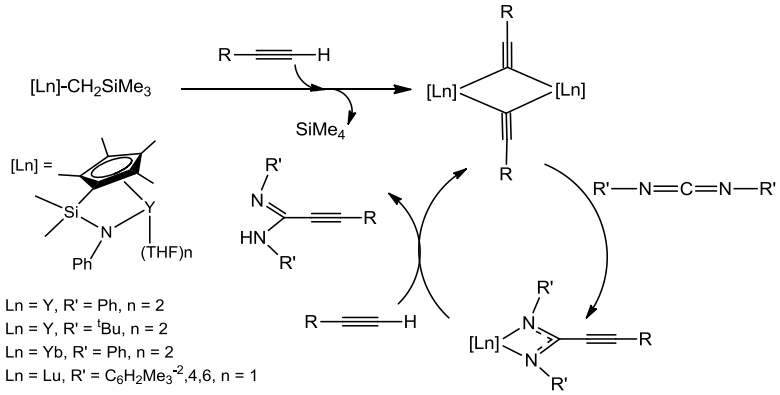

Scheme 47: Catalytic addition of a terminal acetylene to an amidinate complex. [13]

After the formation of the acetylide and the guanidinate and phosphoguanidinate complexes, Hill and co-workers attempted the insertion of 1,3-dialkylcarbodiimide into the calcium-carbon σ-bond. [19] The low solubility of the acetylide complexes in hydrocarbon solvents presented difficulties for performing the reaction. However they were overcome by a single one-pot homogeneous synthesis, scheme 48. The inserted

products were crystallised and characterised by ^{13}C NMR showing a resonance at 159.2 ppm for the central carbon of the amidinate moiety.

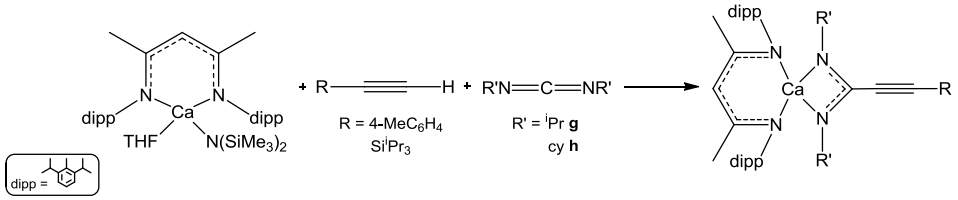

Scheme 48: Amidinate formation via the one-pot insertion of a carbodiimide. [19]

Following the isolation and characterisation of the inserted amidinate products via the stoichiometric addition to a carbodiimide, Hill continued the work to a catalytic scale. Similar to catalytic hydroamination and hydrophosphination of carbodiimides with the heavier group 2 metals, Hill reported a 5 mol catalytic loading of the heteroleptic β-diketiminate calcium amide **C1** with phenyl acetylene and 1,3-di-*iso*-propyl carbodiimide yielding 59 % amidine at 80 ^{o}C in 14 hours, scheme 49.

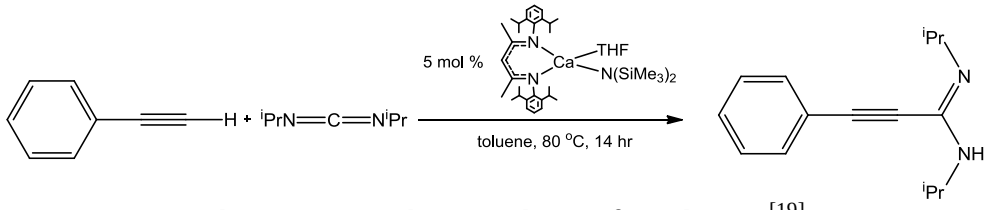

Scheme 49: Catalytic synthesis of amidinate. [19]

1.11 Aims and objectives

After considering the work discussed in this introductory chapter, the subsequent chapters of this thesis will develop and present an extension of the work with the employment of alkaline earth based complexes, **C1**-**9**. The work will centre around the hydroacetylation of terminal acetylenes, proving the catalytic cycle, scheme 50, by the isolation and characterisation of the intermediate acetylide and amidinate complexes formed via σ-bond metathesis and Markovnikov insertion of unsaturated C-C bonds respectively.

The next chapter of this thesis will prove the σ-bond metathesis of a series of terminal acetylenes with the formation of acetylide intermediate complexes. The acetylide

complexes will be isolated and characterised by NMR spectroscopy, elemental analysis and X-ray crystallography.

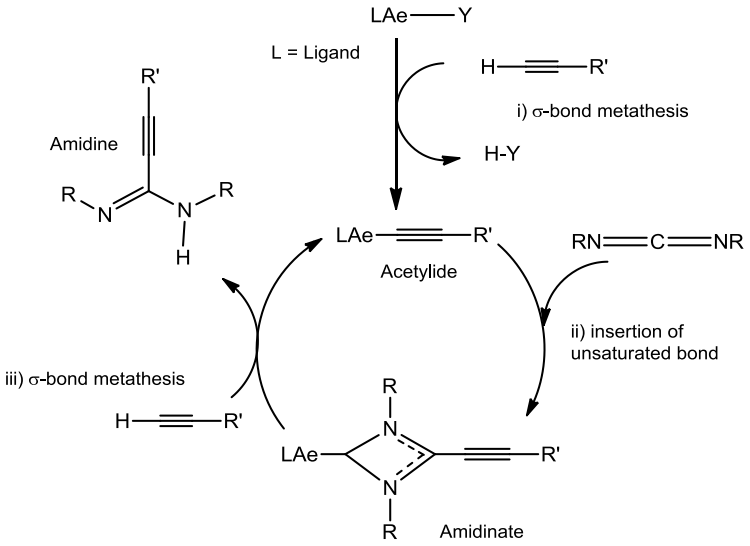

Scheme 50: Catalytic cycle with group 2 metal catalyst.

Both chapters 4 and 5 will discuss the second step of the catalytic cycle in scheme 50 with the insertion of an unsaturated bond to the acetylide complexes described in chapter 2. The insertion of both symmetric and asymmetric double bonds in the form of carbodiimides and an organic isocyanate will ensure the formation of the amidinate and amidate intermediates respectively.

Chapter 3 will discuss the results of an unexpected side reaction observed with the σ-bond metathesis of the donor-functionalised acetylenes, 3-dimethylamino-1-propyne **d**, methyl propargyl ether **e** and phenyl propargyl ether **f**, within the acetylene series employed in chapter 2. Although the acetylide complexes were obtained for all three donor-functionalised acetylenes, the X-ray structures indicated a difference in the final orientation when compared to the predicted orientation obtained from similar reactions. It was expected that the acetylide would insert as a symmetric bridge between the metals of a dimeric acetylide. However, the donor-functionalised acetylenes form an asymmetric bridge within the dimeric acetylide complex resulting in each bridging acetylide unit experiencing an attractive force towards the metal centres. The third chapter looks to explore this differing orientation and its contribution towards the re-distribution within the acetylide complex that results in the acetylides coupling to yield a butatriene derivative.

Chapter 2

2.0 Formation of group 2 acetylides

Following the successful hydroamination and hydrophosphination of a variety of unsaturated small molecules with the group 2 alkaline earth metal catalysts, Hill and co-workers extended this work to hydroacetylation and the addition of acidic alkyne C-H bonds across carbodiimides. This thesis describes the hydroacetylation of a variety of cumulenes with terminal acetylenes and the insertion of unsaturated double bonds via the formation of the intermediate acetylide complexes of the group 2 metals. Like hydroamination and hydrophosphination catalysis, related hydroacetylation reactions have previously been reported with lanthanide metal catalysts. [13a] The general lanthanide-catalysed cycle for the addition of a terminal acetylene to a carbodiimide, scheme 51, illustrates the formation of the lanthanide-acetylide intermediate as a key step in the overall hydroacetylation reaction.

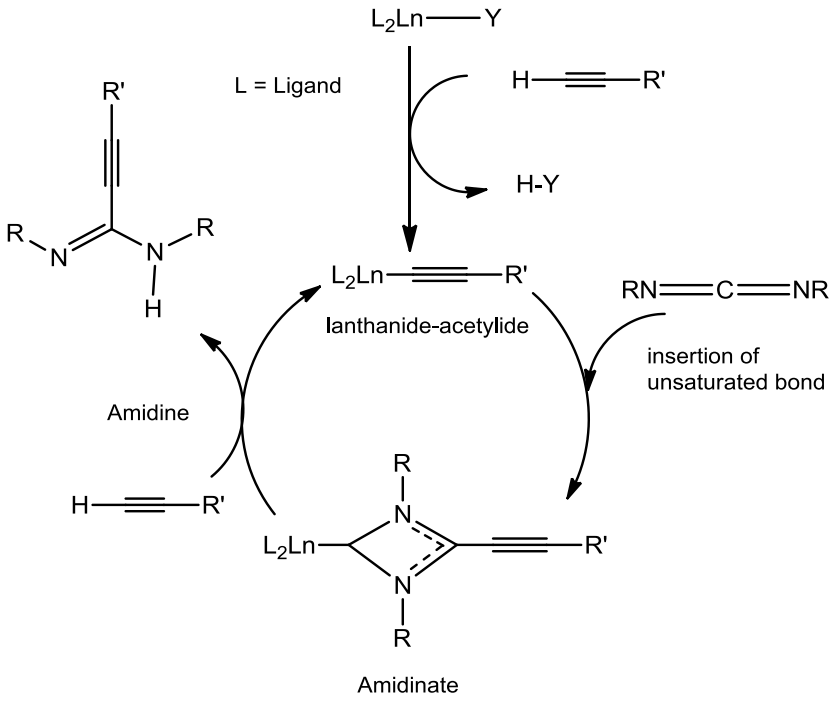

Scheme 51: General catalytic cycle with lanthanide metal catalysts.

Obtained as an isolated complex, acetylide intermediates may be identified via spectroscopic methods and X-ray diffraction analysis. The insertion of the unsaturated double bond assists in the catalysis with the formation of an amidinate intermediate complex and finally the free amidine product is liberated by protonation with a further equivalent of the acidic terminal acetylene in a process not too dis-similar to those of

the guanidinate and guanidine and the phosphoguanidinate and phosphoguanidine formation during the respective carbodiimide hydroamination and hydrophosphination reactions discussed in chapter 1.

Hill proposed the general catalytic cycle for the reaction with group 2 metals and the formation of the group 2-acetylide as the key intermediate, scheme 52, based upon that of the lanthanide metals.

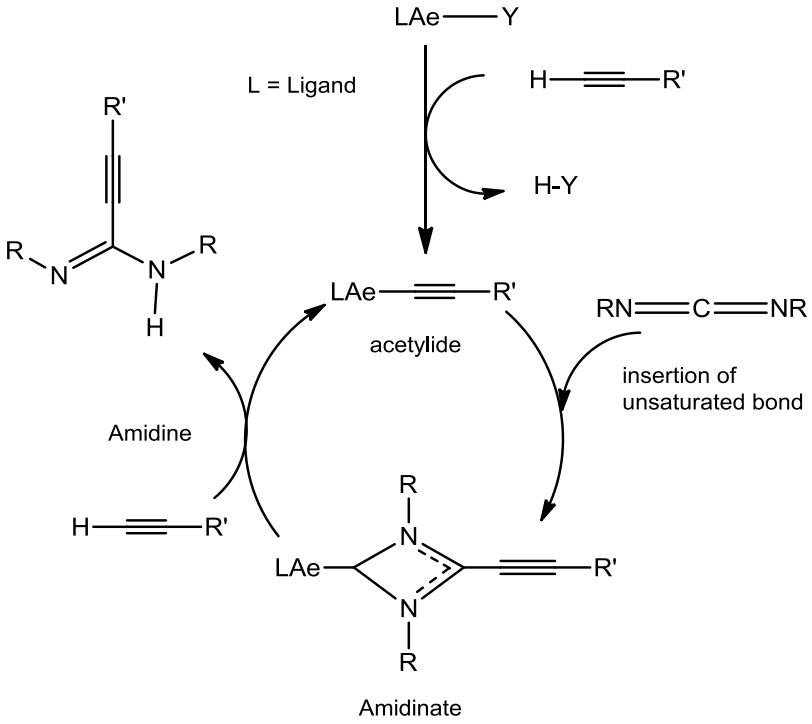

Scheme 52: General catalytic cycle with group 2 metal catalyst.

Following the work discussed in chapter 1 for the hydroamination, hydrophosphination and hydroacetylation catalysis, this chapter of the thesis will present a brief introduction of the formation of acetylide complexes with both the lanthanide and heavier group 2 metals before describing the synthesis and characterisation of a variety of heavier alkaline earth acetylide complexes.

2.1 Introduction

In 2005 Hill and co-workers [8] reported the formation and isolation of terminal dimeric group 2- acetylides by reaction with Chisholm's heteroleptic β-diketiminato calcium amide, **C1**, with a range of terminal alkyl and aryl acetylenes, scheme 53. The enhanced stability of these complexes resulted from an increase in the overall kinetic stability provided from the large bulky diketiminato ligand, **L1**, forming a bidentate chelate on the calcium metal centre.

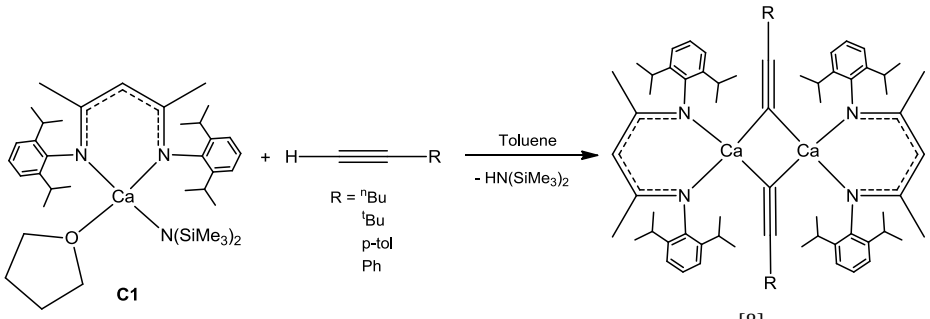

Scheme 53: Formation of dimeric acetylide. [8]

While being extremely air- and moisture-sensitive the acetylides all produced stable complexes with no tendency to re-distribute to insoluble homoleptic complexes hence inhibiting further reaction, scheme 54.

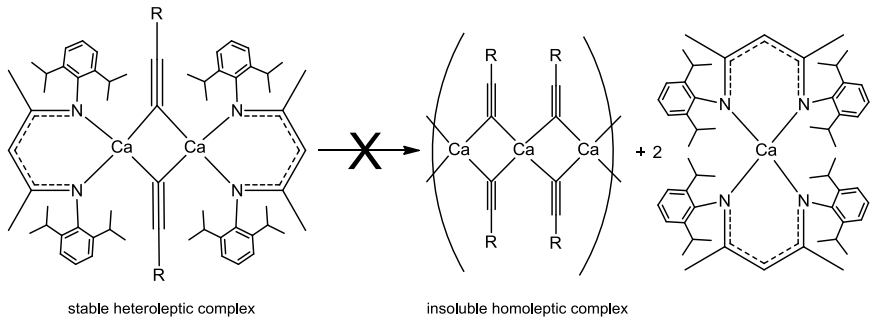

Scheme 54: Stable heteroleptic complex does not re-distribute to the insoluble homoleptic complex.

This chapter will describe the synthesis of a variety of novel calcium acetylides employing phenyl acetylene **a**, tri-*iso*-propylsilyl acetylene, **b**, ethynyl ferrocene, **c**, [54] 3-dimethylamino-1-propyne **d**, methyl propargyl ether **e** [55] and phenyl propargyl ether **f**, figure 11.

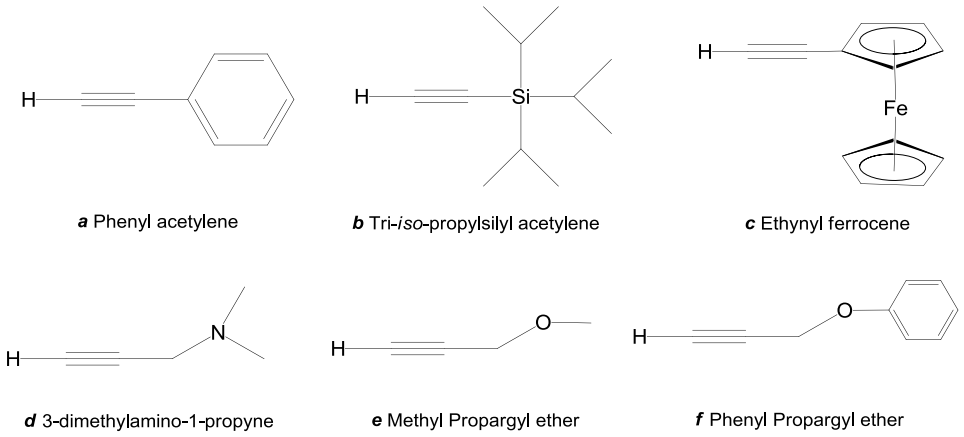

Figure 11: Terminal acetylenes employed in this study.

2.2 Synthesis

2.2.1 [CH{C(Me)N(2,6-$^{i}Pr_2C_6H_3$)}$_2$H] (nacnac) **L1** [12]

Proven to play an important role in the kinetic stability of the air- and moisture sensitive group 2 catalysts, the ligand precursor **L1** itself is air stable and is prepared via an acid-catalysed condensation of 2,6-di-*iso*-propylaniline and 2,4-pentadione followed by separation with dichloromethane, scheme 55. After re-crystallisation from ethanol the nacnac ligand **L1** was identified by ^{1}H NMR spectroscopy displaying a distinctive singlet resonance at 4.76 ppm of the γ-H on the carbon backbone chain. This methine resonance is an important feature of the nacnac ligand **L1** that is also present when the ligand is deprotonated when co-ordinated to a group 2 metal. Other notable resonances are the two doublets at 0.99 and 1.09 ppm that result from the *iso*-propylmethyl protons on the 2,6-di-isopropylphenyl substituents of the ligand and the singlet resonance for the N-H group. This resonance is important as it is absent when the ligand has co-ordinated to a metal.

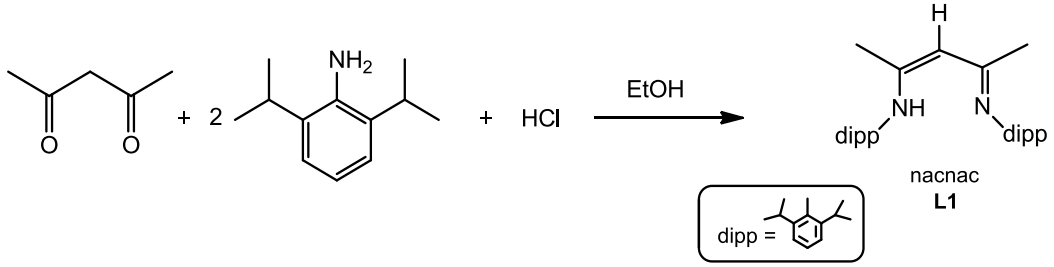

*Scheme 55: Formation of the nacnac ligand **L1**.* [12]

2.2.2 [CH{C(Me)N(2,6-$^{i}Pr_2C_6H_3$)}$_2$H]Ca(N(SiMe$_3$)$_2$(THF) **C1** [2]

The air- and moisture sensitive pre-catalyst **C1**, was prepared and kept under an atmosphere of nitrogen as shown in scheme 56. **C1** was crystallised from hexane at -30 ^{o}C and was identified by ^{1}H NMR spectroscopy. The ^{1}H NMR spectrum for **C1** is similar to that obtained for **L1** except for the absence of the N-H resonance as the H protonates the N(SiMe$_3$)$_2$ anion to HN(SiMe$_3$)$_2$ during the co-ordination of the calcium centre while other notable and useful diagnostic resonances for the γ-H and the *iso*-propylmethyl protons of the 2,6-di-*iso*-propylphenyl substituents of the ligand experience down-field shifts resonating at 4.83 ppm for the γ-H and 1.22 and 1.33 ppm respectively.

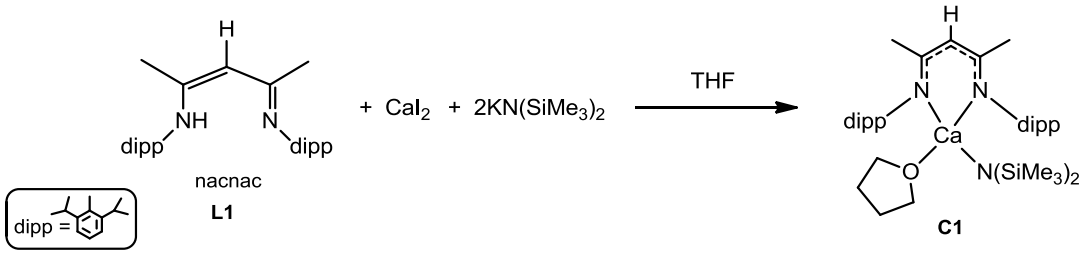

*Scheme 56: Formation of **C1**.* [2]

2.2.3 Acetylide synthesis [19]

A series of β-diketiminato calcium acetylides, **1**-**5** were synthesised by addition of the appropriate terminal acetylene to a stoichiometric quantity of **C1** in toluene at room temperature. The acetylide synthesis was carried out under a nitrogen atmosphere using Schlenk techniques due to the air- and moisture-sensitivity of the compounds. A 1:1 ratio of **C1** and the requisite acetylene were dissolved separately in toluene before reaction. The resultant acetylides crystallised readily after concentration of the toluene solution and storage at -30 ^{o}C and were predicted to form a symmetrical dimeric acetylide complex by analogy with earlier reported complexes, scheme 57.

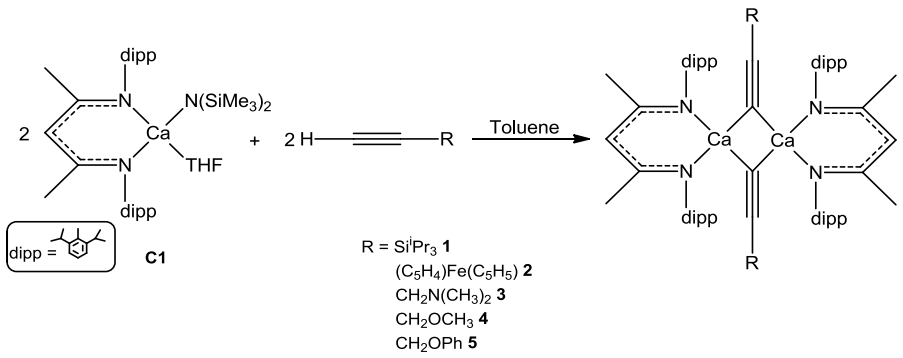

*Scheme 57: Heteroleptic β-diketiminato calcium complex **C1** and the formation of symmetrical dimeric acetylide complexes **1**-**5**.* [19]

2.3 Acetylide characterisation by elemental analysis and NMR spectroscopy

The acetylide products **1**-**5** were crystallised from a concentrated toluene solution at -30 ^{o}C under an atmosphere of nitrogen. Not all of the reactions produced a crystalline product suitable for X-ray crystallography but could be isolated as white/yellow powders. Characterisation was carried out for all of the acetylide products after filtration and drying under vacuum. The initial characterisation of the newly formed acetylide compounds was achieved with both ^{1}H and ^{13}C NMR spectroscopy and the deduced formulations were supported by elemental analysis.

The elemental analysis data for compounds **1**-**5** is displayed in table 12 and was found to be consistent with the expected formulation of the THF-free dimeric acetylide complexes illustrated in scheme 57.

Compound	**1**		**2**		**3**		**4**		**5**	
Formula	$C_{80}H_{124}Ca_2N_4Si_2$		$C_{82}H_{100}Ca_2Fe_2N_4$		$C_{65}H_{98}Ca_2N_6$		$C_{66}H_{94}Ca_2N_4O_2$		$C_{76}H_{96}Ca_2N_4O_2$	
Molc wt.	1278.89		1333.54		1078.71		1053.62		1177.76	
% yield	26		60		72		74		69	
	Calc	Found	Calc	Found	Calc	Found	Calc	Found	Calc	Found
% C	75.17	74.99	73.85	73.79	75.64	75.62	75.24	75.17	77.50	77.42
% H	9.78	9.82	7.56	7.56	9.15	9.16	8.80	8.94	8.22	8.34
% N	4.38	4.45	4.20	4.14	7.78	7.69	5.32	5.27	4.76	4.64

*Table 12: Elemental analysis data for compounds **1**-**5**.*

The ^{1}H NMR spectra indicated the acetylide formation with the complete consumption of the terminal acetylene. The acetylide ligand co-ordinated as a result of the protonation of the $N(SiMe_3)_2$ group on the metal catalyst with the acidic terminal H of the acetylene. The protonation was observed to occur practically instantaneously for all of the acetylides **1**-**5**.

The ^{1}H NMR resonances of the γ-H and *iso*-propylmethyl protons of the acetylide compounds **1**-**5** are presented in table 13. The ^{1}H NMR resonance of the *iso*-propylmethyl protons on the dipp group of acetylide complexes **1**-**5** exhibited slight up-field shifts when compared to the 1.22 and 1.33 ppm resonances observed for the β-diketiminate calcium amide **C1**. The 4.83 ppm resonance observed from the γ-H of **C1** exhibited an up-field shift for compounds **1**, **2**, and **4** while compounds **3** and **5** experienced a down-field shift.

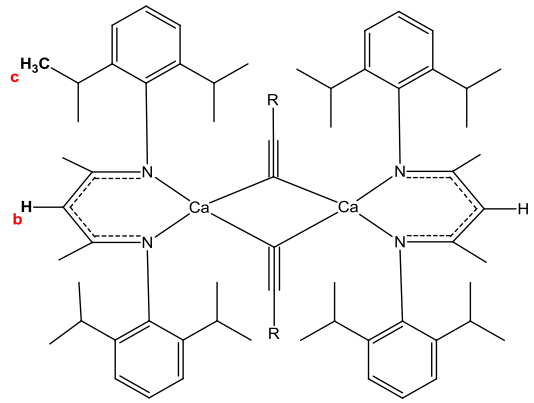

1-5

Compound	b (γ-H)	c (^{i}PrCH$_3$)
1	4.74	1.20 and 1.22
2	4.50	1.00 and 1.11
3	4.88	1.14 and 1.20
4	4.60	1.12 and 1.19
5	4.88	1.13 and 1.19

*Table 13: ^{1}H NMR shifts in ppm for the γ-H and iso-propylmethyl protons of acetylides **1**-**5**.*

The dimeric acetylides form with two bridging C≡C units between the metal centres. These carbon units are clearly identified in the ^{13}C{^{1}H} NMR spectra with all of the acetylides exhibiting similar down-field shifts compared to those observed in the

corresponding free acetylenes, table 14. The difference in shifts results from the change in the electron density of the complex. The co-ordination of the donor-functionalised acetylides experience the greatest shift due to the presence of the electon-donating nitrogen and oxygen atoms and its ability to re-distribute the overall electron-density across the bridging unit. Although the carbon nuclei in compounds **1-5** are deshielded, the compounds containing nitrogen and oxygen donor atoms **3-5**, exhibit a stronger interaction with the calcium metal centre that is not only indicated by a stronger down-field shift in the ^{13}C NMR spectra, but also by the interaction observed in the asymmetric X-ray structures.

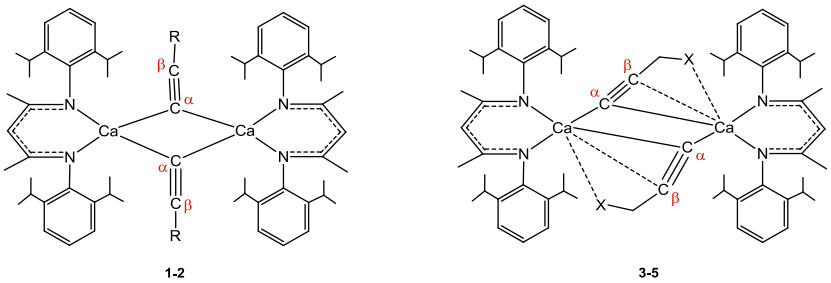

Acetylene			Acetylide		
Compound	α-C	β-C	α-C	β-C	Compound
b	85.9	95.6	96.0	100.8	**1**
c	82.1	93.0	91.6	99.4	**2**
d	83.0	93.7	92.0	102.8	**3**
e	84.9	97.8	93.4	105.6	**4**
f	85.1	97.9	94.3	106.3	**5**

*Table 14: ^{13}C NMR shifts in ppm of the α-C and β-C of acetylides **1-5** show a down-field shift when compared to the α-C and β-C shifts observed for their respective acetylenes **b-f**.*

The structures of the dimeric acetylide complexes **1** and **2** form a four centred Ca-C-Ca-C symmetrical bond and are analogous to those reported previously by Hill and co-workers. [19] This section will therefore concentrate upon the asymmetric dimeric four centred Ca-C-Ca-C bond acetylide complexes **3**, **4** and **5** formed from acetylenes containing the nitrogen and oxygen donor groups, **d**, **e** and **f**, figure 12.

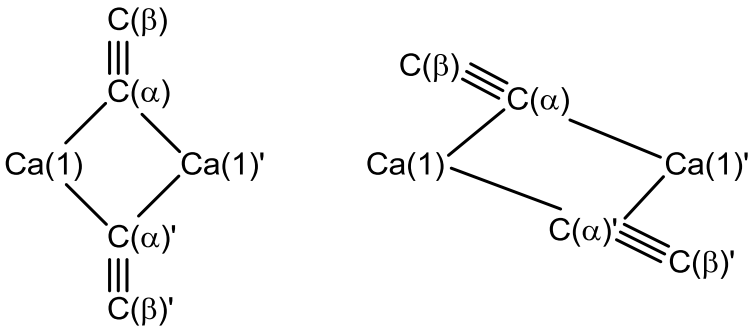

symmetrical acetylide **1**, **2**

asymmetrical acetylide **3**, **4**, **5**

Figure 12: Symmetric and asymmetric dimeric acetylide structures.

The molecular structures of compounds **3**, **4** and **5** are shown in figures 13, 14 and 15 respectively while the selected bond lengths and angle data in table 15 support the formation of the asymmetric structures with comparison with the symmetric acetylide complex formed from reaction of **C1** and phenyl acetylene. As with the previous reported complexes, each structure is dimeric with the acetylide unit providing a μ^2-Ca-C-Ca bridging interaction.

Bond lengths (Å)	**{(nacnac)Ca(CCPh)}$_2$**	**3**	**4**	**5**
Ca(1)-C(α)	2.5056(16)	2.505(2)	2.668(3)	2.6790(17)
Ca(1)'-C(α)	2.5350(16)	2.536(2)	2.497(3)	2.4851(19)
Ca(1)-C(β)	-	2.866(2)	2.721(3)	2.7287(17)
C(α)-C(β)	1.224(2)	1.214(3)	1.221(4)	1.26(3)
Ca(1)-O(1)	-	-	2.5063(18)	2.7413(12)
Bond angles (°)				
C(α)-Ca(1)-C(α)'	89.70(5)	89.23(7)	81.60(10)	78.19(6)
Ca(1)-C(α)-Ca(1)'	90.30(5)	90.77(7)	98.40(10)	101.81(6)
Ca(1)-C(α)-C(β)	172.85(13)	176.3(3)	79.34(18)	79.30(11)
Ca(1)'-C(α)-C(β)	96.68(11)	92.87(16)	172.0(3)	175.01(18)
Ca(1)-C(β)-C(γ)	-	178.7(3)	96.06(17)	102.09(10)
C(α)-C(β)-C(γ)	178.04(13)	178.7(3)	170.5(3)	176.53(19)

C(α) refers to C1 in **3** and C30 in **4** and **5**.
C(β) refers to C2 in **3** and C31 in **4** and **5**.
nacnacCa(CCPh)$_2$ *previously reported by Hill.* [19]

Table 15: Bond lengths and bond angles.

Hill reported the formation of the symmetric dimeric acetylide from reaction of **C1** and phenyl acetylene **a**, [19] in which the bridging bond lengths between the two different calcium metal centres and the bridging α-C, Ca(1)-C(α) 2.5056(16) Å and Ca(1)'-C(α) 2.5350(16) Å differ by only 0.03 Å. However the corresponding bond lengths observed in compounds **4** and **5** indicate the asymmetric bridging of the acetylide units as the C(α) of both compounds express a higher affinity towards the calcium centre denoted Ca(1)', therefore reducing the Ca(1)'-C(α) bond length by almost 0.2 Å. Consequently the Ca(1)-C(α) bond length experienced an equivalent degree of elongation. This shift in bond length produces an asymmetric acetylide that enables further interactions between the β-C and the oxygen atoms of the compounds **4** and **5** with the nearest calcium metal centre. Interestingly, despite compound **3** producing similar bond lengths to that of the phenyl acetylide [19] with a difference around .03 Å between the two calcium metals and the α-C, a bond between the calcium metal and the β-C was observed, Ca(1)-C(β) 2.866(2) Å. However there is no interaction between either caclcium metal and the nitrogen atom, presumably due to the increased steric demands of the two methyl groups of the NMe_2 substituent.

For compounds **4** and **5**, figures 14 and 15, a secondary intermolecular interaction is provided by co-ordination of the OR donors (**4**, R = Me; **5**, R = Ph). This interaction is shown to effectively pull the acetylide towards the metal slightly disrupting the overall symmetry within the complex. This disruption is shown in table 15 through a comparison of the bond lengths of compounds **3**, **4** and **5** with those reported by Hill for $\{(nacnac)Ca(CCPh)\}_2$. [19]

The distorted geometry observed in compounds **4** and **5** also results in differences being observed between their bond angles and those observed for the symmetrically-bridged complexes. The angle between the two bridging acetylides, (C(α)-Ca(1)-C(α)') in compounds **4** and **5**, 81.60(10)^o and 78.19(6)^o respectively, are observed to be slightly lower than the corresponding angle of the $\{nacnacCa(CCPh)\}_2$ of 89.70(5)^o [19] while compound **3** gives the angle at 89.23(7)^o. Compound **3** exerts an angle of Ca(1)-C(α)-Ca(1)' 90.77(7)^o that is close to the angle reported for the symmetric phenyl acetylide compound$\{nacnacCa(CCPh)\}_2$, of 90.30(5)^o, whilst the angles in compounds **4** and **5**, 98.40(10)^o and 101.81(6)^o respectively are increased.

The calcium centres in compounds **4** and **5** are pseudo 6-coordinate with three of the bonds co-ordinated to the acetylide unit at the α-C, β-C and oxygen atom. Although no co-ordination is observed between the calcium and nitrogen in compound **3** in the solid state, the complex still exists with a bent orientation as may be tentatively deduced from the ^{13}C NMR studies.

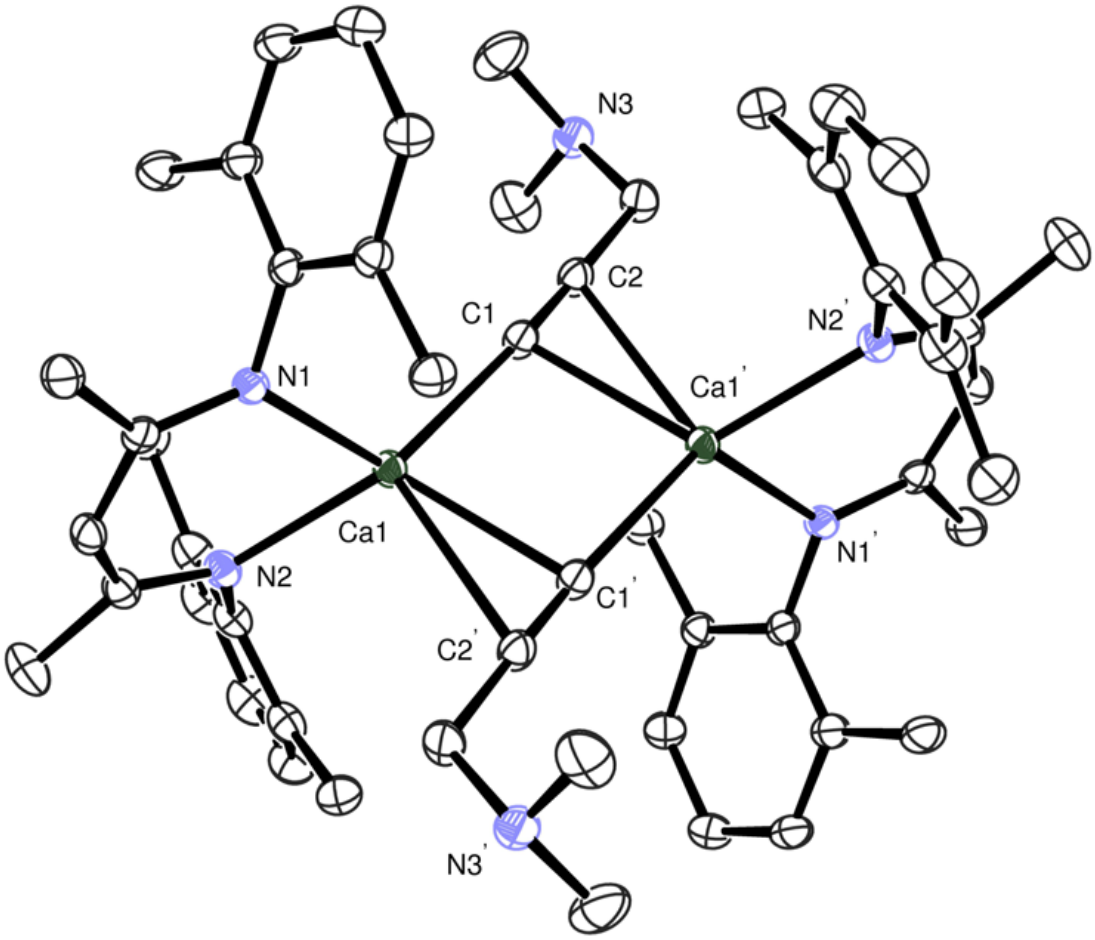

*Figure 13: Compound **3**, ellipsoids drawn at 30% probability. H-atoms and iso-propyl methyl groups removed for clarity.*

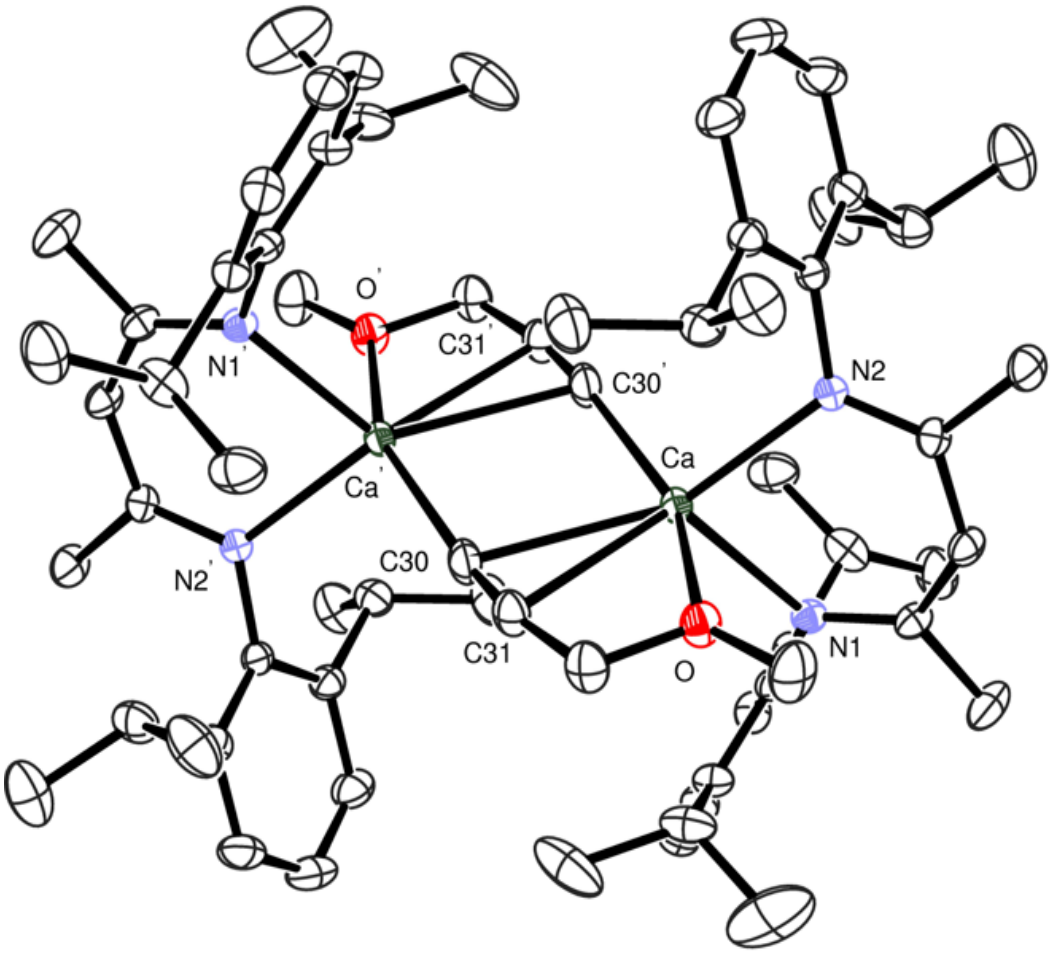

*Figure 14: Compound **4**, ellipsoids drawn at 30% probability. H-atoms and iso-propyl methyl groups removed for clarity.*

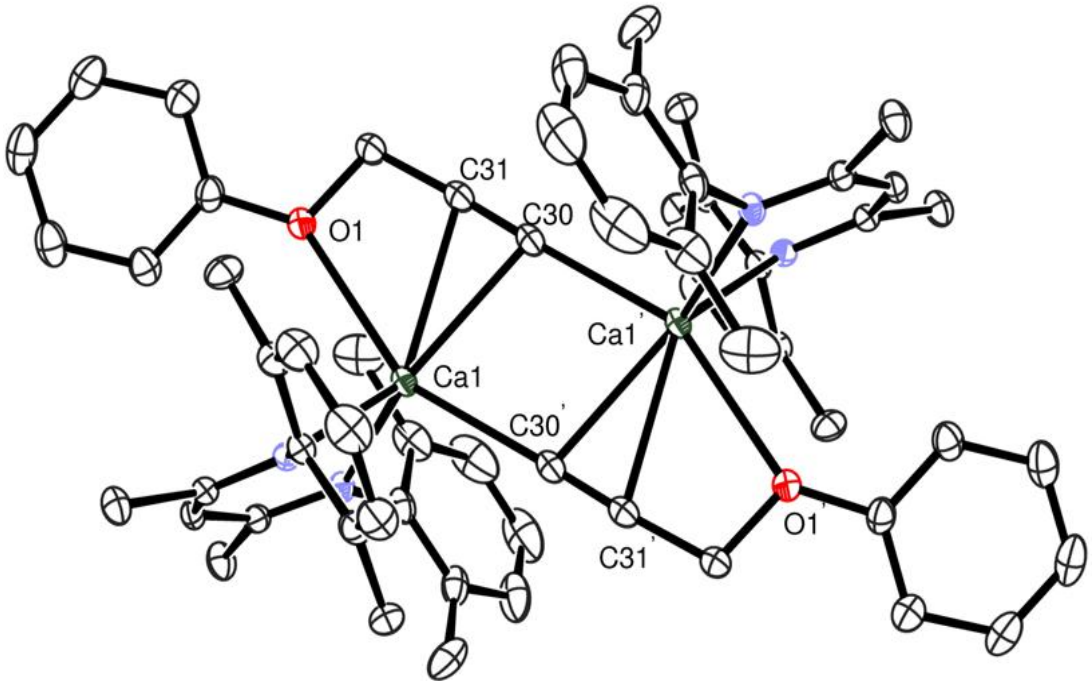

*Figure 15: Compound **5**, ellipsoids drawn at 30% probability. H-atoms and iso-propyl methyl groups removed for clarity.*

2.4 Conclusion

Although elemental analysis and NMR studies indicated that compounds **1**-**5** formed in accordance with previous dimeric acetylide structures reported by Hill and co-workers, the results of the solid state crystallographic analyses allows a division of the compounds into two structural groups; the more conventional symmetric and the newly observed asymmetric acetylides.

The introduction of terminal acetylides with the nitrogen and oxygen donor atoms was found to have a profound effect upon the orientation of the acetylide products **3**-**5** with a reduced angle between the calcium metal and the β-C of the asymmetric bridged acetylide unit, figure 12. In these complexes the electronegative donor atoms encourage a shift in the electron density within the acetylide complex thus encouraging further interactions between the calcium metal and the β-C and oxygen atom of the acetylide unit, hence distorting the symmetry of the complex. This adjustment to the orientation of the acetylide ligand is also found to result in a marked changed in reactivity; observations which will be discussed in chapter 3.

Chapter 3

3.0 Serendipitous observation of acetylene coupling

This chapter describes experimental work derived from the serendipitous observation of a calcium-induced alkyne coupling to form a butatriene derivative. After the formation of the acetylide complexes described in chapter 2, work was extended to studies of the insertion reactivity of the unsaturated double bond of dicyclohexyl carbodiimide. It was proposed that the addition of dicyclohexyl carbodiimide **h** would result in insertion into the calcium-acetylide bond to produce a new amidinate complex and that this reactivity could be extended to a catalytic regime as shown in scheme 58.

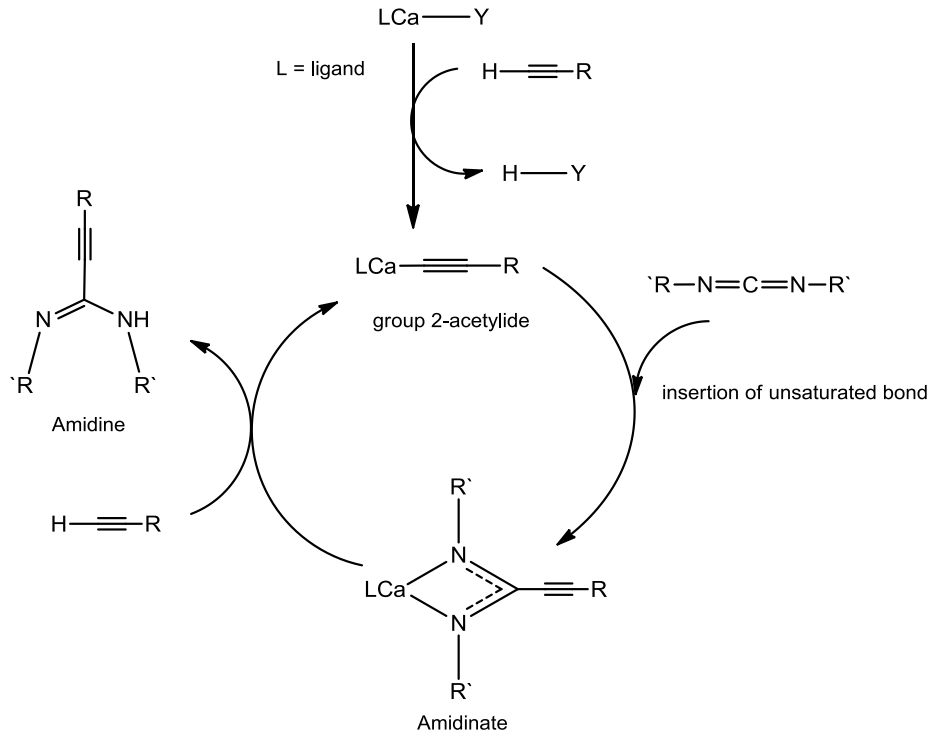

Scheme 58: Proposed catalytic cycle for the formation of an amidinate intermediate complex following the insertion of a carbodiimide into a calcium acetylide.

Although the stoichiometric and catalytic insertion of a carbodiimide will be discussed in chapter 4 of this thesis, a preliminary reaction of **C1** with methyl propargyl ether **e** and dicyclohexyl carbodiimide heated to 65 ^{o}C produced a serendipitous observation in the ^{1}H NMR spectra after recognising that the carbodiimide had been accidently omitted from the reaction. Although the ^{1}H NMR spectra indicated the formation of the bridged, dimeric acetylide, an excess of the acetylene provided the formation of a new unexpected compound with new environments manifested as a singlet at 3.2 ppm, a

doublet at 5.3 ppm and a triplet at 6.8 ppm. Further exploration of these resonances revealed the formation of a butatriene derivative, compound **7**, consisting of three consecutive C=C double bonds, scheme 59. [56a] However, stereoselectivity of the butatriene complex to the *E* or *Z* isomer is still be resolved.

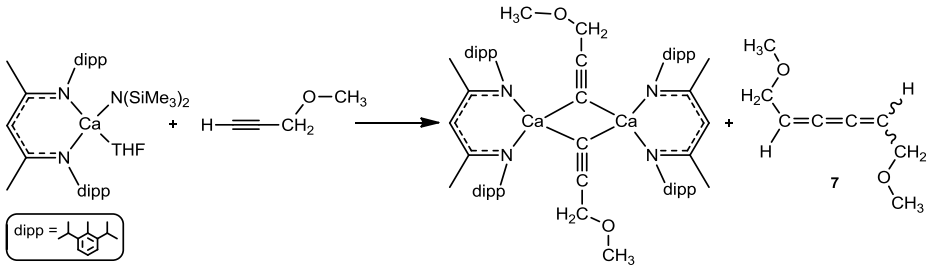

*Scheme 59: Synthesis of the bridged, dimeric acetylide complex and E/Z butatriene derivative identified in ^{1}H NMR spectroscopy from the reaction of **C1** and an excess of methyl propargyl ether.* [56a]

The reaction was repeated with other acetylenes leading to the conclusion that the formation of the butatriene complex was dependent upon the presence of the nitrogen and oxygen donor-functionalised atoms in acetylenes, scheme 60.

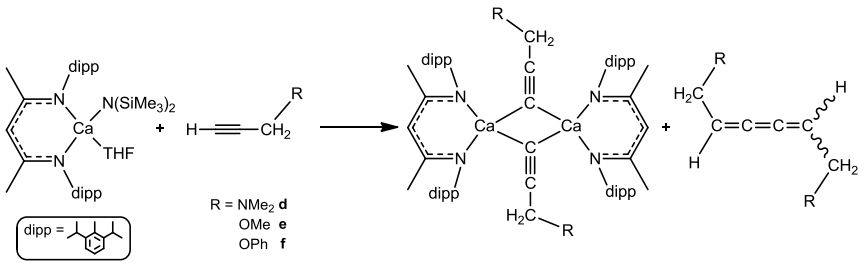

Scheme 60: Proposed synthesis of the bridged, dimeric acetylide complex and the unsaturated triple C=C double bond butatriene derivative.

This chapter therefore seeks to explain the chemistry behind the unexpected coupling of two acetylide units with the donor-functionalised acetylenes, 3-dimethylamino-1-propyne **d**, methyl propargyl ether **e**, and phenyl propargyl ether **f**, by exploring their reactivity on both catalytic and stoichiometric scales with the heteroleptic calcium and strontium β-diketiminato amides **C1**-**2**, the homoleptic calcium, strontium and barium bis(bis(trimethylsilyl)amides) **C3**-**5**, the calcium and strontium triazenide **C6**-**7** and the larger calcium and strontium dipp-BIAN dialkyl complexes **C8**-**9**, figure 16.

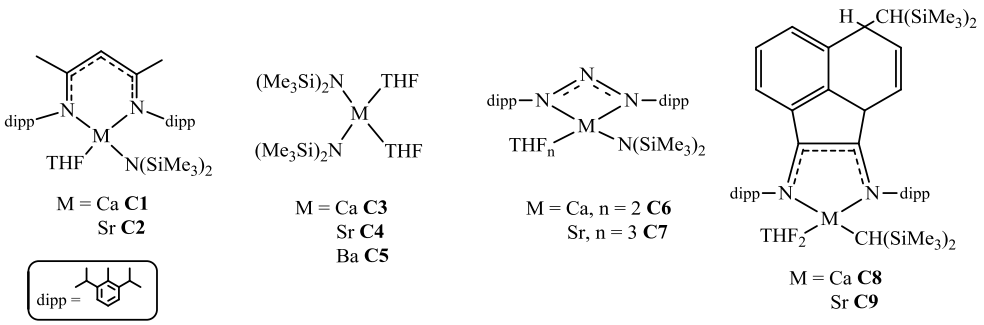

Figure 16: Heavier group 2 complexes employed in the coupling of two acetylide units.

3.1 Previous acetylide-based C-C coupling reactions

Organic chemists have been interested in compounds containing cumulated double bonds, such as the parent butatriene molecule, $H_2C=C=C=CH_2$, from as early as 1888 [57a, b] when the first observations of these compounds were reported. In 1937 Carothers was awarded a patent for recognising the potential of aliphatic unsaturated compounds such as the butatriene as a reactive monomer. [57c] As described in the introduction (section 1.9), previous investigations of C-C coupling reactions to form butatriene moieties have utilised both transition metals and lanthanide metals.

3.2 Results and Discussion

Following the observation of acetylene coupling after the omission of the carbodiimide, the reaction of calcium β-diketiminato amide complex **C1** and methyl propargyl ether **e**, was conducted on an NMR scale at 60 ^{o}C with a stoichiometric 1:2 molar ratio in a Youngs NMR tube in C_6D_6. Monitoring of the reaction by ^{1}H NMR spectroscopy indicated the formation of the butatriene derivative, **7**, by the disappearance of the triplet resonance of the terminal proton of the acetylene at 2.00 ppm and the appearance of the newly formed CH triplet resonance at 6.75 ppm. Both the doublet CH_2 and singlet methyl proton resonances of the methyl propargyl ether **e** were found to experience a down-field shift of 3.75 to 5.21 ppm and 3.08 to 3.16 ppm respectively in the ^{1}H NMR spectra.

The $^{13}C\{^{1}H\}$ NMR spectrum also indicated the acetylene coupling with a highly diagnostic and heavily de-shielded resonance at 201.7 ppm assigned to the quaternary carbons of the butatriene. [56a, b] Although NMR spectroscopy supported the coupling of

two methyl propargyl ether molecules, overall determination of the *E/Z* stereochemistry of the butatriene derivative was inconclusive, scheme 58, due to difficulties in its isolation resulting from its low stability and high tendency towards isomerisation.

This reactivity was extended to 3-dimethylamino-1-propyne **d** and phenyl propargyl ether **f**, under similar conditions. The procedure evidenced the formation of similar butatriene derivatives **6** and **8**, from the observation of similar methine triplet and doublet methylene resonances in the ^{1}H NMR spectra.

The proposed catalytic cycle, scheme 61, indicates the formation of the butatriene derivatives **6**, **7** and **8**, via the sequential addition of the donor-functionalised acetylene to the re-distributed asymmetric acetylide produced from the σ-bond metathesis with the terminal hydrogen of the donor-functionalised acetylene.

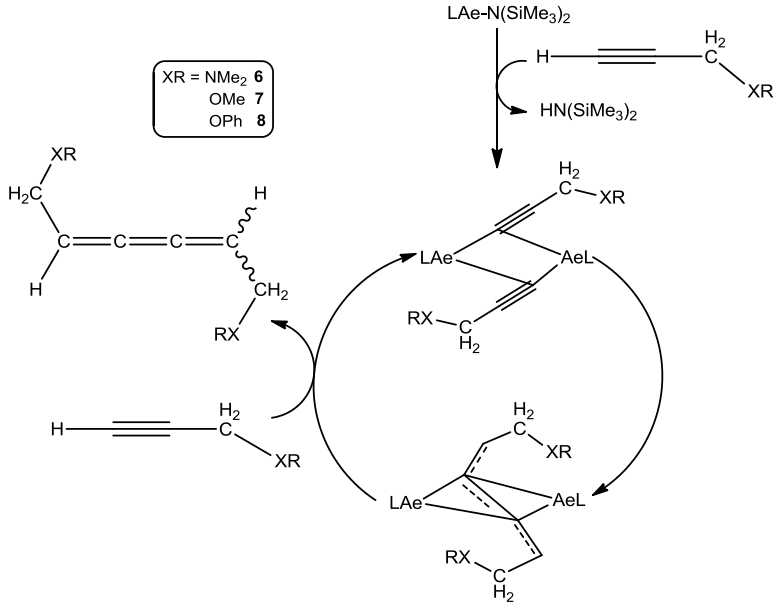

Scheme 61: Proposed catalytic cycle for the donor-functionalised acetylene coupling.

This formation of the three-consequecutive C=C double bonds of the butatriene derivative, compound **7** had not been observed for any previously reported symmetrically bridged, dimeric group 2 acetylides prepared from reaction of non-donor functionalised acetylenes. It was proposed, therefore, that the orientation of the acetylide is the key factor in the butatriene synthesis. The crystal structures of complexes **3**, **4** and **5** described in the previous chapter show the asymmetric orientation of the acetylides where it is proposed that the affinity of the acetylide towards the

calcium metal pulls the two bridging acetylides sufficiently close to the metal so as to allow for polarising interactions, reducing the mutual repulsion of the terminal α-carbon centres and enabling the acetylides to couple and form the butatriene derivative, scheme 62.

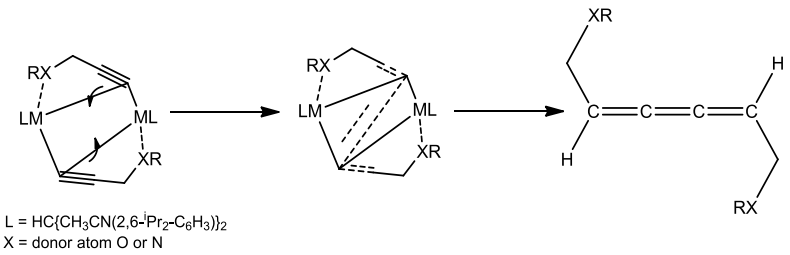

Scheme 62: Proposed acetylene coupling via the polarisation of the bridging acetylide units as a result of the presence of the nitrogen and oxygen donor-atoms.

The progress of the coupling reactions was observed in the ^{1}H NMR spectrum as the proton resonances of the acetylenes were shown to diminish concurrent with the appearance of diagnostic resonances for their corresponding butatriene derivatives **6**-**8**. Compounds **7** and **8** suggest that the more electronegative oxygen atom results in the CH resonance experiencing an increased down-field shift of ca. 1.0 ppm compared to that observed from the nitrogen atom in compound **6**, although the presence of the electronegative atom does not affect the CH_2 resonances of the compounds at ca. 5.3 ppm. The ^{13}C NMR spectra also indicated successful formation of the butatriene complexes with the appearance of the quaternary carbons at ca. 200 ppm, table 16.

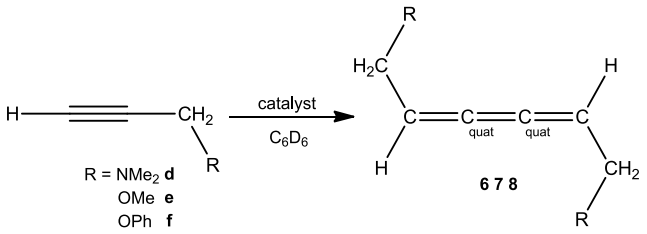

	^{1}H NMR resonance			^{13}C NMR resonance
	HC	CH_2	R	C_{quat}
6	5.97	5.27	2.22	200.4
7	6.75	5.21	3.16	201.7
8	6.63	5.05	6.85 and 7.06	200.3

*Table 16: ^{1}H and ^{13}C NMR shifts given in ppm for the stoichiometric butatriene products **6**-**8**.* [56a]

3.3 Alternative Group 2 metal centred complexes

Several group 2 metal complexes were employed in an effort to increase the scope and overall efficiency of the donor-functionalised acetylene coupling reactions. Although the utility of the β-diketiminato amide derivatives have been more widely explored, the reactions were limited to the stoichiometric case due to protonation of the solubilising β-diketiminato, nacnac ligand, **L1**. In a bid to overcome this limitation other group 2 metal complexes were introduced. The homoleptic complexes **C3-4**, crystallised from hexane at -30 ^{o}C were employed and the triazene ligand **L2** utilised in **C6-7**, [58] was introduced as it was considered to be less prone to protonolysis by the free acetylene.

The final set of complexes, **C8-9**, employed contained the dearomatised BIAN ligand making the complexes less prone to re-distribute during the reaction. [59] These complexes possess a more rigid ligand than **L1** and have been found to be less prone to redistribute towards the inactive homoleptic complex and were, thus, considered likely to encourage a catalytic turnover. Both **C8** and **C9** were prepared in the glovebox by stirring the appropriate group 2 alkyl, [M{CH(SiMe$_3$)$_2$}$_2$(THF)$_2$], and the dipp-BIAN ligand in toluene for 10 minutes at room temperature before the solvent was removed in vacuo, scheme 63. Re-crystallisation of the crude products was not possible even following months of storage at -30 ^{o}C. However the purity of the crude products was found to be sufficient for the subsequent reactions.

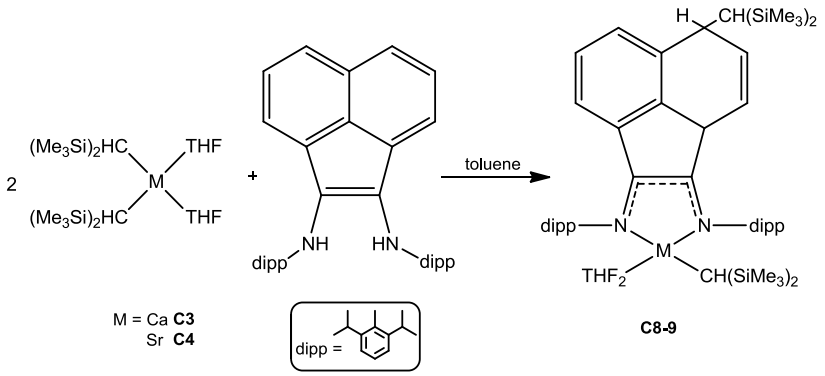

Scheme 63: Formation of calcium and strontium dipp-BIAN dialkyl complexes. [59]

3.4 Stoichiometric carbon-carbon coupling

The stoichiometric coupling reactions proceeded via the addition of an additional donor-functionalised acetylene equivalent to an initial 1:1 solution of group 2 metal complex:acetylene until completion was observed in ^{1}H NMR spectroscopy. In an initial attempt to extend this reactivity to a catalytic regime, a series of reactions were performed with sequential addition of increasing numbers of molar equivalents to the pre-catalysts **C1**, **C3**, **C4** and **C6**-**C9**.

Initial NMR-scale stoichiometric coupling reactions were conducted with the heteroleptic calcium β-diketiminato amide **C1**, however they were found to become limited by the formation an insoluble white/yellow, inactive homoleptic complex [56a] which was found to precipitate during the reaction as a result of β-diketimato protonation, scheme 64, which was clearly observed in the ^{1}H NMR spectra.

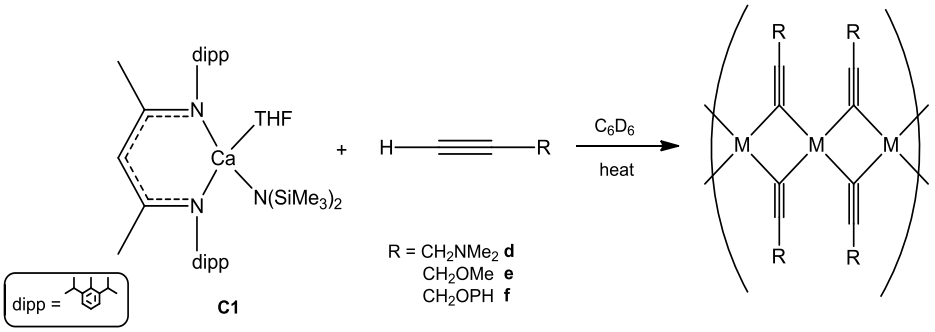

Scheme 64: Formation of the unreactive homoleptic polymeric calcium and strontium acetylides. [56a]

The other group 2 metal complexes were employed in a bid encourage the formation of the butatriene derivative and avoid inhibiting the reaction by preventing the formation the inactive homoleptic complex scheme 65.

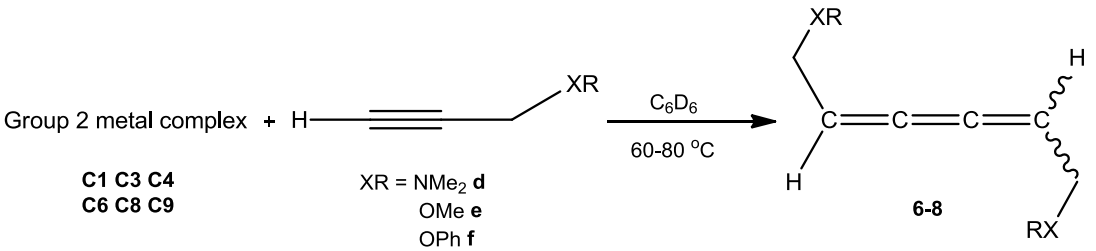

Scheme 65: Donor-functionalised acetylene coupling with a range of group 2 metal complexes.

The final acetylene equivalents added to the reaction are presented in table 17 with the results suggesting the identity of the donor group on the acetylene influences the overall coupling activity. The most successful results were found for the simplest methyl propargyl ether, **e**, while the larger, bulkier acetylenes 3-dimethylamino-1-propyne **d** and phenyl propargyl ether **f** with donor groups NMe_2 and OPh respectively, were found to provide significantly less facile coupling.

Group 2 metal complex	Acetylene	Final acetylene equivalents	Temperature ^oC	Compound
C1	**d**	3	65	**6**
C3	**d**	1[a]	65	**6**
C6	**d**	2	65	**6**
C1	**e**	4	60	**7**
C3	**e**	4	60	**7**
C4	**e**	4	60	**7**
C6	**e**	12	65	**7**
C8	**e**	4	60[c]	**7**
C9	**e**	8	60[c]	**7**
C3	**f**	3	75	**8**
C6	**f**	3	65[b]	**8**

[a] no indication of product formation after 1 week
[b] temperature increased 75 ^oC after 48 hours
[c] temperature increased 80 ^oC after 48 hours
Table 17: Acetylene coupling monitored by ^1H NMR.

The bulkier NMe_2 group of 3-dimethylamino-1-propyne **d** proved too sterically demanding to yield compound **6** on reaction with calcium bis(bis(trimethylsilyl)amide) **C3**. However, 3-dimethylamino-1-propyne **d** did prove successful in forming compound **6** for up to 3 and 2 equivalents upon reaction with calcium diketiminato amide **C1** and calcium triazenide **C6** respectively. While compound **8** was formed from reaction of 3 equivalents of phenyl propargyl ether **f** to a single equivalent of both bis(bis(trimethylsilyl)amide) **C3** and calcium triazenide **C6**.

Compound **7** was most readily produced with 12 equivalents of methyl propargyl ether **e** reacting with the calcium triazene complex **C6** before catalyst deactivation, scheme 66. [56a] The coupling was not only limited to the calcium centred catalysts **C1**, **C3**, **C6** and **C8**, as the strontium complexes, strontium bis(bis(trimethylsilyl)amide) **C4** and strontium dipp-BIAN dialkyl **C9** also provided similar coupling activity. The strontium dipp-BIAN dialkyl **C9** produced compound **7** upon the sequential addition of 8 equivalents of methyl propargyl ether **e**.

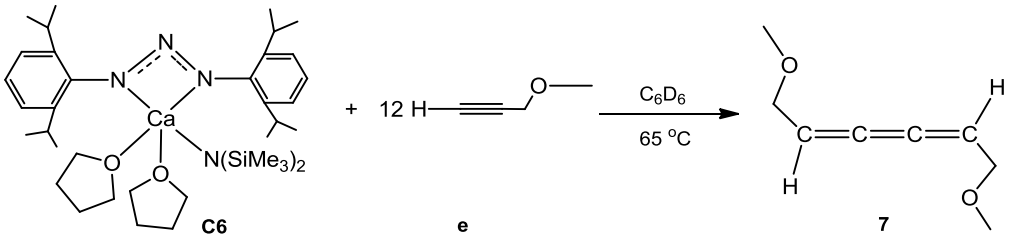

C6 e 7

*Scheme 66: Formation of compound **7** with 12 equivalents of **e**.* [56a]

3.5 Catalytic carbon-carbon coupling

The reactions performed with sequential addition of increasing equivalents of acetylene indicated the viability of a potential catalytic variant. The reactions were thus repeated for the three donor-functionalised acetylenes, 3-dimethylamino-1-propyne **d**, methyl propargyl ether **e** and phenyl propargyl ether **f** with 5 mol % catalytic loading of the heteroleptic strontium β-diketiminato amide, **C2** and the calcium and strontium triazenide and dipp-BIAN dialkyl complexes **C6**-**C9**.

Catalytic turnover to form the coupled butatriene products was observed from the ^{1}H NMR spectra following the consumption of the acetylene, table 18. Although catalytic turnover was initially observed to proceed within a couple of hours, reactions with the calcium **C6** and strontium triazenide **C7** complexes were found to be a little sluggish in comparison. Consequently, inorder to encourage catalytic turnover, their catalytic loadings were increased by 10 mol% after 2 hours.

Catalyst	Acetylene	Time	% Conversion	Compound
C2	**d**	4 weeks	4	**6**
[a]**C6**	**d**	1 weeks	11	**6**
C2	**e**	2 weeks	5	**7**
[b]**C6**	**e**	2 days	91	**7**
[a]**C7**	**e**	10 days	15	**7**
[c]**C8**	**e**	2 weeks	86	**7**
[c]**C9**	**e**	2 weeks	7	**7**
[d]**C6**	**f**	2 weeks	17	**8**

[a] Catalytic loading increased to 20 mol%
[b] 6.25 mol% catalytic loading
[c] reaction at 60 ^{o}C
[d] Catalytic loading increased to 10 mol% after 2 hours
Table 18: Catalytic reactions with 5 mol% catalytic loading of the group 2 metal complexes at 75 ^{o}C.

The least effective catalyst was the strontium β-diketiminato amide **C2**. As well as undergoing protonolysis of the β-diketiminato ligand **L1**, use of the large strontium ion resulted in very low 4 % conversion to compound **6**, most likely due to the insolubility of the intermediate acetylide. The catalyst was also found to be inefficient with the most reactive of the acetylenes methyl propargyl ether **e** with just 5 % conversion to compound **7**. As was the case for the earlier stoichiometric reactions, catalytic turnover was found to depend upon the acetylene employed with the smaller methyl propargyl ether **e** producing the most successful reaction to produce 91 % of compound **7**. For the larger phenyl propargyl ether **f** and 3-dimethylamino-1-propyne **d** the most successful reactions resulted in only 17 % conversion to compound **8** and 11 % conversion to compound **6** respectively with the calcium triazenide complex **C6**.

Although the calcium triazenide derivative **C6** was found to be productive in the coupling of methyl propargyl ether **e** its strontium analogue, **C7** only yielded 15 % of compound **7** despite an increase of catalytic loading to 20 mol%. The metal dipp-BIAN dialkyl complexes **C8** and **C9** also gave contrasting results with the calcium derivative **C8** proving to be the second most productive complex in yielding compound **7** with 86 % conversion. In contrast the strontium complex **C9** provided only very limited reactivity and only 7 % conversion to compound **7**.

The catalysis of the two most efficient reactions was monitored by ^{1}H NMR spectroscopy with their results presented as stack plots in figures 17 and 18. The plots illustrate the formation of the coupled butatriene product over a period of time from reaction of methyl propargyl ether **e** and calcium triazenide **C6** and calcium dipp-BIAN alkyl **C8** respectively, figure 17 and 18. [56a]

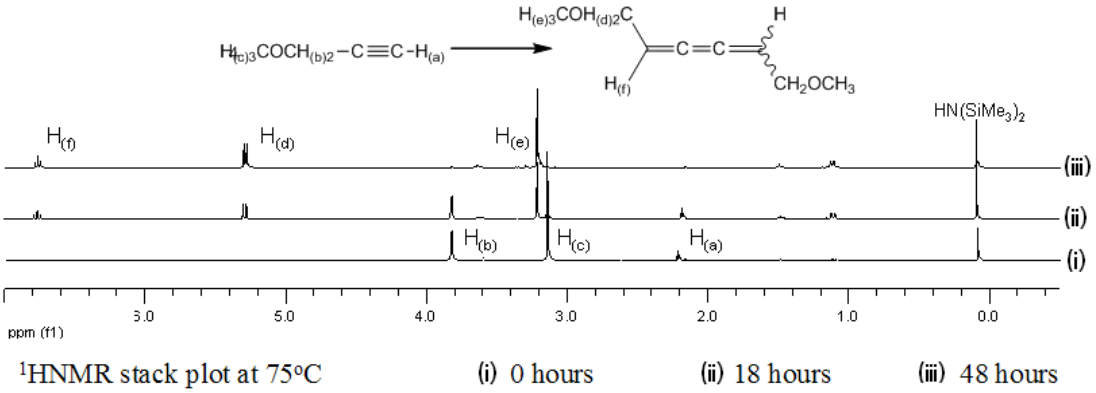

*Figure 17: ^{1}H NMR stack plot of the formation of butatriene compound **7** by the coupling of two methyl propargyl ether molecules **e** catalysed by calcium triazenide **C6** at 75°C over 48 hours in C_6D_6.* [56a]

Spectrum (i) of figure 17 shows the resonances of the methyl propargyl ether **e** at the start of the reaction. The terminal H is observed as a triplet at 2.20 ppm. A singlet ascribed to the CH_3 is observed at 3.07 ppm and a doublet at 3.73 ppm to the CH_2. After heating at 75 ^{0}C for 18 hours plot (ii) shows a decrease in the initial resonances accompanied by the appearance of three new resonances of the newly coupled butatriene. The CH_3 resonance is now observed as a singlet at 3.16 ppm while the CH_2 and CH resonances are clearly observed as doublet and triplet signals at 5.21 and 6.76 ppm respectively. The reaction is shown to be complete after 48 hours as plot (iii) only contains the butatriene resonances. At this point all of the acetylene has successfully coupled together to form the butatriene compound **7**.

The stack plot of the reaction between methyl propargyl ether **e** and 5 mol% of calcium dipp-BIAN **C8**, figure 18, shows the catalysis to be not too dissimilar to that of the reaction with calcium triazenide **C6** in figure 17, with the consumption of methyl propargyl ether **e** resonances (i) and the sole formation and the production of the butatriene derivative compound **7** (iv) with complete atom efficiency.

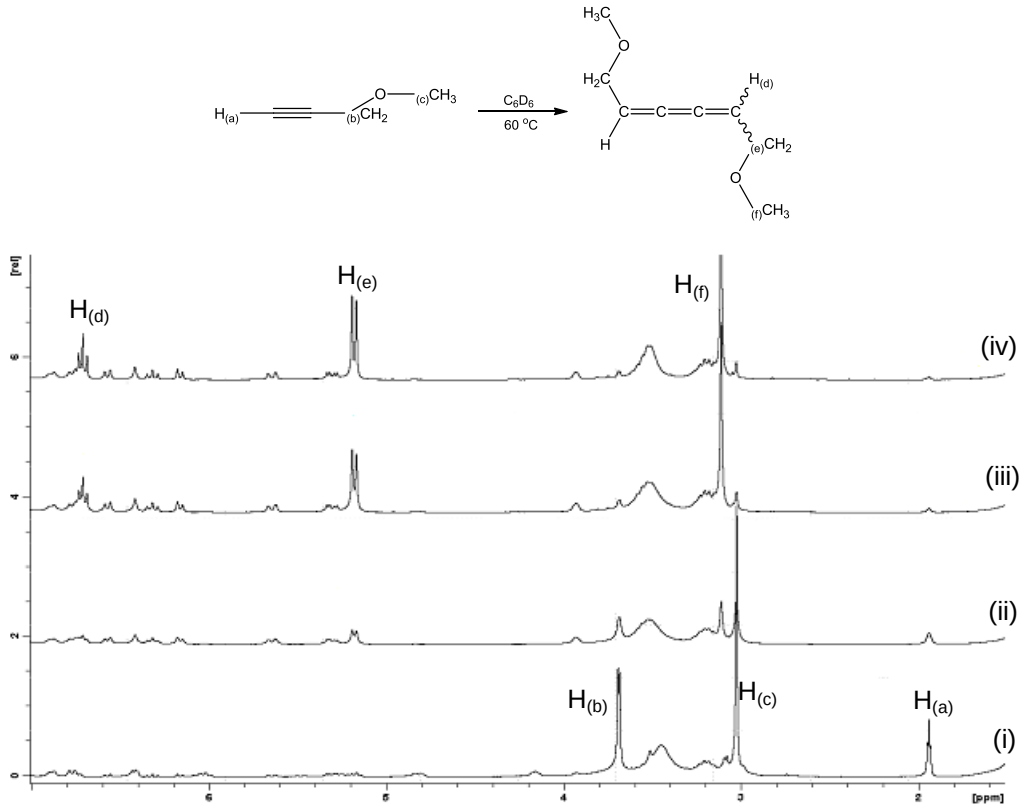

*Figure 18: ^{1}H NMR stack plot of the formation of butatriene compound **7** by the coupling of methyl propargyl ether molecules **e** catalysed by 5 mol% of calcium triazenide **C8** at 60 ^{o}C for 1week in C_6D_6.*

3.6 Conclusion

It is proposed that the formation of the butatriene derivatives is influenced by the orientation of the co-ordinated acetylenes when forming the dimeric acetylides discussed in chapter 2 with the observation of the asymmetric dimeric acetylide complexes with the donor functionalised acetylenes, 3-dimethylamino-1-propyne **d**, methyl propargyl ether **e** and phenyl propargyl ether **f**, scheme 67.

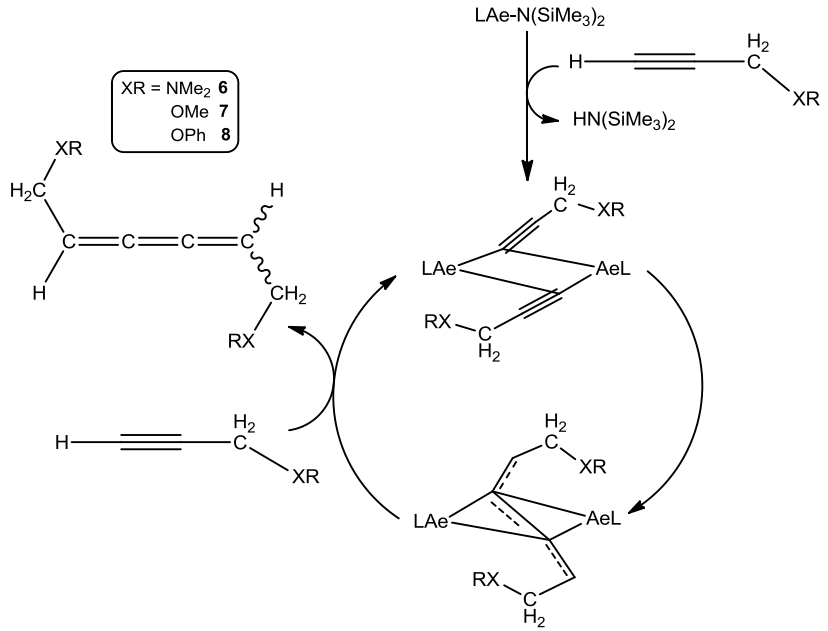

Scheme 67: Proposed catalytic cycle for the donor-functionalised acetylene coupling.

Unlike previously reported symmetric acetylide complexes formed from the non-donor functionalised acetylenes, the asymmetric complexes were found to exert additional interactions between the group 2 metal and the β-C of the asymmetric donor-functionalised dimeric acetylides. An interaction between the metal and the oxygen atom of methyl propargyl ether **e** and phenyl propargyl ether **f** is also observed.

It is therefore proposed that the extra interactions encourage both structural and electronic changes that result in the formation of the asymmetric acetylide complexes. The two possible extremes of these co-ordination modes are illustrated in figure 19 in which the extent of distortion maybe quantified by the two different bridging angles θ and φ around the co-ordinated acetylide. When both angles, θ and φ, are equal, they produce the symmetric structure (a). However when θ and φ are different they produce the asymmetric orientation (b). [56a]

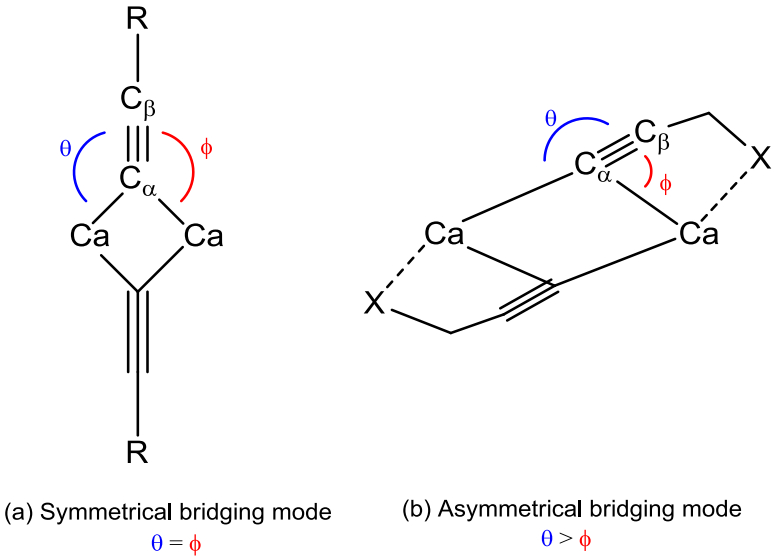

(a) Symmetrical bridging mode
$\theta = \phi$

(b) Asymmetrical bridging mode
$\theta > \phi$

Figure 19: Possible acetylide bridging co-ordination modes. [56a]

It is proposed that there is a shift in electron density with the α-C experiencing a negative charge reduction that is contrasted by an increased negative charge exerted on the β-C, thus inducing a slight polarising effect within the complex. This induced polarisation effect upon the acetylide complex makes the negatively charged β-C more attractive towards the group 2 metal, hence making an interaction more likely. Consequently this interaction increases the polarisation of the complex with the α-C becoming more positive while weakening the strength of its bond with the calcium metal, therefore making the insertion of an unsaturated molecule more viable.

The nature of the (side-on) acetylide-calcium interaction has previously been investigated with density functional theory (DFT) calculations for the model complex $[Ca\{(NHCH)_2CH\}\{C{\equiv}CH\}]_2$, figure 20. [8] Although these results show little change in the overall energy of the system when $(\theta - \varphi) < 50^o$ (ca. 1 KJ mol^{-1}), there was an energy increase of 6-10 KJ mol^{-1} between values of 50-90^o illustrating a destabilising influence within the dimeric acetylide structure. The crystallographic results show the orientations of the structures are strongly influenced by the steric factors.

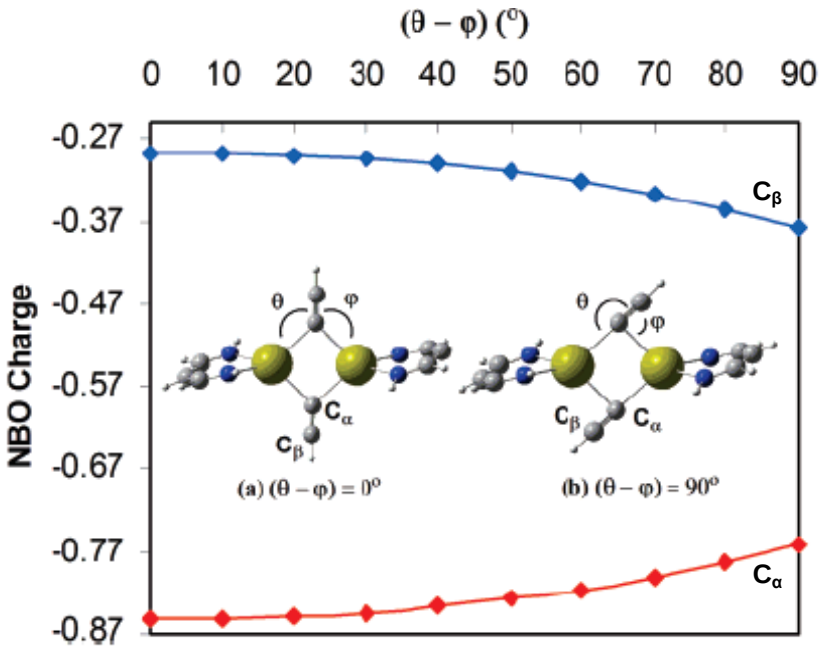

Figure 20: Calculated variation of natural bond orbital (NBO) negative charge on C_α and C_β for $0^o < (\theta - \varphi) < 90^o$. [8]

Higher values of (θ - φ) result in a relatively minor dissipation of negative charge over both carbon centres of the acetylides while the positive charge on the metal remains unchanged. It is suggested, therefore, that it is the presence of the electronegative nitrogen atom in **d** and the oxygen atom in **e** and **f** initiate the formation of the butatriene. With the evidence obtained from the crystal structure data, the proposed mechanism for the acetylide coupling suggests the electronegative atom causes an electron shift in the co-ordinated complex due to its attraction with the metal centre.

Consequently it is proposed that this shift in the electron density from the α-C to β-C of the acetylide unit results in a reduction in the repulsion between the two metal centres. This shift in electron density allows the acetylides to re-distribute, most likely via an un-observed butatrienyl intermediate of the type isolated in previously reported organolanthanide chemistry [21a, b, 34a, 35, 37] and eventually lead to the formation of a butatriene upon protonation with a further acetylene equivalent, scheme 68.

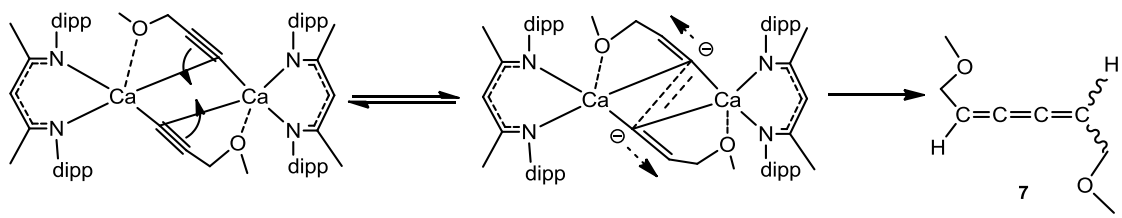

Scheme 68: Proposed mechanism for butatriene formation.

Chapter 4

4.0 Calcium propiolamidinate and catalytic propiolamidine synthesis

The initial motivation for the work described in this thesis was a study of the insertion reactivity of a carbodiimide to a group 2 metal acetylide. Taking into account the catalytic insertion of the carbodiimide with the lanthanide metals it was proposed that the reaction with group 2 metals would proceed via the formation of an amidinate intermediate complex, scheme 69.

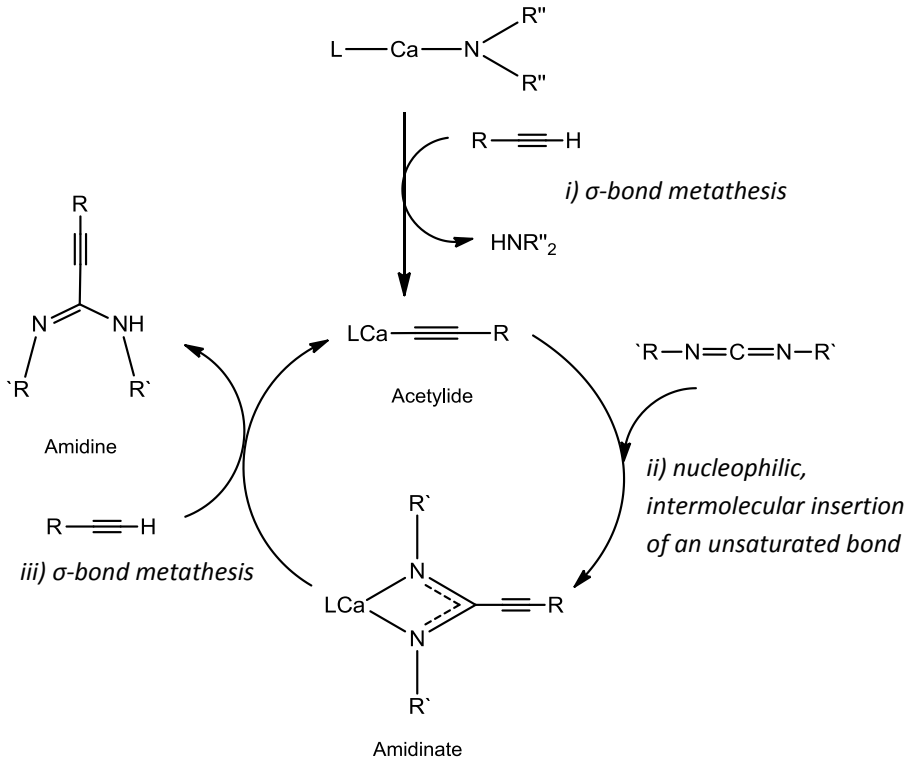

Scheme 69: Proposed catalytic cycle of the carbodiimide insertion to a group 2 acetylide.

Initial reactions involved co-ordination of the acetylides with the heteroleptic calcium β-diketiminato amide **C1**, as discussed in chapter 2, before extending the work to include the homoleptic calcium, strontium and barium bis(bis(trimethylsilyl)amides) **C3-5** complexes with a range of different acetylenes and carbodiimides illustrated in figure 21.

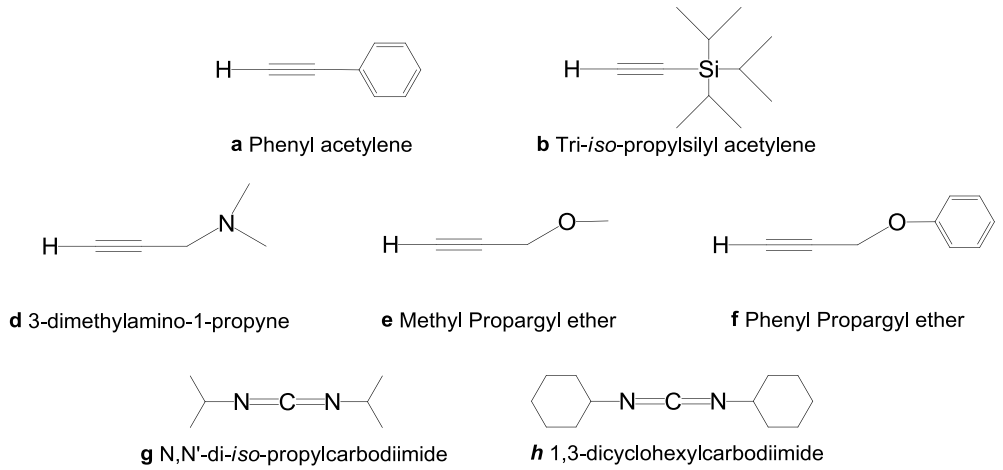

Figure 21: Terminal acetylenes and carbodiimides.

The work described in this chapter aims to expand upon the results presented in chapter 2 through the insertion of unsaturated N-substituted symmetrical carbodiimides, (R'N=C=NR'), into the M-C bonds of calcium acetylides. Following the formation of the acetylide complexes in the proposed catalytic cycle, scheme 69, the carbodiimide insert into the C_{α}-metal bond of the acetylide to form an amidinate intermediate complex that affords the free amidine product upon protonation by a further equivalent of the acetylene. This chapter will describe the formation and isolation of a range of amidinate intermediate complexes and their ability to proceed catalytically with the formation of the free amidine, (R'N=C(R)-NHR).

4.1 Introduction

4.1.1 Amidine synthesis with lanthanide metal complexes

The amidinate unit is well established as an ancillary ligand for the stabilisation of metal compounds such as the early transition and lanthanide metals. Until 2005 further protonation of these complexes to initiate catalysis and production of amidines had proven difficult due to the stability and high sensitivity of the free amidine product towards hydrolysis. However in 2005 Hou et al. [53] reported the first catalytic route to the atom-efficient formation of the free propiolamidine product via the nucleophilic insertion of a carbodiimide to form a propiolamidinate intermediate complex of a half-sandwich yttrium metal catalyst, scheme 70.

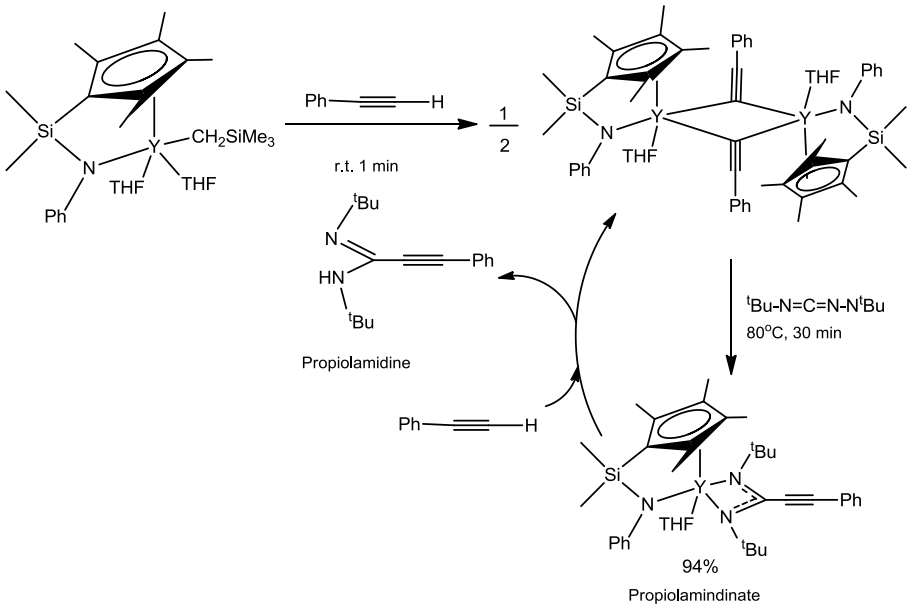

Scheme 70: The catalytic formation of a free propiolamidine product via the carbodiimide insertion to the half-sandwich yttrium propiolamindinate intermediate complex. [53]

Hou found this catalytic reaction to be efficient with other lanthanide metals Yb, Lu and Sm and extended his work to a range of terminal acetylenes and carbodiimides, scheme 71.

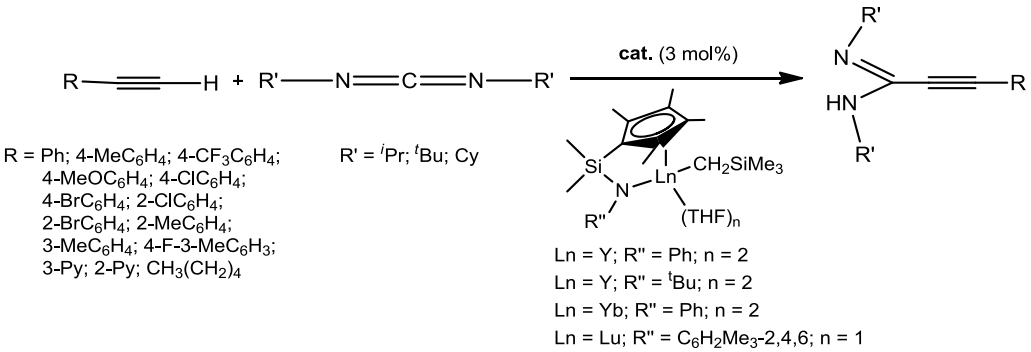

Scheme 71: Extension of Hou's work for the range of catalysts, terminal acetylenes and carbodiimides. [53]

The yields of the isolated free amidine products during the insertion of di-*iso*-propyl carbodiimide **g** to the range of terminal acetylenes with the yttrium catalyst are shown in table 19. [53] Each reaction was carried out at 80 ^{o}C for 1 hour in THF producing yields of 93-99 %.

entry	R	Temp (^{o}C)	Time (h)	Isolated yield (%)
1	Ph	80	1	>99
2	4-MeOC_6H_4	80	1	96
3	4-BrC_6H_4	80	1	93
4	2-ClC_6H_4	80	1	97
5	2-BrC_6H_4	80	1	94
6	2-MeC_6H_4	80	1	97
7	3-MeC_6H_4	80	1	97
8	4-F-3-MeC_6H_3	80	1	95
9	3-Py	80	1	98

Tale 19: Catalytic addition of terminal acetylenes to di-iso-propylcarbodiimide with the half-sandwich yttrium metal complex were R'' = Ph in THF-$_{d8}$. [53]

The results show that although high yields are achieved for all of the reactions, the size and nature of the R groups on the acetylene can affect the overall yield. The highest yield of more than 99 % was obtained during the reaction with the simplest acetylene, phenyl acetylene **a** (entry 1), however the addition of substituents on the phenyl ring reduced the yield. The introduction of a methoxy group on the 4 position of the phenyl ring resulted in a 3 % decrease (entry 2).

The lowest yield of 93 % was found with the bromine atom in position 4 (entry 3) however, there was a 1 % increase when the bromine was in position 2 (entry 5) due to the increased electron with-drawing influence of the bromine in the reaction making it slightly more efficient.

4.2 Synthesis of alkaline earth propiolamidinates

The insertion of the unsaturated double bond of the carbodiimide into the alkaline earth acetylide forms a key intermediate step of the overall insertion catalysis, scheme 72. In order to ascertain and prove the formation of this propiolamidinate intermediate, the reaction was carried out on a stoichiometric scale allowing for the isolation and characterisation of the propiolamidinates. However, before proceeding with the stoichiometric insertion of the carbodiimide on the preparative scale, catalytic turn-over was first established by conducting the reaction on a catalytic scale.

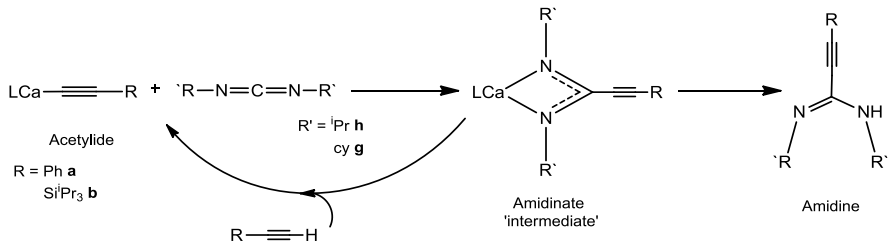

Scheme 72: Proposed catalytic cycle of the insertion of an unsaturated carbodiimide to a group 2 acetylide.

4.3 Catalytic synthesis of alkaline earth propiolamidinates

Following the unexpected coupling observed with the donor-functionalised acetylenes **d-f** discussed in the previous chapter, the catalytic insertion of di-*iso*-propylcarbodiimide **g** and dicyclohexyl carbodiimide **h** was only conducted with phenyl acetylene **a** and tri-*iso*-propylsilyl acetylene **b** despite the inclusion of the donor-functionalised acetylenes in the stoichiometric synthesis, scheme 72.

The catalytic reactions were prepared in Youngs NMR tubes with deuterated benzene (C_6D_6) as the solvent and 5 mol% catalytic loading of calcium bis(bis(trimethylsilyl)amide) **C3**. Due to a slow catalytic rate the reactions were heated for fourteen days at 75 ^{o}C, ^{1}H NMR spectroscopy indicated catalytic turn-over with % conversions presented in table 20. The results suggest the overall conversion is influenced by the size of the R group on the acetylene as the bulkier tri-*iso*-propylsilyl acetylene **b** yielded a lower conversion than that of the phenyl acetylene **a** regardless of the inserting carbodiimide. However the carbodiimide is dependent upon the acetylene with the conversion of compound **19** from reaction of dicyclohexyl carbodiimide **h** and phenyl acetylene **a** being the most efficient with 48 % conversion while the same carbodiimide only yielded 18 % of compound **13** with tri-*iso*-propylsilyl acetylene **b**.

Catalyst	Acetylene	carbodiimide	% Conversion	Compound
C3	**a**	**g**	24	**18**
C3	**a**	**h**	48	**19**
C3	**b**	**g**	22	**12**
C3	**b**	**h**	18	**13**

Table 20: Catalytic reactions with catalyst loading at 5 mol% at 75 ^{o}C for fourteen days.

4.4 Stoichiometric synthesis of heteroleptic alkaline earth propiolamidinates

The initial carbodiimide insertion reactions were undertaken with the heteroleptic group 2 acetylides described in chapter 2. It was proposed that the unsaturated bond of the carbodiimide would insert into the metal-carbon bond of the acetylide, compounds **3-5**, resulting in the formation of the amidate complexes, compounds **9-11**. However, it was found to be more convenient and efficient to prepare the reaction in a single step with a 1:1:1 ratio of group 2 metal complex, acetylene and carbodiimide rather than adding the carbodiimide to the pre-prepared acetylide, scheme 73.

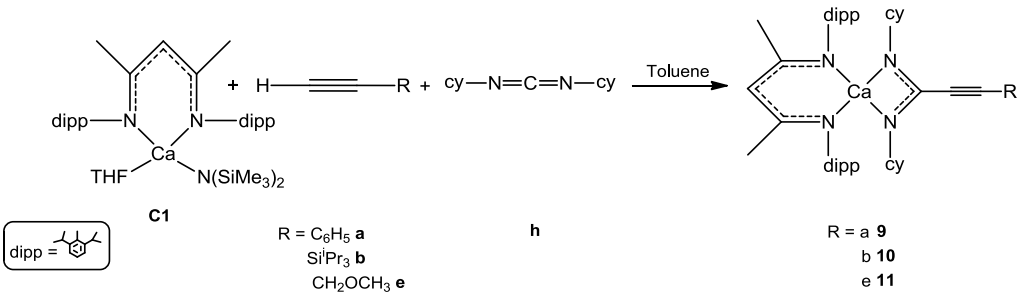

*Scheme 73: Amidinate formation with the heteroleptic β-diketiminato calcium **C1**.*

The propiolamidinate complexes were crystallised from a concentrated toluene solution at -30 ^{o}C under a nitrogen atmosphere. However with the precipitation of a white powder, the reactions did not produce crystalline material suitable for X-ray crystallography. Characterisation of the propiolamidinate products was thus carried out after filtration and drying under vacuum. The initial characterisation was achieved with both ^{1}H and ^{13}C NMR spectroscopy and elemental analysis of the final complex.

4.4.1 Characterisation by elemental analysis and NMR spectroscopy of heteroleptic complexes

The elemental analysis results indicated the formation of the proposed amidinate complexes with the actual % values of the product supporting those calculated theoretically, table 21.

Compound	Formula	Molc. Wt(g)	% Yield	calculated % C	calculated % H	calculated % N	found % C	found % H	found % N
9	$C_{50}H_{68}CaN_4$	765.18	49	78.48	8.96	7.32	76.14	9.01	6.63
10	$C_{53}H_{84}CaN_4Si$	845.45	52	75.30	10.01	6.63	74.30	9.93	4.07
11	$C_{46}H_{68}CaN_4O$	733.14	53	75.36	9.35	7.64	75.62	9.16	7.65

*Table 21: Carbodiimide insertion with heteroleptic catalyst **C1**.*

As observed during the acetylide synthesis in chapter 2, the ^{1}H NMR spectra confirm the reaction progress by the absence of the terminal proton resonance of the acetylene whilst the remaining acetylene protons experience down-field shifts. Comparisons in the ^{1}H NMR spectra between the proton resonances of the β-diketiminato ligand on the calcium β-diketiminato amide complex **C1** and the propiolamidinate compounds **10** and **11** indicated a down-field shift with the donor-functionalised propiolamidinate **11** experiencing the largest shift, table 22.

	C1	**10**	**11**
^{i}PrCH$_3$	1.22 and 1.33	1.29 and 1.40	1.87 and 2.06
γH	4.35	4.96	5.71

*Table 22: Comparison between the ^{1}H NMR shifts in ppm of the β-diketiminato ligand **L1** on the calcium β-diketiminato amide complex **C1** and the propiolamidinates **10** and **11**.*

4.5 Synthesis of homoleptic alkaline earth propiolamidinates

The synthesis of a series of homoleptic group 2 propiolamidinates, **12-41** followed the same synthetic route as that of the heteroleptic compounds. However the ratio of acetylene and carbodiimide to group 2 metal complex was increased to 2:2:1 respectively due to the absence of the β-diketiminato ligand on the metal.

The homoleptic insertion reactions were proposed to proceed via the formation of a polymeric homoleptic acetylide intermediate complex before the ready insertion of the carbodiimide to the M-C bond to produce the terminally inserted amidinate complex, scheme 74.

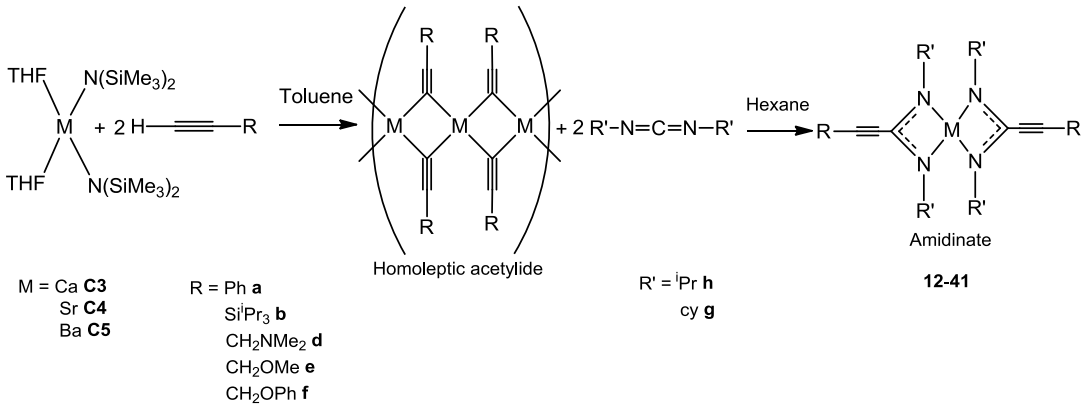

Scheme 74: Proposed homoleptic insertion of a carbodiimide into a group 2 acetylide.

A third carbodiimide, N,N′-di-*tert*-butylcarbodiimide was included in the initial reactions but after numerous attempts the carbodiimide proved to be unreactive. It seems apparent that the size of the substituent on the carbodiimide does affect its overall insertion reactivity as the large bulky substituent on the carbodiimide was found to presumably prevent pre-coordination prior to the insertion step, scheme 75. As a result the N,N′-di-*tert*-butylcarbodiimide was omitted from further reactions.

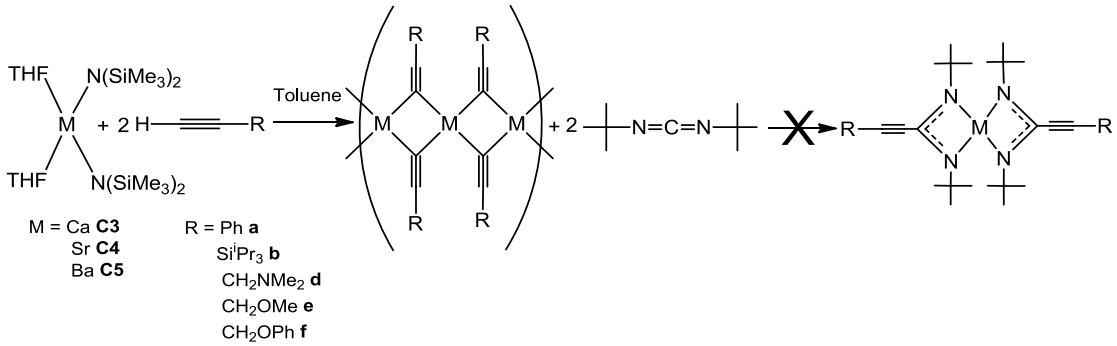

Scheme 75: The bulky substituent on N,N'-di-tert-butylcarbodiimide prevents insertion.

4.5.1 Characterisation by elemental analysis and NMR spectroscopy of homoleptic complexes [60]

Although the monomeric compounds **12-41** were produced at less than 40 % yield the elemental analysis found in table 23 suggested the formation of two different structural products that were dependent upon the identity of the carbodiimide.

Interestingly, the group 2 alkaline earth metal had no overall bearing on the final amidate product. The data obtained from the elemental analysis supported the calculated

data for the insertion of the simplest carbodiimide, N,N'-*di-iso*-propylcarbodiimide **g**, to occur with a double insertion to yield the proposed homoleptic amidate complexes, scheme 76.

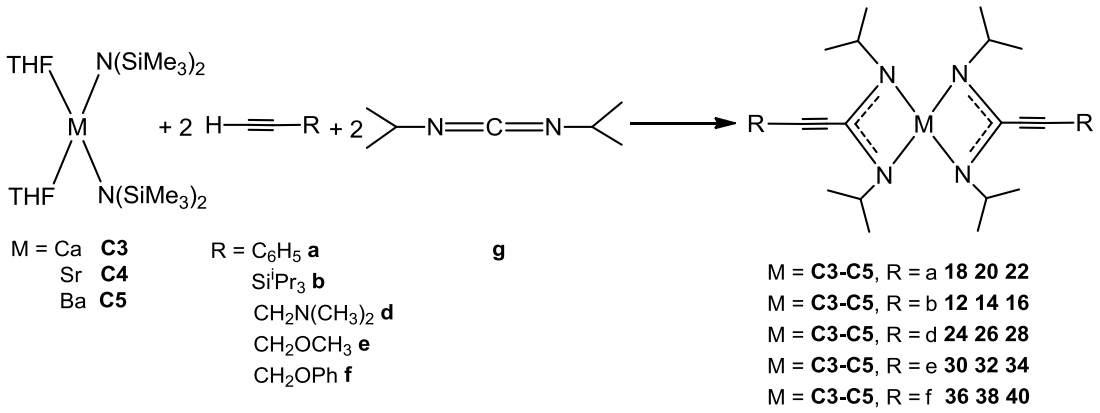

*Scheme 76: Double insertion of N,N'-di-iso-propylcarbodiimide **g**.*

However, replacing the *iso*-propyl groups on the carbodiimide with the larger, more bulky cyclohexyl groups evidently hindered the second insertion reaction. Apparently the complete insertion as observed with the previous carbodiimide was prevented as a result of the increased size of the 1,3-dicyclohexylcarbodiimide, **h**. In this case the carbodiimide was only able to undergo a single insertion process, leaving the second acetylide unit untouched, scheme 77.

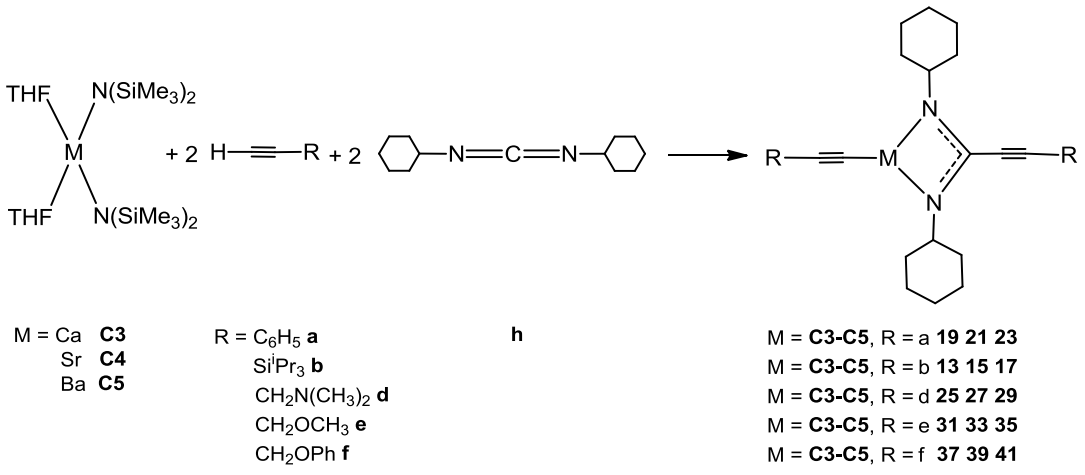

*Scheme 77: Acetylide co-ordination and the single insertion of 1,3-dicyclohexylcarbodiimide **h***

Compound	Formula	Molc. Wt(g)	% Yield	calculated % C	calculated % H	calculated % N	found % C	found % H	found % N
12	$C_{36}H_{70}CaN_4Si_2$	655.22	23	65.99	10.77	8.55	65.96	10.78	8.47
13	$C_{35}H_{64}CaN_2Si_2$	609.15	25	69.01	1059	4.60	68.89	10.50	4.56
14	$C_{36}H_{70}N_4Si_2Sr$	702.76	24	61.53	10.04	7.93	-	-	-
15	$C_{35}H_{64}N_2Si_2Sr$	656.69	25	64.01	9.82	4.27	63.92	9.80	4.37
16	$C_{36}H_{70}BaN_4Si_2$	752.47	8	57.46	9.38	7.45	57.55	9.28	7.39
17	$C_{35}H_{64}BaN_2Si_2$	706.39	38	59.51	9.31	3.97	59.61	9.30	4.05
18	$C_{30}H_{38}CaN_4$	494.73	31	72.83	7.74	11.32	72.82	7.66	11.37
19	$C_{29}H_{32}CaN_2$	448.66	23	77.63	7.19	6.24	77.56	7.12	6.19
20	$C_{30}H_{38}N_4Sr$	542.27	31	66.45	7.06	10.33	65.53	6.96	10.30
21	$C_{29}H_{32}N_2Sr$	496.20	33	70.20	6.50	5.65	69.98	6.56	5.52
22	$C_{30}H_{38}BaN_4$	591.98	31	60.87	6.47	9.46	60.91	6.50	9.51
23	$C_{29}H_{32}BaN_2$	545.90	33	63.80	5.91	5.13	63.78	5.89	5.26
24	$C_{24}H_{44}CaN_6$	456.72	33	63.11	9.71	18.40	63.31	9.36	18.40
25	$C_{23}H_{38}CaN_4$	410.65	37	67.27	9.33	13.64	67.30	9.41	13.61
26	$C_{24}H_{44}N_6Sr$	504.27	33	57.16	8.79	16.67	57.15	8.77	16.53
27	$C_{23}H_{38}N_4Sr$	458.19	36	60.29	8.36	12.23	60.77	8.48	12.08
28	$C_{24}H_{44}BaN_6$	553.97	30	52.03	8.01	15.17	40.47	7.00	9.99
29	$C_{23}H_{38}BaN_4$	507.90	36	54.39	7.54	11.03	54.83	7.66	10.94
30	$C_{22}H_{38}CaN_4O_2$	430.64	36	61.36	8.89	13.01	61.28	8.81	12.97
31	$C_{21}H_{32}CaN_2O_2$	384.57	40	65.59	8.39	7.28	66.04	8.52	7.23
32	$C_{22}H_{38}N_4O_2Sr$	478.18	35	55.26	8.01	11.72	-	-	-
33	$C_{21}H_{32}N_2O_2Sr$	432.11	39	58.37	7.46	6.48	58.47	7.52	6.50
34	$C_{22}H_{38}BaN_4O_2$	527.89	11	50.06	7.26	10.61	49.96	7.25	10.52
35	$C_{21}H_{32}BaN_2O_2$	481.82	15	52.35	6.69	5.81	-	-	-
36	$C_{32}H_{42}CaN_4O_2$	554.78	27	69.28	7.63	10.10	69.29	7.59	9.97
37	$C_{31}H_{36}CaN_2O_2$	508.71	30	73.19	7.13	5.51	73.19	7.23	5.51
38	$C_{32}H_{42}N_4O_2Sr$	602.32	27	63.81	7.03	9.30	-	-	-
39	$C_{31}H_{36}N_2O_2Sr$	556.25	30	66.94	6.52	5.04	66.87	6.62	5.12
40	$C_{32}H_{42}BaN_4O_2$	652.03	19	58.95	6.49	8.59	58.90	6.44	8.57
41	$C_{32}H_{36}BaN_2O_2$	605.96	40	61.45	5.99	4.62	61.45	6.03	4.54

*Table 23: Carbodiimide insertion with homoleptic catalysts **C3-5**.*

Just as with reactions performed with calcium β-diketiminato amide **C1**, the ^{1}H NMR spectra indicated the insertion of the carbodiimide with the homoleptic amides **C3**, **C4** and **C5** for products **12-41** with the disappearance of the terminal proton resonance of the acetylene around 2.0 ppm and the appearance of a sharp singlet resonance at 0.09 ppm for the newly protonated $HN(SiMe_3)_2$.

The ^{1}H NMR spectra from the insertion of di-*iso*-propylcarbodiimide **g** and 1,3-dicyclohexylcarbodiimides **h** with the acetylenes, phenyl acetylene **a**, tri-*iso*-propylsilyl acetylene **b**, 3-dimethylamino-1-propyne **d**, methyl propargyl ether **e** and phenyl propargyl ether **f** showed down-field shifts for amidate compounds **12-41** in comparison to their starting materials, regardless of the group 2 metal employed.

The resonances observed for the tri-*iso*-propylsilyl acetylene/acetylide unit, **b**, of the complexes **12-17**, table 24, displayed down-field shifts of up to 0.1 ppm for the silyl *iso*-propyl methyl resonances and up to 1.78 ppm for the CH signals compared to their respective resonances on the free acetylene. The di-*iso*-propylcarbodiimide **g** also produced down-field shifts of 0.3-0.4 ppm for the ^{i}PrCH$_3$ and 0.9-1.0 ppm for the ^{i}PrCH whilst the larger 1,3-dicyclohexylcarbodiimide **h**, induced similar shifts of up to 0.4 ppm for the cy-CH$_2$ and 0.8 ppm for the cy-CH.

	b		**g**		**h**	
Compound	Si^{i}PrCH$_3$ d	Si^{i}PrCH m	^{i}PrCH$_3$ d	^{i}PrCH m	cy-CH$_2$ m	cy-CH m
12	1.10	3.77	1.35, 1.41	4.23	-	-
13	1.17	3.14	-	-	1.95	3.87
14	1.10	3.80	1.36	4.19	-	-
15	1.17	3.03	-	-	1.81	3.87
16	1.18	3.78	1.34, 1.45	4.35	-	-
17	1.20	3.14	-	-	1.60	3.92

s = singlet, d = doublet and m = multiplet resonances.

*Table 24: ^{1}H NMR resonances in ppm for compounds **12-17**.*

The ^{1}H NMR data for the insertion compounds **18-23** are given in table 25. The resonances observed for the phenyl acetylene/acetylide unit, **a**, indicated no change in the phenyl environments or the CH$_2$ of 1,3-dicylcohexylcarbodiimide, **h**, while the CH experienced down-field shifts between 0.82-1.14 ppm compared to the respective resonances on the free acetylene and carbodiimide. However, the di-*iso*-propylcarbodiimide **g**, produced down-field shifts of up to 0.31 ppm for the ^{i}PrCH$_3$ and 0.28-0.93 ppm for the ^{i}PrCH.

Compound	**a** Ph m	**g** $^{i}PrCH_3$ d	$^{i}PrCH$ m	**h** cy-CH_2 m	cy-CH m
18	6.95, 7.36	0.97, 1.39	4.26	-	-
19	6.96, 7.44	-	-	1.53	4.00
20	6.90, 7.38	1.17, 1.22	3.61	-	-
21	6.95, 7.39	-	-	1.57	4.25
22	6.95, 7.39	0.98, 1.40	4.25	-	-
23	6.96, 7.42	-	-	1.53	3.93

d = doublet and m = multiplet resonances.

*Table 25: ^{1}H NMR resonances in ppm for compounds **18-23**.*

Summarised in tables 26-28, the ^{1}H NMR data from compounds **24-41**, obtained from carbodiimide insertion with donor-functionalised acetylenes, displayed down-field shifts for both carbodiimide compounds and the 3-dimethylamino-1-propyne **d** and methyl propargyl ether **e** derivatives while phenyl propargyl ether **f** experienced an up-field shift. The acetylene CH_2 resonances in compounds **24-35** were found to undergo down-field shifts of 0.24 ppm. Both methyl units on 3-dimethylamino-1-propyne **d** and methyl propargyl ether **e** gave shifts of more than 0.12 ppm and 0.89 ppm respectively while no comparisons were observed in the phenyl region of the spectrum.

Di-*iso*-propylcarbodiimide **g**, produced down-field shifts of up to 0.43 ppm for the $^{i}PrCH_3$ and 0.9 ppm for $^{i}PrCH$ when inserted to 3-dimethylamino-1-propyne, **d**, while the more sterically demanding 1,3-dicyclohexylcarbodiimide **h**, was found to have experienced a shift of up to 0.78 ppm for the cy-CH. Similar results were observed with the other donor-functionalised acetylenes, methyl propargyl ether **e** and phenyl propargyl ether **f**, tables 26-28.

Compound	d		g		h	
	NCH_2 d	NMe_2 s	$^iPrCH_3$ m	^iPrCH m	cy-CH_2 m	cy-CH m
24	3.22	2.18	1.37, 1.47	4.22	-	-
25	3.27	2.25	-	-	1.54	3.82
26	3.13	2.12	1.16	3.73	-	-
27	3.19	2.17	-	-	1.54	3.88
28	2.52	2.22	1.00, 1.42	4.23	-	-
29	2.55	2.22	-	-	1.57	3.86

s = singlet, d = doublet and m = multiplet resonances.

*Table 26: ^1H NMR resonances in ppm for compounds **24-29**.*

Compound	e		g		h	
	OCH_2 d	OMe s	$^iPrCH_3$ m	^iPrCH m	cy-CH_2 m	cy-CH m
30	3.90	3.97	1.04, 1.43	3.79	-	-
31	3.99	3.24	-	-	1.47	3.77
32	3.42	2.91	1.10, 1.42	4.51	-	-
33	4.00	3.24	-	-	1.33	3.86
34	3.84	3.05	0.94, 1.33	4.11	-	-
35	3.86	3.11	-	-	1.47	3.81

s = singlet, d = doublet and m = multiplet resonances.

*Table 27: ^1H NMR resonances in ppm for compound **30-35**.*

Compound	f		g		h	
	OCH_2 d	OPh m	$^iPrCH_3$ m	^iPrCH m	cy-CH_2 m	cy-CH m
36	4.30	6.80, 7.04	0.89, 1.03	4.03	-	-
37	4.37	6.81, 7.08	-	-	1.56	3.61
38	4.29	6.81, 7.04	1.22	4.05	-	-
39	4.42	6.91, 7.07	-	-	1.72	3.65
40	4.32	6.89, 7.04	1.30, 1.47	4.41	-	-
41	4.53	6.82, 6.96	-	-	1.57	4.46

d = doublet and m = multiplet resonances.

*Table 28: ^1H NMR resonances in ppm for compounds **36-41**.*

The $^{13}C\{^{1}H\}$ NMR spectra of compounds **12-41** also indicated that the stoichiometry of the insertion reactions and the amidinate compounds formed was dependent upon the carbodiimide employed. As proposed earlier, the carbodiimides were observed to undergo either mono or bis insertion dependent upon the steric demands of the carbodiimide, figure 22. The different C≡C environments generated during the insertion reactions are indicated in the ^{13}C NMR spectra, table 29.

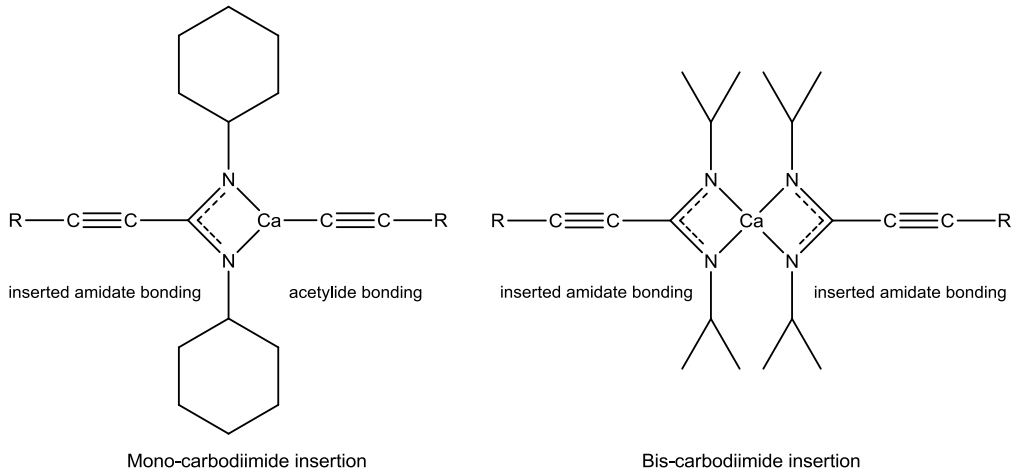

Figure 22: Mono and bis carbodiimide insertion.

The less sterically hindered di-*iso*-propylcarbodiimide **g**, underwent a double insertion thus producing a single C≡C environment observed in the NMR spectra with two resonances between 72 and 100 ppm.

In contrast, the more sterically demanding 1,3-dicyclohexylcarbodiimide **h**, underwent single insertion resulting in the formation of a single amidinate and retention of an acetylide ligand. The structure was supported in the ^{13}C NMR spectra with a resonance that was not only similar to those observed with di-*iso*-propylcarbodiimide **g**, with the two resonances between 74 and 98 ppm for the amidinate environment, but also resonances slightly further up-field between 78 and 99 ppm corresponding to the C≡C of the terminal acetylide. In the absence of any corroborative X-ray data however, (*vide infra*) it was not possible to determine whether the acetylide existed as a terminal or bridging moiety.

Bis-insertion g		Compound	Mono-insertion h			
$N_2C\mathbf{C}{\equiv}CR$	$N_2CC{\equiv}\mathbf{C}R$		$N_2C\mathbf{C}{\equiv}CR$	$N_2CC{\equiv}\mathbf{C}R$	$RC{\equiv}\mathbf{C}M$	$R\mathbf{C}{\equiv}CM$
96.0	100.8	**12**	-	-	-	-
-	-	**13**	96.0	96.4	97.8	99.6
92.8	97.6	**14**	-	-	-	-
-	-	**15**	95.2	95.7	98.2	99.0
93.8	99.7	**16**	-	-	-	-
-	-	**17**	94.3	94.8	97.8	98.7
79.7	95.3	**18**	-	-	-	-
-	-	**19**	80.1	94.8	81.1	97.2
85.5	90.3	**20**	-	-	-	-
-	-	**21**	81.2	82.5	90.2	97.0
80.9	90.3	**22**	-	-	-	-
-	-	**23**	80.9	81.2	90.2	97.1
90.2	94.6	**24**	-	-	-	-
-	-	**25**	93.7	94.0	97.5	98.8
77.0	86.6	**26**	-	-	-	-
-	-	**27**	94.6	95.2	97.7	98.6
82.3	84.9	**28**	-	-	-	-
-	-	**29**	89.6	94.7	96.6	98.4
72.2	82.4	**30**	-	-	-	-
-	-	**31**	82.8	85.8	96.4	97.5
89.4	95.1	**32**	-	-	-	-
-	-	**33**	74.3	78.2	94.4	97.5
77.8	86.7	**34**	-	-	-	-
-	-	**35**	78.1	85.3	86.7	95.4
78.6	91.4	**36**	-	-	-	-
-	-	**37**	77.8	78.8	90.1	92.7
83.9	92.3	**38**	-	-	-	-
-	-	**39**	83.3	86.6	92.7	95.1
84.2	95.4	**40**	-	-	-	-
-	-	**41**	81.3	84.9	90.0	91.2

*Table 29: ^{13}C NMR resonances in ppm for compounds **12-41**.*

Due to the highly soluble nature of the amidinate compounds the only isolated crystal suitable for X-ray crystallography was obtained for compound **19**. Interestingly the X-ray structure obtained for compound **19** did not support the structure proposed from the elemental and NMR analyses for a single amidinate insertion and a single acetylide ligand. Instead the X-ray structure revealed a structure which was the product of complete insertion of the larger 1,3-dicyclohexylcarbodiimide **h**, around the calcium metal centre resulting in the formation of the dimeric amidinate complex with both terminal and bridging modes, figure 23. However, this bis-insertion was only considered to occur with the simpler di-*iso*-propylcarbodiimide **g**, as it is less bulky and therefore less hindered around the metal centre, thus making insertion more likely.

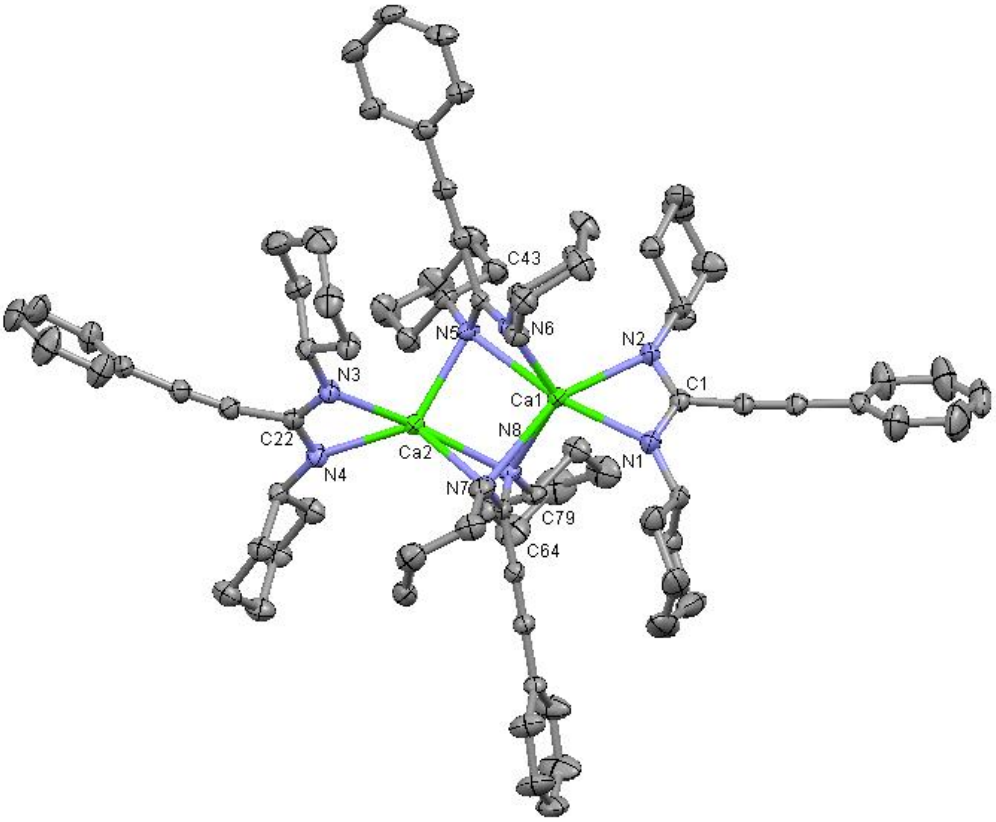

*Figure 23: Compound **19**, ellipsoids drawn at 30% probability. H-atoms and iso-propyl methyl groups removed for clarity. Shows the insertion of bridging and terminal phenyl acetylide to 1,3-dicyclohexyl carbodiimide **h** with the homoleptic calcium bis(bis(trimethylsilyl)amide) **C3**.*

Although bridging and terminal carbodiimide insertion was not predicted in this compound, the bond lengths and angles were found to be similar to those previously reported by Hill and co-workers for the dimeric guanidinate complex [10] consisting of both bridging and terminal carbodiimide insertion, figure 24.

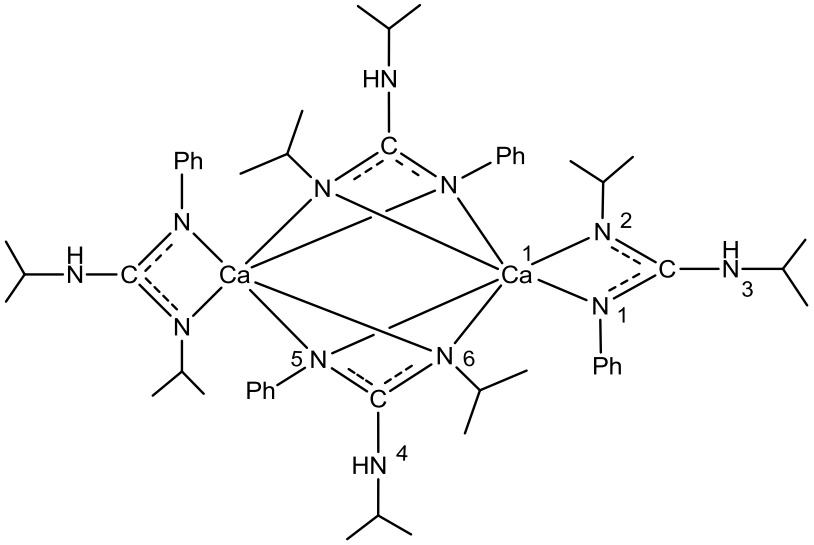

Figure 24: Dimeric guanidinate compound reported by Hill and co-workers shows both the terminal and bridging carbodiimide insertion. [10]

Comparisons between the bond lengths and angles of these two compounds are shown in table 30. Whilst the bridging bond length, Ca(1)-N(5), show a difference of almost 0.2 Å between the two compounds, the bridging Ca(1)-N(6) bond length and bond angle N(1)-C(1)-N(2), along with the terminal bond lengths are consistent for both compounds, **19** and guanidinate.

Bond lengths (Å)	**19**	**Guanidinate (fig 24)** [10]
Ca(1)-N(1)	2.3860(16)	2.3748(11)
Ca(1)-N(2)	2.3889(16)	2.3604(11)
Ca(1)-N(5)	2.6082(16)	2.4269(11)
Ca(1)-N(6)	2.4067(15)	2.4009(11)
N(1)-C(1)	1.330(2)	-
N(2)-C(1)	1.327(3)	-
N(2)-C(43)	1.350(2)	-
N(6)-C(43)	1.321(2)	-
Bond angles (°)		
N(1)-C(1)-N(2)	57.09(6)	57.45(4)
N(1)-Ca(1)-N(6)	124.86(6)	-
N(2)-Ca(1)-N(6)	106.44(6)	-

*Table 30: Selected bond lengths and bond angles of compound **19** and the guanidinate complex reported by Hill and co-workers.* [10]

4.6 Conclusion

This chapter has discussed how the heteroleptic or the homoleptic nature of the group 2 starting material, and the size of the substituents on a di-*iso*-propylcarbodiimide **g** and 1,3-dicyclohexylcarbodiimide **h**, can influence the structure of the final amidinate insertion product.

The insertion with the homoleptic group 2 bis(bis(trimethylsilyl)amides), **C3-C5**, gave the most interesting results as it was observed from the elemental analysis and the NMR data that the size of the substituent on the carbodiimide did in fact determine the composition of the final amidinate compound. From the elemental analysis and the NMR data it was observed that the insertion of the smaller, less sterically demanding N,N'-di-*iso*-propylcarbodiimide **g**, would produce an amidinate complex where the group 2 metal acetylide underwent a double insertion, while the larger 1,3-dicyclohexylcarbodiimide **h**, would only be capable of a single insertion.

However, the structural assumptions resulting from the insertion of these carbodiimides were re-addressed following the X-ray diffraction of compound, **19**. The crystal structure of compound **19** indicated that the insertion had produced a dimeric bis insertion product rather than the monomeric structure initially proposed. Although the formation of monomeric complexes was initially proposed, the elemental analyses and NMR data obtained and presented in this chapter for compounds **12-41** was found to support the formation of both monomeric and dimeric stuctures. The crystal structure of compound **19** however, did not comply with this assumption. After considering this structure comparisons were made between its data and the data leading to the proposed structures. Although the ^{1}H and ^{13}C NMR spectras were unable to explicitly support the formation of either the proposed structures or that of the crystal structure, the elemental analysis was found to lie in favour of the proposed structures. Comparisons between the actual elemental analysis data and the theoretical data of the proposed monomeric/dimeric partial inserted structure **19** and the crystal structure shown in table 31.

Proposed monomeric structure		Found %	Crystal stucture	
$C_{29}H_{32}CaN_2$	Calculated %		Calculated %	$C_{42}H_{54}CaN_4$
C	77.63	77.56	77.02	C
H	7.19	7.12	8.31	H
N	6.24	6.19	8.55	N

*Table 31: Elemental analysis data supports the proposed formation of **19** but does not support the formation of its crystal structure.*

An explanation for the structural differences observed from **19**, scheme 78, is given by the stability of the complex. The high solubility of the complex makes the isolation of its crystals difficult. It is also likely that this species is highly susceptible to re-distribute in solution to its more stable bis-amidinate form. It is this stable form that is consequently characterised by elemental analysis and NMR spectroscopy.

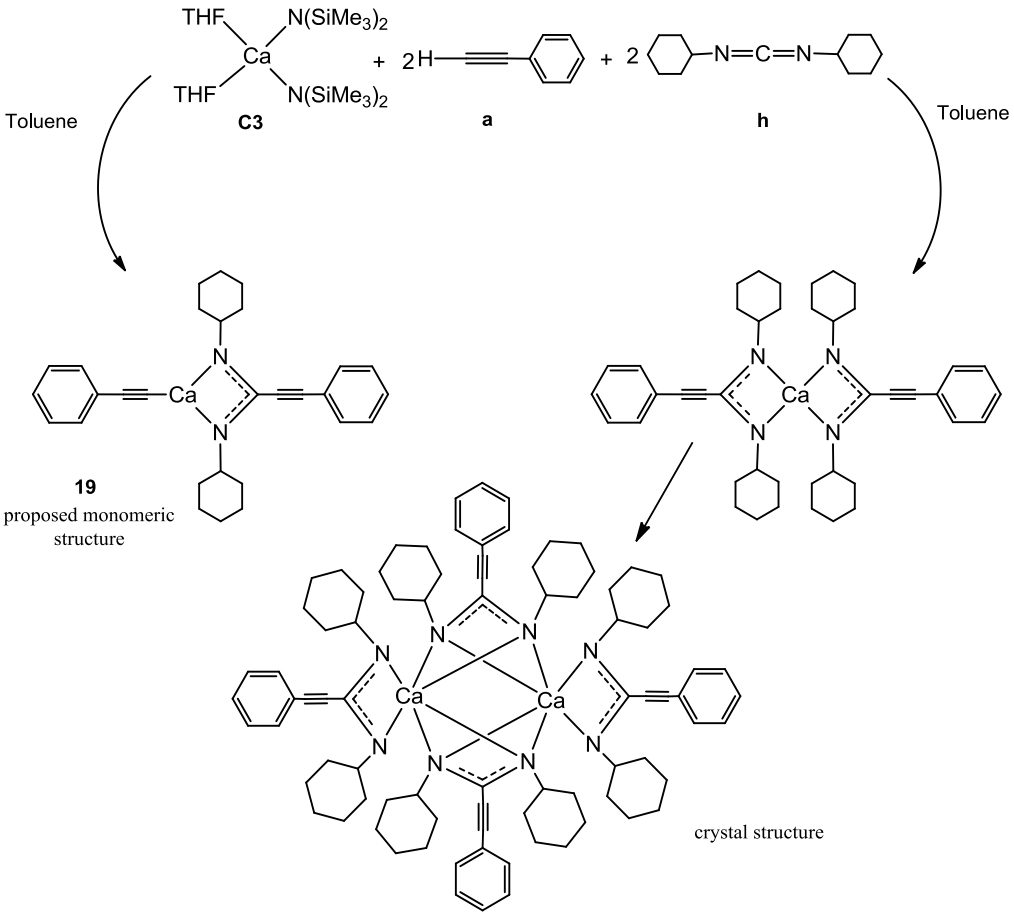

*Scheme 78: Mechanism of possible insertion of compound **19**. Supported by ^{1}H NMR spectroscopy, the proposed monomeric structure shows both insertion and terminal acetylide co-ordination. The crystal structure is a dimer of the proposed bis insertion amidinate.*

Consequently the new proposed route to the formation of the dimeric complex with the insertion of the N'N'-di-*iso*-propyl carbodiimide, **g**, results in both terminal and bridging insertion, scheme 79. While the new proposed mechanism for the insertion of the 1,3-dicyclohexylcarbodiimide, **h**, results in a partial insertion with a bridging dimer and a terminal acetylide, scheme 80.

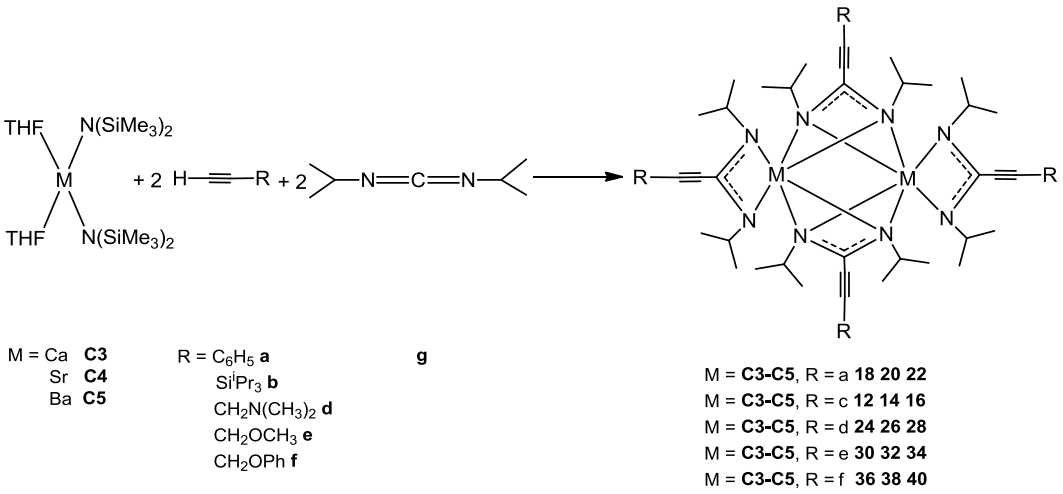

*Scheme 79: Proposed mechanism of the terminal and bridged inserted dimer with N,N'-di-iso-propylcarbodiimide **g**.*

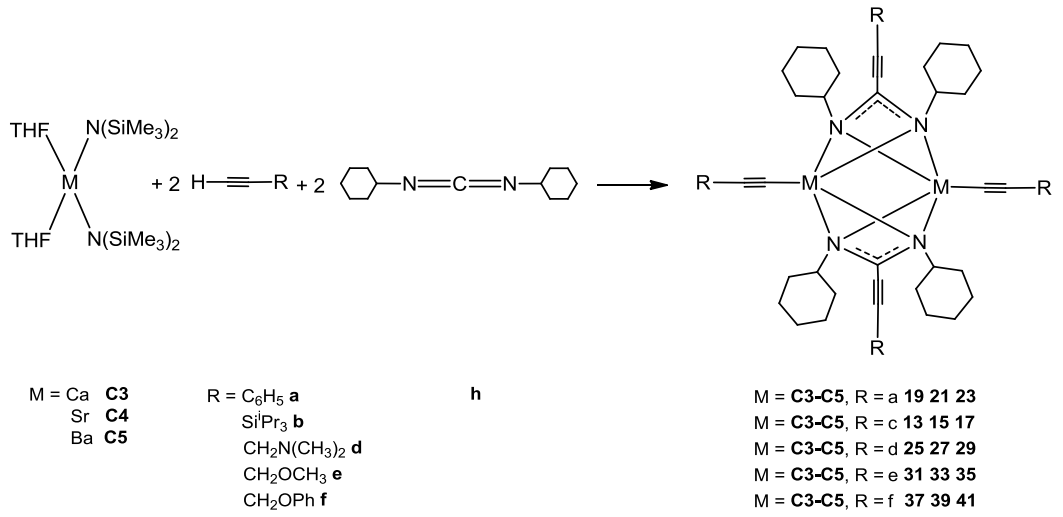

*Scheme 80: Revised mechanism of the terminal acetylide and the inserted bridged dimer with 1,3-dicyclohexylcarbodiimide **h**.*

Chapter 5

5.0 Isocyanate insertion of group 2 acetylides

5.1 Introduction

This chapter aims to develop the work discussed in the previous chapter on the insertion of the symmetrically unsaturated RN=C=NR bonds of a carbodiimide with the insertion of an unsymmetrically unsaturated isocyanate (RN=C=O). This thesis seeks to present the formation of the first C-C bond via the insertion reactivity of an isocyanate with a heavier alkaline earth metal acetylide. Following the same principles as outlined with the carbodiimide insertion in chapter 4, the mechanism for the insertion of an isocyanate is proposed to proceed via the formation of an acetylide intermediate, scheme 81.

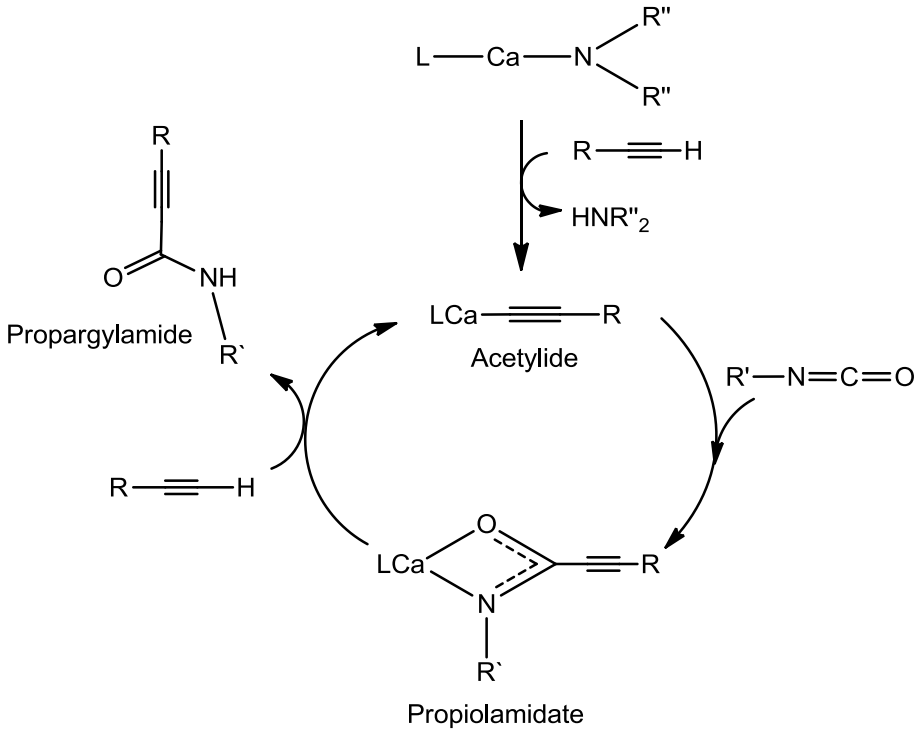

Scheme 81: Proposed catalytic cycle of the isocyanate insertion to a group 2 acetylide.

The chapter looks toward the formation and isolation of a range of amidate intermediate complexes with group 2 metal catalysts and the ability to proceed catalytically with the formation of the free propargylamide product, (R'NH=C(R)=O).

5.1.1 Isocyanate insertion chemistry

This thesis strives present the first known direct insertion of an isocyanate derivative to a metal-carbon bond of an acetylide. Before proceeding with the isocyanate insertion, this chapter will aim to provide a brief understanding of the range of chemistry previously reported for the isocyanate derivatives.

Huang et al. reported [61] the insertion of phenyl isocyanate and a re-arrangement to an aluminium compound $[C_4H_3N(CH_2NMe_2)]AlMe_2$ to yield a seven-membered cycloaluminium compound, scheme 82.

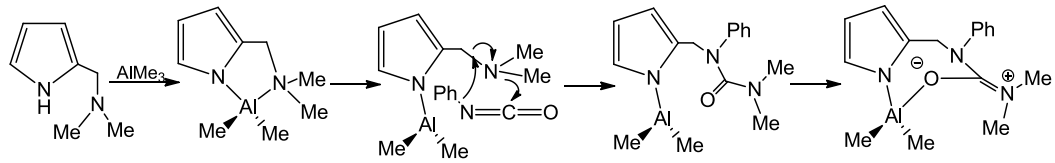

Scheme 82: Phenyl isocyanate insertion and re-arrangement via C-N bond breaking and forming. [61]

Ruthenium half-sandwich metal complexes stabilised by a silylene moiety $[Cp^*(PMe_3)_2Ru{=}Si(SR)_2]^+ \ ^-X$, where R = Me, Ph, *p*-Tol and X = BPh_4, OTf, were reportedby by Tilley and co-workers [62] for the addition of isocyanates via the displacement of $^-BPh_4$ and $^-$OTf units, scheme 83.

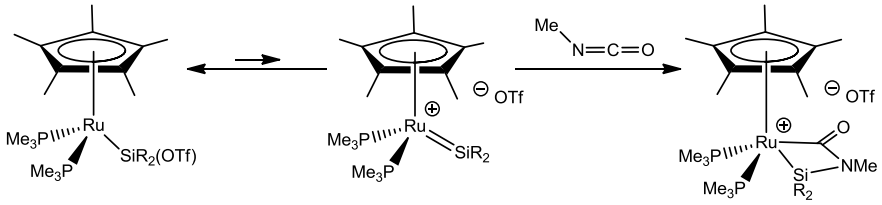

Scheme 83: Isocyanate insertion to a ruthenium complex via $^-$OTf displacement. [62]

Matsuda and co-workers [63] studied the hydrocarbymoylation of alkenes with a rhodium catalyst $[Rh(cod)\{P(OPh)_3\}_2]OTf$, (cod = 1,5-cyclooctadiene), via a three-component coupling. The reaction rate and yield was found to be dependent upon the phosphine and was significantly decreased with a bulkier bidentate, phosphine ligand 1,4-bis(diphenylphosphine)butane, (dppb). Insertion of the isocyanate was not affected by the phenyl substituents.

Reporting Rh(I)P(4-MeO-C_6H_4)$_3$ catalysed (2+2+2) cycloaddition of pentenyl isocyanate and a range of terminal acetylenes, Rovis and co-workers [64-68] continued their work by controlling the enantioselectivity of the reaction by changing the ligand, scheme 84. Large substituents were found to favour the vinylogous amides while the lactam derivative is favoured by smaller substituents.

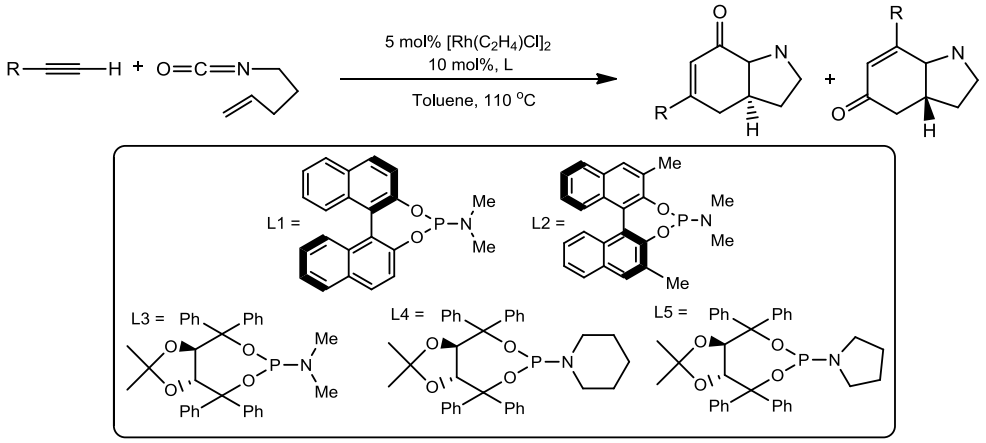

Scheme 84: Ligand dependent enantioselective synthesis. [65]

Samuelson and co-workers [69] reported the single and double insertion reaction of phenyl isocyanate with the titanium and zirconium metal complexes, Ti(O^{n}Bu)$_4$ and Zr(O^{n}Bu)$_4$. The insertion of a single phenyl isocyanate into a Ti-OR bond of Ti(O^{n}Bu)$_4$ resulted in mono-insertion to one oxygen-titanium bond while forming a dimeric complex scheme 85 (a). The addition of two equivalents of the isocyanate to Zr(O^{n}Bu)$_4$ required hydrolysis to isolate the products, (b) whereas the double insertion of Zr(O^{n}Bu)$_4$ was observed with three equivalents (c).

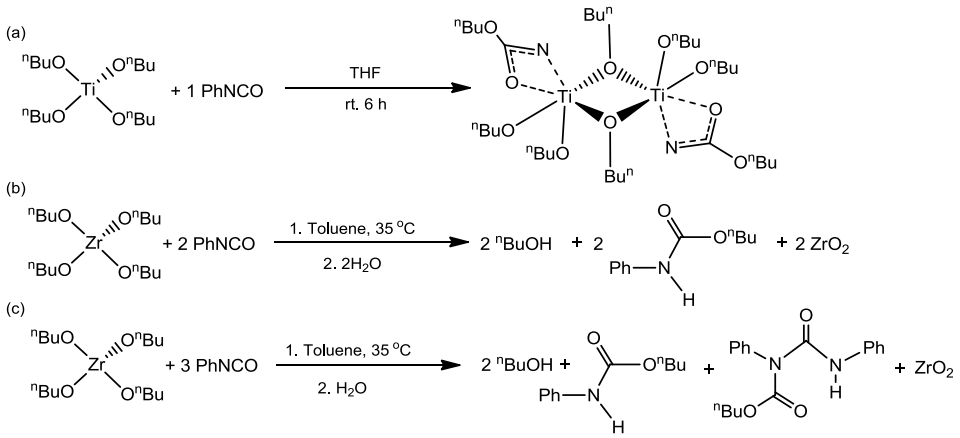

Scheme 85: Mono-insertion of phenyl isocyanate to (a) Ti(O^{n}Bu)$_4$, (b) Zr(O^{n}Bu)$_4$. Bis-insertion of phenyl isocyanate to (c) Zr(O^{n}Bu)$_4$. [69]

Schulz and co-workers [70] synthesised zinc amidate complexes via the insertion of a range of isocyanates with $ZnMe_2$, $[MeZnOC(Me)NR]_x$, R = ^{i}Pr, ^{t}Bu. Shen and co-workers [71] reported the insertion of phenyl isocyanate into an Nd-S bond to yield $[(CH_3C_5H_4)_2Nd]_2[\mu\text{-}\eta^2\text{-}OC(SPh)NPh]_2$. Zhou and co-workers [72] reported isocyanate insertion into a Ln-C σ-bond with the formation of a dinuclear $[Cp^*_2LnOC(^{n}Bu)NPh]_2$, Ln = Sm, Dy, Er, scheme 86.

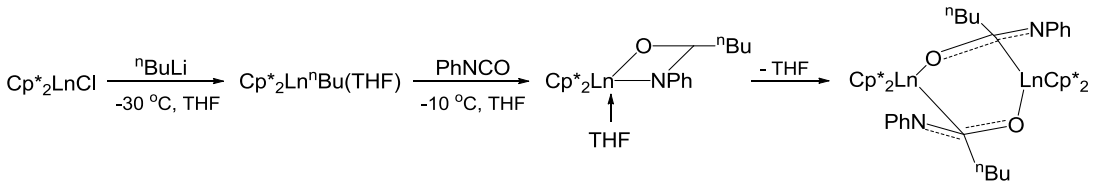

Scheme 86: Isocyanate insertion into a Ln-C σ-bond. [72]

A tetranuclear tetrahydride yttrium complex was reported by Hou et al. [73] following aryl isocyanate insertion. The insertion of an isocyanate into a lanthanide-sulphur bond was reported by Zhang [74] resulting in the formation of a four-centred σ-bond metathesis, scheme 87.

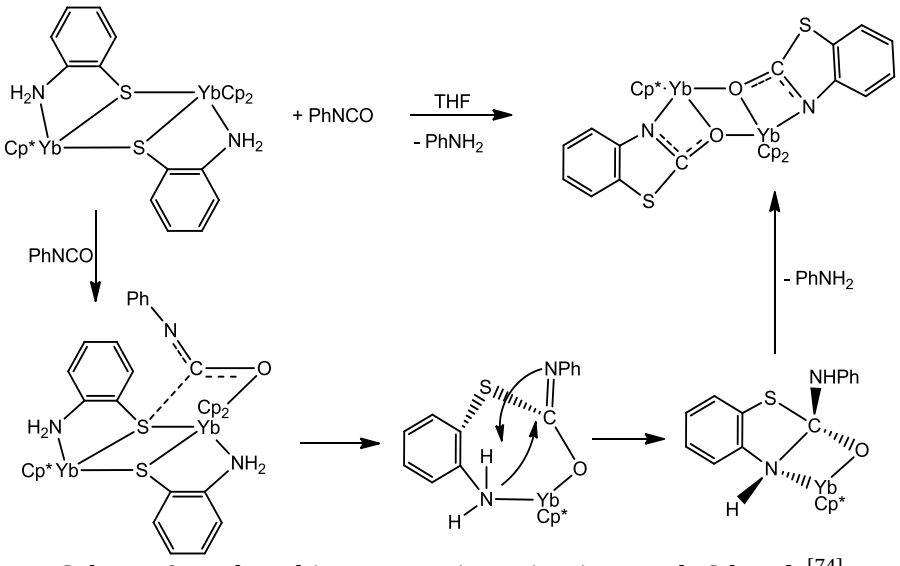

Scheme 87: Phenyl isocyanate insertion into a Yb-S bond. [74]

In 2006 Zhang and co-workers [75] extended their work to lanthanocene hydroxides with the formation of $[Cp_2Y(THF)]_2(\mu\text{-}\eta^2\text{:}\eta^2\text{-}O_2CNPh)$. The addition of phenyl isocyanate to a trinuclear lanthanide cyclic complex $[Cp_2Ln(\mu\text{-}Im)]_3$ Ln = Yb, Er yielded a bridging metallomacrocycle, [76] scheme 88.

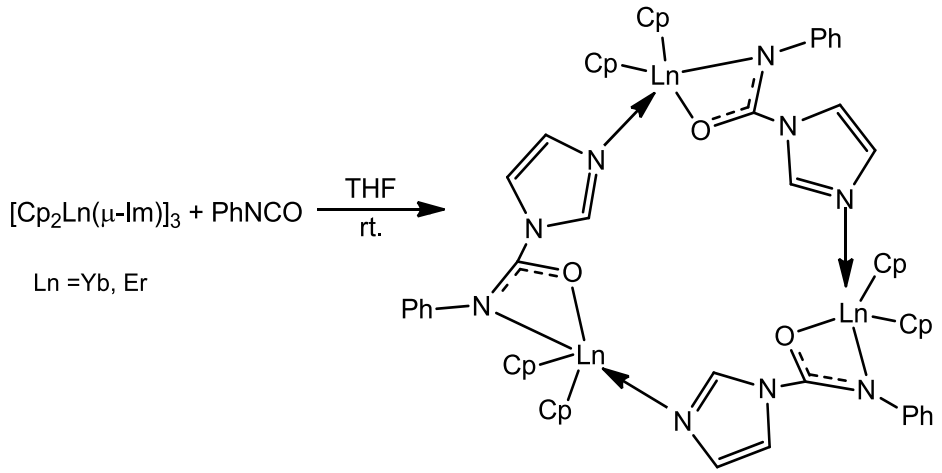

Scheme 88: Formation of a bridging lanthanide metallocenemacrocycle. [76]

Cyclopentadienyl ligands are employed to stabilise the lanthanide metal during the insertion of an isocyanate. However, Wang and co-workers [77] reported the stabilisation with a bidentate amide ligand, scheme 89.

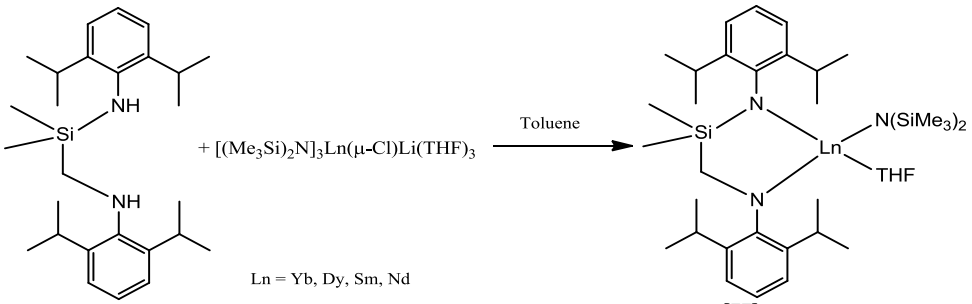

Scheme 89: Amide ligand stabilisation. [77]

Evans and co-workers [78] inserted an isocyanate into the uranium-alkynyl bonds of $[Cp^*_2U(C{\equiv}CPh)_2]$. The uranium centre stabilised by two Cp^* ligands underwent a double insertion, scheme 90.

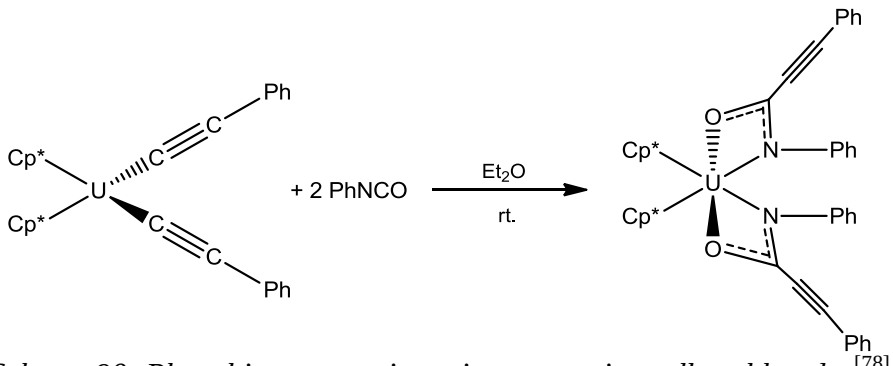

Scheme 90: Phenyl isocyanate insertion to uranium-alkynyl bonds. [78]

Use of a lanthanide thiolate in the cyclisation of isocyanates [79] was found to proceed more efficiently in polar solvents such as 1,3-diphenylurea while no reaction was observed in non-polar solvents. Following cyclisation, carbon monoxide elimination yielded the free product, scheme 91.

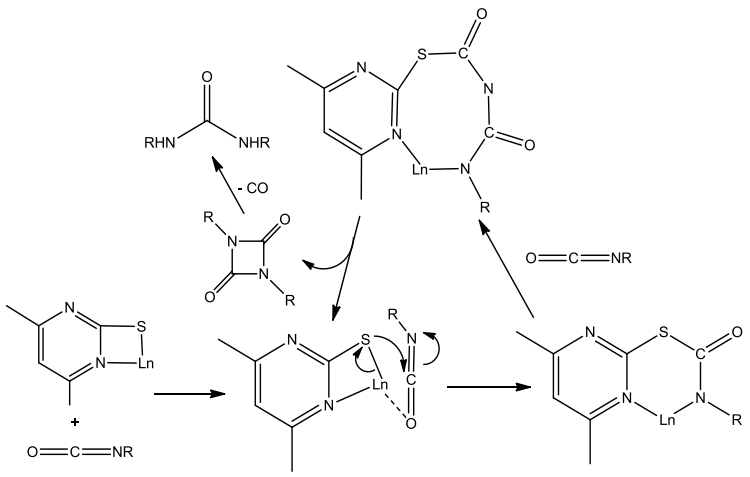

Scheme 91: Proposed catalytic mechanism for the cyclo-dimerisation of isocyanate. [79]

5.2 Synthesis of alkaline earth propiolamidates with isocyanates

Similar to the work in the previous chapter, the isocyanate insertion to alkaline earth acetylide complexes was conducted on both catalytic and preparative scales with phenyl acetylene **a**, tri-*iso*-propylsilyl acetylene **b**, 3-dimethylamino-1-propyne **d**, methyl propargyl ether **e** and phenyl propargyl ether **f**. The insertion was proposed to occur via the formation of the intermediate propargylamidate complexes, scheme 92, which could be isolated and characterised under stoichiometric conditions. However, before proceeding with the insertion of the isocyanate, the reaction catalysis was first initially conducted catalytically.

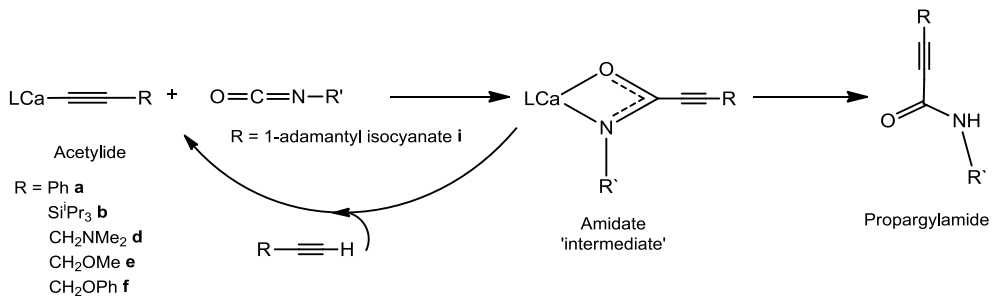

Scheme 92: Proposed catalytic cycle of the insertion of an unsaturated isocyanate to a group 2 acetylide.

5.3 Attempted catalytic synthesis of alkaline earth propiolamidates

The catalytic insertion of 1-adamantyl isocyanate **i** was initially conducted in a Youngs NMR tube in deuterated benzene (C_6D_6) with 5 mol% catalytic loadings of calcium β-diketiminato amide **C1** and calcium, strontium and barium bis(bis(trimethylsilyl)amides) **C3**-**C5**. However the reaction progress, monitored by ^{1}H NMR spectroscopy gave no indication of the reactions being catalytic. The absence of catalysis within these reactions was proposed to result from the acidity of the acetylenes being insufficient in the protonolysis of the amidate intermediate.

Interestingly, reaction with the donor-functionalised acetylenes, 3-dimethylamino-1-propyne **d**, methyl propargyl ether **e** not only failed to inspire catalytic turnover for the insertion of 1-adamantyl isocyanate **i** but also the observation of the C-C coupling discussed in chapter 3 of this thesis. Consequently, further 1-adamantyl isocyanate **i** insertion reactions were only conducted on preparative scales.

5.4 Stoichiometric synthesis of alkaline earth propiolamidates

Despite unsuccessful catalytic insertion of 1-adamantyl isocyanate **i** to alkaline earth acetylides, stoichiometric insertion was found to be productive with several alkaline earth metal complexes; the calcium β-diketiminato amide **C1** and calcium, strontium and barium bis(bis(trimethylsilyl)amides) **C3**-**C5** and calcium and strontium triazenide **C6**-**C7**. Although it is likely that the isocyanate inserts into the metal-carbon bond of the acetylide intermediate complex, for convenience, subsequent reactions were undertaken in a single step from the acetylide starting materials.

5.4.1 Synthesis of heteroleptic alkaline earth propiolamidates

The insertion reaction of 1-adamantyl isocyanate **i** with the heteroleptic calcium β-diketiminato amide **C1** and acetylene was conducted in a 1:1:1 ratio. The acetylene and 1-adamantyl isocyanate **i** were mixed together in a Schlenk flask with 10 ml of toluene while the calcium β-diketiminato amide **C1** was mixed in a separate flask with 10 ml of

toluene before the solutions were combined and left to stir at room temperature, scheme 93.

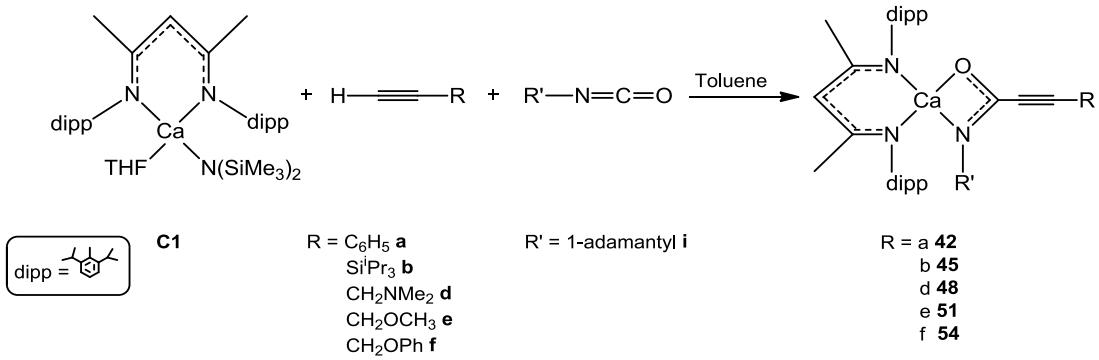

*Scheme 93: Proposed insertion of an isocyanate with the calcium β-diketiminato amide **C1** in the presence of a terminal acetylene.*

Due to the high solubility of the amidate compounds the only crystal data obtained was with compound **42**, figure 25. Similar to the amidinate complexes described earlier in this thesis, the solid state structures assume dimeric structures with the oxygen atom of the 1-adamantyl isocyanate **i** providing the bridge between the two calcium metal centres. The bridging Ca(1)-O(1) bond length of 2.4011(15) Å in compound **42** was found to correspond to the respective bridging Ca(1)-N(6) bond in compound **19** with a length of 2.4067(15) Å (chapter 4). Further interactions between the central calcium metal and the β-C of the donor-functionalised acetlyides **3**-**5** (chapter 2) is also observed in compound **42** with a bond length of 2.5317(17) Å between the calcium and the nitrogen of the 1-adamantyl isocyanate, table 32.

Bond lengths (Å)		**Bond angles (°)**	
Ca(1)-N(1)	2.3569(18)	N(1)-C(1)-N(2)	81.93(6)
Ca(1)-N(2)	2.3905(17)	C(30)-N(3)-C(39)	123.35(18)
Ca(1)-N(3)	2.5317(17)	C(30)-O(1)-Ca(1)	94.71(12)
Ca(1)-O(1)	2.4011(15)	C(30)-N(3)-Ca(1)	89.60(12)
O(1)-C(30)	1.320(2)	C(39)-N(3)-Ca(1)	145.15(13)
N(3)-C(30)	1.290(3)	N(3)-C(30)-O(1)	119.45(19)
C(30)-C(31)	1.457(3)	N(3)-Ca(1)-O(1)	54.29(5)
C(31)-C(32)	1.190(3)		

*Table 32: Selected bond lengths and bond angles of compound **42**.*

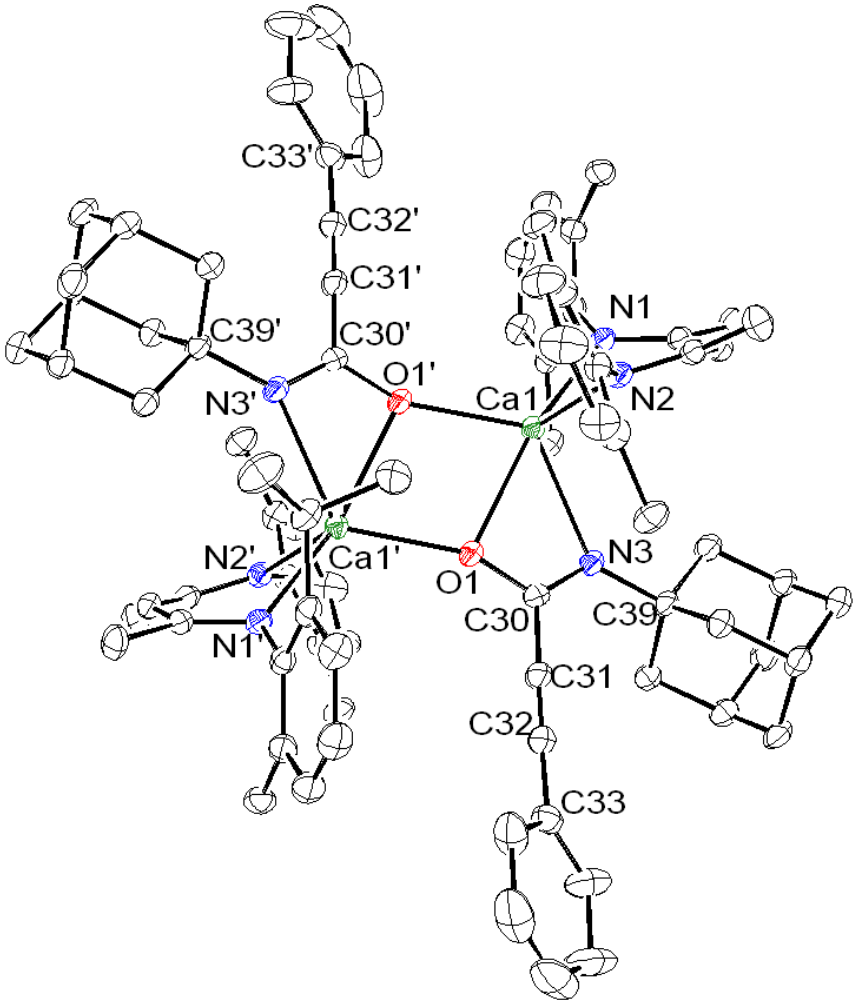

*Figure 25: Compound **42**, ellipsoids drawn at 30% probability. H-atoms and iso-propyl methyl groups removed for clarity.*

5.4.2 Synthesis of homoleptic alkaline earth propiolamidates

Although this insertion reactivity was proven to be non-catalytic the second group of catalysts employed were the homoleptic calcium, strontium and barium bis(bis(trimethylsilyl)amides) **C3-5**. As discussed earlier in this thesis, the omission of the large bulky β-diketiminato ligand, **L1** was suggested to increase the efficiency of the isocyanate insertion by preventing ligand depletion to the inactive homoleptic complex. However it is proposed the absence of this ligand enabled a double insertion on the metal centre with the formation a homoleptic inserted propargylamidate, scheme 94.

Compared to the previous methodology, the stoichiometry of these reactions was altered in order to compensate for the absence of the β-diketiminato ligand **L1** attached to the group 2 centre. Consequently both acetylene and 1-adamantyl isocyanate **i** equivalents

were doubled in respect to the calcium, strontium and barium bis(bis(trimethylsilyl)amide) complexes **C3-5**. The acetylene and 1-adamantyl isocyanate **i** were mixed in a Schlenk flask with 10 ml of toluene while the group 2 bis(bis(trimethylsilyl)amide) was dissolved in a separate Schlenk flask with 10 ml of toluene before combining and leaving to stir at room temperature. The resultant amidate complexes were obtained at -30 ^{o}C from a concentrated toluene solution.

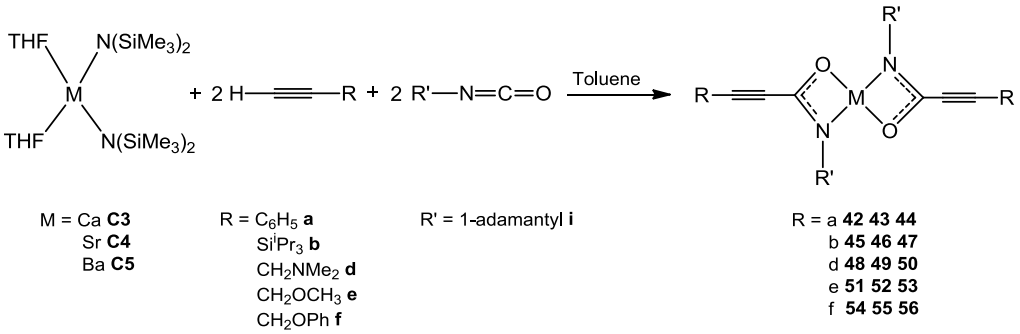

*Scheme 94: Insertion of 1-adamantyl isocyanate **i** with homoleptic group 2 metal bis(bis(trimethylsilyl)amides **C3-5**.*

5.4.3 Synthesis of the triazenide alkaline earth propiolamidates

The final group of reagents used for the insertion of the isocyanate were the calcium and strontium triazenide complexes, **C6-7**. As discussed earlier in this thesis, use of the more acidic triazene pre-ligand, **L2**, makes it less susceptible towards protonation to form inactive homoleptic complexes. It is proposed that like the heteroleptic complexes, these triazenide complexes will allow for a single insertion on the metal centre whilst remaining co-ordinated to the ligand, scheme 95.

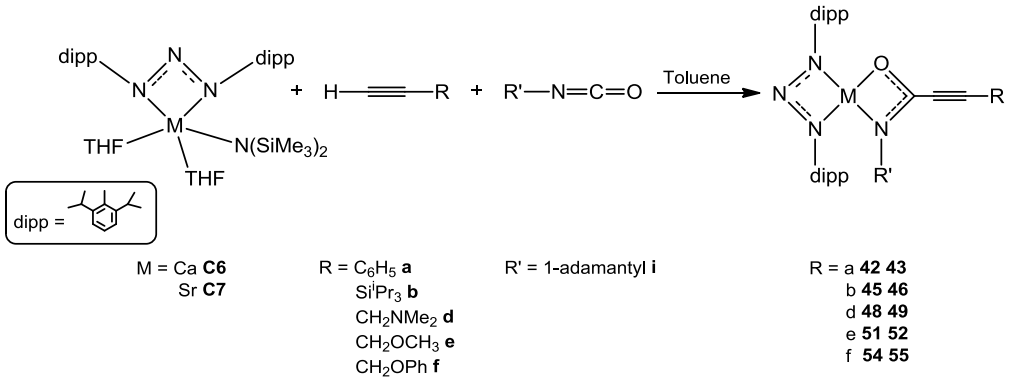

*Scheme 95: Proposed insertion reaction of 1-adamantyl isocyanate **i** with triazenide supported group 2 metal acetylides.*

5.4.4 Characterisation by elemental analysis and spectroscopy

Although the co-ordination of the β-diketimato, **L1** and triazene, **L2** ligands on the group 2 metal were proposed to discourage protonation by the formation of the inactive homoleptic complex, hence inhibit the reaction, the elemental analyses obtained for the amidates did not support the proposed 1-adamantyl isocycanate mono-insertion with the respective ligand remaining co-ordinated to the group 2 metal, schemes 93 and 95. Interestingly, the elemental analysis obtained for componds **42-56** table 33, was found to support a bis-insertion of the 1-adamantyl isocyanate, an insertion initially proposed with the homoleptic group 2 bis(bis(trimethylsilyl)amide **C3-5**, scheme 94.

Compound	Formula	Molc. Wt(g)	% Yield	calculated			found		
				% C	% H	% N	% C	% H	% N
42	$C_{38}H_{40}CaN_2O_2$	596.81	57	76.47	6.67	4.69	76.51	6.85	4.77
43	$C_{38}H_{40}N_2O_2Sr$	644.36	71	70.83	6.26	4.35	70.79	6.36	4.38
44	$C_{38}H_{40}BaN_2O_2$	694.06	50	65.76	5.81	4.04	65.63	5.84	3.96
45	$C_{44}H_{72}CaN_2O_2Si_2$	757.30	65	69.78	9.58	3.70	69.76	9.69	3.58
46	$C_{44}H_{72}N_2O_2Si_2Sr$	804.85	62	65.66	9.02	3.48	65.51	9.13	3.40
47	$C_{44}H_{72}BaN_2O_2Si_2$	854.55	71	61.84	8.49	3.28	61.76	8.51	3.28
48	$C_{32}H_{46}CaN_4O_2$	558.81	73	68.78	8.30	10.03	68.62	8.31	9.76
49	$C_{32}H_{46}N_4O_2Sr$	606.35	61	63.39	7.65	9.24	63.49	7.53	9.20
50	$C_{32}H_{46}BaN_4O_2$	656.06	55	58.58	7.07	8.54	58.47	7.15	8.54
51	$C_{30}H_{40}CaN_2O_4$	532.73	99	67.64	7.57	5.26	67.53	7.59	5.19
52	$C_{30}H_{40}N_2O_4Sr$	580.27	14	62.10	6.95	4.83	61.99	7.00	4.85
53	$C_{30}H_{40}BaN_2O_4$	629.98	83	57.20	6.40	4.45	57.16	6.47	4.50
54	$C_{40}H_{44}CaN_2O_4$	656.87	84	73.14	6.75	4.26	73.17	6.81	4.29
55	$C_{40}H_{44}N_2O_4Sr$	704.41	20	68.20	6.30	3.98	68.03	6.37	4.02
56	$C_{40}H_{44}BaN_2O_4$	754.12	56	63.71	5.88	3.71	63.63	5.93	3.76

*Table 33: CHN microanalytical results for homoleptic group 2 amidate complexes **42-56**.*

In accordance to earlier work discussed in this thesis, reaction of the acetylene starting materials are observed in ^{1}H NMR spectra by the absence of the terminal hydrogen resonance around 2.00 ppm *ca*. following the protonolysis of the ligand. While the remaining acetylene resonances experience a down-field shift. The γH of the β-diketimato ligand, **L1** was found to be relatively unchanged when co-ordinated to the

amidate compounds, while the *iso*-propyl CH_3 protons of the dipp part of the ligand were found to have shifted up-field.

Further characterisation techniques, however, were found to support the heteroleptic amidate compounds produced from a mono-insertion of 1-adamantyl isocyanate **i** with compounds **42**, **45**, **48**, **51** and **54** displaying similar shifts in their ^{1}H NMR spectra. Interestingly the five compounds provided a resonances for the 1-adamantyl isocyanate **i** component of the propiolamidate compound with up-field shifts of 0.06 and 0.13 ppm for the triplet CH_2 and CH resonances respectively while the other CH_2 displayed a doublet with a 0.11 ppm down-field shift, table 34.

Compound	γH	^{i}Pr CH_3	3×C**H**$_2$, t	3×C**H**$_2$, d	3×C**H**, brs
C1	4.83	1.22 and 1.33	-	-	-
i	-	-	1.28	1.55	1.68
42	4.88	1.17 and 1.20	1.22	1.66	1.55
45	4.84	1.16 and 1.19	1.22	1.66	1.55
48	4.81	1.16 and 1.20	1.22	1.66	1.55
51	4.88	1.16 and 1.22	1.22	1.66	1.55
54	4.88	1.16 and 1.20	1.22	1.66	1.55

s= singlet, d = doublet, t =triplet and brs = broad singlet resonances.

*Table 34: Comparing the β-diketiminato ligand **L1** and 1-adamantyl isocyanate **i** proton shifts of compounds **42**, **45**, **48**, **51** and **54**.*

Similar ^{1}H NMR resonances were observed with the amidate compounds **42**-**56** following reaction with the homoleptic group 2 bis(bis(trimethylsilyl)amide **C3**-**5**, the triplet resonace observed for the CH_2 of the 1-adamantyl isocyanate experienced an up-field shift of 0.06 ppm whilst the doublet CH_2 was found to have experienced an up-field shift of 0.1 ppm. A down-field shift of up to 0.2 ppm was observed for the CH, table 35.

Compound	3×C**H**$_2$, t	3×C**H**$_2$, d	3×C**H**, brs
i	1.28	1.55	1.68
42	1.22	1.55	1.66
43	1.22	1.44	1.86
44	1.23	1.44	1.86
45	1.22	1.55	1.66
46	1.23	1.45	1.85
47	1.25	1.45	1.85
48	1.22	1.55	1.66
49	1.22	1.55	1.86
50	1.22	1.44	1.86
51	1.22	1.55	1.66
52	1.23	1.44	1.85
53	1.26	1.46	1.86
54	1.22	1.55	1.66
55	1.22	1.44	1.86
56	1.21	1.44	1.86

*Table 35: ^{1}H NMR resonances in ppm for the insertion of 1-adamantyl isocyanate **i** with the homoleptic group 2 bis(bis(trimethylsilyl)amides **C3-5**.*

In comparison to the 1-adamantyl isocyanate **i** starting material, the $^{13}C\{^1H\}$ NMR spectra of compounds **42**, **45**, **48**, **51** and **54** from reaction with β-diketiminato calium amide **C1** displayed down-field shifts of 40 ppm for the N**C**O unit whilst the remaining 1-adamantyl isocyanate **i** resonances were relatively unaffected, table 36. Interestingly the C≡C shifts observed for those compounds containing nitrogen and oxygen atoms, compounds **48**, **51** and **54** experienced further down-field shifts than the corresponding resonances observed in compounds **42** and **45**.

The $^{13}C\{H\}$ NMR spectra of the amidate compounds **42**-**56** from reaction with the homoleptic group 2 bis(bis(trimethylsilyl)amide **C3-5**, also indicated a difference in the chemical shifts between the non-donor **42**, **45** and donor-functionalised **48**, **51** and **54** compounds with the C≡C resonances experiencing the highest down-field shift in the donor-functionalised compounds, table 37. Similar to the heteroleptic compounds, the NCO resonance of the 1-adamantly isocyanate underwent a 40 ppm down-field shift.

The other resonances of the isocyanate remained unchanged in comparison to those observed in the free 1-adamantyl isocyanate compound.

Compound	**C**≡CR	C≡**C**R	N**C**O	N**C**	3×**C**H_2(C)	3×**C**H_2(CH)	3×**C**H
i	-	-	124.3	55.4	45.1	35.7	29.9
42	85.7	90.0	164.5	55.4	45.8	36.3	30.3
45	85.2	90.0	164.6	54.6	45.8	36.3	30.3
48	93.4	114.8	165.6	52.1	45.8	36.3	30.5
51	97.4	116.2	164.2	53.3	45.2	36.7	29.9
54	97.4	114.7	167.0	56.6	45.2	36.3	30.3

*Table 36: Comparing carbon shifts of amidate compounds **42**, **45**, **48**, **51** and **54** with 1-adamantyl isocyanate **i** and β-diketiminato calium amide **C1**.*

Compound	**C**≡CR	C≡**C**R	N**C**O	N**C**	3×**C**H_2(C)	3×**C**H_2(CH)	3×**C**H
i	-	-	124.3	55.4	45.1	35.7	29.9
42	88.1	92.9	167.5	55.6	45.8	36.3	30.3
43	87.0	91.8	168.8	58.3	45.8	36.2	30.2
44	89.8	93.3	167.7	53.8	42.3	37.1	30.2
45	85.9	95.7	167.6	54.6	45.8	36.3	30.3
46	85.9	95.6	168.5	54.6	45.8	36.3	30.3
47	83.5	95.7	163.1	58.7	44.8	37.4	31.0
48	104.7	115.9	176.9	54.6	45.8	36.3	30.3
49	105.7	115.7	176.2	54.6	45.8	36.3	30.3
50	104.8	114.0	176.7	53.8	44.0	37.5	30.9
51	111.7	114.4	176.9	54.6	45.8	36.3	30.3
52	110.2	115.3	177.3	54.6	45.7	36.2	30.2
53	111.0	114.8	177.2	53.3	46.3	37.1	31.1
54	113.5	115.2	176.1	54.6	45.8	36.3	30.3
55	111.3	115.2	176.9	54.6	45.7	36.2	30.2
56	113.4	115.2	177.1	55.4	45.8	36.2	31.0

*Table 37: ^{13}C NMR resonances in ppm for the homoleptic group 2 amidate complexes **42**-**56**.*

5.5 Conclusion

Although the stoichiometric insertion reaction of 1-adamantyl isocyanate **i** with group 2 acetylides was found to be successful, the catalytic reaction proved unsuccessful. This is proposed to be a consequence of the inability of the terminal acetylene substrate to protonate the co-ordinated amidate ligand to regenerate the intermediate acetylide. Consequently any further insertion of an unsaturated oxygen containing molecule such as an isocyanate will be futile.

Unlike the catalytic reactions, the stoichiometric insertion reactions were successful with each reaction producing a positive result. Both the calcium β-diketiminate amide **C1** and calcium and strontium triazenide complexes **C6** and **C7** produced elemental analyses that did not comply with the formation of the proposed amidate complexes inwhich the respective ligands remained co-ordinated to the metal centre with a single insertion of 1-adamantyl isocyante **i**. Instead the results suggested the formation of a bis-insertion of the 1-adamantyl isocyanate **i** to yield the homoleptic amidate complex, the same structure proposed from reactions of the homoleptic calcium, strontium and barium bis(bis(trimethylsilyl)amide **C3-5**, scheme 96.

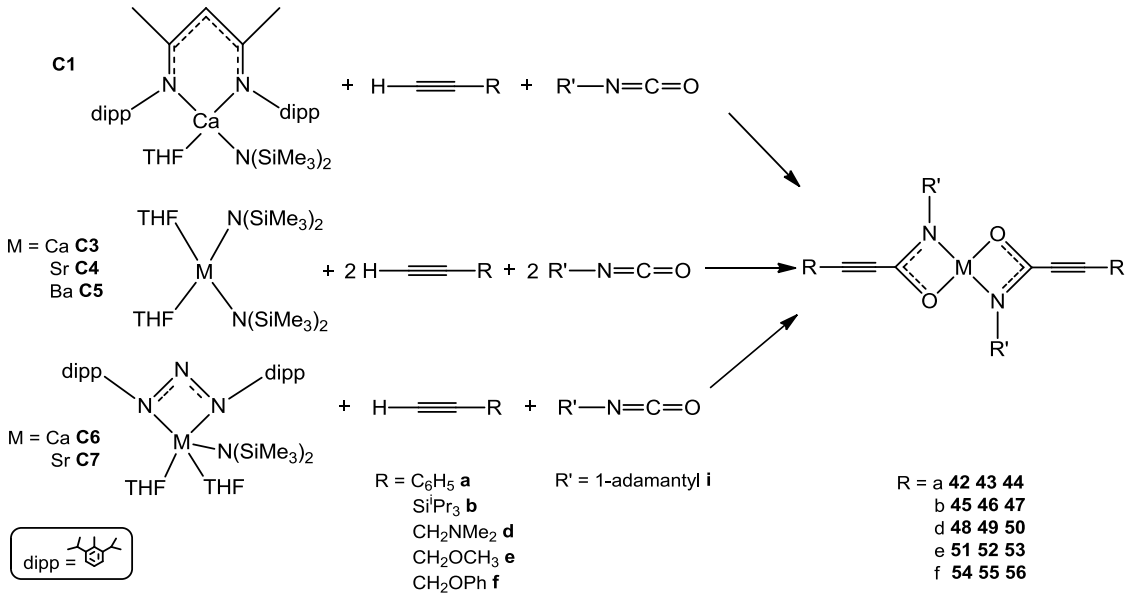

*Scheme 96: Stoichiometric insertion of 1-adamantyl isocyanate **i** to the homoleptic amidate compounds with the group 2 metal complexes **C1**, **C3-7** supported by the elemental analysis.*

However the formation of the initially proposed heteroleptic amidate compounds with the calcium β-diketiminate amide **C1** and calcium and strontium triazenide complexes **C6** and **C7** complexes are supported by the NMR data. As in the previous chapters the amidate products possessed a high solubility highlighted by the isolation of a single X-ray structure of compound **42**. The remaining compounds were obtained as white powders from concentrated hexane solutions. Interestingly the X-ray structure of compound **42** was found to support the formation of the proposed amidate complex consisting of a single insertion and the β-diketiminate ligand, **L1**.

Chapter 6

6.0 Conclusion and future plans

6.1 Conclusion

This thesis has successfully explored and developed the catalytic activity of the heavier alkaline earth metals, calcium, strontium and barium through the hydroacetylation of terminal acetylenes and the insertion of both symmetric and asymmetric double bonds.

Despite chapter 2 expanding the range of alkaline earth acetylides reported Hill and co-workers, [8] the introduction of the donor-functionalised acetylenes 3-dimethylamino-1-propyne **d**, methyl propargyl ether **e** and phenyl propargyl ether **f**, proved very interesting. It was therefore proposed that the presence of the nitrogen and oxygen atoms prevented the formation of symmetric acetylide complexes. A shift in electron density promoted by the nitrogen and oxygen atoms resulted in the formation of a less conventional asymmetric orientation that gave rise to the possibility of acetylide coupling.

Although the coupling of the acteylides were observed serendipitously it proved to be of significant interest. However, although the coupling was found to occur on stoichiometric and catalytic scales, isolation of the final butatriene product was found more difficult due to the low thermodynamic stability of the complex and its high tendency to re-distribute to its more stable enyne form.

The amidinate compounds discussed in chapter 4 were found to be dependent upon the carbodiimide employed. The insertion was found to be determined by the R groups present on the carbodiimide with either mono- or bis-insertion to the group 2 acetylide. Despite initially proposing the amidinate compounds would possess a monomeric structure they were found to be dimeric, bridged by the carbodiimide.

Although the insertion of a carbodiimide was catalytic, the catalytic insertion of 1-adamantyl isocyanate was futile due to the lack of acidity of the terminal acetylene in protonating the amidinate intermediate to yield the free propiolamide.

6.2 Future plans

The coupling reactions in chapter 3 would be of significant interest to any future work. Observed by chance this area of work presented the first carbon-carbon coupling with a heavier alkaline earth metal complex. Future work in this area would strive to fully characterise the butatriene complex and determine its stereochemistry either as a single isolated complex, or due to its low stability, through other reactions such as η^2-co-ordination to a rhodium metal complexes, as discussed earlier in this thesis.

It may be proposed that further information obtained through expanding the range and scope of the ligands and terminal acetylenes of the heavier alkaline earth acetylide compounds may not provide any advantage at this time. However, expanding the carbodiimide range may allow for further understanding of the different amidinate structures in both solution and solid state. An understanding of the futile catalysis in chapter 5 may be achieved by the employment of other isocyante compounds.

Chapter 7

7.0 Experimental

7.1 General experimental procedures

All reactions dealing with air- and moisture-sensitive compounds were carried out under a nitrogen atmosphere using standard Schlenk line and glovebox techniques. NMR experiments using air sensitive compounds were conducted in Youngs tap NMR tubes prepared and sealed in a glovebox under nitrogen and are referenced using residual solvent resonances. Except if stated otherwise, all NMR spectroscpic data was acquired on a Bruker 250 Avance NMR spectrometer at ^{1}H (250 MHz) and a Bruker 300 Avance NMR spectrometer at ^{1}H (300 MHz) and ^{13}C (75.48 MHz) at 298K.

Melting points were determined in sealed capillaries. Elemental analysis of all air- and moisture-sensitive compounds were prepared in a glovebox, flame sealed and sent to London Metropolitan University with Stephen Boyer performing the analysis.

X-ray diffraction data was collected at 150 K on a single crystal FR590 Nonius KappaCCD diffractometer equipped with an Oxford Cryosystem using graphite-monochromated Mo Kα radiation (λ = 0.71073 Å) by Dr G. Kociok-Köhn, Dr M. Mahon or Dr D. MacDougall at the University of Bath. Data was processed using Nonius Software. Crystal parameters and details on data collection, solution and refinement of all the complexes are presented in the appendix section. Structure solution, followed by full matrix least-squares refinement, was performed using the WINGX-1.70 suite of programs throughout.

7.1.2 Ligand and catalyst synthesis

7.1.2.1 Synthesis of *[CH{C(Me)N(2,6-$^{i}Pr_2C_6H_3$)}$_2$H] [nacnacH]* **L1** [12]

5ml (12M) of concentrated hydrochloric acid was added to 4.45 g (44.4 mmol) of 2,4-pentanedione and 19.10 g (107 mmol) of 2,6-di-*iso*-propylaniline. The solution was refluxed for three days in 200 ml ethanol. The pink hydrochloride salt was filtered and washed with hexane. 200 ml of an aqueous solution of sodium hydrocarbonate and 300 ml of dichloromethane was used to dissolve the solid. The organic phase was separated and dried with $MgSO_4$ and the organic solvent removed to give the crude product. The (BDI)H was re-crystallised in ethanol and dried under reduced pressure to give a yield of 14.5 g (34.63 mmol 78 %) of compound **L1**. ^{1}H NMR (250 MHz, 298K, C_6D_6) 0.99 (d, $^3J_{HH}$ = 6.7 Hz, 12H, CH*Me$_2$*), 1.09 (d, $^3J_{HH}$ = 6.9 Hz, 12H, CH*Me$_2$*), 1.61 (s, 6H, {C(*Me*)}$_2$CH), 3.00 (m, $^3J_{HH}$ = 6.9 Hz, 4H, C*H*Me$_2$), 4.76 (s, 1H, {C(Me)}$_2$C*H*), 7.01 (m, 6H, Ar*H*), 12.01 (s, 1H, N*H*).

7.1.2.2 Synthesis of *(nacnac)Ca(N(SiMe$_3$)$_2$(THF)* **C1** [2]

2.00 g (4.78 mmol) of **L1**, 1.40 g (4.78 mmol) of calcium iodide and 1.90 g (9.56 mmol) of KN(SiMe$_3$)$_2$ was left stirring overnight in 15 ml of THF. The solvent was removed under vacuum and hexane was added and stirred for half an hour. The solution was filtered from the KI solid and the volume reduced. Crystallisation occurred overnight at -30 ^{o}C. The hexane was filtered and the solid dried under vacuum yielding 1.48 g (2.14 mmol 45 %) of compound **C1**. ^{1}H NMR (250 MHz, 298K, C_6D_6) 0.19 (s, 18H Si*Me$_3$*), 1.07 (m, 4H, *THF*), 1.22 (d, $^3J_{HH}$ = 6.7 Hz, 12H, CH*Me$_2$*), 1.33 (d, $^3J_{HH}$ = 6.9 Hz, 12H, CH*Me$_2$*), 1.67 (s, 6H, {C(*Me*)}$_2$CH), 3.23 (m, $^3J_{HH}$ = 6.9 Hz, 4H, C*H*Me$_2$), 3.34 (m, $^3J_{HH}$ = 6.4 Hz, 4H, *THF*), 4.83 (s, 1H, {C(Me)}$_2$C*H*), 7.13 (m, 6H, Ar*H*).

7.1.2.3 Synthesis of *(nacnac)Sr(N(SiMe$_3$)$_2$(THF)* **C2** [2]

2.00 g (4.78 mmol) of **L1**, 1.63 g (4.78 mmol) of strontium iodide and 1.90 g (9.56 mmol) of KN(SiMe$_3$)$_2$ was left stirring overnight in 15 ml of THF. The solvent was removed under vacuum and hexane was added and stirred for half an hour. The solution

was filtered from the KI solid and the volume reduced. Crystallisation occurred overnight at -30 ^{o}C. The hexane was filtered and the solid dried under vacuum yielding 1.13 g (1.56 mmol 33 %) of compound **C2**. ^{1}H NMR (250 MHz, 298K, C_6D_6) 0.19 (s, 18H Si*Me$_3$*), 1.10 (m, 4H, *THF*), 1.22 (d, $^{3}J_{HH}$ = 6.7 Hz, 12H, CH*Me$_2$*), 1.36 (d, $^{3}J_{HH}$ = 6.9 Hz, 12H, CH*Me$_2$*), 1.66 (s, 6H, {C(*Me*)}$_2$CH), 3.22 (m, $^{3}J_{HH}$ = 6.9 Hz, 4H, C*H*Me$_2$), 3.35 (m, 4H, *THF*), 4.81 (s, 1H, {C(Me)}$_2$C*H*), 7.12 (m, 6H, Ar*H*).

7.1.2.4 Synthesis of *[M(N(SiMe$_3$)$_2$(THF)$_2$]* **C3-5** [14a]

The appropriate group 2 metal iodide and KN(SiMe$_3$)$_2$ were stirred in THF overnight. The THF was removed under vacuum and replaced by hexane. After stirring for a few minutes the hexane solution was filtered into another Schlenk flask and concentrated. On formation of the product, the solution was left to crystallise at -30 ^{o}C. The hexane was filtered and the residual solvent removed by vacuum to yield compounds **C3-5** as colourless crystalline materials.

1.00 g (3.40 mmol) of calcium iodide and 1.36 g (6.82 mmol) of KN(SiMe$_3$)$_2$ yield 1.38 g (2.73 mmol 81 %) of compound **C3** [(Me$_3$Si)$_2$N]$_2$Ca(THF)$_2$. ^{1}H NMR (250 MHz, 298K, C_6D_6) 0.35 (s, 36H SiMe$_3$), 1.28 (m, 8H, THF), 3.57 (m, 8H, THF).

1.00 g (2.93 mmol) of strontium iodide and 1.17 g (5.87 mmol) of KN(SiMe$_3$)$_2$ yield 0.81 g (0.15 mmol 50 %) of compound **C4** [(Me$_3$Si)$_2$N]$_2$Sr(THF)$_2$. ^{1}H NMR (250 MHz, 298K, C_6D_6) 0.35 (s, 36H SiMe$_3$), 1.27 (m, 8H, THF), 3.52 (m, 8H, THF).

1.00 g (2.56 mmol) of barium iodide and 1.02 g (5.11 mmol) of KN(SiMe$_3$)$_2$ yield 1.12 g (1.87 mmol 73 %) of compound **C5** [(Me$_3$Si)$_2$N]$_2$Ba(THF)$_2$. ^{1}H NMR (250 MHz, 298K, C_6D_6) 0.30 (s, 36H SiMe$_3$), 1.43 (m, 8H, THF), 3.56 (m, 8H, THF).

7.1.2.5 Synthesis of *[N(H){N(2,6-^{i}Pr$_2$C$_6$H$_3$)}$_2$]* **L2** [58]

13.42 ml (99.89 mmol) of *iso*-amylnitrite was slowly added to a 250 ml beaker containing 9.41 ml (49.89 mmol) of cold distilled 2,6-diisopropylaniline and 100 ml of diethyl ether. The solution was stirred overnight before removal of volatiles under reduced pressure. The solution was left to crystallise at -30 ^{o}C overnight before being

filtered and dried to yield 5.5 g (16.1 mmol 60 %) of compound **L2**. ^{1}H NMR (500 MHz, 298K, d_8-toluene) 1.17 (d, $^{3}J_{HH}$ = 6.9 Hz, 24H, CH*Me*$_2$), 3.30 (m, $^{3}J_{HH}$ = 6.9 Hz, 4H, C*H*Me$_2$), 7.06-7.13 (m, 6H, Ar*H*).

7.1.2.6 Synthesis of *[N(H){N(2,6-^{i}Pr$_2$C$_6$H$_3$)}$_2$]Ca{N(SiMe$_3$)$_2$}$_2$(THF)$_2$* **C6** [58]

0.50 g (1.37 mmol) of **L2** and 0.69 g (1.37 mmol) of bis((bistrimethylsilyl)amide) **C3** was dissolved in 20 ml of toluene and stirred for 2 hours. The volume of toluene was reduced under vacuum and the solution left to crystallise overnight at -30 ^{o}C. The toluene was removed by filtration and the product was dried under vacuum yielding 0.48 g (0.7 mmol 48 %) of compound **C6**. ^{1}H NMR (250 MHz, 298K, C_6D_6) 0.25 (s, 18H Si*Me*$_3$), 1.16 (m, 8H, THF), 1.23 (d, $^{3}J_{HH}$ = 6.9 Hz, 24H, CH*Me*$_2$), 3.31 (m, $^{3}J_{HH}$ = 6.9 Hz, 4H, C*H*Me$_2$), 3.47 (m, 8H, THF), 7.08 (m, 5H, Ar*H*), 7.18 (m, 1H, Ar*H*).

7.1.2.7 Sythesis of *[N(H){N(2,6-^{i}Pr$_2$C$_6$H$_3$)}$_2$]Sr{N(SiMe$_3$)$_2$}$_2$(THF)$_3$* **C7** [58]

0.50 g (1.37 mmol) of **L2** and 0.76 g (1.37 mmol) of **C4** was dissolved in 20 ml of toluene and stirred for 2 hours. The volume of toluene was reduced under vacuum and the solution left to crystallise overnight at - 30 ^{o}C. The toluene was removed by filtration and the product was dried under vacuum yielding 0.37 g (0.5 mmol 34 %) of compound **C7**. ^{1}H NMR (250 MHz, 298K, C_6D_6) 0.25 (s, 18H Si*Me*$_3$), 1.08 (d, $^{3}J_{HH}$ = 6.9 Hz, 12H, CH*Me*$_2$), 1.13 (d, $^{3}J_{HH}$ = 6.9 Hz, 12H, CH*Me*$_2$), 1.16 (m, 12H, THF), 3.31 (m, $^{3}J_{HH}$ = 6.9 Hz, 4H, C*H*Me$_2$), 3.34 (m, 12H, THF), 7.08 (m, 5H, Ar*H*), 7.18 (m, 1H, Ar*H*).

7.1.2.8 Alkyl metal complex **C8** and **C9** [59]

Both **C8** and **C9** catalysts were prepared by another member of the Hill group.

7.1.3 Acetylene preparation

The acetylenes that could be purchased were done so from Sigma Aldrich or Fisher and were transferred into the glovebox following vacuum transfer over CaH_2. Those

acetylenes not purchased, ethynyl ferrocene **c** [54] and methyl propargyl ether **e** [55] were prepared in the lab according to literature procedures.

7.2 Acetylide insertion

7.2.1 Synthesis of *[(nacnac)Ca(C≡CSi^{i}Pr$_3$)]$_2$* **1** [19]

0.15 ml (0.74 mmol) of **b** in 10 ml of toluene was added to 0.5 g (0.74 mmol) of **C1** in 10 ml of toluene. After stirring for 15 minutes at room temperature the volume of toluene was reduced under vacuum and the solution left to crystallise overnight at – 30 ^{o}C. The toluene was removed by filtration and the product was dried under vacuum yielding 0.12 g (0.094 mmol 26 %) of compound **1**. ^{1}H NMR (400 MHz, 298 K, C_6D_6) 1.08 (m, 2 x 3H, Si^{i}Pr*H*), 1.06 (d, $^3J_{HH}$ = 6.8 Hz, 2 x 18H, Si^{i}Pr*Me*), 1.20 (d, $^3J_{HH}$ = 6.7 Hz, 2 x 12H, CH*Me$_2$*), 1.22 (d, $^3J_{HH}$ = 6.7 Hz, 2 x 12H, CH*Me$_2$*), 1.41 (s, 2 x 6H, {C(*Me*)}$_2$CH), 3.30 (hept, $^3J_{HH}$ = 6.7 Hz, 2 x 4H, C*H*Me$_2$), 4.74 (s, 2 x 1H, {C(Me)}$_2$C*H*), 7.12 (m, 2 x 6H, Ar*H*); ^{13}C NMR (100 MHz, 298K, C_6D_6) 12.0 (Si^{i}Pr*C*H), 19.2 (Si^{i}Pr*Me*), 24.4 ({C(*Me*)}$_2$CH), 25.2 (*C*HMe$_2$), 26.5 (CH*Me$_2$*), 96.0 (C≡*C*Ca), 100.8 (*C*≡CCa), 123.9 (*p*-*C*$_6$H$_3$), 141.9 (*m*-*C*$_6$H$_3$), 146.6 (*o*-*C*$_6$H$_3$), 147.9 (*i*-*C*$_6$H$_3$), 163.6 ({C(Me)}$_2$*C*H), 166.8(*C*N); Analysis calculated for $C_{80}H_{124}Ca_2N_4Si_2$: C, 75.17; H, 9.78; N, 4.38. Found: C, 74.99; H, 9.82; N, 4.45.

7.2.2 Synthesis of *[(nacnac)Ca(C≡C(C$_5$H$_4$)Fe(C$_5$H$_5$)]$_2$* **2** [19]

0.78g (0.37 mmol) of **c** in 10 ml of toluene was added to 0.25 g (0.37 mmol) of **C1** in 10 ml of toluene. After stirring for 15 minutes at room temperature the volume of toluene was reduced under vacuum and the solution left to crystallise overnight at -30 ^{o}C. The toluene was removed by filtration and the product was dried under vacuum yielding 1.49 g (0.11mmol 60 %) of compound **2**. ^{1}H NMR (400 MHz, 298K, d_8-THF) 1.00 (d, $^3J_{HH}$ = 6.8 Hz, 2 x 12H, CH*Me$_2$*), 1.11 (d, $^3J_{HH}$ = 6.8 Hz, 2 x 12H, CH*Me$_2$*), 1.43 (s, 2 x 6H, {C(*Me*)}$_2$CH), 3.11 (hept, $^3J_{HH}$ = 6.8 Hz, 2 x 4H, C*H*Me$_2$), 3.60 (m, 2 x 2H, C*H* of cyclopentene), 3.72 (m, 2 x 7H, C*H* of cyclopentene), 4.50 (s, 2 x 1H, {C(Me)}$_2$C*H*), 6.79 (t, $^3J_{HH}$ = 7.2 Hz, 2 x 2H, Ar*H*), 6.90 (d, $^3J_{HH}$ = 7.2 Hz, 2 x 4H, Ar*H*); ^{13}C NMR (100 MHz, 298K, d_8-THF) 22.1 ({C(*Me*)}$_2$CH), 22.8 (*C*HMe$_2$),

25.8(CH*Me*$_2$),63.9 (*C*H of cyclopentene), 67.2 (*C*H of cyclopentene), 68.1 (*C*H of cyclopentene), 72.1 (*C*H of cyclopentene), 91.6 (C≡*C*Ca), 99.4 (*C*≡CCa), 121.3 (*p*-*C*$_6$H$_3$), 121.5 (*m*-*C*$_6$H$_3$), 136.7 (*o*-*C*$_6$H$_3$), 139.9 (*i*-*C*$_6$H$_3$), 146.0 ({C(Me)}$_2$*C*H), 162.7(*C*N); Analysis calculated for $C_{82}H_{100}Ca_2Fe_2N_4$: C, 73.85; H, 7.56; N, 4.20. Found: C, 73.79; H, 7.56; N, 4.14.

7.2.3 Synthesis of *[(nacnac)Ca(C≡CCH$_2$NMe$_2$)]$_2$* **3**

0.08 ml (0.037 mmol) of **d** in 10 ml of toluene was added to 0.5 g (0.037 mmol) of **C1** in 10 ml of toluene. After stirring for 15 minutes at room temperature the volume of toluene was reduced under vacuum and the solution left to crystallise overnight at -30 ^{o}C. The toluene was removed by filtration and the product was dried under vacuum yielding 0.28 g (0.268 mmol 72 %) of compound **3**. ^{1}H NMR (250 MHz, 298K, C_6D_6) 1.14 (d, $^{3}J_{HH}$ = 6.8 Hz, 2 x 12H, CH*Me*$_2$), 1.20 (d, $^{3}J_{HH}$ = 6.9 Hz, 2 x 12H, CH*Me*$_2$), 1.55 (s, 2 x 6H, {C(*Me*)}$_2$CH), 1.66 (s, 2 x 6H, N*Me*$_2$), 2.12 (s, 2 x 2H, NC*H*$_2$), 2.98 (m, 2 x 4H, C*H*Me$_2$), 4.88 (s, 2 x 1H, {C(Me)}$_2$C*H*), 7.12 (m, 2 x 6H, Ar*H*); ^{13}C NMR (75.48 MHz, 298K, C_6D_6) 20.8 ({C(*Me*)}$_2$CH), 24.5 (*C*HMe$_2$), 28.7 (CH*Me*$_2$), 60.2 (N*Me*$_2$), 61.0 (N*C*H$_2$), 92.0 (C≡*C*Ca), 102.8 (*C*≡CCa), 123.6 (*p*-*C*$_6$H$_3$), 125.8 (*m*-*C*$_6$H$_3$), 142.8 (*o*-*C*$_6$H$_3$), 146.8 (*i*-*C*$_6$H$_3$), 157.2 ({C(Me)}$_2$*C*H), 164.1 (*C*N); Analysis calculated for $C_{65}H_{98}Ca_2N_6$: C, 75.64; H, 9.15; N, 7.78. Found: C, 75.62; H, 9.16; N, 7.69. X-ray crystallography data, see appendix.

7.2.4 Sythesis of *[(nacnac)Ca(C≡CCH$_2$OMe)]$_2$* **4**

0.06 ml (0.037 mmol) of **e** in 10 ml of toluene was added to 0.5 g (0.037 mmol) of **C1** in 10 ml of toluene. After stirring for 15 minutes at room temperature the volume of toluene was reduced under vacuum and the solution left to crystallise overnight at -30 ^{o}C. The toluene was removed by filtration and the product was dried under vacuum yielding 0.29 g (0.275 mmol 74 %) of compound **4**. ^{1}H NMR (300 MHz, 298K, C_6D_6) 1.12 (d, $^{3}J_{HH}$ = 6.5 Hz, 2 x 12H, CH*Me*$_2$), 1.19 (d, $^{3}J_{HH}$ = 6.7 Hz, 2 x 12H, CH*Me*$_2$), 1.59 (s, 2 x 6H, {C(*Me*)}$_2$CH), 2.91 (s, 2 x 3H, O*Me*), 3.11 (m, 2 x 4H, C*H*Me$_2$), 3.17 (s, 2 x 2H, OC*H*$_2$), 4.60 (s, 2 x 1H, {C(Me)}$_2$C*H*), 7.10 (m, 2 x 6H, Ar*H*); ^{13}C NMR (75.48 MHz, 298K, C_6D_6) 20.5 ({C(*Me*)}$_2$CH), 24.7 (*C*HMe$_2$), 28.1 (CH*Me*$_2$), 58.9 (O*Me*), 62.9 (O*C*H$_2$), 93.4 (C≡*C*Ca), 105.6 (*C*≡CCa), 123.6 (*p*-*C*$_6$H$_3$), 129.3 (*m*-*C*$_6$H$_3$), 141.9

(*o*-C_6H_3), 146.0 (*i*-C_6H_3), 146.4 ({C(Me)}$_2$*C*H), 165.0 (*C*N); Analysis calculated for $C_{66}H_{94}Ca_2N_4O_2$: C, 75.24; H, 8.80; N, 5.32. Found: C, 75.17; H, 8.94; N, 5.27. X-ray crystallography data, see appendix.

7.2.5 Synthesis of *[(nacnac)Ca(C≡CCH$_2$OPh)]$_2$* **5**

0.049 ml (0.037 mmol) of **f** in 10 ml of toluene was added to 0.25 g (0.037 mmol) of **C1** in 10 ml of toluene. After stirring for 15 minutes at room temperature the volume of toluene was reduced under vacuum and the solution left to crystallise overnight at -30 ^{o}C. The toluene was removed by filtration and the product was dried under vacuum yielding 0.15 g (0.127 mmol 69 %) of compound **5**. Decomposed at 200 ^{o}C; ^{1}H NMR (300 MHz, 298K, C_6D_6) 1.13 (d, $^{3}J_{HH}$ = 6.8 Hz, 2 x 12H, CH*Me$_2$*), 1.19 (d, $^{3}J_{HH}$ = 6.7 Hz, 2 x 12H, CH*Me$_2$*), 1.55 (s, 2 x 6H, {C(*Me*)}$_2$CH), 3.10 (m, 2 x 4H, C*H*Me$_2$), 4.06 (s, 2 x 2H, OC*H*$_2$), 4.88 (s, 2 x 1H, {C(Me)}$_2$C*H*), 6.89 (m, 2 x 5H, OAr*H*), 7.06 (m, 2 x 6H, Ar*H*); ^{13}C NMR (75.48 MHz, 298K, C_6D_6) 20.8 ({C(*Me*)}$_2$CH), 24.3 (*C*HMe$_2$), 28.6 (CH*Me$_2$*), 60.0 (O*C*H$_2$), 94.3 (C≡*C*Ca), 106.3 (*C*≡CCa), 115.5 (*o*-C_6H_5), 123.6 (*p*-C_6H_5), 123.8 (*p*-C_6H_3), 129.6 (*m*-C_6H_5), 130.0 (*m*-C_6H_3), 141.3 (*o*-C_6H_3), 142.1 (*i*-C_6H_3), 156.6 (*C*H), 161.5 (*i*-C_6H_5), 165.6 (*C*N); Analysis calculated for $C_{76}H_{96}Ca_2N_4O_2$: C, 77.50; H, 8.22; N, 4.76. Found: C, 77.42; H, 8.34; N, 4.64. X-ray crystallography data, see appendix.

7.3 Coupling of terminal acetylenes [56a]

The coupling reactions were prepared in the glovebox and carried out in Youngs NMR tubes with C_6D_6 as the solvent. The tubes were heated in an oil bath for the stated time and temperature with the reaction progress monitored by ^{1}H NMR.

7.3.1 Stoichiometric reactions

7.3.1.1 Synthesis of *(CH$_2$NMe$_2$)(H)C=C=C=C(H)(CH$_2$NMe$_2$)* **6**

Initially a 1:1 ratio of 50 mg (0.07 mmol) of **C1** and 0.008 ml (0.07 mmol) of **d** was heated at 65 ^{o}C overnight. This was subsequently increased to 1:3 equivalents to form compound **6**. ^{1}H NMR (250 MHz, 298K, C_6D_6) 1.91 (t, 1H, C*H* unreacted), 2.10 (s, 6H, N*Me$_2$* unreacted), 2.22 (s, 12H, N*Me$_2$*), 3.01 (d, 2H, NC*H$_2$* unreacted), 5.27 (d, 4H NC*H$_2$*), 5.97 (t, 2H, C*H*); ^{13}C NMR (75.48 MHz, 298K, C_6D_6) 67.8 (**C**H$_2$NCH$_3$), 94.3 (N*Me$_2$*), 142.8 (=*C*H), 200.4 (=*C*=).

The synthesis was subsequently repeated for both calcium bis(bis(trimethylsilyl)amide) **C3** and calcium triazenide **C6**.

7.3.1.2 Synthesis of *(CH$_2$OMe)(H)C=C=C=C(H)(CH$_2$OMe)* **7**

Initially a 1:1 ratio of 16 mg (0.02 mmol) **C1** and 0.002 ml (0.02 mmol) of **e** was heated at 60 ^{o}C overnight. This was subsequently increased to 1:4 equivalents upon complete reaction of the acetylene to form compound **7**. ^{1}H NMR (250 MHz, 298K, C_6D_6) 2.00 (t, 1H, C*H* unreacted), 3.08 (s, 3H, O*Me* unreacted), 3.16 (s, 6H, O*Me*), 3.57 (d, 2H, OC*H$_2$* unreacted), 5.21 (d, 4H OC*H$_2$*), 6.75 (t, 2H, C*H*); ^{13}C NMR (75.48 MHz, 298K, C_6D_6) 55.6 (O*Me*), 91.0 (N*C*H$_2$), 142.8 (*C*H), 201.7 (=*C*=).

The synthesis was repeated for both calcium and strontium bis(bis(trimethylsilyl)amides) **C3**-**C4**, and calcium and strontium dipp-BIAN alkyls **C8**-**9**. Reaction with the calcium triazenide **C6** proved the most efficient, reacting with 12 acetylene equivalents.

7.3.1.3 Synthesis of *($CH_2OPh)(H)C=C=C=C(H)(CH_2OPh)$* **8**

Initially a 1:1 ratio of 25 mg (0.05 mmol) of **C3** and 0.006 ml (0.05 mmol) of **f** was heated at 75 ^{o}C overnight. This was subsequently increased to 1:3 equivalents to form compound **8**. ^{1}H NMR (250 MHz, 298K, C_6D_6) 1.98 (t, 1H, C*H*, unreacted), 4.16 (d, 2H, OCH_2, unreacted), 5.05 (d, 4H, OCH_2), 6.63 (t, 2H, C*H*), 6.85 (m, 3H, O**Ph**), 7.06 (m, 2H, O**Ph**); ^{13}C NMR (75.48 MHz, 298K, C_6D_6) 89.1 (OCH_2), 117.2 (*i*-*C*Ph), 118.2 (*m*-*C*Ph), 122.9 (*p*-*C*Ph), 129.7 (*o*-*C*Ph), 146.9 (*C*H), 200.3 (=*C*=).

The synthesis was also repeated with calcium triazenide **C6**.

7.3.2 Catalytic reactions

7.3.2.1 Synthesis of *($CH_2NMe_3)(H)C=C=C=C(H)(CH_2NMe_3)$* **6**

40 mg (0.06 mmol, 5 mol %) of **C2** and 0.13 ml (1. 2 mmol) of **d** was heated at 75 ^{o}C for 4 weeks giving *ca*. 4 % conversion of compound **6**. ^{1}H NMR (250 MHz, 298K, C_6D_6) 1.97 (t, 1H, C*H* unreacted), 2.06 (s, 6H, NMe_2 unreacted), 2.12 (s, 12H, NMe_2), 2.21 (d, 2H, NCH_2 unreacted), 5.27 (d, 4H NCH_2), 5.98 (t, 2H, C*H*).

The synthesis was repeated with 20 mol% calcium triazenide **C6**.

7.3.2.2 Synthesis of *($CH_2OMe)(H)C=C=C=C(H)(CH_2OMe)$* **7**

60 mg (0.07 mmol, 5 mol %) of **C6** and 100 mg (1.4 mmol) of **e** were heated to 75 ^{o}C. The reaction monitored by ^{1}H NMR indicated *ca*. 91% conversion of compound **7** after 48 hours. The complex was isolated from the NMR tube by vacuum transfer. ^{1}H NMR (250 MHz, 298K, C_6D_6) 1.98 (t, 1H, C*H* unreacted), 3.07 (s, 6H, O*Me* unreacted), 3.16 (s, 12H, O*Me*), 3.73 (d, 2H, OCH_2 unreacted), 5.21 (d, 4H OCH_2), 6.76 (t, 2H, C*H*).

Producing a lower % yield conversion the synthesis was repeated with the strontium triazenide derivative **C7**, β-diketiminato strontium amide **C2** and both calcium and strontium dipp-BIAN alkyls **C8** and **C9**.

7.3.2.6 Synthesis of *($CH_2OPh)(H)C=C=C=C(H)(CH_2OPh)$* **8**

27 mg (0.04 mmol, 5 mol %) of **C6** and 0.10 ml (0.76 mmol) of **f** was heated at 75 ^oC for 10 days The catalyst loading was increased to 10 mol% and heated for a further 2 days at 75 ^oC giving *ca.* 17 % conversion of compound **14**. ^1H NMR (250 MHz, 298K, C_6D_6) 2.00 (t, 1H, C*H* unreacted), 4.17 (d, 2H, OCH_2 unreacted), 5.06 (d, 4H, OCH_2), 6.64 (t, 2H, C*H*), 6.85 (m, 3H, O*Ph*), 7.06 (m, 2H, O*Ph*).

7.4 Hydroacetylation of carbodiimides

7.4.1 Catalytic insertion

7.4.1.1 Synthesis of *Ca[($^iPrNC(C\equiv CSi^iPr_3)N^iPr]_2$* **12**

7 mg (0.01 mmol, 5mol %) of **C3**, 62 μl (0.27 mmol) of **b** and 37 μl (0.27 mmol) of **g** was heated at 75 ^oC for 14 days giving *ca.* 22 % conversion of compound **12**. ^1H NMR (250 MHz, 298K, C_6D_6) 1.04 (d, 12H, N^{i}Pr*Me*, unreacted), 1.08 (d, 18H, Si^{i}PrMe_3, unreacted), 1.13 (d, 18, Si^{i}PrMe_3), 1.23 (d, 12H, N^{i}Pr*Me*), 1.41 (d, 12H, N^{i}Pr*Me*), 2.08 (s, 1H, C*H*, unreacted), 3.33 (m, 2H, N^{i}Pr*H*, unreacted), 3.87 (m, 6H, Si^{i}Pr*H*, unreactive), 3.96 (m, 6H, Si^{i}Pr*H*), 4.23 (m, 4H, N^{i}Pr*H*).

7.4.1.2 Synthesis of *Ca[(cyNC(C≡CSi^{i}Pr$_3$)Ncy]$_2$* **13**

7 mg (0.01 mmol, 5mol %) of **C3**, 62 μl (0.27 mmol) of **b** and 60 mg (0.27 mmol) of **h** was heated at 75 ^oC for 14 days giving *ca.* 18 % conversion of compound **13**. ^1H NMR (250 MHz, 298K, C_6D_6) 1.07 (d, 18, Si^{i}PrMe_3), 1.14 (d, 18H, Si^{i}PrMe_3 unreacted), 1.24 (d, 12H, N^{i}Pr*Me*), 1.34, 1.65, 1.76, 1.89 (m, 20H, CH_2 of cy), 2.14 (s, 1H, C*H*, unreacted), 3.12 (m, 2H, C*H* of cy, unreacted), 3.33 (m, 2H, N^{i}Pr*H*), 3.38 (m, 4H, C*H* of cy), 3.88 (m, 6H, Si^{i}Pr*H*, unreactive), 4.02 (m, 6H, Si^{i}Pr*H*).

7.4.1.3 Synthesis of *Ca[(^{i}PrNC(C≡CPh)N^{i}Pr]$_2$* **18**

10 mg (0.02 mmol, 5mol %) of **C3**, 50 µl (0.49 mmol) of **a** and 0.48 µl (0.49 mmol) of **g** was heated at 75 ^{o}C for 14 days giving *ca*. 24 % conversion of compound **18**. ^{1}H NMR (250 MHz, 298K, C_6D_6) 1.04 (d, 12H, N^{i}Pr*Me*, unreacted), 1.23 (d, 12H, N^{i}Pr*Me*), 1.41 (d, 12H, N^{i}Pr*Me*), 2.76 (s, 1H, C*H*, unreacted), 3.33 (m, 2H, N^{i}Pr*H*, unreacted), 4.23 (m, 4H, N^{i}Pr*H*), 6.85 (m, 6H, Ph, unreacted), 6.99 (m, 6H, Ph), 7.26 (m, 4H, Ph, unreacted), 7.36 (m, 4H, *Ph*).

7.4.1.4 Synthesis of *Ca[(cyNC(C≡CPh)Ncy]$_2$* **19**

10 mg (0.02 mmol, 5mol %) of **C3**, 50 µl (0.49 mmol) of **a** and 100 mg (0.49 mmol) of **h** was heated at 75 ^{o}C for 14 days giving *ca.* 48 % conversion of compound **19**. ^{1}H NMR (250 MHz, 298K, C_6D_6) 1.02, 1.34, 1.39, 1.63, 1.95 (m, 20H, CH_2 of cy), 2.81 (s, 1H, C*H*, unreacted), 3.11 (m, 2H, C*H* of cy, unreacted), 3.86 (m, 4H, C*H* of cy), 6.85 (m, 6H, Ph, unreacted), 6.99 (m, 6H, Ph), 7.27 (m, 4H, Ph, unreacted), 7.41 (m, 4H, Ph).

7.4.2 Stoichiometric carbodiimide insertion with the heteroleptic complexes

7.4.2.1 Synthesis of *[(nancnac)Ca{cyN=C(C≡CC$_6$H$_5$)=Ncy}]* **9**

0.04 ml (0.37 mmol) of **a** and 76 mg (0.37 mmol) of **h** in 10 ml of toluene was added to 0.25 g (0.37mmol) of **C1** in10 ml of toluene. After stirring overnight at room temperature the solvent volume was reduced in *vacuo* and left to crystallise at -30 ^{o}C for 48 hours. The product was isolated by filtration to yield 0.14 g (0.18 mmol 49 %) of compound **9**. ^{1}H NMR (250 MHz, 298K, C_6D_6) 1.35 (d, $^{3}J_{HH}$ = 6.8 Hz, 2 x 12H, CH*Me$_2$*), 1.41 (m, 2 x 2H, CH_2 of cy), 1.54 (m, 2 x 4H, CH_2 of cy), 1.87 (m, 2 x 4H, CH_2 of cy), 1.92 (s, 2×3H, {C(*Me*)}$_2$CH), 3.11 (m, 2 × 1H, C*H* of cy), 3.41 (hept, 4H, $^{3}J_{HH}$ = 6.8 Hz, C*H*Me$_2$), 4.88 (s, 1H, {C(Me)}$_2$C*H*), 7.12 (m, 6H, Ar*H*); ^{13}C NMR (75.48 MHz, 298K, C_6D_6) 24.8 (*C*HMe$_2$), 25.5, 26.8 (*C*H$_2$ of cy), 28.2 (CH*Me$_2$*), 26.9, 37.4 (*C*H$_2$ of cy), 58.9, 68.3(*C*H of cy), 93.7 (*C*≡CPh), 95.4 (C≡*C*Ph), 98.5 ({C(*Me*)}$_2$CH), 123.6 (*p*-*C*$_6$H$_5$), 123.9 (*m*-*C*$_6$H$_5$), 141.8 (*o*-*C*$_6$H$_5$), 148.0 (*i*-*C*$_6$H$_5$),

158.8(**C**N), 165.1 (**C**N_2); Analysis calculated for $C_{50}H_{68}CaN_4$: C, 78.48; H, 8.96; N, 7.32. Found: C, 76.14; H, 9.01; N, 6.15.

7.4.2.2 Synthesis of *[(nacnac)Ca{cyN=C(C≡CSi^{i}Pr$_3$)=Ncy}]* **10**

0.08ml (0.37 mmol) of **b** and 76 mg (0.37 mmol) of **h** in 10 ml of toluene was added to 0.25 g (0.37 mmol) of **C1** in 10 ml of toluene After stirring overnight at room temperature the solvent volume was reduced in *vacuo* and left to crystallise at -30 ^{o}C for 48 hours. The product was isolated by filtration to yield 0.25 g (0.2 mmol 52 %) of compound **10**. ^{1}H NMR (250 MHz, 298K, C_6D_6) 1.26 (d, 18H, $^3J_{HH}$ = 6.4 Hz, Si^{i}Pr*Me*), 1.29 (d, $^3J_{HH}$ = 6.8 Hz, 2 x 12H, CH*Me*$_2$), 1.40 (d, $^3J_{HH}$ = 6.8 Hz, 2 x 12H, CH*Me*$_2$), 1.43, 1.50 (m, 2 x 4H, C*H*$_2$ of cy), 1.71 (m, 2 × 1H, C*H* of cy), 1.80 (s, 2×3H, {C(*Me*)}$_2$CH), 1.82, 1.94 (m, 2 x 4H, C*H*$_2$ of cy), 3.78 (m, 3H, Si^{i}PrC*H*), 3.42 (hept, 4H, $^3J_{HH}$ = 6.8 Hz, C*H*Me$_2$), 4.96 (s, {C(Me)}$_2$C*H*), 7.05 (m, 6H, Ar*H*); ^{13}C NMR (75.48 MHz, 298K, C_6D_6) 11.7 (Si^{i}Pr*Me*), 18.9 (Si^{i}Pr*C*H), 24.8 (CH*Me*$_2$), 25.5, 26.8 (*C*H$_2$ of cy), 28.2 (*C*HMe$_2$), 26.9, 37.4 (*C*H$_2$ of cy), 58.9, 68.3(*C*H of cy), 93.7 (*C*≡CSi), 95.4 (C≡*C*Si), 98.5 ({C(*Me*)}$_2$CH), 123.6 (*p*-*C*$_6$H$_5$), 123.9 (*m*-*C*$_6$H$_5$), 141.8 (*o*-*C*$_6$H$_5$), 148.0 (*i*-*C*$_6$H$_5$), 158.8(**C**N), 165.1 (**C**N_2); Analysis calculated for $C_{53}H_{84}CaN_4Si$: C, 75.30; H, 10.01; N, 6.63. Found: C, 74.30; H, 9.93; N, 4.07.

7.4.2.3 Synthesis of *[(nacnac)Ca{cyN=C(C≡CCH$_2$OMe)=Ncy}]* **11**

0.03 ml (0.37 mmol) of **e** and 76 mg (0.37 mmol) of **h** in 10 ml of toluene was added to 0.25 g (0.37 mmol) of C**1** in 10 ml of toluene. After stirring overnight at room temperature the solvent volume was reduced in *vacuo* and left to crystallise at -30 ^{o}C for 48 hours. The product was isolated by filtration to yield 0.14 g (0.2 mmol 53 %) of compound **11**. ^{1}H NMR (250 MHz, 298K, C_6D_6) 1.44 (m, 2 x 10H, C*H*$_2$ of cy), 1.87 (d, 2 x 12H, CH*Me*$_2$), 1.77 (m, 2 x 1H, C*H* of cy), 2.06 (d, 2 x 12H, CH*Me*$_2$), 3.09 (s, 2×3H, {C(*Me*)}$_2$CH), 3.16 (s, 3H, O*Me*), 3.56 (m, 4H, C*H*Me$_2$), 5.23 (d, 2H, OC*H*$_2$), 5.71 (s, 1H, {C(Me)}$_2$C*H*), 6.74 (m, 6H, Ar*H*); ^{13}C NMR (75.48 MHz, 298K, C_6D_6) 11.7 (Si^{i}Pr*Me*), 18.9 (Si^{i}Pr*C*H), 24.8 (*C*HMe$_2$), 25.5, 26.8 (*C*H$_2$ of cy), 28.2 (CH*Me*$_2$), 26.9, 37.4 (*C*H$_2$ of cy), 58.9, 68.3(*C*H of cy), 93.7 (*C*≡CO), 95.4 (C≡*C*O), 98.5 ({C(*Me*)}$_2$CH), 123.6 (*p*-*C*$_6$H$_5$), 123.9 (*m*-*C*$_6$H$_5$), 141.8 (*o*-*C*$_6$H$_5$), 148.0 (*i*-*C*$_6$H$_5$),

158.8(**C**N), 165.1 (**C**N_2); Analysis calculated for $C_{46}H_{68}CaN_4O$: C, 75.36; H, 9.35; N, 7.64. Found: C, 75.62; H, 9.16; N, 7.65.

7.4.3 Stoichiometric carbodiimide insertion with the homoleptic complexes

7.4.3.1 Synthesis of *Ca[{^{i}PrNC(C≡CSi^{i}Pr$_3$)N^{i}Pr}]$_2$* **12**

0.45 ml (2.0 mmol) of **b** and 0.31 ml (2.0 mmol) of **g** in 10 ml of toluene was added to 0.5 g (0.99 mmol) of **C3** in 10 ml of toluene. After stirring overnight at room temperature the solvent volume was reduced in *vacuo* and left to crystallise at -30 ^{o}C for 48 hours. The product was isolated by filtration to yield 0.30 g (0.23 mmol 23 %) of compound **12**. ^{1}H NMR (300 MHz, 298K, C_6D_6) 1.10 (s, 36H, Si^{i}Pr*Me$_3$*), 1.35 (d, $^3J_{HH}$ = 6.2, 2 x 6H, N^{i}Pr*Me$_2$*), 1.41 (d, $^3J_{HH}$ = 6.4, 2 x 6H, N^{i}Pr*Me$_2$*), 3.77 (m, 6H, Si^{i}Pr*H*), 4.23 (m, 4H, N^{i}Pr*H*); ^{13}C NMR (75.48 MHz, 298K, C_6D_6) 11.5 (Si^{i}Pr*C*H), 18.7 (Si^{i}Pr*Me$_3$*), 26.1, 27.2, (N^{i}Pr*Me$_2$*), 50.0, 50.4 (N^{i}Pr*C*H), 96.0 (*C*≡CSi), 100.8 (C≡*C*Si), 159.8 (*C*N$_2$); Analysis calculated for $C_{36}H_{70}CaN_4Si_2$: C, 65.99; H, 10.77; N, 8.55. Found: C, 65.96; H, 10.78; N, 8.47.

7.4.3.2 Synthesis of *[{cyNC(C≡CSi^{i}Pr$_3$)Ncy}]Ca[C≡C Si^{i}Pr$_3$]* **13**

0.45 ml (2.0 mmol) of **b** and 0.41 g (2.0 mmol) of **h** in 10 ml of toluene was added to 0.5 g (0.99 mmol) of **C3** in 10 ml of toluene. After stirring overnight at room temperature the solvent volume was reduced in *vacuo* and left to crystallise at -30 ^{o}C for 48 hours. The product was isolated by filtration to yield 0.30 g (0.25 mmol 25 %) of compound **12**. ^{1}H NMR (300 MHz, 298K, C_6D_6) 1.17 (s, 36H, Si^{i}Pr*Me$_3$*), 1.95 (m, 2 × 10H, C*H$_2$* of cy), 3.14 (m, 6H, Si^{i}Pr*H*), 3.87 (m, 2 × 1H, C*H* of cy); ^{13}C NMR (75.48 MHz, 298K, C_6D_6) 26.2, 26.4, 26.7, 26.8, 37.2, 38.1 (*C*H$_2$ of cy), 58.6, 59.0 (*C*H of cy), 96.0 (*C*≡CSi), 96.4 (C≡*C*Si), 97.8 (SiC≡*C*Ca), 99.6 (Si*C*≡CCa), 157.8, 159.4 (*C*N$_2$); Analysis calculated for $C_{35}H_{64}CaN_2Si_2$: C, 69.01; H, 10.59; N, 4.60. Found: C, 68.89; H, 10.50; N, 4.56.

7.4.3.3 Synthesis of *Sr[{^{i}PrNC(C≡CSi^{i}Pr$_3$)N^{i}Pr}]$_2$* **14**

0.41 ml (1.8 mmol) of **b** and 0.28 ml (1.8 mmol) of **g** in 10 ml of toluene was added to 0.5 g (0.91 mmol) of **C4** in 10 ml of toluene. After stirring overnight at room temperature the solvent volume was reduced in *vacuo* and left to crystallise at -30 ^{o}C for 48 hours. The product was isolated by filtration to yield 0.30 g (0.21 mmol 24 %) of compound **14**. ^{1}H NMR (300 MHz, 298K, C_6D_6) 1.10 (s, 36H, Si^{i}Pr*Me$_3$*), 1.36 (d, 2 x 6H, N^{i}Pr*Me$_2$*), 3.80 (m, 6H, Si^{i}Pr*H*), 4.19 (m, 4H, N^{i}Pr*H*); ^{13}C NMR (75.48 MHz, 298K, C_6D_6) 11.5 (Si^{i}Pr*C*H), 18.7 (Si^{i}Pr*Me$_3$*), 22.7, 25.3 (N^{i}Pr*Me$_2$*), 42.7, 53.1 (N^{i}Pr*C*H), 92.8 (*C*≡CSi), 97.6 (C≡*C*Si), 140.3 (*C*N$_2$); The elemental analysis for $C_{36}H_{70}N_4Si_2Sr$ was unsuccessful.

7.4.3.4 Synthesis of *[{cyNC(C≡CSi^{i}Pr$_3$)Ncy}]Sr[C≡C Si^{i}Pr$_3$]* **15**

0.41 ml (1.8 mmol) of **b** and 0.37 g (1.8 mmol) of **h** in 10 ml of toluene was added to 0.5 g (0.91 mmol) of **C4** in 10 ml of toluene. After stirring overnight at room temperature the solvent volume was reduced in *vacuo* and left to crystallise at -30 ^{o}C for 48 hours. The product was isolated by filtration to yield 0.30 g (0.23 mmol 25 %) of compound **15**. ^{1}H NMR (300 MHz, 298K, C_6D_6) 1.17 (s, 36H, Si^{i}Pr*Me$_3$*), 1.81 (m, 2 × 20H, C*H$_2$* of cy), 3.03 (m, 6H, Si^{i}Pr*H*), 3.87 (m, 2 × 1H, C*H* of cy); ^{13}C NMR (75.48 MHz, 298K, C_6D_6) 26.1, 26.4, 26.7, 26.8, 35.4, 37.4 (*C*H$_2$ of cy), 55.7, 59.3 (*C*H of cy), 95.2 (*C*≡CSi), 95.7 (C≡*C*Si), 98.2 (SiC≡*C*Sr), 99.0 (Si*C*≡CSr), 157.8 (*C*N$_2$); Analysis calculated for $C_{35}H_{64}N_2Si_2Sr$: C, 64.01; H, 9.82; N, 4.27. Found: C, 63.92; H, 9.80; N, 4.37.

7.4.3.5 Synthesis of *Ba[{^{i}PrNC(C≡CSi^{i}Pr$_3$)N^{i}Pr}]$_2$* **16**

0.15 ml (0.83 mmol) of **b** and 0.13 ml (0.83 mmol) of **g** in 10 ml of toluene was added to 0.25 g (0.42 mmol) of **C5** in toluene. After stirring overnight at room temperature the solvent volume was reduced in *vacuo* and left to crystallise at -30 ^{o}C for 48 hours. The product was isolated by filtration to yield 0.05 g (0.03 mmol 8 %) of compound **16**. ^{1}H NMR (300 MHz, 298K, C_6D_6) 1.18 (s, 36H, Si^{i}Pr*Me$_3$*), 1.34 (d, $^{3}J_{HH}$ = 6.2, 2 x 6H, N^{i}Pr*Me$_2$*), 1.45 (d, $^{3}J_{HH}$ = 5.3, 2 x 6H, N^{i}Pr*Me$_2$*), 3.78 (m, 6H, Si^{i}Pr*H*), 4.35 (m, 4H, N^{i}Pr*H*); ^{13}C NMR (75.48 MHz, 298K, C_6D_6) 11.7 (Si^{i}Pr*C*H), 18.9 (Si^{i}Pr*Me$_3$*), 22.6, 26.1

(N^{i}Pr*Me$_2$*), 44.3, 49.1 (N^{i}Pr*C*H), 93.8 (*C*≡CSi), 99.7 (C≡*C*Si), 146.2 (*C*N$_2$); Analysis calculated for $C_{36}H_{70}BaN_4Si_2$: C, 57.46; H, 9.38; N, 7.45. Found: C, 57.55; H, 9.28; N, 7.39.

7.4.3.6 Synthesis of *[{cyNC(C≡CSi^{i}Pr$_3$)Ncy}]Ba[C≡C Si^{i}Pr$_3$]* **17**

0.15 ml (0.83 mmol) of **b** and 0.17 g (0.83 mmol) of **h** in 10 ml of toluene was added to 0.25 g (0.42 mmol) of **C5** in 10 ml of toluene. After stirring overnight at room temperature the solvent volume was reduced in *vacuo* and left to crystallise at -30 ^{o}C for 48 hours. The product was isolated by filtration to yield 0.22 g (0.16 mmol 38 %) of compound **17**. ^{1}H NMR (300 MHz, 298K, C_6D_6) 1.20 (s, 36H, Si^{i}PrMe**$_3$**), 1.60 (m, 2 × 10H, CH_2 of cy), 3.14 (m, 6H, Si^{i}PrH), 3.92 (m, 2 × 1H, CH of cy); ^{13}C NMR (75.48 MHz, 298K, C_6D_6) 25.9, 26.02, 26.5, 26.6, 26.9, 27.0 (*C*H$_2$ of cy), 60.0, 61.0 (*C*H of cy), 94.3 (*C*≡CSi), 94.8 (C≡*C*Si), 97.8 (SiC≡*C*Ba), 98.7 (Si*C*≡CBa), 157.9 (*C*N$_2$); Analysis calculated for $C_{35}H_{64}BaN_2Si_2$: C, 59.51; H, 9.31; N, 3.97. Found: C, 59.61; H, 9.30; N, 4.05.

7.4.3.7 Synthesis of *Ca[{^{i}PrNC(C≡CPh)N^{i}Pr}]$_2$* **18**

0.22 ml (1.98 mmol) of **a** and 0.31 ml (1.98 mmol) of **g** in 10 ml of toluene was added to 0.5 g (0.99 mmol) of **C3** in 10 ml of toluene. After stirring overnight at room temperature the solvent volume was reduced in *vacuo* and left to crystallise at -30 ^{o}C for 48 hours. The product was isolated by filtration to yield 0.30 g (0.3 mmol 31 %) of compound **18** with a melting point of 85 ^{0}C. ^{1}H NMR (300 MHz, 298K, C_6D_6) 0.97 (d, $^{3}J_{HH}$ = 6.4 Hz, 2 x 6H, N^{i}Pr*Me$_2$*), 1.39 (d, $^{3}J_{HH}$ = 6.2 Hz, 2 x 6H, N^{i}Pr*Me$_2$*), 4.26 (m, 2 x 2H, N^{i}Pr*H*), 6.95 (m, 6H, Ar*H*), 7.36 (m, 4H, Ar*H*); ^{13}C NMR (75.48 MHz, 298K, C_6D_6) 26.2, 27.2 (N^{i}Pr*Me$_2$*) 50.0, 50.6 (N^{i}Pr*C*H), 79.7 (*C*≡CPh), 95.3 (C≡*C*Ph), 122.1 (*i*- *C*$_6$H$_5$), 123.3 (*m*- *C*$_6$H$_5$), 129.5 (*p*- *C*$_6$H$_5$), 132.2 (*o*- *C*$_6$H$_5$), 158.0 (*C*N$_2$); Analysis calculated for $C_{30}H_{38}CaN_4$: C, 72.83; H, 7.74; N, 11.32. Found: C, 72.82; H, 7.66; N, 11.37.

7.4.3.8 Synthesis of *[{cyNC(C≡CPh)Ncy}]Ca[C≡CPh]* **19**

0.22 ml (1.98 mmol) of **a** and 0.41 g (1.98 mmol) of **h** in 10 ml of toluene was added to 0.5 g (0.99 mmol) of **C3** in 10 ml of toluene. After stirring overnight at room temperature the solvent volume was reduced in *vacuo* and left to crystallise at -30 ^{o}C for 48 hours. The product was isolated by filtration to yield 0.30 g (0.23 mmol 23 %) of compound **19** with a melting point greater than 85 ^{0}C. ^{1}H NMR (300 MHz, 298K, C_6D_6) 1.53 (m, 2 × 10H, C*H*$_2$ of cy), 4.00 (m, 2 × 1H, C*H* of cy), 6.96 (m, 6H, Ar*H*), 7.44 (m, 4H, Ar*H*); ^{13}C NMR (75.48 MHz, 298K, C_6D_6) 26.2, 26.4, 26.6, 26.8, 37.2, 38.2 (*C*H$_2$ of cy), 58.6, 59.3 (*C*H of cy), 80.1 (*C*≡CPh), 94.8 (C≡*C*Ph), 81.1 (PhC≡*C*Ca), 97.2 (Ph*C*≡CCa), 122.3 (*i*- *C*$_6$H$_5$), 123.5 (*m*- *C*$_6$H$_5$), 128.8 (*p*- *C*$_6$H$_5$), 132.2 (*o*- *C*$_6$H$_5$), 159.9 (*C*N$_2$); Analysis calculated for $C_{29}H_{32}CaN_4$: C, 77.63; H, 7.19; N, 6.24. Found: C, 77.56; H, 7.12; N, 6.19; X-ray crystallography data, see appendix.

7.4.3.9 Synthesis of *Sr[{^{i}PrNC(C≡CPh)N^{i}Pr}]$_2$* **20**

0.20 ml (1.8 mmol) of **a** and 0.28 ml (1.8 mmol) of **g** in 10 ml of toluene was added to 0.5 g (0.91 mmol) of **C4** in 10 ml of toluene. After stirring overnight at room temperature the solvent volume was reduced in *vacuo* and left to crystallise at -30 ^{o}C for 48 hours. The product was isolated by filtration to yield 0.30 g (0.28 mmol 31 %) of compound **20** decomposing at 120 ^{o}C. ^{1}H NMR (300 MHz, 298K, C_6D_6) 1.17 (d, 2 x 6H, N^{i}Pr*Me*$_2$), 1.22 (d, 2 x 6H, N^{i}Pr*Me*$_2$), 3.61 (m, 2 x 2H, N^{i}Pr*H*), 6.90 (m, 6H, Ar*H*), 7.38 (m, 4H, Ar*H*); ^{13}C NMR (75.48 MHz, 298K, C_6D_6) 22.6, 25.4 (N^{i}Pr*Me*$_2$), 42.6, 53.2 (N^{i}Pr*C*H), 85.5 (*C*≡CPh), 90.3 (C≡*C*Ph), 122.1 (*i*- *C*$_6$H$_5$), 123.2 (*m*- *C*$_6$H$_5$), 128.7 (*p*- *C*$_6$H$_5$), 132.1 (*o*- *C*$_6$H$_5$), 157.6 (*C*N$_2$); Analysis calculated for $C_{30}H_{38}N_4Sr$: C, 66.45; H, 7.06; N, 10.33. Found: C, 66.53; H, 6.96; N, 10.30.

7.4.3.10 Synthesis of *[{cyNC(C≡CPh)Ncy}]Sr[C≡CPh]* **21**

0.20 ml (1.8 mmol) of **a** and 0.37 g (1.8 mmol) of **h** in 10 ml of toluene was added to 0.5 g (0.91 mmol) of **C4** in 10 ml of toluene. After stirring overnight at room temperature the solvent volume was reduced in *vacuo* and left to crystallise at -30 ^{o}C for 48 hours. The product was isolated by filtration to yield 0.30 g (0.3 mmol 33 %) of compound **21** decomposing above 120 ^{o}C. ^{1}H NMR (300 MHz, 298K, C_6D_6) 1.57 (m, 2

× 10H, CH_2 of cy), 4.25 (m, 2 × 1H, C*H* of cy), 6.95 (m, 6H, Ar*H*), 7.39 (m, 4H, Ar*H*); ^{13}C NMR (75.48 MHz, 298K, C_6D_6) 25.3, 25.5, 26.2, 26.5, 33.3, 35.8(*C*H_2 of cy), 49.7, 61.4 (*C*H of cy), 81.2 (*C*≡CPh), 82.5 (C≡*C*Ph), 90.2 (PhC≡*C*Sr), 97.0 (Ph*C*≡CSr), 122.2 (*i*- *C*$_6$H$_5$), 123.9 (*m*- *C*$_6$H$_5$), 128.7 (*p*- *C*$_6$H$_5$), 131.2 (*o*- *C*$_6$H$_5$), 152.2 (*C*N_2); Analysis calculated for $C_{29}H_{32}N_2Sr$: C, 70.20; H, 6.50; N, 5.65. Found: C, 69.98; H, 6.56; N, 5.52.

7.4.3.11 Synthesis of *Ba[{^{i}PrNC(C≡CPh)N^{i}Pr}]$_2$* **22**

0.18 ml (1.7 mmol) of **a** and 0.26 ml (1.7 mmol) of **g** in 10 ml of toluene was added to 0.5 g (0.83 mmol) of **C5** in 10 ml of toluene. After stirring overnight at room temperature the solvent volume was reduced in *vacuo* and left to crystallise at -30 ^{o}C for 48 hours. The product was isolated by filtration to yield 0.30 g (0.25 mmol 31 %) of compound **27** decomposing above 120 ^{o}C. ^{1}H NMR (300 MHz, 298K, C_6D_6) 0.98 (d, 2 x 6H, N^{i}Pr*Me$_2$*), 1.40 (d, 2 x 6H, N^{i}Pr*Me$_2$*), 4.25 (m, 2 x 2H, N^{i}Pr*H*), 6.95 (m, 6H, Ar*H*), 7.39 (m, 4H, Ar*H*); ^{13}C NMR (75.48 MHz, 298K, C_6D_6) 22.7, 25.4 (N^{i}Pr*Me$_2$*), 49.2, 53.1 (N^{i}Pr*C*H), 80.9 (*C*≡CPh), 90.3 (C≡*C*Ph), 122.1 (*i*- *C*$_6$H$_5$), 123.7 (*m*- *C*$_6$H$_5$), 128.7 (*p*- *C*$_6$H$_5$), 132.2 (*o*- *C*$_6$H$_5$), 140.0 (*C*N_2); Analysis calculated for $C_{30}H_{38}BaN_4$: C, 60.87; H, 6.47; N, 9.46. Found: C, 60.91; H, 6.50; N, 9.51.

7.4.3.12 Synthesis of *[{cyNC(C≡CPh)Ncy}]Ba[C≡CPh]* **23**

0.18 ml (1.7 mmol) of **a** and 0.34 g (1.7 mmol) of **h** in 10 ml of toluene was added to 0.5 g (0.83 mmol) of **C5** in 10 ml of toluene. After stirring overnight at room temperature the solvent volume was reduced in *vacuo* and left to crystallise at -30 ^{o}C for 48 hours. The product was isolated by filtration to yield 0.30 g (0.27 mmol 33 %) of compound **23** decomposing above 120 ^{o}C. ^{1}H NMR (300 MHz, 298K, C_6D_6) 1.53 (m, 2 × 10H, CH_2 of cy), 3.93 (m, 2 × 1H, C*H* of cy), 6.96 (m, 6H, Ar*H*), 7.42 (m, 4H, Ar*H*); ^{13}C NMR (75.48 MHz, 298K, C_6D_6) 25.3, 25.5, 26.4, 26.5, 33.3, 35.8 (*C*H_2 of cy), 49.7, 58.7 (*C*H of cy), 80.9 (*C*≡CPh), 81.2 (C≡*C*Ph), 90.2 (PhC≡*C*Ba), 97.1 (Ph*C*≡CBa), 122.2 (*i*- *C*$_6$H$_5$), 123.0 (*m*- *C*$_6$H$_5$), 128.7 (*p*- *C*$_6$H$_5$), 132.2 (*o*- *C*$_6$H$_5$), 139.2 (*C*N_2); Analysis calculated for $C_{29}H_{32}BaN_2$: C, 63.80; H, 5.91; N, 5.13. Found: C, 63.78; H, 5.89; N, 5.26.

7.4.3.13 Synthesis of *Ca[{^{i}PrNC(C≡CCH$_2$NMe$_2$)N^{i}Pr}]$_2$* **24**

0.21 ml (2.0 mmol) of **d** and 0.31 ml (2.0 mmol) of **g** in 10 ml of toluene was added to 0.5 g (0.99 mmol) of **C3** in 10 ml of toluene. After stirring overnight at room temperature the solvent volume was reduced in *vacuo* and left to crystallise at -30 ^{o}C for 48 hours. The product was isolated by filtration to yield 0.3 g (0.37 mmol 33 %) of compound **24**. ^{1}H NMR (300 MHz, 298K, C_6D_6) 1.37 (d, $^{3}J_{HH}$ = 6.2, 2 x 6H, ^{i}Pr*Me$_2$*), 1.47 (d, $^{3}J_{HH}$ = 6.4, 2 x 6H, ^{i}Pr*Me$_2$*), 2.18 (s, 2 x 6H, N*Me$_2$*), 3.22 (d, $^{2}J_{HH}$ = 11.5, 2 x 2H, C*H$_2$*NMe$_2$), 4.22 (m, 4H, ^{i}Pr*H*); ^{13}C NMR (75.48 MHz, 298K, C_6D_6) 26.2, 27.2 (^{i}Pr*Me$_3$*), 43.9 (N*Me$_2$*), 49.9 (*C*H$_2$NMe$_2$), 50.4 (^{i}Pr*C*H), 90.2 (*C*≡CCH$_2$), 94.6 (C≡*C*H$_2$), 145.3 (*C*N$_2$); Analysis calculated for $C_{24}H_{44}CaN_6$: C, 63.11; H, 9.71; N, 18.40. Found: C, 63.31; H, 9.36; N, 18.40.

7.4.3.14 Synthesis of *[{cyNC(C≡CCH$_2$NMe$_2$)Ncy}]Ca[C≡CCH$_2$NMe$_2$]* **25**

0.21 ml (2.0 mmol) of **d** and 0.41 g (2.0 mmol) of **h** in 10 ml of toluene was added to 0.5 g (0.99 mmol) of **C3** in 10 ml of toluene. After stirring overnight at room temperature the solvent volume was reduced in *vacuo* and left to crystallise at -30 ^{o}C for 48 hours. The product was isolated by filtration to yield 0.3 g (0.37 mmol 37 %) of compound **25**. ^{1}H NMR (300 MHz, 298K, C_6D_6) 1.54 (m, 2 × 10H, C*H$_2$* of cy), 2.25 (d, 12H, N*Me$_2$*), 3.27 (d, 4H, C*H$_2$*NMe$_2$), 3.82 (m, 2 × 1H, C*H* of cy); ^{13}C NMR (75.48 MHz, 298K, C_6D_6) 25.8, 26.2, 26.7, 26.8, 35.4, 35.9 (*C*H$_2$ of cy), 43.9 (N*Me$_2$*), 49.3 (*C*H$_2$NMe$_2$), 58.9, 59.2 (*C*H of cy), 93.7 (*C*≡CCH$_2$), 94.0 (C≡*C*CH$_2$), 97.5 (CH$_2$C≡*C*Ca), 98.8 (CH$_2$*C*≡CCa), 146.8 (*C*N$_2$); Analysis calculated for $C_{23}H_{38}CaN_4$: C, 67.27; H, 9.33; N, 13.64. Found: C, 67.30; H, 9.41; N, 13.61.

7.4.3.15 Synthesis of *Sr[{^{i}PrNC(C≡CCH$_2$NMe$_2$)N^{i}Pr}]$_2$* **26**

0.19 ml (1.8 mmol) of **d** and 0.28 ml (1.8 mmol) of **g** in 10 ml of toluene was added to 0.5 g (0.99 mmol) of **C4** in 10 ml of toluene. After stirring overnight at room temperature the solvent volume was reduced in *vacuo* and left to crystallise at -30 ^{o}C for 48 hours. The product was isolated by filtration to yield 0.3 g (0.33 mmol 33 %) ofcompound **26**. ^{1}H NMR (300 MHz, 298K, C_6D_6) 1.16 (brs, 24H, ^{i}Pr*Me$_3$*), 2.12 (s, 2 x 6H, N*Me$_2$*), 3.13 (d, 2 x 2H, C*H$_2$*NMe$_2$), 3.73 (m, 4H, ^{i}Pr*H*); ^{13}C NMR (75.48 MHz,

298K, C_6D_6) 23.5, 24.0 (^{i}Pr*Me*$_3$), 44.0 (N*Me*$_2$), 48.0 (*C*H$_2$NMe$_2$), 52.9 (^{i}Pr*C*H), 77.0 (*C*≡CCH$_2$), 86.6 (C≡*C*H$_2$), 140.0 (*C*N$_2$); Analysis calculated for $C_{24}H_{44}N_6Sr$: C, 57.16; H, 8.79; N, 16.67. Found: C, 57.15; H, 8.77; N, 16.53.

7.4.3.16 Synthesis of *[{cyNC(C≡CH$_2$NMe$_2$)Ncy}]Sr[C≡CH$_2$NMe$_2$]* **27**

0.19 ml (1.8 mmol) of **d** and 0.37 g (1.8 mmol) of **h** in 10 ml of toluene was added to 0.5 g (0.99 mmol) of **C4** in 10 ml of toluene. After stirring overnight at room temperature the solvent volume was reduced in *vacuo* and left to crystallise at -30 ^{o}C for 48 hours. The product was isolated by filtration to yield 0.3 g (0.33 mmol 36 %) of compound **27**. ^{1}H NMR (300 MHz, 298K, C_6D_6) 1.54 (m, 2 × 10H, C*H*$_2$ of cy), 2.17 (d, 2 × 6H, N*Me*$_2$), 3.19 (d, 2 × 2H C*H*$_2$NMe$_2$), 3.88 (m, 2 × 1H, C*H* of cy); ^{13}C NMR (75.48 MHz, 298K, C_6D_6) 25.7, 26.5, 35.4 (*C*H$_2$ of cy), 44.0 (N*Me*$_2$), 48.2 (*C*H$_2$NMe$_2$), 55.7 (*C*H of cy), 94.6 (*C*≡CCH$_2$), 95.2 (C≡*C*CH$_2$), 97.7 (CH$_2$C≡*C*Sr), 98.6 (CH$_2$*C*≡CSr), 138.5 (***C***N$_2$); Analysis calculated for $C_{23}H_{38}N_4Sr$: C, 60.29; H, 8.36; N, 12.23. Found: C, 60.77; H, 8.48; N, 12.08.

7.4.3.17 Synthesis of *Ba[{^{i}PrNC(C≡CH$_2$NMe$_2$)N^{i}Pr}]$_2$* **28**

0.09 ml (0.83 mmol) of **d** and 0.13 ml (0.83 mmol) of **g** in 10 ml of toluene was added to 0.25 g (0.42 mmol) of **C5** in 10 ml of toluene. After stirring overnight at room temperature the solvent volume was reduced in *vacuo* and left to crystallise at -30 ^{o}C for 48 hours. The product was isolated by filtration to yield 0.14 g (0.12 mmol 30 %) of compound **28**. ^{1}H NMR (300 MHz, 298K, C_6D_6) 1.00 (s, $^{3}J_{HH}$ = 7.0, 2 x 6H, ^{i}Pr*Me*$_3$), 1.42 (s, $^{3}J_{HH}$ = 5.8, 2 x 6H, ^{i}Pr*Me*$_3$), 2.22 (s, 2 x 6H, N*Me*$_2$), 2.52 (d, 2 x 2H, C*H*$_2$NMe$_2$), 4.23 (m, 4H, ^{i}Pr*H*); ^{13}C NMR (75.48 MHz, 298K, C_6D_6) 22.4, 23.3 (^{i}Pr*Me*$_3$), 44.1 (N*Me*$_2$), 46.9 (*C*H$_2$NMe$_2$), 48.3(^{i}Pr*C*H), 82.3 (**C**≡CCH$_2$), 84.9 (*C*≡CCH$_2$), 143.6 (*C*N$_2$); Analysis calculated for $C_{24}H_{44}BaN_6$: C, 52.03; H, 8.01; N, 15.17. Found: C, 40.47; H, 7.00; N, 9.99.

7.4.3.18 Synthesis of *[{cyNC(C≡CH$_2$NMe$_2$)Ncy}]Ba[C≡CH$_2$NMe$_2$]* **29**

0.09 ml (0.83 mmol) of **d** and 0.17 g (0.83 mmol) of **h** in 10 ml of toluene was added to 0.25 g (0.42 mmol) of **C5** in 10 ml of toluene. After stirring overnight at room

temperature the solvent volume was reduced in *vacuo* and left to crystallise at -30 ^{o}C for 48 hours. The product was isolated by filtration to yield 0.15 g (0.15 mmol 36 %) of compound **29**. ^{1}H NMR (300 MHz, 298K, C_6D_6) 1.57 (m, 2 × 10H, CH_2 of cy), 2.22 (d, 2 × 6H, NMe_2), 2.55 (d, 2 × 2H CH_2NMe_2), 3.86 (m, 2 × 1H, CH of cy); ^{13}C NMR (75.48 MHz, 298K, C_6D_6) 24.8, 25.8, 26.5, 27.3, 35.4(CH$_2$ of cy), 44.1 (NMe_2), 47.1 (CH$_2$NMe_2), 55.7 (CH of cy), 89.6 (C≡CCH$_2$), 94.7 (C≡CCH$_2$), 96.6 (CH$_2$C≡CBa), 98.4 (CH$_2C$≡CBa), 143.3 (CN$_2$); Analysis calculated for $C_{23}H_{38}BaN_4$: C, 54.39; H, 7.54; N, 11.03. Found: C, 54.83; H, 7.66; N, 10.94.

7.4.3.19 Synthesis of *Ca[{^{i}PrNC(C≡CCH$_2$OMe)N^{i}Pr}]$_2$* **30**

0.17 ml (1.98 mmol) of **e** and 0.31 ml (1.98 mmol) of **g** in 10 ml of toluene was added to 0.5 g (0.99 mmol) of **C3** in 10 ml of toluene. After stirring overnight at room temperature the solvent volume was reduced in *vacuo* and left to crystallise at -30 ^{o}C for 48 hours. The product was isolated by filtration to yield 0.3 g (0.35 mmol 36 %) of compound **30**. ^{1}H NMR (300 MHz, 298K, C_6D_6) 1.04 (d, $^{3}J_{HH}$ = 6.4, 2 x 6H, terminal ^{i}PrMe_3), 1.26 (d, $^{3}J_{HH}$ = 6.1, 2 x 6H, terminal ^{i}PrMe_3), 1.32 (d, $^{3}J_{HH}$ = 6.2, 2 x 6H, bridging ^{i}PrMe_3), 1.43 (d, $^{3}J_{HH}$ = 6.4, 2 x 6H, bridging ^{i}PrMe_3), 3.14 (d, 12H, OMe), 3.79 (m, 2 x 2H, ^{i}PrH), 3.90 (brs, 4H, CH_2OMe), 3.97 (brs, 4H, CH_2OMe), 4.11 (m, 2 x 2H, ^{i}PrH); ^{13}C NMR (75.48 MHz, 298K, C_6D_6) 23.1 (^{i}PrMe_3), 46.9 (OMe), 51.8 (^{i}PrCH), 58.4 (CH$_2$OMe), 72.2 (C≡CCH$_2$), 82.4 (C≡CH$_2$), 146.8 (CN$_2$); Analysis calculated for $C_{22}H_{38}CaN_4O_2$: C, 61.36; H, 8.89; N, 13.01. Found: C, 61.28; H, 8.81; N, 12.97.

7.4.3.20 Synthesis of *[{cyNC(C≡CCH$_2$OMe)Ncy}]Ca[C≡CCH$_2$OMe]* **31**

0.17 ml (2.0 mmol) of **e** and 0.41 g (2.0 mmol) of **h** in 10 ml of toluene was added to 0.5 g (0.99 mmol) of **C3** in 10 ml of toluene. After stirring overnight at room temperature the solvent volume was reduced in *vacuo* and left to crystallise at -30 ^{o}C for 48 hours. The product was isolated by filtration to yield 0.3 g (0.39 mmol 40 %) of compound **31**. ^{1}H NMR (300 MHz, 298K, C_6D_6) 1.47 (m, 2 × 10H, CH_2 of cy), 3.24 (s, 2 × 6H, OMe), 3.99 (m, 2 × 2H CH_2OMe), 3.77 (m, 2 × 1H, CH of cy); ^{13}C NMR (75.48 MHz, 298K, C_6D_6) 24.2, 24.3, 26.1, 26.2, 26.5, 26.7 (CH$_2$ of cy), 49.7 (CH of cy), 62.5 (OMe), 67.6 (CH$_2$OMe), 82.8 (C≡CCH$_2$), 85.8 (C≡CCH$_2$), 96.4 (CH$_2$C≡CCa), 97.5

(CH_2C≡CCa), 143.8 (CN_2); Analysis calculated for $C_{21}H_{32}CaN_2O_2$: C, 65.59; H, 8.39; N, 7.28. Found: C, 66.04; H, 8.52; N, 7.23.

7.4.3.21 Synthesis of *Sr[{^{i}PrNC(C≡CCH$_2$OMe)N^{i}Pr}]$_2$* **32**

0.15 ml (1.8 mmol) of **e** and 0.28 ml (1.8 mmol) of **g** in 10 ml of toluene was added to 0.5 g (0.9 mmol) of **C4** in 10 ml of toluene. After stirring overnight at room temperature the solvent volume was reduced in *vacuo* and left to crystallise at -30 ^{o}C for 48 hours. The product was isolated by filtration to yield 0.3 g (0.31 mmol 35 %) of compound **32**. ^{1}H NMR (300 MHz, 298K, C_6D_6) 1.10 (d, $^{3}J_{HH}$ = 6.6, 2 x 6H, terminal ^{i}Pr*Me$_3$*), 1.22 (d, $^{3}J_{HH}$ = 6.4, 2 x 6H, terminal ^{i}Pr*Me$_3$*), 1.28 (d, $^{3}J_{HH}$ = 6.8, 2 x 6H, bridging ^{i}Pr*Me$_3$*), 1.42 (d, $^{3}J_{HH}$ = 7.0, 2 x 6H, bridging ^{i}Pr*Me$_3$*), 2.89 (s, 2 x 6H, O*Me*), 2.91 (s, 2 x 6H, O*Me*), 3.11 (d, $^{2}J_{HH}$ = 4.5, 2 x 2H, C*H$_2$*OMe), 3.42 (d, 2 x 2H, C*H$_2$*OMe), 4.51 (m, 2 x 2H, ^{i}Pr*H*), 4.72 (m, 2 x 2H, ^{i}Pr*H*); ^{13}C NMR (75.48 MHz, 298K, C_6D_6) 21.8 (^{i}Pr*Me$_3$*), 48.6 (O*Me*), 50.1 (^{i}Pr*C*H), 56.5 (*C*H$_2$OMe), 89.4 (*C*≡CCH$_2$), 95.1 (C≡*C*CH$_2$), 146.6 (*C*N$_2$); The elemental analysis for $C_{22}H_{38}N_4O_2Sr$ was unsuccessful.

7.4.3.22 Synthesis of *[{cyNC(C≡CCH$_2$OMe)Ncy}]Sr[C≡CCH$_2$OMe]* **33**

0.15 ml (1.8 mmol) of **e** and 0.37 g (1.8 mmol) of **h** in 10 ml of toluene was added to 0.5 g (0.9 mmol) of **C4** in 10 ml of toluene. After stirring overnight at room temperature the solvent volume was reduced in *vacuo* and left to crystallise at -30 ^{o}C for 48 hours. The product was isolated by filtration to yield 0.3 g (0.35 mmol 39 %) of compound **33**. ^{1}H NMR (300 MHz, 298K, C_6D_6) 1.43 (m, 2 × 10H, C*H$_2$* of cy), 3.24 (s, 2 × 6H, O*Me*), 3.86 (m, 2 × 1H, C*H* of cy), 4.00 (m, 2 × 2H C*H$_2$*OMe); ^{13}C NMR (75.48 MHz, 298K, C_6D_6) 25.1, 25.2, 26.0, 26.3, 37.2 (*C*H$_2$ of cy), 50.2 (*C*H of cy), 59.3 (O*Me*), 66.7 (*C*H$_2$OMe), 74.3 (*C*≡CCH$_2$), 78.2 (C≡*C*CH$_2$), 94.4 (CH$_2$C≡*C*Sr), 97.5 (CH$_2$*C*≡CSr), 155.1 (*C*N$_2$); Analysis calculated for $C_{21}H_{32}N_2O_2Sr$: C, 58.37; H, 7.46; N, 6.48. Found: C, 58.47; H, 7.52; N, 6.50.

7.4.3.23 Synthesis of *Ba[{^{i}PrNC(C≡CCH$_2$OMe)N^{i}Pr}]$_2$* **34**

0.07 ml (0.83 mmol) of **e** and 0.13 ml (0.83 mmol) of **g** in 10 ml of toluene was added to 0.25 g (0.42 mmol) of **C5** in 10 ml of toluene. After stirring overnight at room

temperature the solvent volume was reduced in *vacuo* and left to crystallise at -30 ^{o}C for 48 hours. The product was isolated by filtration to yield 0.05 g (0.05 mmol 11 %) of compound **34**. ^{1}H NMR (300 MHz, 298K, C_6D_6) 0.94 (d, $^{3}J_{HH}$ = 6.4, 2 x 6H, ^{i}Pr*Me*$_3$), 1.33 (d, $^{3}J_{HH}$ = 6.2, 2 x 6H, ^{i}Pr*Me*$_3$), 3.05 (s, 2 x 6H, O*Me*), 3.84 (d, 2 x 2H, C*H*$_2$OMe), 4.11 (m, 2 x 2H, ^{i}Pr*H*); ^{13}C NMR (75.48 MHz, 298K, C_6D_6) 22.6, 25.3 (^{i}Pr*Me*$_3$), 42.5 (O*Me*), 53.1 (^{i}Pr*C*H), 57.4, 59.6 (*C*H$_2$OMe), 77.8 (*C*≡CCH$_2$), 86.7 (C≡*C*H$_2$), 149.4 (*C*N$_2$); Analysis calculated for $C_{22}H_{38}BaN_4O_2$: C, 50.06; H, 7.26; N, 10.61. Found: C, 49.96; H, 7.25; N, 10.52.

7.4.3.24 Synthesis of *[{cyNC(C≡CCH$_2$OMe)Ncy}]Ba[C≡CCH$_2$OMe]* **35**

0.07ml (0.83 mmol) of **e** and 0.17 g (0.83 mmol) of **h** in 10 ml of toluene was added to 0.25 g (0.42 mmol) of **C5** in 10 ml of toluene. After stirring overnight at room temperature the solvent volume was reduced in *vacuo* and left to crystallise at -30 ^{o}C for 48 hours. The product was isolated by filtration to yield 0.06 g (0.06 mmol 15 %) of compound **35**. ^{1}H NMR (300 MHz, 298K, C_6D_6) 1.47 (m, 2 × 10H, C*H*$_2$ of cy), 3.11 (s, 2 × 6H, O*Me*), 3.81 (m, 2 × 1H, C*H* of cy), 3.86 (m, 2 × 2H C*H*$_2$OMe); ^{13}C NMR (75.48 MHz, 298K, C_6D_6) 25.2, 25.4, 26.2, 26.4, 33.2, 35.7 (*C*H$_2$ of cy), 49.7 (O*Me*), 57.3, 59.6 (*C*H of cy), 61.3 (*C*H$_2$OMe), 78.1 (*C*≡CCH$_2$), 85.3 (C≡*C*CH$_2$), 86.7 (CH$_2$C≡*C*Ba), 95.4 (CH$_2$*C*≡CBa), 139.4 (*C*N$_2$); The elemental analysis for $C_{21}H_{32}BaN_2O_2$ was unsuccessful.

7.4.3.25 Synthesis of *Ca[{^{i}PrNC(C≡CCH$_2$OPh)N^{i}Pr}]$_2$* **36**

0.25 ml (1.98 mmol) of **f** and 0.31 ml (1.98 mmol) of **g** in 10 ml of toluene was added to 0.5 g (0.99 mmol) of **C3** in 10 ml of toluene. After stirring overnight at room temperature the solvent volume was reduced in *vacuo* and left to crystallise at -30 ^{o}C for 48 hours. The product was isolated by filtration to yield 0.3 g (0.27 mmol 27 %) of compound **36**. ^{1}H NMR (300 MHz, 298K, C_6D_6) 0.89 (d, $^{3}J_{HH}$ = 6.4, 2 x 6H, ^{i}Pr*Me*$_3$), 1.03 (d, $^{3}J_{HH}$ = 6.4, 2 x 6H, ^{i}Pr*Me*$_3$), 4.03 (m, 2 x 2H, ^{i}Pr*H*); 4.30 (d, 2 x 2H, C*H*$_2$OPh), 6.80 (m, 2 x 3H, O*Ph*), 7.04 (m, 2 x 2H, O*Ph*); ^{13}C NMR (75.48 MHz, 298K, C_6D_6) 23.0(^{i}Pr*Me*$_3$), 55.6 (*C*H$_2$OPh), 78.6 (*C*≡CCH$_2$), 91.4 (C≡*C*H$_2$), 115.3 (*i*-*C*OPh), 121.3 (*m*-*C*OPh), 121.8 (*p*-*C*OPh), 129.7 (*o*-*C*OPh), 158.0 (*C*N$_2$); Analysis calculated for $C_{32}H_{42}CaN_4O$: C, 69.28; H, 7.63; N, 10.10. Found: C, 69.29; H, 7.59; N, 9.97.

7.4.3.26 Synthesis of *[{cyNC(C≡CCH$_2$OPh)Ncy}]Ca[C≡CCH$_2$OPh]* **37**

0.25 ml (1.98 mmol) of **f** and 0.41 g (1.98 mmol) of **h** in 10 ml of toluene was added to 0.5 g (0.99 mmol) of **C3** in 10 ml of toluene. After stirring overnight at room temperature the solvent volume was reduced in *vacuo* and left to crystallise at -30 ^{o}C for 48 hours. The product was isolated by filtration to yield 0.3 g (0.27 mmol 30 %) of compound **37**. ^{1}H NMR (300 MHz, 298K, C_6D_6) 1.56 (m, 2 × 10H, C*H$_2$* of cy), 3.61 (m, 2 × 1H, C*H* of cy), 4.37 (d, $^{3}J_{HH}$ = 3.8MHz, 4H, C*H$_2$*OPh), 6.81 (m, 2 × 3H O*Ph*), 7.08 (m, 2 × 2H, O*Ph*); ^{13}C NMR (75.48 MHz, 298K, C_6D_6) 25.8, 26.2, 26.4, 26.7, 37.0, 38.1 (*C*H$_2$ of cy), 55.2, 55.64 (*C*H of cy), 58.7 (*C*H$_2$OPh), 77.8 (*C*≡CCH$_2$), 78.8 (C≡*C*CH$_2$), 90.1 (CH$_2$C≡*C*Ca), 92.7 (CH$_2$*C*≡CCa), 115.0 (*i*-*C*OPh), 121.3 (*m*-*C*OPh), 121.7 (*p*-*C*OPh), 129.7 (*o*-*C*OPh), 156.7 (*C*N$_2$); Analysis calculated for $C_{31}H_{36}CaN_2O_2$: C, 73.19; H, 7.13; N, 5.51. Found: C, 73.19; H, 7.23; N, 5.51.

7.4.3.27 Synthesis of *Sr[{^{i}PrNC(C≡CCH$_2$OPh)N^{i}Pr}]$_2$* **38**

0.23 ml (1.81 mmol) of **f** and 0.28 ml (1.81 mmol) of **g** in 10 ml of toluene was added to 0.5 g (0.9 mmol) of **C4** in 10 ml of toluene. After stirring overnight at room temperature the solvent volume was reduced in *vacuo* and left to crystallise at -30 ^{o}C for 48 hours. The product was isolated by filtration to yield 0.3 g (0.25 mmol 27 %) of compound **38**. ^{1}H NMR (300 MHz, 298K, C_6D_6) 1.22 (m, 2 x 12H, ^{i}Pr*Me$_3$*), 4.05 (m, 2 x 2H, ^{i}Pr*H*), 4.29 (d, 2 x 2H, C*H$_2$*OPh), 6.81 (m, 2 x 3H, O*Ph*), 7.04 (m, 2 x 2H, O*Ph*); ^{13}C NMR (75.48 MHz, 298K, C_6D_6) 25.0 (^{i}Pr*Me$_3$*), 55.6 (^{i}Pr*C*H), 59.8 (*C*H$_2$OPh), 83.9 (***C***≡CCH$_2$), 92.3 (C≡*C*CH$_2$), 115.2 (*i*-*C*OPh), 121.9 (*m*-*C*OPh), 125.5 (*p*-*C*OPh), 129.74 (*o*-*C*OPh), 152.6 (*C*N$_2$); Analysis calculated for $C_{32}H_{42}N_4O_2Sr$ was unsuccessful.

7.4.3.28 Synthesis of *[{cyNC(C≡CCH$_2$OPh)Ncy}]Sr[C≡CCH$_2$OPh]* **39**

0.23 ml (1.81 mmol) of **f** and 0.37 g (1.81 mmol) of **h** in 10 ml of toluene was added to 0.5 g (0.9 mmol) of **C4** in 10 ml of toluene. After stirring overnight at room temperature the solvent volume was reduced in *vacuo* and left to crystallise at -30 ^{o}C for 48 hours. The product was isolated by filtration to yield 0.3 g (0.27 mmol 30 %) of compound **39**. ^{1}H NMR (300 MHz, 298K, C_6D_6) 1.72 (m, 2 × 10H, C*H$_2$* of cy), 3.65 (m, 2 × 1H, C*H* of cy), 4.42 (d, 4H, C*H$_2$*OPh), 6.91 (m, 2 × 3H O*Ph*), 7.07 (m, 2 × 2H, O*Ph*); ^{13}C NMR

(75.48 MHz, 298K, C_6D_6) 25.6, 25.7, 26.3, 26.4, 38.5, 38.6 (*C*H_2 of cy), 50.4, 55.1 (*C*H of cy), 60.7 (*C*H_2OPh), 83.3 (*C*≡CCH$_2$), 86.6 (C≡*C*CH$_2$), 92.7 (CH$_2$C≡*C*Sr), 95.1 (CH$_2$*C*≡CSr), 115.0 (*i*-*C*OPh), 121.2 (*m*-*C*OPh), 126.4 (*p*-OPh), 129.6 (*o*-*C*OPh), 146.0 (*C*N_2); Analysis calculated for $C_{31}H_{36}N_2O_2Sr$: C, 66.94; H, 6.52; N, 5.04. Found: C, 66.87; H, 6.62; N, 5.12.

7.4.3.29 Synthesis of *Ba[{^{i}PrNC(C≡CCH$_2$OPh)N^{i}Pr}]$_2$* **40**

0.11 ml (0.83 mmol) of **f** and 0.13 ml (0.83 mmol) of **g** in 10 ml of toluene was added to 0.25 g (0.42 mmol) of **C5** in 10 ml of toluene. After stirring overnight at room temperature the solvent volume was reduced in *vacuo* and left to crystallise at -30 ^{o}C for 48 hours. The product was isolated by filtration to yield 0.1 g (0.08 mmol 19 %) of compound **40**. ^{1}H NMR (300 MHz, 298K, C_6D_6) 1.03 (m, 2 x 12H, ^{i}Pr*Me$_3$*), 1.22 (m, 2 x 12H, ^{i}Pr*Me$_3$*), 1.30 (m, 2 x 12H, ^{i}Pr*Me$_3$*), 1.47 (m, 2 x 12H, ^{i}Pr*Me$_3$*), 4.32 (d, 2 x 2H, C*H$_2$*OPh), 4.41 (m, 2 x 2H, ^{i}Pr*H*), 6.80 (m, 2 x 3H, O*Ph*), 7.04 (m, 2 x 2H, O*Ph*); ^{13}C NMR (75.48 MHz, 298K, C_6D_6) 25.9 (^{i}Pr*Me$_3$*), 55.6 (^{i}PrCH), 56.2 (*C*H_2OPh), 84.2 (*C*≡CCH$_2$), 95.4 (C≡*C*CH$_2$), 115.3 (*i*-*C*OPh), 121.1 (*m*-*C*OPh), 126.0 (*p*-*C*OPh), 129.7 (*o*-*C*OPh), 154.9 (*C*N_2); Analysis calculated for $C_{32}H_{42}BaN_4O_2$: C, 58.95; H, 6.49; N, 8.59. Found: C, 58.94; H, 6.44; N, 8.57.

7.4.3.30 Synthesis of *[{cyNC(C≡CCH$_2$OPh)Ncy}]Ba[C≡CCH$_2$OPh]* **41**

0.11 ml (0.83 mmol) of **f** and 0.17 g (0.83 mmol) of **h** in 10 ml of toluene was added to 0.25 g (0.42 mmol) of **C5** in 10 ml of toluene. After stirring overnight at room temperature the solvent volume was reduced in *vacuo* and left to crystallise at -30 ^{o}C for 48 hours. The product was isolated by filtration to yield 0.2 g (0.17 mmol 40 %) of compound **41**. ^{1}H NMR (300 MHz, 298K, C_6D_6) 1.57 (m, 2 × 10H, C*H$_2$* of cy), 4.46 (m, 2 × 1H, C*H* of cy), 4.53 (s, 4H, C*H$_2$*OPh), 6.82 (m, 2 × 3H O*Ph*), 6.96 (m, 2 × 2H, O*Ph*); ^{13}C NMR (75.48 MHz, 298K, C_6D_6) 26.0, 26.1, 26.3, 26.3, 37.2, 38.2 (*C*H_2 of cy), 48.2, 48.4 (*C*H of cy), 6.0 (*C*H_2OPh), 81.3 (*C*≡CCH$_2$), 84.9 (C≡*C*CH$_2$), 90.0 (CH$_2$C≡*C*Ba), 91.2 (CH$_2$*C*≡CBa), 115.3 (*i*-*C*OPh), 121.7 (*m*-*C*OPh), 125.4 (*p*-*C*OPh), 129.8 (*o*-*C*OPh), 158.2 (*C*N_2); Analysis calculated for $C_{32}H_{36}BaN_2O_2$: C, 61.45; H, 5.99; N, 4.62. Found: C, 61.45; H, 6.03; N, 4.54.

7.5 Hydroacetylation of isocyanates

7.5.1 Synthesis of *Ca[{OC(C≡CPh)N$_{(1\text{-}adamantyl)}$}]$_2$* **42**

0.03 ml (0.3 mmol) of **a** and 0.05 g (0.3 mmol) of **i** in 10 ml of toluene was added to 0.2 g (0.3 mmol) of **C1** in 10 ml of toluene. After stirring overnight at room temperature the solvent volume was reduced in *vacuo* and left to crystallise at -30 ^{o}C for 48 hours. The product was isolated by filtration to yield 0.10 g (0.108 mmol 57 %) of compound **42**. ^{1}H NMR (300 MHz, 298K, C_6D_6) 1.17 (m, 2 x 12H, ^{i}Pr*Me$_3$*), 1.20 (m, 2 x 12H, ^{i}Pr*Me$_3$*), 1.22 (t, 6H, C*H$_2$* of 1-adamantyl), 1.55 (d, 6H, C*H$_2$* of 1-adamantyl), 1.66 (m, 2H, C*H* of 1-adamantyl), 2.10 (s, 2 x 3H, {C(*Me*)}$_2$CH), 2.98 (m, 4 x 1H, ^{i}Pr*H*), 4.88 (s, 1H, {C(Me)}$_2$C*H),* 7.02 (m, 5H, Ar*H*), 7.12 (m, 6H, Ar*H*); ^{13}C NMR (75.48 MHz, 298K, C_6D_6) 21.4 ({C(*Me*)}$_2$CH), 24.7 (^{i}Pr*Me$_3$*), 28.4 (^{i}Pr*C*H), 30.3 (*C*H of 1-adamantyl), 36.3, 45.8 (*C*H$_2$ of 1-adamantyl), 55.4 (N*C* of 1-adamantyl), 85.7 (*C*≡CPh), 90.0 (C≡*C*Ph), 123.4 (*i*-*C*$_6$H$_5$), 124.0 (*m*-*C*$_6$H$_3$), 124.1 {*C*(Me)}$_2$CH), 125.7 (*p*-*C*$_6$H$_3$), 128.5 (*m*-*C*$_6$H$_5$), 129.3 (*p*-*C*$_6$H$_5$), 131.5 (*o*-*C*$_6$H$_5$), 136.4 (*o*-*C*$_6$H$_3$), 141.6 (*i*-*C*$_6$H$_3$), 164.5 (N*C*O), 192.4 ({C(Me)}$_2$*CH)*; Analysis calculated for $C_{38}H_{40}CaN_2O_2$: C, 76.47; H, 6.67; N, 4.69. Found: C, 76.51; H, 6.85; N, 4.77; X-ray crystallography data, see appendix.

The synthesis of compound **42** was repeated with calcium bis(bis(trimethylsilyl)amide) **C3** yielding 0.18 g (0.3 mmol 70 %) and with calcium triazenide **C6** yielding 0.04 g (0.067 mmol 48 %).

7.5.2 Synthesis of *Sr[{OC(C≡CPh)N$_{(1\text{-}adamantyl)}$}]$_2$* **43**

0.08 ml (0.724 mmol) of **a** and 0.128 g (0.724 mmol) of **i** in 10 ml of toluene was added to 0.2 g (0.362 mmol) of **C4** in 10 ml of toluene. After stirring overnight at room temperature the solvent volume was reduced in *vacuo* and left to crystallise at -30 ^{o}C for 48 hours. The product was isolated by filtration to yield 0.165 g (0.256 mmol 71 %) of compound **43**. ^{1}H NMR (300 MHz, 298K, C_6D_6) 1.22 (t, 2 × 6H, C*H$_2$* of 1-adamantyl), 1.44 (d, 2 × 6H, C*H$_2$* of 1-adamantyl), 1.86 (m, 2 × 1H, C*H* of 1-adamantyl), 6.99 (m, 2 × 5H, Ar*H*); ^{13}C NMR (75.48 MHz, 298K, C_6D_6), 30.2 (*C*H of 1-adamantyl), 36.2, 45.8

(*C*H_2 of 1-adamantyl), 58.3 (N*C* of 1-adamantyl), 87.0 (*C*≡CPh), 91.8 (C≡*C*Ph), 121.5 (*i*-C_6H_5), 128.8(*m*-C_6H_3), 129.3 (*p*-C_6H_3), 131.6 (*o*-C_6H_5), 168.8 (N*C*O); Analysis calculated for $C_{38}H_{40}N_2O_2Sr$: C, 70.83; H, 6.26; N, 4.35. Found: C, 70.79; H, 6.36; N, 4.38.

The synthesis was repeated with strontium triazende **C7** yielding 0.135 g (0.21 mmol 79 %) of compound **43**.

7.5.3 Synthesis of *Ba[{OC(C≡CPh)N$_{(1\text{-}adamantyl)}$}]$_2$* **44**

0.07 ml (0.664 mmol) of **a** and 0.118 g (0.664 mmol) of **i** in 10 ml of toluene was added to 0.2 g (0.332 mmol) of **C5** in 10 ml of toluene. After stirring overnight at room temperature the solvent volume was reduced in *vacuo* and left to crystallise at -30 ^oC for 48 hours. The product was isolated by filtration to yield 0.115 g (0.166 mmol 50 %) of compound **44**. ^1H NMR (300 MHz, 298K, C_6D_6) 1.23 (t, 2 × 6H, C*H*$_2$ of 1-adamantyl), 1.44 (d, 2 × 6H, C*H*$_2$ of 1-adamantyl), 1.86 (m, 2 × 1H, C*H* of 1-adamantyl), 6.99 (m, 2 × 5H, Ar*H*); ^{13}C NMR (75.48 MHz, 298K, C_6D_6) 30.2 (*C*H of 1-adamantyl), 37.1, 42.3 (*C*H_2 of 1-adamantyl), 53.8 (N*C* of 1-adamantyl), 89.8 (*C*≡CPh), 93.3 (C≡*C*Ph), 122.0 (*i*-C_6H_5), 128.7 (*m*-C_6H_3), 129.3 (*p*-C_6H_3), 132.0 (*o*-C_6H_5), 167.7 (N*C*O); Analysis calculated for $C_{38}H_{40}BaN_2O_2$: C, 65.76; H, 5.81; N, 4.04. Found: C, 65.63; H, 5.84; N, 3.96.

7.5.4 Synthesis of *Ca[{OC(C≡CSi^{i}Pr$_3$)N$_{(1\text{-}adamantyl)}$}]$_2$* **45**

0.07 ml (0.295 mmol) of **b** and 0.05 g (0.295 mmol) of **i** in 10 ml of toluene was added to 0.2 g (0.295 mmol) of **C1** in 10 ml of toluene. After stirring overnight at room temperature the solvent volume was reduced in *vacuo* and left to crystallise at -30 ^oC for 48 hours. The product was isolated by filtration to yield 0.115 g (0.19 mmol 65 %) of compound **45**. ^1H NMR (300 MHz, 300K, C_6D_6) 1.10 (d, 18H, Si^{i}Pr*Me*$_3$), 1.16 (d, 2 x 12H, ^{i}Pr*Me*), 1.19 (d, 2 x 12H, ^{i}Pr*Me*), 1.22 (t, 12H, C*H*$_2$ of 1-adamantyl), 1.55 (d, 12H, C*H*$_2$ of 1-adamantyl), 1.66 (m, 6H, C*H* of 1-adamantyl), 1.86 (s, 3 x 1H, Si^{i}Pr*H*), 2.10 (s, 2 x 3H, {C(*Me*)}$_2$CH), 2.93 (m, 4 x 1H, ^{i}PrC*H*), 4.84 (s, 1H, {C(Me)}$_2$C*H*), 7.12 (m, 6H, Ar*H*); ^{13}C NMR (75.48 MHz, 298K, C_6D_6) 11.4 (Si^{i}Pr*C*), 18.7 (Si^{i}Pr*Me*$_3$), 21.4 {C(*Me*)}$_2$CH), 24.5 (^{i}Pr*Me*$_3$), 28.4 (^{i}Pr*C*H), 30.3 (*C*H of 1-adamantyl), 36.3, 45.8 (*C*H_2

of 1-adamantyl), 54.6 (N*C* of 1-adamantyl), 85.2 (*C*≡CSi), 90.0 (C≡*C*Si), 124.0 (*m*-C_6H_3), 124.2 ({*C*(Me)}$_2$CH), 125.6 (*p*-C_6H_3), 138.3 (*o*-C_6H_3), 143.6 (*i*-C_6H_3), 164.6 (N*C*O), 192.3 ({C(Me)}$_2$*CH)*; Analysis calculated for $C_{44}H_{72}CaN_2O_2Si_2$: C, 69.78; H, 9.58; N, 3.70. Found: C, 69.76; H, 9.69; N, 3.58.

The synthesis was repeated with calcium bis(bis(trimethylsilyl)amide) **C3** and calcium triazenide **C6** yielding 0.055 g (0.09 mmol 23 %) and 0.04 g (0.053 mmol 52 %) of compound **45** respectively.

7.5.5 Synthesis of *Sr[{OC(C≡CSi^{i}Pr$_3$)N$_{(1\text{-}adamantyl)}$}]$_2$* **46**

0.16 ml (0.72 mmol) of **b** and 0.128 g (0.72 mmol) of **i** in 10 ml of toluene was added to 0.2 g (0.36 mmol) of **C4** in 10 ml of toluene. After stirring overnight at room temperature the solvent volume was reduced in *vacuo* and left to crystallise at -30 ^{o}C for 48 hours. The product was isolated by filtration to yield 0.18 g (0.224 mmol 62 %) of compound **46**. ^{1}H NMR (300 MHz, 298K, C_6D_6) 1.10 (d, 2 × 18H, Si^{i}Pr*Me$_3$*), 1.23 (t, 2 × 6H, C*H$_2$* of 1-adamantyl), 1.45 (d, 2 × 6H, C*H$_2$* of 1-adamantyl), 1.85 (m, 2 × 1H, C*H* of 1-adamantyl), 2.18 (d, 2 × 3H, Si^{i}Pr*H*); ^{13}C NMR (75.48 MHz, 298K, C_6D_6) 11.4 (Si^{i}Pr*C*), 18.7 (Si^{i}Pr*Me*$_3$), 30.3 (*C*H of 1-adamantyl), 36.3, 45.77 (*C*H$_2$ of 1-adamantyl), 54.6 (N*C* of 1-adamantyl), 85.9 (*C*≡CPh), 95.6 (C≡*C*Ph), 168.5 (N**C**O); Analysis calculated for $C_{44}H_{72}N_2O_2Si_2Sr$: C, 65.66; H, 9.02; N, 3.48. Found: C, 65.51; H, 9.13; N, 3.40.

The synthesis was repeated with strontium triazenide **C7** yielding 0.11 g (0.137 mmol 52 %) of compound **46**

7.5.6 Synthesis of *Ba[{OC(C≡CSi^{i}Pr$_3$)N$_{(1\text{-}adamantyl)}$}]$_2$* **47**

0.15 ml (0.66 mmol) of **b** and 0.118 g (0.66 mmol) of **i** in 10 ml of toluene was added to 0.2 g (0.33 mmol) of **C5** in 10 ml of toluene. After stirring overnight at room temperature the solvent volume was reduced in *vacuo* and left to crystallise at -30 ^{o}C for 48 hours. The product was isolated by filtration to yield 0.2 g (0.23 mmol 71 %) of compound **47**. ^{1}H NMR (300 MHz, 298K, C_6D_6) 1.14 (d, 2 × 18H, Si^{i}Pr*Me$_3$*), 1.25 (t, 2 × 6H, C*H$_2$* of 1-adamantyl), 1.45 (d, 2 × 6H, C*H$_2$* of 1-adamantyl), 1.85 (m, 2 × 1H, C*H*

of 1-adamantyl), 2.26 (d, 2 × 3H, Si^{i}Pr*H*); ^{13}C NMR (75.48 MHz, 298K, C_6D_6) 11.5 (Si^{i}Pr*C*), 18.8 (Si^{i}Pr*Me*$_3$), 31.0 (*C*H of 1-adamantyl), 37.4, 44.8 (*C*H$_2$ of 1-adamantyl), 58.7 (N*C* of 1-adamantyl), 83.5 (*C*≡CPh), 95.7 (C≡*C*Ph), 163.1 (N*C*O); Analysis calculated for $C_{44}H_{72}BaN_2O_2Si_2$: C, 61.84; H, 8.49; N, 3.28. Found: C, 61.76; H, 8.51; N, 3.28.

7.5.7 Synthesis of *Ca[{OC(C≡CCH$_2$NMe$_2$)N$_{(1\text{-}adamantyl)}$}]$_2$* **48**

0.03 ml (0.295 mmol) of **d** and 0.05 g (0.295 mmol) of **i** in 10 ml of toluene was added to 0.2 g (0.295 mmol) of **C1** in 10 ml of toluene. After stirring overnight at room temperature the solvent volume was reduced in *vacuo* and left to crystallise at -30 ^{o}C for 48 hours. The product was isolated by filtration to yield 0.12 g (0.21 mmol 73 %) of compound **48**. ^{1}H NMR (300 MHz, 300K, C_6D_6) 1.16 (d, 2 x 6H, ^{i}Pr*Me*), 1.20 (d, 2 x 6H, ^{i}Pr*Me*), 1.22 (t, 12H, C*H*$_2$ of 1-adamantyl), 1.55 (d, 12H, C*H*$_2$ of 1-adamantyl), 1.66 (m, 6H, C*H* of 1-adamantyl), 2.11 (s, 2 x 3H, {C(*Me*)}$_2$CH), 2.73 (s, 2 x 3H, N*Me*$_2$), 2.98 (m, 4 x 1H, ^{i}PrC*H*), 3.75 (d, 2H, NC*H*$_2$), 4.81 (s, 1H, {C(Me)}$_2$C*H*), 7.13 (m, 6H, Ar*H*); ^{13}C NMR (75.48 MHz, 298K, C_6D_6) 21.4 {C(*Me*)}$_2$CH), 24.7 (^{i}Pr*Me*$_3$), 28.4 (^{i}Pr*C*H), 30.5 (*C*H of 1-adamantyl), 36.3, 45.8 (*C*H$_2$ of 1-adamantyl), 52.1 (N*C* of 1-adamantyl), 69.2 (N*Me*$_2$), 75.5 (N*C*H$_2$), 93.4 (*C*≡CCH$_2$), 114.8 (C≡*C*CH$_2$), 123.3 (*m*-*C*$_6$H$_3$), 124.0 ({*C*(Me)}$_2$CH), 125.6 (*p*-*C*$_6$H$_3$), 136.4 (*o*-*C*$_6$H$_3$), 142.8 (*i*-*C*$_6$H$_3$), 165.6 (N*C*O), 190.9 ({C(Me)}$_2$*CH*); Analysis calculated for $C_{32}H_{46}CaN_4O_2$: C, 68.78; H, 8.30; N, 10.03. Found: C, 68.62; H, 8.31; N, 9.76.

The synthesis was repeated with calcium bis(bis(trimethylsilyl)amide) **C3** and calcium triazenide **C6** yielding 0.04 g (0.0716 mmol 18 %) and 0.05 g (0.089 mmol 59 %) of compound **48** respectively.

7.5.8 Synthesis of *Sr[{OC(C≡CCH$_2$NMe$_2$)N$_{(1\text{-}adamantyl)}$}]$_2$* **49**

0.028 ml (0.26 mmol) of **d** and 0.05 g (0.28 mmol) of **i** in 10 ml of toluene was added to 0.2 g (0.26 mmol) of **C7** in 10 ml of toluene. After stirring overnight at room temperature the solvent volume was reduced in *vacuo* and left to crystallise at -30 ^{o}C for 48 hours. The product was isolated by filtration to yield 0.135 g (0.22 mmol 61 %) of compound **49**. ^{1}H NMR (300 MHz, 298K, C_6D_6) 1.17 (d, 2 x 6H, ^{i}Pr*Me*), 1.20 (d, 2 x

6H, ^{i}Pr*Me*), 1.22 (t, 12H, CH_2 of 1-adamantyl), 1.55 (d, 12H, CH_2 of 1-adamantyl), 1.86 (m, 6H, C*H* of 1-adamantyl), 2.10 (s, 2 x 3H, NMe_2), 3.01 (m, 4 x 1H, ^{i}PrC*H*), 3.75 (d, 2 x 2H, NCH_2), 7.12 (m, 6H, Ar*H*); ^{13}C NMR (75.48 MHz, 298K, C_6D_6) 24.5 (^{i}PrMe_3), 28.6 (^{i}Pr*C*H), 30.9 (*C*H of 1-adamantyl), 36.3, 45.4 (*C*H_2 of 1-adamantyl), 55.5 (N*C* of 1-adamantyl), 75.7 (NMe_2), 78.3 (N*C*H_2), 108.4 (*C*≡CCH$_2$), 114.8 (C≡*C*CH$_2$), 123.3 (*m*-C_6H_3), 125.8 (*p*-C_6H_3), 136.5 (*o*-C_6H_3), 140.4 (*i*-C_6H_3), 175.4 (N**C**O); Analysis calculated for $C_{32}H_{46}N_4O_2Sr$: C, 63.39; H, 7.65; N, 9.24. Found: C, 63.49; H, 7.53; N, 9.20.

The synthesis was repeated with β-diketiminato strontium amide **C2** yielding 0.15 g (0.247 mmol 68 %) of compound **49**.

7.5.9 Synthesis of *Ba[{OC(C≡CCH$_2$NMe$_2$)N$_{(1\text{-}adamantyl)}$}]$_2$* **50**

0.07 ml (0.66 mmol) of **d** and 0.118 g (0.66 mmol) of **i** in10 ml of toluene was added to 0.2 g (0.33 mmol) of **C5** in 10 ml of toluene. After stirring overnight at room temperature the solvent volume was reduced in *vacuo* and left to crystallise at -30 ^{o}C for 48 hours. The product was isolated by filtration to yield 0.12 g (0.183 mmol 55 %) of compound **50**. ^{1}H NMR (300 MHz, 298K, C_6D_6) 1.22 (t, 12H, CH_2 of 1-adamantyl), 1.44 (d, 12H, CH_2 of 1-adamantyl), 1.86 (m, 6H, C*H* of 1-adamantyl), 3.13 (s, 2 x 3H, NMe_2**)**, 4.25 (d, 2 x 2H, NCH_2); ^{13}C NMR (75.48 MHz, 298K, C_6D_6) 30.9 (*C*H of 1-adamantyl), 37.5, 44.00 (*C*H_2 of 1-adamantyl), 53.8 (N*C* of 1-adamantyl), 74.2 (NMe_2), 79.1 (N*C*H_2), 104.8 (*C*≡CCH$_2$), 114.0 (C≡*C*CH$_2$), 176.7 (N*C*O); Analysis calculated for $C_{32}H_{46}BaN_4O_2$: C, 58.58; H, 7.07; N, 8.54. Found: C, 58.47; H, 7.15; N, 8.54.

7.5.10 Synthesis of *Ca[{OC(C≡CCH$_2$OMe)N$_{(1\text{-}adamantyl)}$}]$_2$* **51**

0.03 ml (0.295 mmol) of **e** and 0.05 g (0.295 mmol) of **i** in 10 ml of toluene was added to 0.2 g (0.295 mmol) of **C1** in 10 ml of toluene. After stirring overnight at room temperature the solvent volume was reduced in *vacuo* and left to crystallise at -30 ^{o}C for 48 hours. The product was isolated by filtration to yield 0.155 g (0.291 mmol 99 %) of compound **51**. ^{1}H NMR (300 MHz, 298K, C_6D_6) 1.16 (d, 2 x 6H, ^{i}Pr*Me*), 1.22 (d, 2 x 6H, ^{i}Pr*Me*), 1.22 (t, 12H, CH_2 of 1-adamantyl), 1.55 (d, 12H, CH_2 of 1-adamantyl), 1.66 (m, 6H, C*H* of 1-adamantyl), 2.11 (s, 2 x 3H, {C(*Me*)}$_2$CH), 2.73 (s, 2 x 3H, O*Me*),

2.98 (m, 4 x 1H, ^{i}PrC*H*), 4.26 (d, 2 x 2H, OCH_2), 4.88 (s, 1H, {C(Me)}$_2$C*H*), 7.10 (m, 6H, Ar*H*); ^{13}C NMR (75.48 MHz, 298K, C_6D_6) 21.4 {C(*Me*)}$_2$CH), 23.7 (^{i}Pr*Me*$_3$), 28.4 (^{i}Pr*C*H), 29.9 (*C*H of 1-adamantyl), 36.7, 45.2 (*C*H_2 of 1-adamantyl), 53.3 (N*C* of 1-adamantyl), 70.2 (O*Me*), 76.4 (O*C*H_2), 97.4 (*C*≡CCH$_2$), 116.2 (C≡*C*CH$_2$), 123.4 (*m*-*C*$_6$H$_3$), 123.8 ({*C*(Me)}$_2$CH), 125.6 (*p*-*C*$_6$H$_3$), 136.4 (*o*-*C*$_6$H$_3$), 142.8(*i*-*C*$_6$H$_3$), 164.2 (N*C*O), 192.4 ({C(Me)}$_2$*CH*); Analysis calculated for $C_{30}H_{40}CaN_2O_4$: C, 67.64; H, 7.57; N, 5.26. Found: C, 67.53; H, 7.59; N, 5.19.

The synthesis was repeated with calcium bis(bis(trimethylsilyl)amide) **C3** and calcium triazenide **C6** yielding 0.135 g (0.25 mmol 64 %) and 0.04 g (0.075 mmol 54 %) of compound **51** respectively.

7.5.11 Synthesis of *Sr[{OC(C≡CCH$_2$OMe)N$_{(1\text{-}adamantyl)}$}]$_2$* **52**

0.06 ml (0.72 mmol) of **e** and 0.128 g (0.72 mmol) of **i** in 10 ml of toluene was added to 0.2 g (0.36 mmol) of **C4** in 10 ml of toluene. After stirring overnight at room temperature the solvent volume was reduced in *vacuo* and left to crystallise at -30 ^{o}C for 48 hours. The product was isolated by filtration to yield 0.03 g (0.052 mmol 14 %) of compound **52**. ^{1}H NMR (300 MHz, 298K, C_6D_6) 1.23 (t, 12H, CH_2 of 1-adamantyl), 1.44 (d, 12H, CH_2 of 1-adamantyl), 1.85 (m, 6H, C***H*** of 1-adamantyl), 3.20 (s, 2 x 3H, O*Me*), 4.27 (d, 2 x 2H, OCH_2); ^{13}C NMR (75.48 MHz, 298K, C_6D_6) 30.2 (*C*H of 1-adamantyl), 36.2, 45.7 (*C*H_2 of 1-adamantyl), 54.6 (N*C* of 1-adamantyl), 76.8 (O*Me*), 79.9 (O*C*H_2), 110.2 (*C*≡CCH$_2$), 115.3 (C≡***C***CH$_2$), 177.3 (N*C*O); Analysis calculated for $C_{30}H_{40}N_2O_4Sr$: C, 62.10; H, 6.95; N, 4.83. Found: C, 61.99; H, 7.00; N, 4.85.

The synthesis was repeated with strontium triazenide **C7** yielding 0.145 g (0.25 mmol 97 %) of compound **52**.

7.5.12 Synthesis of *Ba[{OC(C≡CCH$_2$OMe)N$_{(1\text{-}adamantyl)}$}]$_2$* **53**

0.056 ml (0.66 mmol) of **e** and 0.118 g (0.66 mmol) of **i** in 10 ml of toluene was added to 0.2 g (0.33 mmol) of **C5** in 10 ml of toluene. After stirring overnight at room temperature the solvent volume was reduced in *vacuo* and left to crystallise at -30 ^{o}C for 48 hours. The product was isolated by filtration to yield 0.165 g (0.261 mmol 83 %) of

compound **53** ^{1}H NMR (300 MHz, 298K, C_6D_6) 1.26 (t, 12H, C*H*$_2$ of 1-adamantyl), 1.46 (d, 12H, C*H*$_2$ of 1-adamantyl), 1.86 (m, 6H, C*H* of 1-adamantyl), 3.13 (s, 2 × 3H, O*Me*), 4.14 (d, 2 × 2H, OC*H*$_2$); ^{13}C NMR (75.48 MHz, 298K, C_6D_6) 31.1 (*C*H of 1-adamantyl), 37.1, 46.3 (*C*H$_2$ of 1-adamantyl), 53.3 (N*C* of 1-adamantyl), 77.7 (O*Me*), 79.62 (O*C*H$_2$), 110.96 (*C*≡CCH$_2$), 114.80 (C≡*C*CH$_2$), 177.16 (N*C*O); Analysis calculated for $C_{30}H_{40}BaN_2O_4$: C, 57.20; H, 6.40; N, 4.45. Found: C, 57.16; H, 6.47; N, 4.50.

7.5.13 Synthesis of *Ca[{OC(C≡CCH$_2$OPh)N$_{(1\text{-}adamantyl)}$}]$_2$* **54**

0.038 ml (0.295 mmol) of **f** and 0.05 g (0.295 mmol) of **f** in 10 ml of toluene was added to 0.2 g (0.295 mmol) of **C1** in 10 ml of toluene. After stirring overnight at room temperature the solvent volume was reduced in *vacuo* and left to crystallise at -30 ^{o}C for 48 hours. The product was isolated by filtration to yield 0.160 g (0.244 mmol 84 %) of compound **54**. ^{1}H NMR (300 MHz, 298K, C_6D_6) 1.16 (d, 2 x 6H, ^{i}Pr*Me*), 1.20 (d, 2 x 6H, ^{i}Pr*Me*), 1.22 (t, 12H, C*H*$_2$ of 1-adamantyl), 1.55 (d, 12H, C*H*$_2$ of 1-adamantyl), 1.66 (m, 6H, C*H* of 1-adamantyl), 2.11 (s, 2 x 3H, {C(*Me*)}$_2$CH), 2.98 (m, 4 x 1H, ^{i}PrC*H*), 4.17 (d, 2 x 2H, OC*H*$_2$), 4.88 (s, 1H, {C(Me)}$_2$C*H*), 7.02 (m, 5H, C_6H_5), 7.13 (m, 6H, Ar*H*); ^{13}C NMR (75.48 MHz, 298K, C_6D_6) 21.4 {C(*Me*)}$_2$CH), 23.7 (^{i}Pr*Me$_3$*), 28.3 (^{i}Pr*C*H), 30.3 (*C*H of 1-adamantyl), 36.3, 45.2 (*C*H$_2$ of 1-adamantyl), 56.6 (N*C* of 1-adamantyl), 77.4 (O*C*H$_2$), 97.4 (*C*≡CCH$_2$), 114.7 (C≡*C*CH$_2$), 114.8 (*o*-C_6H_5), 120.48 (*p*-C_6H_5), 123.34 (*m*-*C*$_6$H$_3$), 123.55 ({*C*(Me)}$_2$CH), 125.64 (*p*-*C*$_6$H$_3$), 130.71 (*m*-C_6H_5), 136.38 (*o*-*C*$_6$H$_3$), 142.75 (*i*-*C*$_6$H$_3$), 165.48 (*i*-C_6H_5), 167.00 (N*C*O), 191.75 ({C(Me)}$_2$*CH*); Analysis calculated for $C_{40}H_{44}CaN_2O_4$: C, 73.14; H, 6.75; N, 4.26. Found: C, 73.17; H, 6.81; N, 4.29.

The synthesis was repeated with calcium bis(bis(trimethylsilyl)amide) **C3** and calcium triazenide **C6** yielding 0.10 g (0.152 mmol 38 %) and 0.045 g (0.0685 mmol 49 %) of compound **54** respectively.

7.5.14 Synthesis of *Sr[{OC(C≡CCH$_2$OPh)N$_{(1\text{-}adamantyl)}$}]$_2$* **55**

0.09 ml (0.72 mmol) of **f** and 0.128 g (0.72 mmol) of **i** in 10 ml of toluene was added to 0.2 g (0.36 mmol) of **C4** in 10 ml of toluene. After stirring overnight at room

temperature the solvent volume was reduced in *vacuo* and left to crystallise at -30 ^{o}C for 48 hours. The product was isolated by filtration to yield 0.05 g (0.071 mmol 20 %) of compound **55**. ^{1}H NMR (300 MHz, 298K, C_6D_6) 1.22 (t, 12H, CH_2 of 1-adamantyl), 1.44 (d, 12H, CH_2 of 1-adamantyl), 1.86 (m, 6H, C*H* of 1-adamantyl), 4.15 (d, 2 × 2H, OCH_2), 6.85 (m, 2 × 5H, C_6H_5); ^{13}C NMR (75.48 MHz, 298K, C_6D_6) 30.2 (*C*H of 1-adamantyl), 36.2, 45.7 (*C*H_2 of 1-adamantyl), 54.6 (N*C* of 1-adamantyl), 75.5 (O*C*H_2), 111.3 (*C*≡CCH$_2$), 115.2 (C≡*C*CH$_2$), 121.5 (*o*-C_6H_5), 125.6 (*p*-C_6H_5), 129.6 (*m*-C_6H_5), 158.1 (*i*-C_6H_5), 176.9 (N*C*O); Analysis calculated for $C_{40}H_{44}N_2O_4Sr$: C, 68.20; H, 6.30; N, 3.98. Found: C, 68.03; H, 6.37; N, 4.02.

The synthesis was repeated with strontium triazenide **C7** yielding 0.17 g (0.24 mmol 91 %) of compound **55**.

7.5.15 Synthesis of *Ba[{OC(C≡CCH$_2$OPh)N$_{(1\text{-}adamantyl)}$}]$_2$* **56**

0.085 ml (0.66 mmol) of **f** and 0.118 g (0.66 mmol) of **i** in 10 ml of toluene was added to 0.2 g (0.33 mmol) of **C5** in 10 ml of toluene. After stirring overnight at room temperature the solvent volume was reduced in *vacuo* and left to crystallise at -30 ^{o}C for 48 hours. The product was isolated by filtration to yield 0.14 g (0.186 mmol 56 %) of compound **56**. ^{1}H NMR (300 MHz, 298K, C_6D_6) 1.21 (t, 12H, CH_2 of 1-adamantyl), 1.44 (d, 12H, CH_2 of 1-adamantyl), 1.86 (m, 6H, C***H*** of 1-adamantyl), 4.15 (d, 2 × 2H, OCH_2), 6.85 (m, 2 × 5H, C_6H_5); ^{13}C NMR (75.48 MHz, 298K, C_6D_6) 31.0 (*C*H of 1-adamantyl), 36.2, 45.8 (*C*H_2 of 1-adamantyl), 55.4 (N*C* of 1-adamantyl), 75.5 (O*C*H_2), 113.43 (*C*≡CCH$_2$), 115.17 (C≡*C*CH$_2$), 121.57 (*o*-C_6H_5), 125.38 (*p*-C_6H_5), 129.63 (*m*-C_6H_5), 158.42 (*i*-C_6H_5), 177.06 (N*C*O); Analysis calculated for $C_{40}H_{44}BaN_2O_4$: C, 63.71; H, 5.88; N, 3.71. Found: C, 63.63; H, 5.93; N, 3.76.

Chapter 8

8.0 References

1. V. C. R. Grignard, ***Acad. Sci*, 1900**, 130, 1322-1324.

2. M. H. Chisholm, J. C. Gallucci, K. Phomphra,. ***Inorg Chem***, **2004**, 43, 6717-6725.

3. N. Nimitsiriwat, V. C. Gibson, E. L. Marshall, P. Takolpuckdee, A. K. Tomov, A. J. P. White, D. J. Williams, M. R. J. Elsegood, S. H. Dale, ***Inorg Chem***. **2007**, 46, 9988-9997.

4. (a) A. G. Avent, M. R. Crimmin, M. S. Hill, P. B. Hitchcock, ***Dalton Trans***. **2005**, 278-284.
   (b) S. C. Stockwell, T. P. Hanusa, J. C. Huffman, ***J. Am. Chem. Soc***, **1992**, 114, 3393-3399.
   (c) F. Feil, C. Muller, S. Harder, ***J. Organomet. Chem***. **2003**, 683, 56-63.
   (d) F. T. Edelmann, **Comprehensive Organometallic Chemistry II edition, E. W. Abel, F. G. A. Stone, G. Wilkinson, M. F. Lappert, Pergamon,Oxford**, **1995**, vol. 4.
   (e) M. H. Chisholm, J. C. Gallucci, K. Phomphra, ***Chem Comm***. **2003**, 48-49.

5. (a) M. R. Crimmin, I. J. Casely, M. S. Hill, ***J. Am. Chem. Soc*. 2005.** 127, 2042-2043.
   (b) Y. K. Kim. T. Livinghouse, J. E. Bercaw, **Tet Lett. 2001**, 42, 2933-2935.

6. A. G. M. Barrett, I. J. Casely, M. R. Crimmin, M. S. Hill, J.R. Lachs, M. F. Mahon, P. A. Procopiou. ***Inorg. Chem***. **2009**, 48, 4445-4453.

7. (a) M. R. Crimmin, A. G. M. Barrett, M. S. Hill, P. B. Hitchcock, P. A. Procopiou, ***Organometallics*, 2007**, 26, 2953-2956.
   (b) A. Motta, I. L. Fragala, T. J. Marks, ***Organometallics***, **2005**, 24, 4995-5003.
   (c) M. Westerhausen, W. Schwarz, ***J. Organomet. Chem***. **1993**, 463, 51-63.

8. A. G. M. Barrett, M. R. Crimmin, M. S. Hill, P. B. Hitchcock, ***Organometallics***, **2005**, 24, 1184-1188.

9. A. G. M. Barrett, M. R. Crimmin, M. S. Hill, P. B. Hitchcock, P. A. Procopiou, ***Dalton. Trans***. **2008**, 4474-4481.

10. J. R. Lachs, A. G. M. Barrett, M. R. Crimmin, G. Kociok-Kohn, M. S. Hill, M. F. Mahon, P. A. Procopiou, ***Eur. J. Chem***. **2008**, 4173-4179.

11. M. R. Crimmin, A. G. M. Barrett, M. S. Hill, P. B. Hitchcock, P. A. Procopiou, ***Organometallics***, **2008**, 27, 497-499.

12 M. Stender, R. J. Wright, B. E. Eichler, J. Prust, M. M. Olmstead, H. W. Roesky, P. Power, ***J. Chem. Soc. Dalton Trans***. **2001**, 34565-3469.

13. X. Zhang, Z. Hou, ***Org. Biomol. Chem***. **2008**, 6, 1720-1730.

14 (a) M. Westerhausen, ***Inorg Chem***, **1991**, 30, 96-101.
(b) H. Burger, C. Forker, J. Goubeau, **Monatsh, Chem, 1965**, 96, 597-601.
(c) L. M. Engelhardt, B. S. Jolly, P. C. Junk, C. L. Raston, B. W. Skelton, A. H. White, ***Aust. J. Chem***. **1986**, 39, 1377-1383.
(d) A. R. Utke, R. T. Sanderson, ***J. Org. Chem***, **1964**, 29, 1261-1264.
(e) S. Cucinella, G. Dozzi, G. Perego, A. Mazzei, ***J. Organomet. Chem***. **1977**, 137, 257-264.
(f) M. Veith, ***Chem. Rev***, **1990**, 90, 1, 3-16.

15. (a) M. R. Gagne, T. J. Marks, ***J. Am. Chem. Soc***. **1989**, 111, 4108-4109.
(b) M. R. Burggstein, H. Berberich, P. W. Roesky, ***Chem. Euro. J***. **2001**, 7 No 14, 3078-3085.
(c) F. T. Edelman, ***Top. Curr. Chem***. **1996**, 176, 247-276.
(d) V. M. Arredondo, F. E. M^{c}Donald, T. J. Marks, ***J. Am. Chem. Soc***. **1998**, 120, 4871-4872.
(e) M. R. Douglass, T. J. Marks, ***J. Am. Chem. Soc***. **2000**, 122, 1824-1825.

16. M. R. Crimmin, A. G. M. Barrett, M. S. Hill, P. B. Hitchcock, P. A. Procopiou, **Inorg. Chem**. **2007**, 46, 10410-10415.

17. (a) D. J. Burkey, T. P. Hanusa, ***Organometallics***, **1996**, 15, 4971-4976.
(b) D. J. Burkey, E. K. Alexander, T. P. Hanusa, ***Organometallics***, **1994**, 13, 2773-2786.

18. D. C. Green, U. Englich, K. Ruhlandt-Senge, ***Angew. Chem. Int. Ed.*** **1999**, 38, No 3, 354-357.

19. A. G. M. Barrett, M. R. Crimmin, M. S. Hill, P. B. Hitchcock, S. L. Lomas, M. F. Mahon, P. A. Procopiou and K. Suntharalingam, ***Organometallics*** **2008**, *27*, 6300-6306.

20. H. Yamazaki, J. C. S. ***Chem. Comm***., **1976**, 841-842.

21. (a) H. J. Heeres, J. Nijhoff, J. H. Teuben and R. D. Rogers, ***Organometallics*** **1993**, *12*, 2609-2617.
(b) H. J. Heeres, J. H. Teuben, ***Organometallics***, **1991**, 10, 1980-1986.

22. (a) Y. Wakatsuki, H. Yamazaki, N. Kumegawa, T. Satoh and J. Y. Satoh, ***J. Am. Chem. Soc***. **1991**, 113, 9604-9610.
(b) M. Akita, H. Yasuda, A. Nakamura, ***Bull. Chem. Jpn***. **1984**, 57, 480-487.
(c) B. M. Trost, C. Chan, G. Ruhter, ***J. Am. Chem. Soc***. **1987**, 109, 3486-3487.
(d) M. Ishikawa, J. Ohshita, A. Minato, ***J. Organomet. Chem***. **1988**, 346, C58-C60.
(e) J. Ohshita, K. Furumori, A. Matsuguchi, M. Ishikawa, ***J, Org. Chem***, **1990**, 55, 3277-3280.
(f) I. P. Kovalev, K. V. Yevdakov, Yu. A. Strelenko, M. G. Vinogradov, G. I. Nikishin, ***J. Organomet. Chem***. **1990**, 386, 139-146.

23. (a) C. Bruneau and P. H. Dixneuf, ***Acc. Chem. Res***. **1999**, *32*, 311-323.
(b) S. J. Landon, P. M. Shulman, G. L. Geoffroy, ***J. Am. Chem. Soc***. **1985**, 107, 6739-6740.

(c) B. E. Boland-Lussier, M. R. Churchill, R. P. Hugues, A. L. Rheingold. ***Organometallics***, **1982**, 1, 628-634.

(d) S. R. Bly, M.Raya, R. K.Bly, ***Organometallic***, **1992**, 11, 1220-1228.

(e) P. K. Baker, G. K. Barber, M. Green, A. J. Welch, ***J. Am. Chem. Soc***. **1980**, 102, 7811-7812.

(f) D. S. Gill, M. Green, ***J. Chem. Soc., Chem. Commun***. **1981**, 1037-1038.

(g) S. L Buchwald, R. H. Grubbs, ***J. Am. Chem. Soc***. **1983**, 105, 5490-5491.

(h) I. M. Bruce, A. G. Swincer, R. C. Wallis***, J. Organomet. Chem***. **1979**, 171, C5-C8.

(i) A.Davidson, J. P. Selegue, ***J. Am. Chem. Soc***. **1978**, 100, 7763-7765.

(j) S. Abbott, S. G.Davis, P. Warner. ***J. Organomet. Chem***. ***1983***, 246, C65-C68.

(k) M. P. Gamasa, J.Gimeno, E.Lastra,B. M. Martin, ***Organometallics, 1992***, 11, 1373-1381.

24. C. S. Yi, and N. Liu, ***Organometallics*** **1996**, *15*, 3968-3971.

25. T. Ohmura, S-I. Yorozuya, Y. Yamamoto and N. Miyaura, ***Organometallics***, **2000**, *19*, 4, 365-367

26. (a) A. Nakamura, P-J. Kim and N. Hagihara, ***J. Organometal. Chem***. **1965**, 3, 7-15.

(b) A. Nakamura, P-J. Kim and N. Hagihara. ***This Bulletin***, 37, 292 **1964**.

(c) W. M. Schubert, T. H. Liddicoet and W. A. Lanka, ***J. Am. Chem. Soc***. **1954**, 76, 1929-1932.

27. (a) G. Maas, P. J. Stang and M. R. White, ***Organometallics*** **1983**, *2*, 720-725.

(b) Osborn, J. A.; Jardine, F. H.; Young, J. F.; Wilkinson, G. ***J. Chem. Soc. A***, **1966**, 1711-1732.

28. N. Suzuki, Y. Fukuda, C. E. Kim, H. Takahara, M. Iwasaki, M. Saburi, M. Nishiura and Y. Wakatsuki, ***Chem Lett***, 2, **2003**, 16-17.

29. M. Schafer, J. Wolf and H. Werner, ***Dalton Trans.***, **2005**, 1468-1481.

30. (a) F. A. Akkerman and D. Lentz, ***Angew. Chem. Int. Ed***. **2007**, 46, 4902-4904.
(b) J.P. Collman, J. W. Kang, ***J. Am. Chem. Soc***. **1967**, 89, 844-851.

31. V. V. Burlakov, P. Arndt, W. Baumann, A. Spannenberg, U. Rosenthal, P. Parameswaran and E.D. Jemmis, ***Chem. Commun***., **2004**, 2074-2075.

32. S. K. Pollack, A. Fiseha and B. Narayanswamy, ***Macromolecules*** **1997**, *30*, 5265-5270.

33. H. J. Heeres, J. Nijhoff, J. H. Teuben, ***Organometallics***, **1993**, 12, 2609-2617.

34. (a) W. J. Evans, R. A. Keyer and J. W. Ziller, ***Organometallics*** **1990**, *9*, 2628-2631.
(b) S. P. Nolan, D. Stern, T. J. Marks, ***J. Am. Chem. Soc***. **1989**, 111, 7844-7853.
(c) W. J. Evans, T. A. Ulibarri, L. R. Chamberlain, J. W. Ziller, D. Jr. Alvarez, ***Organometallics***, **1990**, 9, 2124-2130.
(d) D. G. Sekutowski, G. D. Stucky, ***J. Am. Chem. Soc***. **1976**, 98, 1376-1382.

35. W. J. Evans, R. A. Keyer and J. W. Ziller, ***Organometallics*** **1993**, *12*, 2618-2633.

36. L. Lee, D. J. Berg and G. W. Bushnell, ***Organometallics*** **1995**, *14*, 5021-5023.

37. C. M. Forsyth, S. P. Nolan, C. L. Stern and T. J. Marks, ***Organometallics*** **1993**, *12*, 3618-3623.

38. (a) C. Pi, R. Liu, P. Zheng, Z. Chen, X. Zhou, ***Inorg. Chem***, **2007**, 46, 5252-5259.
(b) C. F. Pi, F. X. Zhang, Z. Pang, J. Zheng, J. Luo, Z. X. Chen, L. H. Weng, X. G. Zhou, ***Organometallics***, **2007**, 26, 1934-1946.

39. J. Zhang, Y. Han, F. Han, Z. Chen, L. Weng, X.Zhou, ***Inorg. Chem***, **2008**, 47, 5552-5554.

40. F. Han, J. Zhang, W. Yi, Z. Zhang, J. Yu, L. Weng, X.Zhou, ***Inorg. Chem***, **2010**, 49, 2793-2798.

41. S. Yao, H-S. Chan, C-K. Lam, H. K. Lee, ***Inorg. Chem***. **2009**, 48, 9936-9946.

42. G. B. Deacon, C. M. Forsyth, P. C. Junk, J. Wanf, ***Inorg. Chem***. **2007**, 46, 10022-10030.

43. Y. Cao, Z. Du, W. Li, J.Li, Y. Zhang, F. Xu, Q. Shen, ***Inorg. Chem***. **2011**, 50, 3729-3737.

44. Z. Du, W. Li, X. Zhu, F. Xu, Q. Shen, ***J. Org. Chem***. **2008**, 73, 8966-8972.

45. (a) S. Zhou, S. Wang, G. Yang,Q. L. L. Zhang, Z. Yao, H. Song, ***Organometallics***, **2007**, 26, 3755-3561.
(b) E. W. Thomas, E. E. Nishizawa, D. C. Zimmermann, D. J. Williams, ***J. Med. Chem***, **1989**, 32, 228-236.
(c) T. G. Ong, J. S. O'Brien, I. Korobkov, D. S. Richeson, ***Organometallics***, **2006**, 25, 4728-4730.
(d) W. X. Zhang, M. Nishiura, Z. Hou, ***Chem. Eur. J***. **2007**, 13, 4037-4051.

46. F. Feil, S. Harder, ***Eur. J.Inorg. Chem***, **2005**, 4438-4443.

47. W-X. Zhang, D. Li, Z. Wang, Z. Xi, ***Organometallics***, **2009**, 28, 882-887.

48. T-G. Ong, J. S. O'Brien, I. Korobkov, D. S. Richeson, ***Organometallics***, **2006**, 25, 4728-4730.

49. X. Zhu, Z. Du, F. Xu, Q. Shen, ***J. Org. Chem***. **2009**, 74, 6347-6349.

50. D. Li, Y. Wang, W-X. Zhang, S. Zhang, J. Guang, Z. Xi, ***Organometallics***, **2011**, 30, 5278-5283.

51. F. Wang, S. Cai, Q.Liao,C. Xi, ***J. Org. Chem***. **2011**, 76, 3174-3180.

52. T. K. Panda, H. Tsurugi, K.Pal, H. Kaneko, K. Mashima, ***Organometallic***, **2010**, 29, 34-37.

53. W-X. Zhang, M. Nishiura, Z. Hou, ***J. Am. Chem. Soc***. **2005**, 127, 16788-16789.

54. J. Polin, H. Schottenberger, ***Org Syn,*** **1998**, 9, 411-413.

55. W. C. Lee, M. W. Huh, Y. S. Gal, S, K. Cho, ***Polymer (Korea),*****1989**, 13, 520-528.

56. (a) A. G. M. Barrett, M. R. Crimmin, M. S. Hill, P. B. Hitchcock, S. L. Lomas, P. A. Procopiou and K. Suntharalingam, ***Chem. Commun***., **2009**, 2299 – 2301.
(b) J. P. C. M. van Dongen, M. J. A. de Bie and R. Steur, ***Tetrahedron Lett***, **1973**, 1371-1374.

57. (a) Gustavson, G.; Demjanov, N.J.Prakt. ***Chem***. **1888**, 146, 201-207.
(b) L. M Morton, A. A Noyes,. ***Am. Chem. J***. 1888, 10, 430-433.
(c) W. H. Carothers, G. J. Berchet, ***U.S. Patent 2136178***, E.I du Pont de Nemours, Willmington, DE, **1937**.

58. A. G. M. Barrett, M. R. Crimmin, M. S. Hill, P. B. Hitchcock, G. Kociok-Hohn, P. A. Procopiou, ***Inorg Chem,*** **2008**, 47, 7366-7376.

59. M. Arrowsmith, M. S. Hill, G. Kociok-Kohn, ***Organometallics,*** **2011**, 30, 6, 1291-1294.

60. A. G. M. Barrett, M. R. Crimmin, M. S. Hill, P. B. Hitchcock, S. L. Lomas, M. F. Mahon and P. A. Procopiou, ***Dalton Trans***., **2010**, 39, 7393 – 7400.

61. C-F. Tsai, H-J. Chen, J-C. Chang, C-H. Hung, C-C. Lai, C-H. Hu, J-H. Huang, ***Inorg. Chem***. **2004**, 43, 2183-2188

62. G. P. Mitchell, T. D. Tilley, ***J. Am. Chem. Soc***. **1997**, 119, 11236-11243.

63. T. Muraoko, I. Matsuda, K. Itoh, ***Organometallics***. **2001**, 20, 4676-4682.

64. R. T. Yu, T. Rovis, ***J. Am. Chem. Soc***. **2006**, 128, 2782-2783.

65. R. T. Yu, T. Rovis, ***J. Am. Chem. Soc***. **2006**, 128, 12370-12371.

66. E. E. Lee, T. Rovis, ***Org. Lett.*** **2008**, vol. 10, 1231-1234.

67. R. K. Friedman, T. Rovis, ***J. Am. Chem. Soc***. **2009**, 131, 10775-10782.

68. D. M. Dalton, K. M. Oberg, R. T. Yu, E. E. Lee, S. Perreault, M. E. Oinen, M. L. Pease, G. Malik, T. Rovis, ***J. Am. Chem. Soc***. **2009**, 131, 15717-15728.

69. A. Kumar, S. De, A. G. Samuelson, E. D. Jemmis, ***Organometallics***, **2008**, 27, 955-960.

70. S. Schmidt, R. Schaper, S. Schulz, D. Blaser, C. Wolper, ***Organometallics***, **2011**, 31, 1073-1078.

71. Q. Shen, H. Li, C. Yao, Y. Yao, L. Zhang, K.Yu., ***Organometallics***, **2001**, 20, 3070-3073.

72. X-G. Zhou, L-B. Zhang, M. Zhu, R-F. Cai, L-H. Weng, ***Organometallics***, **2001**, 20, 5700-5706.

73. O. Tardif, D. Hashizume, Z. Hou, ***J. Am. Chem. Soc***. **2004**, 126, 8080-8081.

74. J. Zhang, L. Ma, R. Cai, L. Weng, X. Zhou, ***Organometallics***, **2005**, 24, 738-742.

75. C. Zhang, R. Liu, J. Zhang, Z. Chen, ***Inorg. Chem***. **2006**, 45, 5867-5877.

76. J. Zhang, R. Cai, Z. Chen, X. Zhou, ***Inorg. Chem***. **2007**, 46, 321-327.

77. Y. Wu, S. Wang, X. Zhu, G. Yang, Y. Wei, L. Zhang, H-B. Song, ***Inorg. Chem***. **2008**, 47, 5503-5511.

78. W. J. Evans, J. R. Walensky, J. W. Ziller, ***Organometallics***, **2010**, 29, 945-950.

79. H-X. Li, L. Cheng, H-M. Wang, X-J. Yang, Z-G.Ren, J-P. Lang, ***Organometallics***, **2011**, 30, 208-214.

Appendix

9.0 X-ray crystallography

Compound **3**

Table A1. Crystal data and structure refinement for **3**.

Empirical formula	C_{37} H_{52} Ca N_3
Formula weight	578.90
Temperature	150(2) K
Wavelength	0.71073 Å
Crystal system	Triclinic
Space group	P-1
Unit cell dimensions	a = 11.8480(4)Å α = 98.268(1)°
	b = 13.0650(5)Å β = 109.380(2)°
	c = 13.4040(6)Å γ = 110.718(2)°
Volume	1748.67(12) $Å^3$
Z	2
Density (calculated)	1.099 Mg/m^3
Absorption coefficient	0.207 mm^{-1}
F(000)	630
Crystal size	0.40 x 0.40 x 0.20 mm
Theta range for data collection	4.05 to 27.69°
Index ranges	-15<=h<=15; -16<=k<=16; -17<=l<=17
Reflections collected	30955
Independent reflections	30971 [R(int) = 0.0000]
Reflections observed (>2σ)	20563
Data Completeness	0.966
Absorption correction	Semi-empirical from equivalents
Max. and min. transmission	0.97 and 0.84
Refinement method	Full-matrix least-squares on F^2
Data / restraints / parameters	30971 / 0 / 376
Goodness-of-fit on F^2	1.048
Final R indices [I>2σ(I)]	R1 = 0.0888 wR2 = 0.2078
R indices (all data)	R1 = 0.1386 wR2 = 0.2491
Largest diff. peak and hole	0.580 and -0.388 $eÅ^{-3}$

Notes: Asymmetric unit consists of ½ of a dimer and ½ of a benzene molecule. Convergence optimized once account of pseudo-merohedral twinning (25%) about the (0, 1, 1) direction was included in the refinement.

Table A2. Atomic coordinates (x 10^4) and equivalent isotropic displacement parameters ($Å^2$ x 10^3) for **3**.U(eq) is defined as one third of the trace of the orthogonalized Uij tensor.

Atom	x	y	z	U(eq)
Ca(1)	1547(1)	6092(1)	1040(1)	32(1)
N(1)	3095(2)	7799(2)	1065(2)	32(1)
N(2)	3141(2)	6557(2)	2817(2)	35(1)
N(3)	-3529(2)	6250(2)	692(2)	48(1)
C(1)	-836(2)	5730(2)	442(2)	36(1)
C(2)	-1968(2)	5604(2)	205(2)	39(1)
C(3)	-3359(2)	5475(2)	-72(2)	44(1)
C(4)	-3177(3)	6082(3)	1764(3)	70(1)
C(5)	-2853(3)	7441(3)	733(4)	79(1)
C(6)	4418(2)	7273(2)	3199(2)	38(1)
C(7)	4974(2)	8000(2)	2646(2)	37(1)
C(8)	4391(2)	8311(2)	1730(2)	32(1)
C(9)	5297(2)	9312(2)	1501(2)	45(1)
C(10)	5375(3)	7369(3)	4329(2)	58(1)
C(11)	2566(2)	8327(2)	279(2)	33(1)
C(12)	2225(2)	9201(2)	649(2)	38(1)
C(13)	1678(2)	9695(2)	-118(2)	44(1)
C(14)	1463(3)	9355(2)	-1213(2)	46(1)
C(15)	1780(3)	8472(2)	-1574(2)	45(1)
C(16)	2314(2)	7946(2)	-840(2)	35(1)
C(17)	2410(3)	9585(2)	1832(2)	48(1)
C(18)	3344(4)	10871(3)	2387(3)	86(1)
C(19)	1098(4)	9357(4)	1891(3)	97(1)
C(20)	2595(2)	6967(2)	-1282(2)	42(1)
C(21)	1378(3)	6023(2)	-2247(2)	54(1)
C(22)	3765(3)	7409(3)	-1625(3)	60(1)
C(23)	2693(2)	5970(2)	3544(2)	39(1)
C(24)	2285(2)	6507(2)	4262(2)	48(1)
C(25)	1843(3)	5917(3)	4946(3)	60(1)
C(26)	1800(3)	4849(3)	4932(3)	63(1)
C(27)	2170(3)	4324(3)	4210(2)	55(1)
C(28)	2598(2)	4864(2)	3490(2)	43(1)
C(29)	2259(3)	7652(3)	4257(2)	55(1)
C(30)	874(4)	7531(4)	3792(5)	105(2)
C(31)	3014(6)	8533(4)	5417(4)	129(2)
C(32)	2942(3)	4238(2)	2677(2)	46(1)
C(33)	4177(3)	4058(3)	3233(3)	69(1)
C(34)	1782(3)	3087(3)	1935(3)	62(1)
C(35)	-860(3)	9621(4)	3911(3)	77(1)
C(36)	-1005(3)	8919(3)	4565(3)	70(1)
C(37)	140(4)	10699(4)	4339(3)	76(1)

Table A3. Bond lengths [Å] and angles [^{o}] for **3**.

Ca(1)-N(1)	2.3196(17)	Ca(1)-N(2)	2.323(2)
Ca(1)-C(1)	2.505(2)	Ca(1)-C(1)#1	2.536(2)
Ca(1)-C(2)#1	2.866(2)	N(1)-C(8)	1.339(3)
N(1)-C(11)	1.434(3)	N(2)-C(6)	1.332(3)
N(2)-C(23)	1.445(3)	N(3)-C(4)	1.430(4)
N(3)-C(3)	1.449(3)	N(3)-C(5)	1.460(4)
C(1)-C(2)	1.214(3)	C(1)-Ca(1)#1	2.536(2)
C(2)-C(3)	1.504(3)	C(3)-H(3A)	0.9900
C(3)-H(3B)	0.9900	C(4)-H(4A)	0.9800
C(4)-H(4B)	0.9800	C(4)-H(4C)	0.9800
C(5)-H(5A)	0.9800	C(5)-H(5B)	0.9800
C(5)-H(5C)	0.9800	C(6)-C(7)	1.403(3)
C(6)-C(10)	1.517(4)	C(7)-C(8)	1.389(3)
C(7)-H(7)	0.9500	C(8)-C(9)	1.516(3)
C(9)-H(9A)	0.9800	C(9)-H(9B)	0.9800
C(9)-H(9C)	0.9800	C(10)-H(10A)	0.9800
C(10)-H(10B)	0.9800	C(10)-H(10C)	0.9800
C(11)-C(16)	1.404(3)	C(11)-C(12)	1.419(3)
C(12)-C(13)	1.392(3)	C(12)-C(17)	1.508(4)
C(13)-C(14)	1.378(4)	C(13)-H(13)	0.9500
C(14)-C(15)	1.405(4)	C(14)-H(14)	0.9500
C(15)-C(16)	1.388(3)	C(15)-H(15)	0.9500
C(16)-C(20)	1.521(3)	C(17)-C(19)	1.508(4)
C(17)-C(18)	1.543(4)	C(17)-H(17)	1.0000
C(18)-H(18A)	0.9800	C(18)-H(18B)	0.9800
C(18)-H(18C)	0.9800	C(19)-H(19A)	0.9800
C(19)-H(19B)	0.9800	C(19)-H(19C)	0.9800
C(20)-C(21)	1.522(4)	C(20)-C(22)	1.548(4)
C(20)-H(20)	1.0000	C(21)-H(21A)	0.9800
C(21)-H(21B)	0.9800	C(21)-H(21C)	0.9800
C(22)-H(22A)	0.9800	C(22)-H(22B)	0.9800
C(22)-H(22C)	0.9800	C(23)-C(28)	1.399(4)
C(23)-C(24)	1.416(4)	C(24)-C(25)	1.394(4)
C(24)-C(29)	1.509(4)	C(25)-C(26)	1.377(4)
C(25)-H(25)	0.9500	C(26)-C(27)	1.379(4)
C(26)-H(26)	0.9500	C(27)-C(28)	1.397(4)
C(27)-H(27)	0.9500	C(28)-C(32)	1.515(4)
C(29)-C(30)	1.489(5)	C(29)-C(31)	1.541(5)
C(29)-H(29)	1.0000	C(30)-H(30A)	0.9800
C(30)-H(30B)	0.9800	C(30)-H(30C)	0.9800
C(31)-H(31A)	0.9800	C(31)-H(31B)	0.9800
C(31)-H(31C)	0.9800	C(32)-C(33)	1.525(4)
C(32)-C(34)	1.529(4)	C(32)-H(32)	1.0000
C(33)-H(33A)	0.9800	C(33)-H(33B)	0.9800
C(33)-H(33C)	0.9800	C(34)-H(34A)	0.9800
C(34)-H(34B)	0.9800	C(34)-H(34C)	0.9800
C(35)-C(37)	1.361(5)	C(35)-C(36)	1.364(5)
C(35)-H(35)	0.9500	C(36)-C(37)#2	1.373(5)
C(36)-H(36)	0.9500	C(37)-C(36)#2	1.373(5)

C(37)-H(37)	0.9500		
N(1)-Ca(1)-N(2)	81.70(6)	N(1)-Ca(1)-C(1)	120.52(7)
N(2)-Ca(1)-C(1)	128.68(7)	N(1)-Ca(1)-C(1)#1	118.90(7)
N(2)-Ca(1)-C(1)#1	121.72(7)	C(1)-Ca(1)-C(1)#1	89.23(7)
N(1)-Ca(1)-C(2)#1	102.87(7)	N(2)-Ca(1)-C(2)#1	102.57(7)
C(1)-Ca(1)-C(2)#1	114.25(7)	C(1)#1-Ca(1)-C(2)#1	25.02(7)
C(8)-N(1)-C(11)	118.99(17)	C(8)-N(1)-Ca(1)	126.47(14)
C(11)-N(1)-Ca(1)	114.54(12)	C(6)-N(2)-C(23)	118.16(19)
C(6)-N(2)-Ca(1)	125.89(15)	C(23)-N(2)-Ca(1)	115.90(14)
C(4)-N(3)-C(3)	112.0(2)	C(4)-N(3)-C(5)	112.7(3)
C(3)-N(3)-C(5)	111.9(2)	C(2)-C(1)-Ca(1)	176.3(2)
C(2)-C(1)-Ca(1)#1	92.87(16)	Ca(1)-C(1)-Ca(1)#1	90.77(7)
C(1)-C(2)-C(3)	178.7(3)	N(3)-C(3)-C(2)	116.5(2)
N(3)-C(3)-H(3A)	108.2	C(2)-C(3)-H(3A)	108.2
N(3)-C(3)-H(3B)	108.2	C(2)-C(3)-H(3B)	108.2
H(3A)-C(3)-H(3B)	107.3	N(3)-C(4)-H(4A)	109.5
N(3)-C(4)-H(4B)	109.5	H(4A)-C(4)-H(4B)	109.5
N(3)-C(4)-H(4C)	109.5	H(4A)-C(4)-H(4C)	109.5
H(4B)-C(4)-H(4C)	109.5	N(3)-C(5)-H(5A)	109.5
N(3)-C(5)-H(5B)	109.5	H(5A)-C(5)-H(5B)	109.5
N(3)-C(5)-H(5C)	109.5	H(5A)-C(5)-H(5C)	109.5
H(5B)-C(5)-H(5C)	109.5	N(2)-C(6)-C(7)	124.9(2)
N(2)-C(6)-C(10)	119.7(2)	C(7)-C(6)-C(10)	115.4(2)
C(8)-C(7)-C(6)	131.34(19)	C(8)-C(7)-H(7)	114.3
C(6)-C(7)-H(7)	114.3	N(1)-C(8)-C(7)	124.14(19)
N(1)-C(8)-C(9)	119.1(2)	C(7)-C(8)-C(9)	116.76(19)
C(8)-C(9)-H(9A)	109.5	C(8)-C(9)-H(9B)	109.5
H(9A)-C(9)-H(9B)	109.5	C(8)-C(9)-H(9C)	109.5
H(9A)-C(9)-H(9C)	109.5	H(9B)-C(9)-H(9C)	109.5
C(6)-C(10)-H(10A)	109.5	C(6)-C(10)-H(10B)	109.5
H(10A)-C(10)-H(10B)	109.5	C(6)-C(10)-H(10C)	109.5
H(10A)-C(10)-H(10C)	109.5	H(10B)-C(10)-H(10C)	109.5
C(16)-C(11)-C(12)	120.6(2)	C(16)-C(11)-N(1)	121.24(19)
C(12)-C(11)-N(1)	118.0(2)	C(13)-C(12)-C(11)	118.2(2)
C(13)-C(12)-C(17)	119.8(2)	C(11)-C(12)-C(17)	122.0(2)
C(14)-C(13)-C(12)	121.9(2)	C(14)-C(13)-H(13)	119.1
C(12)-C(13)-H(13)	119.1	C(13)-C(14)-C(15)	119.3(2)
C(13)-C(14)-H(14)	120.3	C(15)-C(14)-H(14)	120.3
C(16)-C(15)-C(14)	120.8(2)	C(16)-C(15)-H(15)	119.6
C(14)-C(15)-H(15)	119.6	C(15)-C(16)-C(11)	119.1(2)
C(15)-C(16)-C(20)	118.7(2)	C(11)-C(16)-C(20)	122.2(2)
C(12)-C(17)-C(19)	110.8(2)	C(12)-C(17)-C(18)	111.8(2)
C(19)-C(17)-C(18)	108.9(3)	C(12)-C(17)-H(17)	108.4
C(19)-C(17)-H(17)	108.4	C(18)-C(17)-H(17)	108.4
C(17)-C(18)-H(18A)	109.5	C(17)-C(18)-H(18B)	109.5
H(18A)-C(18)-H(18B)	109.5	C(17)-C(18)-H(18C)	109.5
H(18A)-C(18)-H(18C)	109.5	H(18B)-C(18)-H(18C)	109.5
C(17)-C(19)-H(19A)	109.5	C(17)-C(19)-H(19B)	109.5
H(19A)-C(19)-H(19B)	109.5	C(17)-C(19)-H(19C)	109.5
H(19A)-C(19)-H(19C)	109.5	H(19B)-C(19)-H(19C)	109.5
C(16)-C(20)-C(21)	112.1(2)	C(16)-C(20)-C(22)	111.0(2)
C(21)-C(20)-C(22)	110.3(2)	C(16)-C(20)-H(20)	107.8

C(21)-C(20)-H(20)	107.8	C(22)-C(20)-H(20)	107.8
C(20)-C(21)-H(21A)	109.5	C(20)-C(21)-H(21B)	109.5
H(21A)-C(21)-H(21B)	109.5	C(20)-C(21)-H(21C)	109.5
H(21A)-C(21)-H(21C)	109.5	H(21B)-C(21)-H(21C)	109.5
C(20)-C(22)-H(22A)	109.5	C(20)-C(22)-H(22B)	109.5
H(22A)-C(22)-H(22B)	109.5	C(20)-C(22)-H(22C)	109.5
H(22A)-C(22)-H(22C)	109.5	H(22B)-C(22)-H(22C)	109.5
C(28)-C(23)-C(24)	120.8(2)	C(28)-C(23)-N(2)	120.1(2)
C(24)-C(23)-N(2)	119.0(2)	C(25)-C(24)-C(23)	117.9(3)
C(25)-C(24)-C(29)	120.3(3)	C(23)-C(24)-C(29)	121.7(2)
C(26)-C(25)-C(24)	121.6(3)	C(26)-C(25)-H(25)	119.2
C(24)-C(25)-H(25)	119.2	C(25)-C(26)-C(27)	119.9(2)
C(25)-C(26)-H(26)	120.0	C(27)-C(26)-H(26)	120.0
C(26)-C(27)-C(28)	121.0(3)	C(26)-C(27)-H(27)	119.5
C(28)-C(27)-H(27)	119.5	C(27)-C(28)-C(23)	118.6(3)
C(27)-C(28)-C(32)	119.3(2)	C(23)-C(28)-C(32)	122.0(2)
C(30)-C(29)-C(24)	111.2(3)	C(30)-C(29)-C(31)	108.6(3)
C(24)-C(29)-C(31)	113.0(3)	C(30)-C(29)-H(29)	108.0
C(24)-C(29)-H(29)	108.0	C(31)-C(29)-H(29)	108.0
C(29)-C(30)-H(30A)	109.5	C(29)-C(30)-H(30B)	109.5
H(30A)-C(30)-H(30B)	109.5	C(29)-C(30)-H(30C)	109.5
H(30A)-C(30)-H(30C)	109.5	H(30B)-C(30)-H(30C)	109.5
C(29)-C(31)-H(31A)	109.5	C(29)-C(31)-H(31B)	109.5
H(31A)-C(31)-H(31B)	109.5	C(29)-C(31)-H(31C)	109.5
H(31A)-C(31)-H(31C)	109.5	H(31B)-C(31)-H(31C)	109.5
C(28)-C(32)-C(33)	113.3(2)	C(28)-C(32)-C(34)	111.7(2)
C(33)-C(32)-C(34)	109.7(2)	C(28)-C(32)-H(32)	107.3
C(33)-C(32)-H(32)	107.3	C(34)-C(32)-H(32)	107.3
C(32)-C(33)-H(33A)	109.5	C(32)-C(33)-H(33B)	109.5
H(33A)-C(33)-H(33B)	109.5	C(32)-C(33)-H(33C)	109.5
H(33A)-C(33)-H(33C)	109.5	H(33B)-C(33)-H(33C)	109.5
C(32)-C(34)-H(34A)	109.5	C(32)-C(34)-H(34B)	109.5
H(34A)-C(34)-H(34B)	109.5	C(32)-C(34)-H(34C)	109.5
H(34A)-C(34)-H(34C)	109.5	H(34B)-C(34)-H(34C)	109.5
C(37)-C(35)-C(36)	120.3(3)	C(37)-C(35)-H(35)	119.8
C(36)-C(35)-H(35)	119.8	C(35)-C(36)-C(37)#2	119.9(4)
C(35)-C(36)-H(36)	120.0	C(37)#2-C(36)-H(36)	120.0
C(35)-C(37)-C(36)#2	119.8(3)	C(35)-C(37)-H(37)	120.1
C(36)#2-C(37)-H(37)	120.1		

Symmetry transformations used to generate equivalent atoms:

#1 -x,-y+1,-z #2 -x,-y+2,-z+1

Table A4. Anisotropic displacement parameters ($Å^2$ x 10^3) for **3**. The anisotropic displacement factor exponent takes the form: -2 gpi^2 [h^2 a^{*2} U11 + ... + 2 h k a* b* U

Atom	U11	U22	U33	U23	U13	U12
Ca(1)	26(1)	32(1)	35(1)	6(1)	11(1)	11(1)
N(1)	27(1)	31(1)	37(1)	9(1)	13(1)	13(1)
N(2)	30(1)	40(1)	34(1)	10(1)	14(1)	16(1)
N(3)	34(1)	46(1)	63(2)	6(1)	20(1)	20(1)
C(1)	35(1)	31(1)	40(1)	5(1)	16(1)	12(1)
C(2)	34(1)	35(1)	43(1)	3(1)	16(1)	14(1)
C(3)	31(1)	50(1)	50(2)	4(1)	18(1)	18(1)
C(4)	57(2)	100(2)	64(2)	13(2)	31(2)	46(2)
C(5)	55(2)	47(2)	138(3)	15(2)	47(2)	24(2)
C(6)	34(1)	45(1)	35(1)	8(1)	13(1)	18(1)
C(7)	24(1)	38(1)	42(1)	5(1)	12(1)	11(1)
C(8)	29(1)	30(1)	41(1)	5(1)	18(1)	15(1)
C(9)	32(1)	41(1)	58(2)	17(1)	16(1)	13(1)
C(10)	39(2)	78(2)	44(2)	23(2)	8(1)	18(1)
C(11)	25(1)	28(1)	42(1)	8(1)	13(1)	9(1)
C(12)	35(1)	35(1)	47(2)	14(1)	17(1)	17(1)
C(13)	45(1)	39(1)	58(2)	16(1)	24(1)	25(1)
C(14)	50(2)	49(1)	51(2)	24(1)	21(1)	28(1)
C(15)	48(2)	45(1)	47(2)	19(1)	22(1)	23(1)
C(16)	34(1)	34(1)	36(1)	10(1)	14(1)	14(1)
C(17)	58(2)	50(2)	49(2)	13(1)	24(1)	35(1)
C(18)	74(2)	78(2)	66(2)	-16(2)	22(2)	12(2)
C(19)	65(2)	130(3)	69(2)	-5(2)	40(2)	17(2)
C(20)	50(2)	43(1)	40(1)	12(1)	23(1)	24(1)
C(21)	65(2)	46(1)	45(2)	6(1)	21(1)	24(1)
C(22)	56(2)	65(2)	72(2)	17(2)	39(2)	31(2)
C(23)	33(1)	50(1)	34(1)	14(1)	13(1)	19(1)
C(24)	42(1)	65(2)	42(2)	16(1)	20(1)	25(1)
C(25)	57(2)	91(2)	47(2)	23(2)	31(2)	36(2)
C(26)	60(2)	83(2)	56(2)	38(2)	33(2)	29(2)
C(27)	56(2)	62(2)	55(2)	30(2)	27(1)	26(1)
C(28)	31(1)	52(2)	42(2)	17(1)	12(1)	14(1)
C(29)	61(2)	63(2)	50(2)	12(1)	30(1)	33(2)
C(30)	75(3)	96(3)	148(4)	38(3)	33(3)	52(2)
C(31)	143(4)	82(3)	107(4)	-11(3)	-5(3)	57(3)
C(32)	51(2)	43(1)	52(2)	19(1)	25(1)	23(1)
C(33)	57(2)	79(2)	72(2)	15(2)	20(2)	39(2)
C(34)	64(2)	56(2)	64(2)	16(2)	25(2)	28(2)
C(35)	55(2)	115(3)	43(2)	11(2)	12(2)	30(2)
C(36)	46(2)	90(2)	59(2)	1(2)	20(2)	22(2)
C(37)	72(2)	103(3)	61(2)	26(2)	33(2)	40(2)

Table A5. Hydrogen coordinates (x 10^4) and isotropic displacement parameters (Å^2 x 10^3) for **3**.

Atom	x	y	z	U(eq)
H(3A)	-3705	5577	-814	53
H(3B)	-3914	4680	-125	53
H(4A)	-3629	5267	1688	104
H(4B)	-3445	6525	2216	104
H(4C)	-2216	6337	2122	104
H(5A)	-1892	7692	1078	119
H(5B)	-3098	7924	1168	119
H(5C)	-3114	7508	-21	119
H(7)	5915	8338	2952	44
H(9A)	5210	9077	740	68
H(9B)	6217	9557	2020	68
H(9C)	5051	9950	1593	68
H(10A)	5132	7668	4900	87
H(10B)	6278	7891	4465	87
H(10C)	5334	6611	4352	87
H(13)	1447	10283	119	53
H(14)	1103	9714	-1719	56
H(15)	1628	8231	-2328	53
H(17)	2810	9139	2256	58
H(18A)	3435	11090	3150	128
H(18B)	2974	11321	1973	128
H(18C)	4216	11020	2390	128
H(19A)	1239	9601	2666	145
H(19B)	512	8535	1570	145
H(19C)	689	9785	1475	145
H(20)	2859	6627	-671	50
H(21A)	1601	5412	-2507	80
H(21B)	1081	6340	-2851	80
H(21C)	667	5711	-2003	80
H(22A)	3928	6764	-1905	90
H(22B)	4562	7968	-981	90
H(22C)	3546	7773	-2205	90
H(25)	1563	6262	5433	72
H(26)	1517	4473	5420	75
H(27)	2133	3585	4202	66
H(29)	2690	7963	3772	66
H(30A)	884	8283	3783	158
H(30B)	427	7219	4251	158
H(30C)	398	7011	3035	158
H(31A)	3928	8620	5735	194
H(31B)	2576	8267	5896	194
H(31C)	3017	9273	5357	194
H(32)	3127	4723	2186	55
H(33A)	4917	4796	3712	104
H(33B)	4402	3724	2666	104
H(33C)	4007	3538	3680	104

H(34A)	2038	2709	1420	92
H(34B)	1017	3215	1516	92
H(34C)	1547	2601	2394	92
H(35)	-1459	9357	3153	92
H(36)	-1704	8167	4263	84
H(37)	239	11186	3881	92

Table A6. Dihedral angles [^{o}] for **3**.

Atom1 - Atom2 - Atom3 - Atom4	Dihedral
N(2) - Ca(1) - N(1) - C(8)	21.31(18)
C(1) - Ca(1) - N(1) - C(8)	151.63(17)
C(1)#1 - Ca(1) - N(1) - C(8)	-100.45(19)
C(2)#1 - Ca(1) - N(1) - C(8)	-79.77(19)
N(2) - Ca(1) - N(1) - C(11)	-158.47(15)
C(1) - Ca(1) - N(1) - C(11)	-28.15(18)
C(1)#1 - Ca(1) - N(1) - C(11)	79.77(16)
C(2)#1 - Ca(1) - N(1) - C(11)	100.45(15)
N(1) - Ca(1) - N(2) - C(6)	-20.50(18)
C(1) - Ca(1) - N(2) - C(6)	-143.22(17)
C(1)#1 - Ca(1) - N(2) - C(6)	98.44(19)
C(2)#1 - Ca(1) - N(2) - C(6)	80.93(19)
N(1) - Ca(1) - N(2) - C(23)	162.18(16)
C(1) - Ca(1) - N(2) - C(23)	39.46(19)
C(1)#1 - Ca(1) - N(2) - C(23)	-78.88(17)
C(2)#1 - Ca(1) - N(2) - C(23)	-96.39(16)
N(1) - Ca(1) - C(1) - C(2)	-65(3)
N(2) - Ca(1) - C(1) - C(2)	39(3)
C(1)#1 - Ca(1) - C(1) - C(2)	171(3)
C(2)#1 - Ca(1) - C(1) - C(2)	171(3)
N(1) - Ca(1) - C(1) - Ca(1)#1	123.58(7)
N(2) - Ca(1) - C(1) - Ca(1)#1	-131.52(8)
C(1)#1 - Ca(1) - C(1) - Ca(1)#1	0.0
C(2)#1 - Ca(1) - C(1) - Ca(1)#1	0.27(9)
Ca(1) - C(1) - C(2) - C(3)	18(15)
Ca(1)#1 - C(1) - C(2) - C(3)	-171(100)
C(4) - N(3) - C(3) - C(2)	-63.8(3)
C(5) - N(3) - C(3) - C(2)	63.9(3)
C(1) - C(2) - C(3) - N(3)	-19(13)
C(23) - N(2) - C(6) - C(7)	-172.4(2)
Ca(1) - N(2) - C(6) - C(7)	10.3(3)
C(23) - N(2) - C(6) - C(10)	5.5(3)
Ca(1) - N(2) - C(6) - C(10)	-171.77(19)
N(2) - C(6) - C(7) - C(8)	12.2(4)
C(10) - C(6) - C(7) - C(8)	-165.8(3)
C(11) - N(1) - C(8) - C(7)	168.1(2)
Ca(1) - N(1) - C(8) - C(7)	-11.7(3)
C(11) - N(1) - C(8) - C(9)	-10.7(3)
Ca(1) - N(1) - C(8) - C(9)	169.54(16)
C(6) - C(7) - C(8) - N(1)	-11.5(4)

C(6) - C(7) - C(8) - C(9)	167.3(2)
C(8) - N(1) - C(11) - C(16)	100.5(2)
Ca(1) - N(1) - C(11) - C(16)	-79.7(2)
C(8) - N(1) - C(11) - C(12)	-83.4(2)
Ca(1) - N(1) - C(11) - C(12)	96.37(19)
C(16) - C(11) - C(12) - C(13)	-2.2(3)
N(1) - C(11) - C(12) - C(13)	-178.34(19)
C(16) - C(11) - C(12) - C(17)	176.5(2)
N(1) - C(11) - C(12) - C(17)	0.4(3)
C(11) - C(12) - C(13) - C(14)	0.2(3)
C(17) - C(12) - C(13) - C(14)	-178.6(2)
C(12) - C(13) - C(14) - C(15)	1.1(4)
C(13) - C(14) - C(15) - C(16)	-0.4(4)
C(14) - C(15) - C(16) - C(11)	-1.6(3)
C(14) - C(15) - C(16) - C(20)	177.9(2)
C(12) - C(11) - C(16) - C(15)	2.9(3)
N(1) - C(11) - C(16) - C(15)	178.92(19)
C(12) - C(11) - C(16) - C(20)	-176.6(2)
N(1) - C(11) - C(16) - C(20)	-0.6(3)
C(13) - C(12) - C(17) - C(19)	61.1(3)
C(11) - C(12) - C(17) - C(19)	-117.6(3)
C(13) - C(12) - C(17) - C(18)	-60.6(3)
C(11) - C(12) - C(17) - C(18)	120.7(3)
C(15) - C(16) - C(20) - C(21)	-54.2(3)
C(11) - C(16) - C(20) - C(21)	125.2(2)
C(15) - C(16) - C(20) - C(22)	69.6(3)
C(11) - C(16) - C(20) - C(22)	-111.0(3)
C(6) - N(2) - C(23) - C(28)	-95.5(3)
Ca(1) - N(2) - C(23) - C(28)	82.1(2)
C(6) - N(2) - C(23) - C(24)	88.0(3)
Ca(1) - N(2) - C(23) - C(24)	-94.5(2)
C(28) - C(23) - C(24) - C(25)	2.7(4)
N(2) - C(23) - C(24) - C(25)	179.2(2)
C(28) - C(23) - C(24) - C(29)	-174.2(2)
N(2) - C(23) - C(24) - C(29)	2.3(4)
C(23) - C(24) - C(25) - C(26)	0.1(4)
C(29) - C(24) - C(25) - C(26)	177.1(3)
C(24) - C(25) - C(26) - C(27)	-1.7(5)
C(25) - C(26) - C(27) - C(28)	0.4(5)
C(26) - C(27) - C(28) - C(23)	2.4(4)
C(26) - C(27) - C(28) - C(32)	-177.5(3)
C(24) - C(23) - C(28) - C(27)	-4.0(4)
N(2) - C(23) - C(28) - C(27)	179.6(2)
C(24) - C(23) - C(28) - C(32)	176.0(2)
N(2) - C(23) - C(28) - C(32)	-0.5(3)
C(25) - C(24) - C(29) - C(30)	-66.9(4)
C(23) - C(24) - C(29) - C(30)	109.9(3)
C(25) - C(24) - C(29) - C(31)	55.5(4)
C(23) - C(24) - C(29) - C(31)	-127.7(4)
C(27) - C(28) - C(32) - C(33)	-67.8(3)
C(23) - C(28) - C(32) - C(33)	112.3(3)
C(27) - C(28) - C(32) - C(34)	56.6(3)
C(23) - C(28) - C(32) - C(34)	-123.3(3)

C(37) - C(35) - C(36) - C(37)#2	0.1(6)
C(36) - C(35) - C(37) - C(36)#2	-0.1(6)

Symmetry transformations used to generate equivalent atoms:

#1 -x,-y+1,-z #2 -x,-y+2,-z+1

Compound **4**

Table A7. Crystal data and structure refinement for **4**. (toluene)

Empirical formula	$C_{66}\ H_{92}\ Ca_2\ N_4\ O_2\quad C_7\ H_8$
Formula weight	1145.73
Temperature	173(2) K
Wavelength	0.71073 Å
Crystal system	Triclinic
Space group	$P\bar{1}$ (No.2)
Unit cell dimensions	a = 13.2296(2) Å α = 91.519(1)°
	b = 14.3726(3) Å β = 104.537(1)°
	c = 21.2865(4) Å γ = 115.640(1)°
Volume	3489.52(11) $Å^3$
Z	2
Density (calculated)	1.09 Mg/m^3
Absorption coefficient	0.21 mm^{-1}
F(000)	1244
Crystal size	0.40 x 0.30 x 0.25 mm^3
Theta range for data collection	3.42 to 26.06°
Index ranges	-16<=h<=16; -17<=k<=17; -26<=l<=26
Reflections collected	54759
Independent reflections	13709 [R(int) = 0.055]
Reflections observed (>2σ)	10036
Data Completeness	99.1 %
Absorption correction	Semi-empirical from equivalents
Max. and min. transmission	0.9531 and 0.9018
Refinement method	Full-matrix least-squares on F^2
Data / restraints / parameters	13709 / 0 / 725
Goodness-of-fit on F^2	1.009
Final R indices [I>2σ(I)]	R1 = 0.059 wR2 = 0.151
R indices (all data)	R1 = 0.087 wR2 = 0.169
Largest diff. peak and hole	1.35 and -0.61 e.$Å^{-3}$ (near solnate)

There are two independent molecules of the complex, each lying on an inversion centre. The disordered toluene solvate was included with isotropic C atoms and H atoms omitted.

Data collection KappaCCD , Program package WinGX , Abs correction MULTISCAN Refinement using SHELXL-97 , Drawing using ORTEP-3 for Windows

Table A8. Atomic coordinates (x 10^4) and equivalent isotropic displacement parameters ($Å^2$ x 10^3) **4**. U(eq) is defined as one third of the trace of the orthogonalized U^{ij} tensor.

Atom	x	y	z	U(eq)
Ca	6165(1)	6117(1)	5716(1)	28(1)
O	7489(2)	5657(2)	6570(1)	40(1)
N(1)	7781(2)	7673(2)	5695(1)	29(1)
N(2)	6047(2)	7151(2)	6531(1)	27(1)
C(1)	8401(2)	8420(2)	6209(1)	32(1)
C(2)	8077(2)	8468(2)	6788(1)	34(1)
C(3)	6988(2)	7952(2)	6924(1)	29(1)
C(4)	9546(2)	9327(3)	6201(2)	52(1)
C(5)	6933(3)	8375(2)	7565(1)	43(1)
C(6)	8139(2)	7783(2)	5103(1)	30()
C(7)	7852(2)	8399(2)	4663(1)	34(1)
C(8)	8174(2)	8461(2)	4084(1)	39(1)
C(9)	8762(3)	7931(2)	3939(1)	43(1)
C(10)	9011(3)	7310(2)	4364(2)	44(1)
C(11)	8710(2)	7215(2)	4951(1)	37(1)
C(12)	7197(3)	8996(2)	4783(1)	45(1)
C(13)	5977(3)	8534(3)	4287(2)	58(1)
C(14)	7875(3)	10168(3)	4750(2)	66(1)
C(15)	9029(3)	6527(3)	5407(2)	53(1)
C(16)	10290(4)	7106(5)	5829(3)	122(2)
C(17)	8774(5)	5483(3)	5034(2)	92(2)
C(18)	4936(2)	6817(2)	6655(1)	28(1)
C(19)	4301(2)	7391(2)	6483(1)	38(1)
C(20)	3188(3)	7012(3)	6563(2)	50(1)
C(21)	2691(3)	6084(3)	6798(2)	55(1)
C(22)	3310(3)	5519(3)	6957(2)	48(1)
C(23)	4439(2)	5872(2)	6895(1)	34(1)
C(24)	4781(3)	8393(2)	6194(2)	48(1)
C(25)	4127(4)	8212(3)	5464(2)	69(1)
C(26)	4705(4)	9285(3)	6557(2)	75(1)
C(27)	5080(3)	5220(2)	7084(1)	40(1)
C(28)	5351(3)	5156(3)	7816(2)	61(1)
C(29)	4400(3)	4122(3)	6688(2)	60(1)
C(30)	5598(3)	4182(2)	5201(2)	42(1)
C(31)	6375(3)	4316(2)	5699(1)	41(1)
C(32)	7303(3)	4639(2)	6325(2)	46(1)
C(33)	8403(3)	6118(3)	7175(2)	62(1)
Ca(1B)	5347(1)	1482(1)	9971(1)	26(1)
O(1B)	5773(2)	2531(1)	11027(1)	37(1)
N(1B)	6705(2)	2945(2)	9659(1)	28(1)
N(2B)	4095(2)	2125(2)	9396(1)	26(1)
C(1B)	6618(2)	3825(2)	9599(1)	32(1)
C(2B)	5579(2)	3913(2)	9533(1)	32(1)
C(3B)	4410(2)	3132(2)	9391(1)	28(1)

C(4B)	7676(3)	4827(2)	9588(2)	49(1)
C(5B)	3487(2)	3515(2)	9203(2)	41(1)
C(6B)	7717(2)	2871(2)	9589(1)	31(1)
C(7B)	7753(2)	2613(2)	8955(1)	36(1)
C(8B)	8710(3)	2482(2)	8892(2)	47(1)
C(9B)	9599(3)	2583(3)	9437(2)	51(1)
C(10B)	9543(3)	2816(3)	10054(2)	48(1)
C(11B)	8615(2)	2963(2)	10145(1)	38(1)
C(12B)	6785(2)	2476(2)	8343(1)	43(1)
C(13B)	7205(3)	3339(3)	7929(2)	70(1)
C(14B)	6278(3)	1412(3)	7929(2)	60(1)
C(15B)	8613(3)	3238(3)	10835(2)	51(1)
C(16B)	9611(4)	4316(3)	11161(2)	74(1)
C(17B)	8685(3)	2427(4)	11271(2)	78(1)
C(18B)	2877(2)	1386(2)	9152(1)	28(1)
C(19B)	2441(2)	864(2)	8499(1)	33(1)
C(20B)	1257(2)	162(3)	8267(1)	47(1)
C(21B)	523(2)	-48(3)	8657(2)	57(1)
C(22B)	974(2)	427(3)	9305(1)	53(1)
C(23B)	2158(2)	1128(2)	9565(1)	37(1)
C(24B)	3251(2)	1054(2)	8069(1)	35(1)
C(25B)	2854(3)	109(2)	7554(1)	47(1)
C(26B)	3431(3)	2017(3)	7742(2)	51(1)
C(27B)	2635(2)	1531(2)	10300(1)	42(1)
C(28B)	2038(3)	2112(3)	10534(2)	53(1)
C(29B)	2534(3)	623(3)	10681(1)	54(1)
C(30B)	5240(3)	101(2)	10817(1)	40(1)
C(31B)	5504(3)	877(2)	11188(1)	37(1)
C(32B)	5795(3)	1898(2)	11535(1)	41(1)
C(33B)	6042(4)	3576(3)	11267(2)	63(1)
C(1S)	9791(8)	2743(7)	7243(4)	79(2)a
C(2S)	9254(5)	1625(5)	7270(3)	104(2)
C(3S)	8194(8)	1118(8)	6738(5)	82(2)a
C(4S)	7689(8)	1573(7)	6254(4)	167(3)
C(5S)	8298(7)	2643(7)	6240(4)	70(2)a
C(6S)	9353(5)	3173(5)	6797(3)	108(2)
C(7S)	10838(5)	3345(5)	7751(3)	117(2)
C(8S)	8796(10)	1985(9)	6840(6)	98(3)a
C(9S)	10438(7)	2327(6)	7803(4)	71(2)a
C(10S)	10219(13)	3620(12)	7232(7)	130(4)a

a occupancy 0.5

Table A9. Bond lengths [Å] and angles [°] **4**.

Ca-N(2)	2.333(2)	Ca-N(1)	2.344(2)
Ca-C(30)’	2.497(3)	Ca-O	2.5063(18)
Ca-C(30)	2.668(3)	Ca-C(31)	2.721(3)
O-C(33)	1.427(4)	O-C(32)	1.434(3)
N(1)-C(1)	1.322(3)	N(1)-C(6)	1.442(3)
N(2)-C(3)	1.328(3)	N(2)-C(18)	1.432(3)

C(1)-C(2)	1.412(4)	C(1)-C(4)	1.517(4)
C(2)-C(3)	1.415(4)	C(3)-C(5)	1.511(3)
C(6)-C(7)	1.401(4)	C(6)-C(11)	1.410(4)
C(7)-C(8)	1.394(4)	C(7)-C(12)	1.516(4)
C(8)-C(9)	1.378(4)	C(9)-C(10)	1.368(4)
C(10)-C(11)	1.396(4)	C(11)-C(15)	1.518(4)
C(12)-C(13)	1.529(5)	C(12)-C(14)	1.542(5)
C(15)-C(16)	1.513(6)	C(15)-C(17)	1.538(5)
C(18)-C(23)	1.403(4)	C(18)-C(19)	1.408(4)
C(19)-C(20)	1.390(4)	C(19)-C(24)	1.518(4)
C(20)-C(21)	1.379(5)	C(21)-C(22)	1.376(5)
C(22)-C(23)	1.398(4)	C(23)-C(27)	1.516(4)
C(24)-C(25)	1.530(5)	C(24)-C(26)	1.532(5)
C(27)-C(28)	1.525(4)	C(27)-C(29)	1.526(4)
C(30)-C(31)	1.221(4)	C(30)-Ca’	2.497(3)
C(31)-C(32)	1.467(4)	Ca(1B)-N(2B)	2.338(2)
Ca(1B)-N(1B)	2.344(2)	Ca(1B)-O(1B)	2.4696(18)
Ca(1B)-C(30B)”	2.492(3)	Ca(1B)-C(30B)	2.697(3)
Ca(1B)-C(31B)	2.741(3)	O(1B)-C(33B)	1.430(3)
O(1B)-C(32B)	1.433(3)	N(1B)-C(1B)	1.324(3)
N(1B)-C(6B)	1.432(3)	N(2B)-C(3B)	1.322(3)
N(2B)-C(18B)	1.436(3)	C(1B)-C(2B)	1.407(4)
C(1B)-C(4B)	1.520(4)	C(2B)-C(3B)	1.410(4)
C(3B)-C(5B)	1.518(3)	C(6B)-C(11B)	1.406(4)
C(6B)-C(7B)	1.407(4)	C(7B)-C(8B)	1.396(4)
C(7B)-C(12B)	1.519(4)	C(8B)-C(9B)	1.380(4)
C(9B)-C(10B)	1.376(4)	C(10B)-C(11B)	1.389(4)
C(11B)-C(15B)	1.513(4)	C(12B)-C(14B)	1.521(4)
C(12B)-C(13B)	1.527(5)	C(15B)-C(17B)	1.529(5)
C(15B)-C(16B)	1.529(5)	C(18B)-C(23B)	1.396(3)
C(18B)-C(19B)	1.413(3)	C(19B)-C(20B)	1.390(4)
C(19B)-C(24B)	1.521(4)	C(20B)-C(21B)	1.375(4)
C(21B)-C(22B)	1.380(4)	C(22B)-C(23B)	1.395(4)
C(23B)-C(27B)	1.522(4)	C(24B)-C(26B)	1.519(4)
C(24B)-C(25B)	1.528(4)	C(27B)-C(28B)	1.522(4)
C(27B)-C(29B)	1.531(5)	C(30B)-C(31B)	1.209(4)
C(30B)-Ca(1B)”	2.492(3)	C(31B)-C(32B)	1.470(4)
N(2)-Ca-N(1)	83.11(7)	N(2)-Ca-C(30)’	101.41(8)
N(1)-Ca-C(30)’	110.70(9)	N(2)-Ca-O	90.08(7)
N(1)-Ca-O	89.65(7)	C(30).-Ca-O	157.53(8)
N(2)-Ca-C(30)	146.17(9)	N(1)-Ca-C(30)	127.81(8)
C(30).-Ca-C(30)	81.60(10)	O-Ca-C(30)	78.23(8)
N(2)-Ca-C(31)	132.77(8)	N(1)-Ca-C(31)	118.54(8)
C(30).-Ca-C(31)	107.53(9)	O-Ca-C(31)	52.09(8)
C(30)-Ca-C(31)	26.17(9)	C(33)-O-C(32)	113.2(2)
C(33)-O-Ca	139.88(19)	C(32)-O-Ca	106.65(15)
C(1)-N(1)-C(6)	119.4(2)	C(1)-N(1)-Ca	122.78(16)
C(6)-N(1)-Ca	117.75(15)	C(3)-N(2)-C(18)	119.7(2)
C(3)-N(2)-Ca	122.16(16)	C(18)-N(2)-Ca	117.62(15)
N(1)-C(1)-C(2)	125.0(2)	N(1)-C(1)-C(4)	120.2(2)
C(2)-C(1)-C(4)	114.8(2)	C(1)-C(2)-C(3)	131.7(2)
N(2)-C(3)-C(2)	124.7(2)	N(2)-C(3)-C(5)	119.7(2)

C(2)-C(3)-C(5)	115.6(2)	C(7)-C(6)-C(11)	120.2(2)
C(7)-C(6)-N(1)	120.0(2)	C(11)-C(6)-N(1)	119.6(2)
C(8)-C(7)-C(6)	118.7(2)	C(8)-C(7)-C(12)	118.3(2)
C(6)-C(7)-C(12)	123.0(2)	C(9)-C(8)-C(7)	121.5(3)
C(10)-C(9)-C(8)	119.4(3)	C(9)-C(10)-C(11)	121.8(3)
C(10)-C(11)-C(6)	118.4(3)	C(10)-C(11)-C(15)	119.3(2)
C(6)-C(11)-C(15)	122.3(2)	C(7)-C(12)-C(13)	110.5(3)
C(7)-C(12)-C(14)	111.7(3)	C(13)-C(12)-C(14)	110.0(3)
C(16)-C(15)-C(11)	110.8(3)	C(16)-C(15)-C(17)	111.6(4)
C(11)-C(15)-C(17)	112.3(3)	C(23)-C(18)-C(19)	120.1(2)
C(23)-C(18)-N(2)	119.9(2)	C(19)-C(18)-N(2)	119.8(2)
C(20)-C(19)-C(18)	118.8(3)	C(20)-C(19)-C(24)	119.1(3)
C(18)-C(19)-C(24)	122.0(2)	C(21)-C(20)-C(19)	121.5(3)
C(22)-C(21)-C(20)	119.4(3)	C(21)-C(22)-C(23)	121.5(3)
C(22)-C(23)-C(18)	118.7(3)	C(22)-C(23)-C(27)	119.0(3)
C(18)-C(23)-C(27)	122.3(2)	C(19)-C(24)-C(25)	110.4(3)
C(19)-C(24)-C(26)	112.0(3)	C(25)-C(24)-C(26)	109.8(3)
C(23)-C(27)-C(28)	112.0(2)	C(23)-C(27)-C(29)	111.8(3)
C(28)-C(27)-C(29)	109.9(3)	C(31)-C(30)-Ca.	172.0(3)
C(31)-C(30)-Ca	79.34(18)	Ca.-C(30)-Ca	98.40(10)
C(30)-C(31)-C(32)	170.5(3)	C(30)-C(31)-Ca	74.49(18)
C(32)-C(31)-Ca	96.06(17)	O-C(32)-C(31)	105.1(2)
N(2B)-Ca(1B)-N(1B)	80.20(7)	N(2B)-Ca(1B)-O(1B)	93.31(7)
N(1B)-Ca(1B)-O(1B)	90.12(7)	N(2B)-Ca(1B)-C(30B)”	100.40(8)
N(1B)-Ca(1B)-C(30B)”	109.08(8)	O(1B)-Ca(1B)-C(30B)”	157.95(8)
N(2B)-Ca(1B)-C(30B)	136.48(8)	N(1B)-Ca(1B)-C(30B)	141.17(8)
O(1B)-Ca(1B)-C(30B)	77.64(7)	C(30B)”-Ca(1B)-C(30B)	80.54(9)
N(2B)-Ca(1B)-C(31B)	128.37(8)	N(1B)-Ca(1B)-C(31B)	128.30(8)
O(1B)-Ca(1B)-C(31B)	51.97(7)	C(30B)”-Ca(1B)-C(31B)	106.21(8)
C(30B)-Ca(1B)-C(31B)	25.68(8)	C(33B)-O(1B)-C(32B)	113.4(2)
C(33B)-O(1B)-Ca(1B)	138.15(18)	C(32B)-O(1B)-Ca(1B)	108.38(14)
C(1B)-N(1B)-C(6B)	120.6(2)	C(1B)-N(1B)-Ca(1B)	123.79(16)
C(6B)-N(1B)-Ca(1B)	115.39(15)	C(3B)-N(2B)-C(18B)	119.4(2)
C(3B)-N(2B)-Ca(1B)	123.40(16)	C(18B)-N(2B)-Ca(1B)	116.02(15)
N(1B)-C(1B)-C(2B)	124.4(2)	N(1B)-C(1B)-C(4B)	120.4(2)
C(2B)-C(1B)-C(4B)	115.2(2)	C(1B)-C(2B)-C(3B)	130.2(2)
N(2B)-C(3B)-C(2B)	124.5(2)	N(2B)-C(3B)-C(5B)	120.3(2)
C(2B)-C(3B)-C(5B)	115.2(2)	C(11B)-C(6B)-C(7B)	120.3(2)
C(11B)-C(6B)-N(1B)	120.8(2)	C(7B)-C(6B)-N(1B)	118.8(2)
C(8B)-C(7B)-C(6B)	118.6(3)	C(8B)-C(7B)-C(12B)	119.5(2)
C(6B)-C(7B)-C(12B)	121.9(2)	C(9B)-C(8B)-C(7B)	121.3(3)
C(10B)-C(9B)-C(8B)	119.6(3)	C(9B)-C(10B)-C(11B)	121.6(3)
C(10B)-C(11B)-C(6B)	118.8(3)	C(10B)-C(11B)-C(15B)	119.2(3)
C(6B)-C(11B)-C(15B)	122.0(2)	C(7B)-C(12B)-C(14B)	111.4(3)
C(7B)-C(12B)-C(13B)	111.9(3)	C(14B)-C(12B)-C(13B)	110.0(3)
C(11B)-C(15B)-C(17B)	112.5(3)	C(11B)-C(15B)-C(16B)	111.6(3)
C(17B)-C(15B)-C(16B)	109.4(3)	C(23B)-C(18B)-C(19B)	120.4(2)
C(23B)-C(18B)-N(2B)	120.8(2)	C(19B)-C(18B)-N(2B)	118.6(2)
C(20B)-C(19B)-C(18B)	118.0(2)	C(19B)-C(24B)	121.2(2)
C(18B)-C(19B)-C(24B)	120.8(2)	C(21B)-C(20B)-C(19B)	121.9(3)
C(20B)-C(21B)-C(22B)	119.4(3)	C(21B)-C(22B)-C(23B)	121.1(3)
C(22B)-C(23B)-C(18B)	118.9(2)	C(22B)-C(23B)-C(27B)	118.7(2)
C(18B)-C(23B)-C(27B)	122.3(2)	C(26B)-C(24B)-C(19B)	112.4(2)

C(26B)-C(24B)-C(25B)	110.2(2)	C(19B)-C(24B)-C(25B)	113.0(2)
C(23B)-C(27B)-C(28B)	113.5(2)	C(23B)-C(27B)-C(29B)	109.7(2)
C(28B)-C(27B)-C(29B)	110.1(2)	C(31B)-C(30B)-Ca(1B)”	178.2(2)
C(31B)-C(30B)-Ca(1B)	79.16(17)	Ca(1B)”-C(30B)-Ca(1B)	99.46(9)
C(30B)-C(31B)-C(32B)	170.2(3)	C(30B)-C(31B)-Ca(1B)	75.16(17)
C(32B)-C(31B)-Ca(1B)	95.08(16)	O(1B)-C(32B)-C(31B)	104.5(2)

Symmetry transformations used to generate equivalent atoms: ‘ -x+1,-y+1,-z+1 “ -x+1,-y,-z+2

Least-squares planes (x,y,z in crystal coordinates) and deviations from them (* indicates atom used to define plane)

8.2939 (0.0092) x - 8.4484 (0.0098) y + 11.9281 (0.0155) z = 6.7632 (0.0097)

* 0.0000 (0.0000) Ca
* 0.0000 (0.0000) N1
* 0.0000 (0.0000) N2

Rms deviation of fitted atoms = 0.0000

7.7881 (0.0098) x - 12.4890 (0.0123) y + 7.8848 (0.0230) z = 0.9470 (0.0257)

Angle to previous plane (with approximate esd) = 24.38 (0.13)

0.0197 (0.0010) N1
-0.0195 (0.0010) N2
* -0.0236 (0.0013) C1
* 0.0235 (0.0012) C3
0.7218 (0.0038) Ca
0.1202 (0.0037) C2

Rms deviation of fitted atoms = 0.0217

- 4.1438 (0.0112) x + 7.5715 (0.0100) y + 17.4843 (0.0101) z = 16.3398 (0.0097)

Angle to previous plane (with approximate esd) = 83.54 (0.08)

* 0.0000 (0.0000) Ca1B_a
* 0.0000 (0.0000) N1B_a
* 0.0000 (0.0000) N2B_a

Rms deviation of fitted atoms = 0.0000

- 2.3808 (0.0118) x + 1.0115 (0.0243) y + 21.0115 (0.0044) z = 18.9893 (0.0032)

Angle to previous plane (with approximate esd) = 27.91 (0.10)

* 0.0075 (0.0010) N1B_a
* -0.0075 (0.0010) N2B_a
* -0.0088 (0.0012) C1B_a
* 0.0088 (0.0012) C3B_a
    0.8382 (0.0038) Ca1B_a
    0.1079 (0.0036) C2B_a

Rms deviation of fitted atoms = 0.0082

Compound **5**

Table A10. Crystal data and structure refinement for **5**.

Empirical formula	$C_{76}\ H_{96}\ Ca_2\ N_4\ O_2$
Formula weight	1177.73
Temperature	132(2) K
Wavelength	0.71073 Å
Crystal system	Monoclinic
Space group	P21/n
Unit cell dimensions	a = 14.5832(2)Å $\alpha = 90^o$
	b = 13.6656(2)Å $\beta = 106.054(1)^o$
	c = 18.4258(3)Å $\gamma = 90^o$
Volume	3528.84(9) $Å^3$
Z	2
Density (calculated)	1.108 Mg/m^3
Absorption coefficient	0.207 mm^{-1}
F(000)	1272
Crystal size	0.15 x 0.10 x 0.10 mm
Theta range for data collection	3.76 to 27.48^o
Index ranges	-18<=h<=18; -17<=k<=17; -23<=l<=23
Reflections collected	57055
Independent reflections	8054 [R(int) = 0.0780]
Reflections observed (>2σ)	6021
Data Completeness	0.997
Absorption correction	Semi-empirical from equivalents
Max. and min. transmission	0.98 and 0.83
Refinement method	Full-matrix least-squares on F^2
Data / restraints / parameters	8054 / 0 / 382
Goodness-of-fit on F^2	1.024
Final R indices [I>2σ(I)]	R1 = 0.0453 wR2 = 0.1105
R indices (all data)	R1 = 0.0682 wR2 = 0.1241
Largest diff. peak and hole	0.461 and -0.330 $eÅ^{-3}$

Notes: Asymmetric unit consists of ½ of a dimer molecule, proximate to a crystallographic inversion centre.

Table A11. Atomic coordinates (x 10^4) and equivalent isotropic displacement parameters ($Å^2$ x 10^3) for **5**.U(eq) is defined as one third of the trace of the orthogonalized Uij tensor.

Atom	x	y	z	U(eq)
Ca(1)	3967(1)	64(1)	525(1)	26(1)
O(1)	4571(1)	813(1)	1959(1)	36(1)
N(1)	2948(1)	-1113(1)	799(1)	24(1)
N(2)	2504(1)	882(1)	113(1)	26(1)
C(1)	1758(1)	762(1)	382(1)	27(1)
C(2)	1642(1)	-35(1)	828(1)	27(1)
C(3)	2152(1)	-923(1)	990(1)	26(1)
C(4)	961(1)	1515(1)	227(1)	39(1)
C(5)	1740(1)	-1668(1)	1421(1)	36(1)
C(6)	3335(1)	-2084(1)	868(1)	26(1)
C(7)	3981(1)	-2402(1)	1541(1)	32(1)
C(8)	4389(1)	-3330(1)	1559(1)	44(1)
C(9)	4177(2)	-3921(1)	935(1)	51(1)
C(10)	3555(1)	-3600(1)	268(1)	46(1)
C(11)	3129(1)	-2678(1)	216(1)	33(1)
C(12)	4268(1)	-1761(1)	2236(1)	39(1)
C(13)	4032(2)	-2231(2)	2916(1)	55(1)
C(14)	5328(1)	-1510(2)	2422(1)	49(1)
C(15)	2464(1)	-2317(2)	-518(1)	39(1)
C(16)	2680(2)	-2744(2)	-1222(1)	54(1)
C(17)	1419(1)	-2493(2)	-555(1)	56(1)
C(18)	2508(1)	1641(1)	-420(1)	34(1)
C(19)	2944(2)	2547(2)	-165(1)	52(1)
C(20)	2994(2)	3245(2)	-712(2)	80(1)
C(21)	2637(2)	3053(2)	-1471(2)	84(1)
C(22)	2231(2)	2168(2)	-1706(1)	65(1)
C(23)	2154(1)	1442(2)	-1198(1)	42(1)
C(24)	3350(2)	2782(2)	667(2)	68(1)
C(25)	4405(2)	3061(2)	855(2)	91(1)
C(26)	2792(2)	3593(2)	926(2)	85(1)
C(27)	1713(2)	474(2)	-1479(1)	56(1)
C(28)	666(2)	456(3)	-1589(2)	100(1)
C(29)	1918(2)	128(3)	-2202(2)	96(1)
C(30)	5792(1)	545(2)	680(1)	40(1)
C(31)	5711(1)	781(1)	1295(1)	39(1)
C(32)	5566(1)	1022(2)	2030(1)	41(1)
C(33)	4291(1)	841(1)	2620(1)	36(1)
C(34)	4915(2)	992(2)	3331(1)	46(1)
C(35)	4562(2)	937(2)	3957(1)	55(1)
C(36)	3613(2)	750(2)	3879(1)	55(1)
C(37)	2996(2)	638(1)	3165(1)	49(1)
C(38)	3329(1)	685(1)	2532(1)	39(1)

Table A12. Bond lengths [Å] and angles [°] for **5**.

Ca(1)-N(1)	2.3372(13)	Ca(1)-N(2)	2.3411(13)
Ca(1)-C(30)#1	2.4851(19)	Ca(1)-C(30)	2.6790(17)
Ca(1)-C(31)	2.7287(17)	Ca(1)-O(1)	2.7413(12)
Ca(1)-C(18)	3.1869(16)	Ca(1)-C(6)	3.1920(16)
Ca(1)-Ca(1)#1	4.0098(6)	O(1)-C(33)	1.388(2)
O(1)-C(32)	1.449(2)	N(1)-C(3)	1.3283(19)
N(1)-C(6)	1.434(2)	N(2)-C(1)	1.324(2)
N(2)-C(18)	1.430(2)	C(1)-C(2)	1.404(2)
C(1)-C(4)	1.520(2)	C(2)-C(3)	1.411(2)
C(2)-H(2)	0.9300	C(3)-C(5)	1.513(2)
C(4)-H(4A)	0.9600	C(4)-H(4B)	0.9600
C(4)-H(4C)	0.9600	C(5)-H(5A)	0.9600
C(5)-H(5B)	0.9600	C(5)-H(5C)	0.9600
C(6)-C(7)	1.403(2)	C(6)-C(11)	1.412(2)
C(7)-C(8)	1.397(2)	C(7)-C(12)	1.512(3)
C(8)-C(9)	1.368(3)	C(8)-H(8)	0.9300
C(9)-C(10)	1.383(3)	C(9)-H(9)	0.9300
C(10)-C(11)	1.397(3)	C(10)-H(10)	0.9300
C(11)-C(15)	1.513(3)	C(12)-C(14)	1.528(3)
C(12)-C(13)	1.529(3)	C(12)-H(12)	0.9800
C(13)-H(13A)	0.9600	C(13)-H(13B)	0.9600
C(13)-H(13C)	0.9600	C(14)-H(14A)	0.9600
C(14)-H(14B)	0.9600	C(14)-H(14C)	0.9600
C(15)-C(17)	1.525(3)	C(15)-C(16)	1.532(3)
C(15)-H(15)	0.9800	C(16)-H(16A)	0.9600
C(16)-H(16B)	0.9600	C(16)-H(16C)	0.9600
C(17)-H(17A)	0.9600	C(17)-H(17B)	0.9600
C(17)-H(17C)	0.9600	C(18)-C(23)	1.408(3)
C(18)-C(19)	1.412(3)	C(19)-C(20)	1.404(3)
C(19)-C(24)	1.516(4)	C(20)-C(21)	1.376(5)
C(20)-H(20)	0.9300	C(21)-C(22)	1.363(4)
C(21)-H(21)	0.9300	C(22)-C(23)	1.389(3)
C(22)-H(22)	0.9300	C(23)-C(27)	1.499(3)
C(24)-C(25)	1.528(4)	C(24)-C(26)	1.528(4)
C(24)-H(24)	0.9800	C(25)-H(25A)	0.9600
C(25)-H(25B)	0.9600	C(25)-H(25C)	0.9600
C(26)-H(26A)	0.9600	C(26)-H(26B)	0.9600
C(26)-H(26C)	0.9600	C(27)-C(28)	1.484(4)
C(27)-C(29)	1.520(3)	C(27)-H(27)	0.9800
C(28)-H(28A)	0.9600	C(28)-H(28B)	0.9600
C(28)-H(28C)	0.9600	C(29)-H(29A)	0.9600
C(29)-H(29B)	0.9600	C(29)-H(29C)	0.9600
C(30)-C(31)	1.216(3)	C(30)-Ca(1)#1	2.4851(19)
C(31)-C(32)	1.465(3)	C(32)-H(32A)	0.9700
C(32)-H(32B)	0.9700	C(33)-C(38)	1.385(3)
C(33)-C(34)	1.389(3)	C(34)-C(35)	1.388(3)
C(34)-H(34)	0.9300	C(35)-C(36)	1.375(3)
C(35)-H(35)	0.9300	C(36)-C(37)	1.382(3)
C(36)-H(36)	0.9300	C(37)-C(38)	1.383(3)
C(37)-H(37)	0.9300	C(38)-H(38)	0.9300

N(1)-Ca(1)-N(2)	79.73(4)	N(1)-Ca(1)-C(30)#1	102.56(5)
N(2)-Ca(1)-C(30)#1	102.21(6)	N(1)-Ca(1)-C(30)	144.90(5)
N(2)-Ca(1)-C(30)	134.96(6)	C(30)#1-Ca(1)-C(30)	78.19(6)
N(1)-Ca(1)-C(31)	133.76(5)	N(2)-Ca(1)-C(31)	129.21(5)
C(30)#1-Ca(1)-C(31)	104.05(5)	C(30)-Ca(1)-C(31)	25.96(5)
N(1)-Ca(1)-O(1)	95.93(4)	N(2)-Ca(1)-O(1)	98.96(4)
C(30)#1-Ca(1)-O(1)	153.98(5)	C(30)-Ca(1)-O(1)	76.16(5)
C(31)-Ca(1)-O(1)	50.21(4)	N(1)-Ca(1)-C(18)	102.41(4)
N(2)-Ca(1)-C(18)	24.36(4)	C(30)#1-Ca(1)-C(18)	88.67(6)
C(30)-Ca(1)-C(18)	112.68(5)	C(31)-Ca(1)-C(18)	115.28(5)
O(1)-Ca(1)-C(18)	105.20(4)	N(1)-Ca(1)-C(6)	24.34(4)
N(2)-Ca(1)-C(6)	102.48(4)	C(30)#1-Ca(1)-C(6)	89.34(5)
C(30)-Ca(1)-C(6)	122.51(5)	C(31)-Ca(1)-C(6)	120.39(5)
O(1)-Ca(1)-C(6)	100.73(4)	C(18)-Ca(1)-C(6)	122.98(4)
N(1)-Ca(1)-Ca(1)#1	132.95(3)	N(2)-Ca(1)-Ca(1)#1	127.10(3)
C(30)#1-Ca(1)-Ca(1)#1	40.84(4)	C(30)-Ca(1)-Ca(1)#1	37.35(4)
C(31)-Ca(1)-Ca(1)#1	63.24(4)	O(1)-Ca(1)-Ca(1)#1	113.40(3)
C(18)-Ca(1)-Ca(1)#1	104.08(3)	C(6)-Ca(1)-Ca(1)#1	110.61(3)
C(33)-O(1)-C(32)	116.41(13)	C(33)-O(1)-Ca(1)	139.63(10)
C(32)-O(1)-Ca(1)	102.01(9)	C(3)-N(1)-C(6)	120.53(13)
C(3)-N(1)-Ca(1)	125.25(10)	C(6)-N(1)-Ca(1)	113.47(9)
C(1)-N(2)-C(18)	120.41(13)	C(1)-N(2)-Ca(1)	126.06(10)
C(18)-N(2)-Ca(1)	113.16(9)	N(2)-C(1)-C(2)	124.06(14)
N(2)-C(1)-C(4)	120.74(14)	C(2)-C(1)-C(4)	115.19(14)
C(1)-C(2)-C(3)	130.47(14)	C(1)-C(2)-H(2)	114.8
C(3)-C(2)-H(2)	114.8	N(1)-C(3)-C(2)	124.06(14)
N(1)-C(3)-C(5)	120.70(14)	C(2)-C(3)-C(5)	115.24(13)
C(1)-C(4)-H(4A)	109.5	C(1)-C(4)-H(4B)	109.5
H(4A)-C(4)-H(4B)	109.5	C(1)-C(4)-H(4C)	109.5
H(4A)-C(4)-H(4C)	109.5	H(4B)-C(4)-H(4C)	109.5
C(3)-C(5)-H(5A)	109.5	C(3)-C(5)-H(5B)	109.5
H(5A)-C(5)-H(5B)	109.5	C(3)-C(5)-H(5C)	109.5
H(5A)-C(5)-H(5C)	109.5	H(5B)-C(5)-H(5C)	109.5
C(7)-C(6)-C(11)	120.42(15)	C(7)-C(6)-N(1)	121.14(14)
C(11)-C(6)-N(1)	118.09(14)	C(7)-C(6)-Ca(1)	107.43(10)
C(11)-C(6)-Ca(1)	111.46(10)	N(1)-C(6)-Ca(1)	42.20(7)
C(8)-C(7)-C(6)	118.68(17)	C(8)-C(7)-C(12)	119.32(16)
C(6)-C(7)-C(12)	121.98(15)	C(9)-C(8)-C(7)	121.37(18)
C(9)-C(8)-H(8)	119.3	C(7)-C(8)-H(8)	119.3
C(8)-C(9)-C(10)	119.99(17)	C(8)-C(9)-H(9)	120.0
C(10)-C(9)-H(9)	120.0	C(9)-C(10)-C(11)	121.14(18)
C(9)-C(10)-H(10)	119.4	C(11)-C(10)-H(10)	119.4
C(10)-C(11)-C(6)	118.36(17)	C(10)-C(11)-C(15)	121.27(16)
C(6)-C(11)-C(15)	120.37(15)	C(7)-C(12)-C(14)	110.21(16)
C(7)-C(12)-C(13)	112.27(17)	C(14)-C(12)-C(13)	110.73(15)
C(7)-C(12)-H(12)	107.8	C(14)-C(12)-H(12)	107.8
C(13)-C(12)-H(12)	107.8	C(12)-C(13)-H(13A)	109.5
C(12)-C(13)-H(13B)	109.5	H(13A)-C(13)-H(13B)	109.5
C(12)-C(13)-H(13C)	109.5	H(13A)-C(13)-H(13C)	109.5
H(13B)-C(13)-H(13C)	109.5	C(12)-C(14)-H(14A)	109.5
C(12)-C(14)-H(14B)	109.5	H(14A)-C(14)-H(14B)	109.5
C(12)-C(14)-H(14C)	109.5	H(14A)-C(14)-H(14C)	109.5
H(14B)-C(14)-H(14C)	109.5	C(11)-C(15)-C(17)	111.95(16)

C(11)-C(15)-C(16)	113.65(17)	C(17)-C(15)-C(16)	109.77(15)
C(11)-C(15)-H(15)	107.0	C(17)-C(15)-H(15)	107.0
C(16)-C(15)-H(15)	107.0	C(15)-C(16)-H(16A)	109.5
C(15)-C(16)-H(16B)	109.5	H(16A)-C(16)-H(16B)	109.5
C(15)-C(16)-H(16C)	109.5	H(16A)-C(16)-H(16C)	109.5
H(16B)-C(16)-H(16C)	109.5	C(15)-C(17)-H(17A)	109.5
C(15)-C(17)-H(17B)	109.5	H(17A)-C(17)-H(17B)	109.5
C(15)-C(17)-H(17C)	109.5	H(17A)-C(17)-H(17C)	109.5
H(17B)-C(17)-H(17C)	109.5	C(23)-C(18)-C(19)	120.84(17)
C(23)-C(18)-N(2)	119.26(16)	C(19)-C(18)-N(2)	119.64(17)
C(23)-C(18)-Ca(1)	115.26(11)	C(19)-C(18)-Ca(1)	103.85(12)
N(2)-C(18)-Ca(1)	42.49(7)	C(20)-C(19)-C(18)	117.7(2)
C(20)-C(19)-C(24)	119.9(2)	C(18)-C(19)-C(24)	122.41(18)
C(21)-C(20)-C(19)	121.3(3)	C(21)-C(20)-H(20)	119.3
C(19)-C(20)-H(20)	119.3	C(22)-C(21)-C(20)	120.0(2)
C(22)-C(21)-H(21)	120.0	C(20)-C(21)-H(21)	120.0
C(21)-C(22)-C(23)	121.9(2)	C(21)-C(22)-H(22)	119.0
C(23)-C(22)-H(22)	119.0	C(22)-C(23)-C(18)	118.2(2)
C(22)-C(23)-C(27)	120.2(2)	C(18)-C(23)-C(27)	121.56(16)
C(19)-C(24)-C(25)	111.6(2)	C(19)-C(24)-C(26)	112.1(2)
C(25)-C(24)-C(26)	109.7(2)	C(19)-C(24)-H(24)	107.7
C(25)-C(24)-H(24)	107.7	C(26)-C(24)-H(24)	107.7
C(24)-C(25)-H(25A)	109.5	C(24)-C(25)-H(25B)	109.5
H(25A)-C(25)-H(25B)	109.5	C(24)-C(25)-H(25C)	109.5
H(25A)-C(25)-H(25C)	109.5	H(25B)-C(25)-H(25C)	109.5
C(24)-C(26)-H(26A)	109.5	C(24)-C(26)-H(26B)	109.5
H(26A)-C(26)-H(26B)	109.5	C(24)-C(26)-H(26C)	109.5
H(26A)-C(26)-H(26C)	109.5	H(26B)-C(26)-H(26C)	109.5
C(28)-C(27)-C(23)	112.9(2)	C(28)-C(27)-C(29)	108.7(2)
C(23)-C(27)-C(29)	114.1(2)	C(28)-C(27)-H(27)	106.9
C(23)-C(27)-H(27)	106.9	C(29)-C(27)-H(27)	106.9
C(27)-C(28)-H(28A)	109.5	C(27)-C(28)-H(28B)	109.5
H(28A)-C(28)-H(28B)	109.5	C(27)-C(28)-H(28C)	109.5
H(28A)-C(28)-H(28C)	109.5	H(28B)-C(28)-H(28C)	109.5
C(27)-C(29)-H(29A)	109.5	C(27)-C(29)-H(29B)	109.5
H(29A)-C(29)-H(29B)	109.5	C(27)-C(29)-H(29C)	109.5
H(29A)-C(29)-H(29C)	109.5	H(29B)-C(29)-H(29C)	109.5
C(31)-C(30)-Ca(1)#1	175.01(18)	C(31)-C(30)-Ca(1)	79.30(11)
Ca(1)#1-C(30)-Ca(1)	101.81(6)	C(30)-C(31)-C(32)	176.53(19)
C(30)-C(31)-Ca(1)	74.74(11)	C(32)-C(31)-Ca(1)	102.09(10)
O(1)-C(32)-C(31)	105.58(14)	O(1)-C(32)-H(32A)	110.6
C(31)-C(32)-H(32A)	110.6	O(1)-C(32)-H(32B)	110.6
C(31)-C(32)-H(32B)	110.6	H(32A)-C(32)-H(32B)	108.8
C(38)-C(33)-O(1)	115.31(16)	C(38)-C(33)-C(34)	120.79(17)
O(1)-C(33)-C(34)	123.89(16)	C(35)-C(34)-C(33)	118.61(19)
C(35)-C(34)-H(34)	120.7	C(33)-C(34)-H(34)	120.7
C(36)-C(35)-C(34)	121.2(2)	C(36)-C(35)-H(35)	119.4
C(34)-C(35)-H(35)	119.4	C(35)-C(36)-C(37)	119.42(19)
C(35)-C(36)-H(36)	120.3	C(37)-C(36)-H(36)	120.3
C(36)-C(37)-C(38)	120.7(2)	C(36)-C(37)-H(37)	119.7
C(38)-C(37)-H(37)	119.7	C(37)-C(38)-C(33)	119.27(19)
C(37)-C(38)-H(38)	120.4	C(33)-C(38)-H(38)	120.4

Symmetry transformations used to generate equivalent atoms:

#1 -x+1,-y,-z

Table A13. Anisotropic displacement parameters ($Å^2$ x 10^3) for **5**. The anisotropic displacement factor exponent takes the form: -2 gpi^2 [h^2 a^{*2} U11 + ... + 2 h k a* b* U

Atom	U11	U22	U33	U23	U13	U12
Ca(1)	21(1)	29(1)	31(1)	2(1)	10(1)	1(1)
O(1)	30(1)	49(1)	32(1)	-7(1)	12(1)	-6(1)
N(1)	23(1)	26(1)	24(1)	1(1)	6(1)	1(1)
N(2)	26(1)	25(1)	29(1)	3(1)	11(1)	4(1)
C(1)	26(1)	28(1)	27(1)	-1(1)	8(1)	3(1)
C(2)	23(1)	32(1)	28(1)	1(1)	12(1)	2(1)
C(3)	24(1)	30(1)	24(1)	0(1)	7(1)	-2(1)
C(4)	34(1)	38(1)	48(1)	10(1)	19(1)	13(1)
C(5)	32(1)	36(1)	43(1)	9(1)	17(1)	2(1)
C(6)	24(1)	25(1)	31(1)	1(1)	10(1)	-1(1)
C(7)	29(1)	30(1)	38(1)	6(1)	9(1)	3(1)
C(8)	39(1)	36(1)	55(1)	11(1)	10(1)	10(1)
C(9)	49(1)	27(1)	78(2)	0(1)	21(1)	9(1)
C(10)	47(1)	34(1)	59(1)	-14(1)	19(1)	-3(1)
C(11)	30(1)	32(1)	39(1)	-6(1)	13(1)	-4(1)
C(12)	41(1)	41(1)	30(1)	6(1)	2(1)	8(1)
C(13)	50(1)	76(2)	38(1)	12(1)	9(1)	7(1)
C(14)	44(1)	53(1)	42(1)	4(1)	-2(1)	0(1)
C(15)	39(1)	44(1)	31(1)	-10(1)	8(1)	-6(1)
C(16)	50(1)	74(2)	42(1)	-22(1)	18(1)	-17(1)
C(17)	38(1)	89(2)	39(1)	-12(1)	7(1)	-1(1)
C(18)	28(1)	35(1)	43(1)	14(1)	17(1)	10(1)
C(19)	44(1)	36(1)	74(2)	20(1)	14(1)	2(1)
C(20)	59(2)	57(2)	120(3)	49(2)	16(2)	-5(1)
C(21)	62(2)	95(2)	101(2)	73(2)	32(2)	16(2)
C(22)	57(1)	91(2)	57(1)	44(1)	30(1)	30(1)
C(23)	38(1)	56(1)	39(1)	18(1)	19(1)	21(1)
C(24)	77(2)	29(1)	86(2)	3(1)	3(1)	-12(1)
C(25)	64(2)	51(2)	137(3)	-34(2)	-6(2)	2(1)
C(26)	87(2)	63(2)	116(2)	-8(2)	46(2)	-16(2)
C(27)	75(2)	63(1)	29(1)	3(1)	10(1)	16(1)
C(28)	85(2)	123(3)	116(3)	-65(2)	67(2)	-37(2)
C(29)	56(2)	160(3)	66(2)	-46(2)	9(1)	29(2)
C(30)	26(1)	53(1)	42(1)	-7(1)	14(1)	-8(1)
C(31)	27(1)	50(1)	40(1)	-8(1)	11(1)	-11(1)
C(32)	31(1)	56(1)	38(1)	-12(1)	12(1)	-12(1)
C(33)	41(1)	34(1)	36(1)	-5(1)	19(1)	-1(1)
C(34)	48(1)	52(1)	39(1)	-7(1)	15(1)	-3(1)
C(35)	74(2)	56(1)	37(1)	-9(1)	22(1)	0(1)
C(36)	83(2)	44(1)	54(1)	-7(1)	45(1)	-3(1)
C(37)	55(1)	37(1)	65(1)	-8(1)	37(1)	-4(1)

C(38)	41(1)	33(1)	49(1)	-8(1)	21(1)	0(1)

Table A14. Hydrogen coordinates (x 10^4) and isotropic displacement parameters ($Å^2$ x 10^3) for **5**.

Atom	x	y	z	U(eq)
H(2)	1148	32	1054	32
H(4A)	935	1854	-235	58
H(4B)	1081	1976	636	58
H(4C)	363	1192	182	58
H(5A)	2009	-2300	1379	54
H(5B)	1060	-1695	1213	54
H(5C)	1891	-1482	1943	54
H(8)	4814	-3550	2004	53
H(9)	4451	-4539	961	61
H(10)	3418	-4006	-154	55
H(12)	3907	-1149	2121	46
H(13A)	4223	-1800	3342	83
H(13B)	4366	-2841	3033	83
H(13C)	3357	-2346	2798	83
H(14A)	5502	-1103	2863	73
H(14B)	5452	-1166	2004	73
H(14C)	5697	-2101	2514	73
H(15)	2552	-1607	-534	46
H(16A)	2239	-2481	-1666	81
H(16B)	2617	-3443	-1220	81
H(16C)	3319	-2575	-1221	81
H(17A)	1021	-2251	-1026	84
H(17B)	1268	-2158	-145	84
H(17C)	1312	-3182	-518	84
H(20)	3275	3849	-558	96
H(21)	2671	3528	-1824	101
H(22)	1999	2047	-2220	78
H(24)	3300	2190	954	81
H(25A)	4639	3202	1384	136
H(25B)	4476	3629	569	136
H(25C)	4760	2527	729	136
H(26A)	3067	3714	1455	128
H(26B)	2139	3395	840	128
H(26C)	2820	4180	646	128
H(27)	1992	-10	-1088	68
H(28A)	527	679	-1137	150
H(28B)	434	-200	-1699	150
H(28C)	360	878	-2001	150
H(29A)	2595	126	-2136	143
H(29B)	1617	561	-2609	143
H(29C)	1672	-522	-2319	143
H(32A)	5976	626	2426	49
H(32B)	5705	1707	2149	49

H(34)	5556	1127	3388	55
H(35)	4974	1029	4437	65
H(36)	3389	698	4304	66
H(37)	2351	530	3110	58
H(38)	2910	612	2052	47

Table A15. Dihedral angles [^{o}] for **5**.

Atom1 - Atom2 - Atom3 - Atom4	Dihedral
N(1) - Ca(1) - O(1) - C(33)	-19.42(17)
N(2) - Ca(1) - O(1) - C(33)	61.08(17)
C(30)#1 - Ca(1) - O(1) - C(33)	-154.71(17)
C(30) - Ca(1) - O(1) - C(33)	-164.66(17)
C(31) - Ca(1) - O(1) - C(33)	-164.36(19)
C(18) - Ca(1) - O(1) - C(33)	85.18(17)
C(6) - Ca(1) - O(1) - C(33)	-43.54(17)
Ca(1)#1 - Ca(1) - O(1) - C(33)	-161.72(15)
N(1) - Ca(1) - O(1) - C(32)	142.83(11)
N(2) - Ca(1) - O(1) - C(32)	-136.67(11)
C(30)#1 - Ca(1) - O(1) - C(32)	7.53(18)
C(30) - Ca(1) - O(1) - C(32)	-2.41(11)
C(31) - Ca(1) - O(1) - C(32)	-2.12(11)
C(18) - Ca(1) - O(1) - C(32)	-112.57(11)
C(6) - Ca(1) - O(1) - C(32)	118.70(11)
Ca(1)#1 - Ca(1) - O(1) - C(32)	0.52(11)
N(2) - Ca(1) - N(1) - C(3)	-31.04(12)
C(30)#1 - Ca(1) - N(1) - C(3)	-131.41(12)
C(30) - Ca(1) - N(1) - C(3)	141.33(12)
C(31) - Ca(1) - N(1) - C(3)	104.69(13)
O(1) - Ca(1) - N(1) - C(3)	67.02(12)
C(18) - Ca(1) - N(1) - C(3)	-40.00(13)
C(6) - Ca(1) - N(1) - C(3)	170.01(19)
Ca(1)#1 - Ca(1) - N(1) - C(3)	-163.03(10)
N(2) - Ca(1) - N(1) - C(6)	158.95(11)
C(30)#1 - Ca(1) - N(1) - C(6)	58.58(11)
C(30) - Ca(1) - N(1) - C(6)	-28.67(15)
C(31) - Ca(1) - N(1) - C(6)	-65.32(12)
O(1) - Ca(1) - N(1) - C(6)	-102.98(10)
C(18) - Ca(1) - N(1) - C(6)	149.99(10)
Ca(1)#1 - Ca(1) - N(1) - C(6)	26.97(12)
N(1) - Ca(1) - N(2) - C(1)	28.71(13)
C(30)#1 - Ca(1) - N(2) - C(1)	129.48(13)
C(30) - Ca(1) - N(2) - C(1)	-145.10(12)
C(31) - Ca(1) - N(2) - C(1)	-110.70(13)
O(1) - Ca(1) - N(2) - C(1)	-65.74(13)
C(18) - Ca(1) - N(2) - C(1)	-172.9(2)
C(6) - Ca(1) - N(2) - C(1)	37.43(14)
Ca(1)#1 - Ca(1) - N(2) - C(1)	165.70(11)
N(1) - Ca(1) - N(2) - C(18)	-158.36(12)
C(30)#1 - Ca(1) - N(2) - C(18)	-57.59(12)

C(30) - Ca(1) - N(2) - C(18)	27.83(14)
C(31) - Ca(1) - N(2) - C(18)	62.22(13)
O(1) - Ca(1) - N(2) - C(18)	107.18(11)
C(6) - Ca(1) - N(2) - C(18)	-149.64(11)
Ca(1)#1 - Ca(1) - N(2) - C(18)	-21.37(13)
C(18) - N(2) - C(1) - C(2)	171.45(16)
Ca(1) - N(2) - C(1) - C(2)	-16.1(2)
C(18) - N(2) - C(1) - C(4)	-9.4(2)
Ca(1) - N(2) - C(1) - C(4)	163.04(12)
N(2) - C(1) - C(2) - C(3)	-11.2(3)
C(4) - C(1) - C(2) - C(3)	169.61(17)
C(6) - N(1) - C(3) - C(2)	-169.37(14)
Ca(1) - N(1) - C(3) - C(2)	21.3(2)
C(6) - N(1) - C(3) - C(5)	11.7(2)
Ca(1) - N(1) - C(3) - C(5)	-157.67(12)
C(1) - C(2) - C(3) - N(1)	8.3(3)
C(1) - C(2) - C(3) - C(5)	-172.71(17)
C(3) - N(1) - C(6) - C(7)	-88.90(18)
Ca(1) - N(1) - C(6) - C(7)	81.63(15)
C(3) - N(1) - C(6) - C(11)	97.83(17)
Ca(1) - N(1) - C(6) - C(11)	-91.64(14)
C(3) - N(1) - C(6) - Ca(1)	-170.53(18)
N(1) - Ca(1) - C(6) - C(7)	-117.44(16)
N(2) - Ca(1) - C(6) - C(7)	-138.66(11)
C(30)#1 - Ca(1) - C(6) - C(7)	118.98(11)
C(30) - Ca(1) - C(6) - C(7)	43.46(12)
C(31) - Ca(1) - C(6) - C(7)	13.03(12)
O(1) - Ca(1) - C(6) - C(7)	-36.87(11)
C(18) - Ca(1) - C(6) - C(7)	-153.04(10)
Ca(1)#1 - Ca(1) - C(6) - C(7)	83.33(11)
N(1) - Ca(1) - C(6) - C(11)	108.65(15)
N(2) - Ca(1) - C(6) - C(11)	87.43(11)
C(30)#1 - Ca(1) - C(6) - C(11)	-14.94(11)
C(30) - Ca(1) - C(6) - C(11)	-90.45(12)
C(31) - Ca(1) - C(6) - C(11)	-120.88(11)
O(1) - Ca(1) - C(6) - C(11)	-170.79(11)
C(18) - Ca(1) - C(6) - C(11)	73.04(12)
Ca(1)#1 - Ca(1) - C(6) - C(11)	-50.58(11)
N(2) - Ca(1) - C(6) - N(1)	-21.22(11)
C(30)#1 - Ca(1) - C(6) - N(1)	-123.59(11)
C(30) - Ca(1) - C(6) - N(1)	160.90(10)
C(31) - Ca(1) - C(6) - N(1)	130.47(10)
O(1) - Ca(1) - C(6) - N(1)	80.57(10)
C(18) - Ca(1) - C(6) - N(1)	-35.61(11)
Ca(1)#1 - Ca(1) - C(6) - N(1)	-159.23(9)
C(11) - C(6) - C(7) - C(8)	-2.2(2)
N(1) - C(6) - C(7) - C(8)	-175.35(15)
Ca(1) - C(6) - C(7) - C(8)	-131.20(14)
C(11) - C(6) - C(7) - C(12)	176.06(15)
N(1) - C(6) - C(7) - C(12)	2.9(2)
Ca(1) - C(6) - C(7) - C(12)	47.09(18)
C(6) - C(7) - C(8) - C(9)	0.6(3)
C(12) - C(7) - C(8) - C(9)	-177.69(18)

C(7) - C(8) - C(9) - C(10)	0.7(3)
C(8) - C(9) - C(10) - C(11)	-0.4(3)
C(9) - C(10) - C(11) - C(6)	-1.1(3)
C(9) - C(10) - C(11) - C(15)	178.74(18)
C(7) - C(6) - C(11) - C(10)	2.5(2)
N(1) - C(6) - C(11) - C(10)	175.78(15)
Ca(1) - C(6) - C(11) - C(10)	129.61(14)
C(7) - C(6) - C(11) - C(15)	-177.40(15)
N(1) - C(6) - C(11) - C(15)	-4.1(2)
Ca(1) - C(6) - C(11) - C(15)	-50.25(17)
C(8) - C(7) - C(12) - C(14)	63.3(2)
C(6) - C(7) - C(12) - C(14)	-115.02(18)
C(8) - C(7) - C(12) - C(13)	-60.7(2)
C(6) - C(7) - C(12) - C(13)	121.03(18)
C(10) - C(11) - C(15) - C(17)	96.2(2)
C(6) - C(11) - C(15) - C(17)	-83.9(2)
C(10) - C(11) - C(15) - C(16)	-28.8(2)
C(6) - C(11) - C(15) - C(16)	151.04(16)
C(1) - N(2) - C(18) - C(23)	-90.17(19)
Ca(1) - N(2) - C(18) - C(23)	96.46(15)
C(1) - N(2) - C(18) - C(19)	95.7(2)
Ca(1) - N(2) - C(18) - C(19)	-77.68(17)
C(1) - N(2) - C(18) - Ca(1)	173.37(19)
N(1) - Ca(1) - C(18) - C(23)	-84.75(13)
N(2) - Ca(1) - C(18) - C(23)	-106.56(18)
C(30)#1 - Ca(1) - C(18) - C(23)	17.81(13)
C(30) - Ca(1) - C(18) - C(23)	94.42(13)
C(31) - Ca(1) - C(18) - C(23)	122.74(13)
O(1) - Ca(1) - C(18) - C(23)	175.50(12)
C(6) - Ca(1) - C(18) - C(23)	-70.53(13)
Ca(1)#1 - Ca(1) - C(18) - C(23)	56.00(13)
N(1) - Ca(1) - C(18) - C(19)	140.81(13)
N(2) - Ca(1) - C(18) - C(19)	119.00(18)
C(30)#1 - Ca(1) - C(18) - C(19)	-116.62(13)
C(30) - Ca(1) - C(18) - C(19)	-40.02(14)
C(31) - Ca(1) - C(18) - C(19)	-11.69(14)
O(1) - Ca(1) - C(18) - C(19)	41.07(13)
C(6) - Ca(1) - C(18) - C(19)	155.04(12)
Ca(1)#1 - Ca(1) - C(18) - C(19)	-78.43(13)
N(1) - Ca(1) - C(18) - N(2)	21.81(12)
C(30)#1 - Ca(1) - C(18) - N(2)	124.37(12)
C(30) - Ca(1) - C(18) - N(2)	-159.02(11)
C(31) - Ca(1) - C(18) - N(2)	-130.70(11)
O(1) - Ca(1) - C(18) - N(2)	-77.94(12)
C(6) - Ca(1) - C(18) - N(2)	36.03(13)
Ca(1)#1 - Ca(1) - C(18) - N(2)	162.56(11)
C(23) - C(18) - C(19) - C(20)	1.3(3)
N(2) - C(18) - C(19) - C(20)	175.32(18)
Ca(1) - C(18) - C(19) - C(20)	132.51(18)
C(23) - C(18) - C(19) - C(24)	-178.83(19)
N(2) - C(18) - C(19) - C(24)	-4.8(3)
Ca(1) - C(18) - C(19) - C(24)	-47.6(2)
C(18) - C(19) - C(20) - C(21)	-0.4(4)

C(24) - C(19) - C(20) - C(21)	179.7(2)
C(19) - C(20) - C(21) - C(22)	-0.6(4)
C(20) - C(21) - C(22) - C(23)	0.8(4)
C(21) - C(22) - C(23) - C(18)	0.1(3)
C(21) - C(22) - C(23) - C(27)	-179.3(2)
C(19) - C(18) - C(23) - C(22)	-1.2(3)
N(2) - C(18) - C(23) - C(22)	-175.22(16)
Ca(1) - C(18) - C(23) - C(22)	-127.31(15)
C(19) - C(18) - C(23) - C(27)	178.26(18)
N(2) - C(18) - C(23) - C(27)	4.2(2)
Ca(1) - C(18) - C(23) - C(27)	52.1(2)
C(20) - C(19) - C(24) - C(25)	-56.9(3)
C(18) - C(19) - C(24) - C(25)	123.2(2)
C(20) - C(19) - C(24) - C(26)	66.6(3)
C(18) - C(19) - C(24) - C(26)	-113.3(2)
C(22) - C(23) - C(27) - C(28)	-89.7(3)
C(18) - C(23) - C(27) - C(28)	90.9(3)
C(22) - C(23) - C(27) - C(29)	35.0(3)
C(18) - C(23) - C(27) - C(29)	-144.4(2)
N(1) - Ca(1) - C(30) - C(31)	-79.95(16)
N(2) - Ca(1) - C(30) - C(31)	89.41(15)
C(30)#1 - Ca(1) - C(30) - C(31)	-175.04(18)
O(1) - Ca(1) - C(30) - C(31)	0.52(13)
C(18) - Ca(1) - C(30) - C(31)	101.46(14)
C(6) - Ca(1) - C(30) - C(31)	-93.51(14)
Ca(1)#1 - Ca(1) - C(30) - C(31)	-175.04(18)
N(1) - Ca(1) - C(30) - Ca(1)#1	95.09(10)
N(2) - Ca(1) - C(30) - Ca(1)#1	-95.54(8)
C(30)#1 - Ca(1) - C(30) - Ca(1)#1	0.0
C(31) - Ca(1) - C(30) - Ca(1)#1	175.04(18)
O(1) - Ca(1) - C(30) - Ca(1)#1	175.56(8)
C(18) - Ca(1) - C(30) - Ca(1)#1	-83.50(7)
C(6) - Ca(1) - C(30) - Ca(1)#1	81.53(8)
Ca(1)#1 - C(30) - C(31) - C(32)	-79(4)
Ca(1) - C(30) - C(31) - C(32)	24(4)
Ca(1)#1 - C(30) - C(31) - Ca(1)	-103.4(17)
N(1) - Ca(1) - C(31) - C(30)	128.37(13)
N(2) - Ca(1) - C(31) - C(30)	-114.05(13)
C(30)#1 - Ca(1) - C(31) - C(30)	5.00(18)
O(1) - Ca(1) - C(31) - C(30)	-179.34(16)
C(18) - Ca(1) - C(31) - C(30)	-90.25(14)
C(6) - Ca(1) - C(31) - C(30)	102.64(14)
Ca(1)#1 - Ca(1) - C(31) - C(30)	3.37(12)
N(1) - Ca(1) - C(31) - C(32)	-50.19(15)
N(2) - Ca(1) - C(31) - C(32)	67.38(15)
C(30)#1 - Ca(1) - C(31) - C(32)	-173.56(13)
C(30) - Ca(1) - C(31) - C(32)	-178.6(2)
O(1) - Ca(1) - C(31) - C(32)	2.09(11)
C(18) - Ca(1) - C(31) - C(32)	91.18(13)
C(6) - Ca(1) - C(31) - C(32)	-75.92(14)
Ca(1)#1 - Ca(1) - C(31) - C(32)	-175.20(14)
C(33) - O(1) - C(32) - C(31)	170.40(15)
Ca(1) - O(1) - C(32) - C(31)	3.15(17)

C(30) - C(31) - C(32) - O(1)	-27(4)
Ca(1) - C(31) - C(32) - O(1)	-3.16(17)
C(32) - O(1) - C(33) - C(38)	177.05(16)
Ca(1) - O(1) - C(33) - C(38)	-22.4(3)
C(32) - O(1) - C(33) - C(34)	-4.3(3)
Ca(1) - O(1) - C(33) - C(34)	156.25(14)
C(38) - C(33) - C(34) - C(35)	3.0(3)
O(1) - C(33) - C(34) - C(35)	-175.60(18)
C(33) - C(34) - C(35) - C(36)	-0.8(3)
C(34) - C(35) - C(36) - C(37)	-1.6(3)
C(35) - C(36) - C(37) - C(38)	1.9(3)
C(36) - C(37) - C(38) - C(33)	0.3(3)
O(1) - C(33) - C(38) - C(37)	175.95(16)
C(34) - C(33) - C(38) - C(37)	-2.7(3)

Symmetry transformations used to generate equivalent atoms:

#1 -x+1,-y,-z

Compound **19**

Table A16. Crystal data and structure refinement **19**.

Empirical formula	$C_{91}\ H_{116}\ Ca_2\ N_4$
Formula weight	1402.08
Temperature	150(2) K
Wavelength	0.71073 Å
Crystal system	Triclinic
Space group	$P\ \bar{1}$
Unit cell dimensions	a = 14.3620(3)Å α = 89.6820(10)^o
	b = 15.1344(3)Å β = 84.4800(10)^o
	c = 21.2566(5)Å γ = 63.8190(10)^o
Volume	4123.57(15) Å^3
Z	2
Density (calculated)	1.129 Mg/m^3
Absorption coefficient	0.187 mm^{-1}
F(000)	1516
Crystal size	0.40 x 0.20 x 0.20 mm
Theta range for data collection	3.59 to 27.39^o
Index ranges	-18<=h<=18; -19<=k<=19; -27<=l<=27
Reflections collected	6299
Independent reflections	18335 [R(int) = 0.1097]
Completeness to theta = 27.39	97.8 %
Max. and min. transmission	0.9636 and 0.9290
Refinement method	Full-matrix least-squares on F^2
Data / restraints / parameters	18335 / 0 / 911
Goodness-of-fit on F^2	1.023
Final R indices [I>2σ(I)]	R1 = 0.0538 wR2 = 0.1141
R indices (all data)	R1 = 0.0976 wR2 = 0.1341
Largest diff. peak and hole	0.492 and -0.397 eÅ^{-3}

Table A17. Atomic coordinates (x 10^4) and equivalent isotropic displacement parameters (A^2 x 10^3) **19**. U(eq) is defined as one third of the trace of the orthogonalized Uij tensor.

Atom	x	y	z	U(eq)
Ca(1)	2222(1)	1772(1)	7085(1)	24(1)
Ca(2)	410(1)	944(1)	7337(1)	26(1)
N(1)	3104(1)	2351(1)	6303(1)	31(1)
N(2)	2928(1)	2885(1)	7332(1)	30(1)
N(3)	533(1)	-561(1)	7729(1)	30(1)
N(4)	-1030(1)	546(1)	7425(1)	30(1)
N(5)	1366(1)	1327(1)	8098(1)	25(1)
N(6)	3061(1)	340(1)	7695(1)	25(1)
N(7)	1429(1)	921(1)	6351(1)	25(1)
N(8)	392(1)	2470(1)	6754(1)	26(1)
C(1)	3211(2)	2937(1)	6725(1)	27(1)
C(2)	3644(2)	3620(1)	6527(1)	28(1)
C(3)	4037(2)	4156(1)	6392(1)	29(1)
C(4)	4510(2)	4807(2)	6248(1)	33(1)
C(5)	5340(2)	4540(2)	5787(1)	58(1)
C(6)	5783(2)	5198(3)	5661(2)	75(1)
C(7)	4590(2)	6077(2)	5996(2)	65(1)
C(8)	4590(2)	6335(2)	6442(2)	70(1)
C(9)	4140(2)	5706(2)	6574(1)	56(1)
C(10)	3255(2)	2477(2)	5629(1)	32(1)
C(11)	3685(2)	1480(2)	5276(1)	46(1)
C(12)	3739(2)	1567(2)	4555(1)	55(1)
C(13)	2685(2)	2237(3)	4358(1)	67(1)
C(14)	2252(2)	3255(2)	4682(1)	62(1)
C(15)	2220(2)	3185(1)	5397(1)	40(1)
C(16)	3044(2)	3508(1)	7808(1)	31(1)
C(17)	2053(2)	4465(2)	7942(1)	45(1)
C(18)	2150(2)	5097(2)	8467(1)	56(1)
C(19)	2402(2)	4537(2)	9068(1)	53(1)
C(20)	3397(2)	3586(2)	8946(1)	45(1)
C(21)	3331(2)	2952(2)	8412(1)	34(1)
C(22)	-482(2)	-290(1)	7701(1)	28(1)
C(23)	-945(2)	-905(1)	7986(1)	29(1)
C(24)	-1184(2)	-1471(2)	8268(1)	30(1)
C(25)	-1387(2)	-2190(2)	8627(1)	31(1)
C(26)	-821(2)	-3179(2)	8452(1)	49(1)
C(27)	-968(2)	-3885(2)	8805(1)	63(1)
C(28)	-1661(2)	-3615(2)	933(1)	58(1)
C(29)	-2219(2)	-2635(2)	9517(1)	58(1)
C(30)	-2097(2)	-1920(2)	9161(1)	45(1)
C(31)	1173(2)	-1441(1)	8055(1)	29(1)
C(32)	2299(2)	-1822(2)	7770(1)	37(1)
C(33)	3028(2)	-2730(2)	8095(1)	49(1)
C(34)	2933(2)	-2544(2)	8802(1)	56(1)

C(35)	1813(2)	-2162(2)	9090(1)	51(1)
C(36)	1091(2)	-1245(2)	8764(1)	38(1)
C(37)	-2095(2)	790(1)	7298(1)	28(1)
C(38)	-2105(2)	255(2)	6693(1)	34(1)
C(39)	-3203(2)	577(2)	6501(1)	42(1)
C(40)	-3771(2)	1685(2)	6449(1)	41(1)
C(41)	-3793(2)	2211(2)	7060(1)	43(1)
C(42)	-2693(2)	1898(2)	7242(1)	39(1)
C(43)	2345(2)	668(1)	8187(1)	24(1)
C(44)	2611(2)	317(1)	8816(1)	28(1)
C(45)	2871(2)	-37(1)	9313(1)	30(1)
C(46)	3207(2)	-477(1)	9899(1)	30(1)
C(47)	4227(2)	-751(2)	10029(1)	37(1)
C(48)	4550(2)	-1160(2)	10601(1)	45(1)
C(49)	3868(2)	-1307(2)	11039(1)	46(1)
C(50)	2856(2)	-1049(2)	10913(1)	45(1)
C(51)	2522(2)	-633(2)	10345(1)	38(1)
C(52)	628(2)	1805(1)	8666(1)	29(1)
C(53)	-483(2)	2098(2)	8517(1)	35(1)
C(54)	-1296(2)	2652(2)	9068(1)	52(1)
C(55)	-1184(2)	3544(2)	9296(1)	57(1)
C(56)	-86(2)	3249(2)	9470(1)	51(1)
C(57)	728(2)	2703(2)	8914(1)	39(1)
C(58)	4108(2)	-424(1)	7784(1)	26(1)
C(59)	4587(2)	-1103(1)	7195(1)	32(1)
C(60)	5659(2)	-1921(1)	7296(1)	35(1)
C(61)	6393(2)	-1503(2)	7471(1)	43(1)
C(62)	5912(2)	-781(2)	8041(1)	45(1)
C(63)	4826(2)	23(2)	7945(1)	36(1)
C(64)	739(2)	1845(1)	6252(1)	26(1)
C(65)	378(2)	2154(1)	5634(1)	27(1)
C(66)	46(2)	2447(1)	5139(1)	28(1)
C(67)	-347(2)	2785(1)	4544(1)	28(1)
C(68)	-18(2)	2149(2)	4020(1)	46(1)
C(69)	-415(2)	2452(2)	3451(1)	56(1)
C(70)	-1133(2)	3394(2)	3394(1)	54(1)
C(71)	-1478(2)	4039(2)	3907(1)	67(1)
C(72)	-1087(2)	3743(2)	4484(1)	52(1)
C(73)	1820(2)	186(1)	5820(1)	26(1)
C(74)	2872(2)	-627(1)	5942(1)	31(1)
C(75)	3311(2)	-1427(2)	5410(1)	41(1)
C(76)	2544(2)	-1841(2)	5303(1)	45(1)
C(77)	1492(2)	-1022(2)	5181(1)	41(1)
C(78)	1059(2)	-247(2)	5725(1)	33(1)
C(79)	-303(2)	3516(1)	6669(1)	30(1)
C(80)	-1444(2)	3758(2)	6830(1)	42(1)
C(81)	-2144(2)	4855(2)	6750(1)	56(1)
C(82)	-1827(2)	5496(2)	7139(2)	67(1)
C(83)	-691(2)	5250(2)	6978(1)	57(1)
C(84)	3(2)	4156(2)	7064(1)	40(1)
C(85)	5797(4)	6694(3)	9029(2)	125(2)
C(86)	5844(2)	5736(2)	8850(2)	77(1)
C(87)	5882(3)	5063(4)	9311(2)	101(1)

C(88)	5878(3)	4186(3)	9134(3)	115(2)
C(89)	5843(3)	3985(3)	8509(3)	105(2)
C(90)	5811(3)	4624(2)	8053(2)	84(1)
C(91)	5820(2)	5504(2)	8232(2)	72(1)

Table A18. Bond lengths [Å] and angles [^{o}] for **19**.

Ca(1)-N(1)	2.3860(16)	Ca(1)-N(2)	2.3989(16)
Ca(1)-N(6)	2.4067(15)	Ca(1)-N(8)	2.5343(16)
Ca(1)-N(5)	2.6082(16)	Ca(1)-N(7)	2.6555(16)
Ca(1)-C(1)	2.7746(19)	Ca(1)-C(43)	2.8429(18)
Ca(1)-C(64)	2.8646(19)	Ca(1)-Ca(2)	3.3519(5)
Ca(2)-N(3)	2.3590(16)	Ca(2)-N(4)	2.3874(17)
Ca(2)-N(7)	2.4293(16)	Ca(2)-N(5)	2.4462(16)
Ca(2)-N(8)	2.6058(16)	Ca(2)-C(22)	2.7622(19)
Ca(2)-C(64)	2.7786(19)	N(1)-C(1)	1.330(2)
N(1)-C(10)	1.454(3)	N(2)-C(1)	1.327(3)
N(2)-C(16)	1.458(2)	N(3)-C(22)	1.336(2)
N(3)-C(31)	1.461(2)	N(4)-C(22)	1.329(2)
N(4)-C(37)	1.457(2)	N(5)-C(43)	1.350(2)
N(5)-C(52)	1.480(2)	N(6)-C(43)	1.321(2)
N(6)-C(58)	1.467(2)	N(7)-C(64)	1.340(2)
N(7)-C(73)	1.472(2)	N(8)-C(64)	1.331(2)
N(8)-C(79)	1.474(2)	C(1)-C(2)	1.465(3)
C(2)-C(3)	1.195(3)	C(3)-C(4)	1.440(3)
C(4)-C(5)	1.379(3)	C(4)-C(9)	1.383(3)
C(5)-C(6)	1.410(4)	C(5)-H(5)	0.9500
C(6)-C(7)	1.367(4)	C(6)-H(6)	0.9500
C(7)-C(8)	1.337(4)	C(7)-H(7)	0.9500
C(8)-C(9)	1.382(4)	C(8)-H(8)	0.9500
C(9)-H(9)	0.9500	C(10)-C(11)	1.524(3)
C(10)-C(15)	1.526(3)	C(10)-H(10)	1.0000
C(11)-C(12)	1.534(3)	C(11)-H(11A)	0.9900
C(11)-H(11B)	0.9900	C(12)-C(13)	1.504(4)
C(12)-H(12A)	0.9900	C(12)-H(12B)	0.9900
C(13)-C(14)	1.523(4)	C(13)-H(13A)	0.9900
C(13)-H(13B)	0.9900	C(14)-C(15)	1.522(3)
C(14)-H(14A)	0.9900	C(14)-H(14B)	0.9900
C(15)-H(15A)	0.9900	C(15)-H(15B)	0.9900
C(16)-C(17)	1.520(3)	C(16)-C(21)	1.521(3)
C(16)-H(16)	1.0000	C(17)-C(18)	1.529(3)
C(17)-H(17A)	0.9900	C(17)-H(17B)	0.9900
C(18)-C(19)	1.512(4)	C(18)-H(18A)	0.9900
C(18)-H(18B)	0.9900	C(19)-C(20)	1.517(3)
C(19)-H(19A)	0.9900	C(19)-H(19B)	0.9900
C(20)-C(20)	1.526(3)	C(20)-H(20A)	0.9900
C(20)-H(20B)	0.9900	C(21)-H(21A)	0.9900
C(21)-H(21B)	0.9900	C(22)-C(23)	1.463(3)
C(23)-C(24)	1.193(3)	C(24)-C(25)	1.442(3)
C(25)-C(30)	1.381(3)	C(25)-C(26)	1.384(3)
C(26)-C(27)	1.381(3)	C(26)-H(26)	0.9500

C(27)-C(28)	1.369(4)	C(27)-H(27)	0.9500
C(28)-C(29)	1.372(4)	C(28)-H(28)	0.9500
C(29)-C(30)	1.382(3)	C(29)-H(29)	0.9500
C(30)-H(30)	0.9500	C(31)-C(32)	1.519(3)
C(31)-C(36)	1.521(3)	C(31)-H(31)	1.0000
C(32)-C(33)	1.523(3)	C(32)-H(32A)	0.9900
C(32)-H(32B)	0.9900	C(33)-C(34)	1.514(4)
C(33)-H(33A)	0.9900	C(33)-H(33B)	0.9900
C(34)-C(35)	1.513(4)	C(34)-H(34A)	0.9900
C(34)-H(34)	0.9900	C(35)-C(36)	1.529(3)
C(35)-H(35A)	0.9900	C(35)-H(35B)	0.9900
C(36)-H(36A)	0.9900	C(36)-H(36B)	0.9900
C(37)-C(42)	1.520(3)	C(37)-C(38)	1.528(3)
C(37)-H(37)	1.0000	C(38)-C(39)	1.528(3)
C(38)-H(38A)	0.9900	C(38)-H(38B)	0.9900
C(39)-C(40)	1.515(3)	C(39)-H(39A)	0.9900
C(39)-H(39B)	0.9900	C(40)-C(41)	1.519(3)
C(40)-H(40A)	0.9900	C(40)-H(40B)	0.9900
C(41)-C(42)	1.525(3)	C(41)-H(41A)	0.9900
C(41)-H(41B)	0.9900	C(42)-H(42A)	0.9900
C(42)-H(42B)	0.9900	C(43)-C(44)	1.458(3)
C(44)-C(45)	1.198(3)	C(45)-C(46)	1.433(3)
C(46)-C(47)	1.392(3)	C(46)-C(51)	1.393(3)
C(47)-C(48)	1.385(3)	C(47)-H(47)	0.9500
C(48)-C(49)	1.375(3)	C(48)-H(48)	0.9500
C(49)-C(50)	1.381(3)	C(49)-H(49)	0.9500
C(50)-C(51)	1.387(3)	C(50)-H(50)	0.9500
C(51)-H(51)	0.9500	C(52)-C(53)	1.522(3)
C(52)-C(57)	1.529(3)	C(52)-H(52)	1.0000
C(53)-C(54)	1.525(3)	C(53)-H(53A)	0.9900
C(53)-H(53B)	0.9900	C(54)-C(55)	1.516(3)
C(54)-H(54A)	0.9900	C(54)-H(54B)	0.9900
C(55)-C(56)	1.520(3)	C(55)-H(55A)	0.9900
C(55)-H(55B)	0.9900	C(456)-C(57)	1.528(3)
C(56)-H(56A)	0.9900	C(56)-H(56)	0.9900
C(57)-H(57A)	0.9900	C(57)-H(57B)	0.9900
C(58)-C(59)	1.523(3)	C(58)-C(63)	1.525(3)
C(58)-H(58)	1.0000	C(59)-C(620)	1.526(3)
C(59)-H(59A)	0.9900	C(59)-H(59B)	0.9900
C(60)-C(61)	1.522(3)	C(60)-H(60A)	0.9900
C(60)-H(60A)	0.9900	C(61)-C(62)	1.525(3)
C(61)-H(61A)	0.9900	C(61)-H(61B)	0.9900
C(62)-C(63)	1.530(3)	C(62)-H(62A)	0.9900
C(62)-H(62B)	0.9900	C(63)-H(63A)	0.9900
C(63)-H(63B)	0.9900	C(64)-C(65)	1.456(3)
C(65)-C(66)	1.200(3)	C(66)-C(67)	1.433(3)
C(67)-C(68)	1.377(3)	C(67)-C(72)	1.382(3)
C(68)-C(69)	1.376(3)	C(68)-H(68)	0.9500
C(69)-C(70)	1.355(3)	C(69)-H(69)	0.9500
C(70)-C(71)	1.365(4)	C(70)-H(70)	0.9500
C(71)-C(72)	1.388(3)	C(71)-H(71)	0.9500
C(72)-H(72)	0.9500	C(73)-C(74)	1.516(3)
C(73)-C(78)	1.528(3)	C(73)-H(73)	1.0000

C(74)-C(75)	1.531(3)	C(74)-H(74A)	0.9900
C(74)-H(74B)	0.9900	C(75)-C(76)	1.522(3)
C(75)-H(75A)	0.9900	C(75)-H(75B)	0.9900
C(76)-C(77)	1.519(3)	C(76)-H(76A)	0.9900
C(76)-H(76B)	0.9900	C(77)-C(78)	1.528(3)
C(77)-H(77A)	0.9900	C(77)-H(77B)	0.9900
C(78)-H(78A)	0.9900	C(76)-H(78B)	0.9900
C(79)-C(84)	1.514(3)	C(79)-C(80)	1.516(3)
C(79)-H(79)	1.0000	C(80)-C(81)	1533(3)
C(80)-H(80A)	0.9900	C(80)-H(80B)	0.9900
C(81)-C(82)	1.516(4)	C(81)-H(81A)	0.9900
C(81)-H(81B)	0.9900	C(82)-C(83)	1.509(4)
C(82)-H(82A)	0.9900	C(82)-H(82B)	0.9900
C(83)-C(84)	1.531(3)	C(83)-H(83A)	0.9900
C(83)-H(83B)	0.9900	C(84)-H(84A)	0.9900
C(84)-H(84B)	0.9900	C(85)-C(86)	1.472(5)
C(85)-H(85A)	0.9800	C(85)-H(85B)	0.9800
C(85)-H(85C)	0.9800	C(86)-C(91)	1.368(5)
C(86)-C(87)	1.397(5)	C(87)-C()	1.384(6)
C(87)-H(87)	0.9500	C(88)-C(89)	1.377(6)
C(88)-H(88)	0.9500	C(89)-C(90)	1.354(5)
C(89)-H(89)	0.9500	C(90)-C(91)	1.394(4)
C(90)-H(90)	0.9500	C(91)-H(91)	0.9500
N(1)-Ca(1)-N(2)	57.09(6)	N(1)-Ca(1)-N(6)	124.86(6)
N(2)-Ca(1)-N(6)	106.44(6)	N(1)-Ca(1)-N(8)	102.76(6)
N(2)-Ca(1)-N(8)	118.91(5)	N(6)-Ca(1)-N(8)	127.19(5)
N(1)-Ca(1)-N(5)	168.63(6)	N(2)-Ca(1)-N(5)	111.58(5)
N(6)-Ca(1)-N(5)	54.46(5)	N(8)-Ca(1)-N(5)	83.34(5)
N(1)-Ca(1)-N(7)	100.34(5)	N(2)-Ca(1)-N(7)	155.34(5)
N(6)-Ca(1)-N(7)	94.60(5)	N(8)-Ca(1)-N(7)	51.76(5)
N(5)-Ca(1)-N(7)	90.98(5)	N(1)-Ca(1)-C(1)	28.63(6)
N(2)-Ca(1)-C(1)	28.56(6)	N(6)-Ca(1)-C(1)	120.76(6)
N(8)-Ca(1)-C(1)	111.95(5)	N(5)-Ca(1)-C(1)	140.10(6)
N(7)-Ca(1)-C(1)	127.87(5)	N(1)-Ca(1)-C(43)	147.41(6)
N(2)-Ca(1)-C(43)	105.05(5)	N(6)-Ca(1)-C(43)	27.59(5)
N(8)-Ca(1)-C(43)	109.83(5)	N(5)-Ca(1)-C(43)	28.25(5)
N(7)-Ca(1)-C(43)	99.56(5)	C(1)-Ca(1)-C(43)	129.92(6)
N(1)-Ca(1)-C(64)	92.53(6)	N(2)-Ca(1)-C(64)	133.48(6)
N(6)-Ca(1)-C(64)	120.06(5)	N(8)-Ca(1)-C(64)	27.69(5)
N(5)-Ca(1)-C(64)	97.06(5)	N(7)-Ca(1)-C(64)	27.77(5)
C(1)-Ca(1)-C(64)	113.46(6)	C(43-Ca(1)-C(64)	116.42(5)
N(1)-Ca(1)-Ca(2)	144.27(4)	N(2)-Ca(1)-Ca(2)	151.12(4)
N(6)-Ca(1)-Ca(2)	76.98(4)	N(8)-Ca(1)-Ca(2)	50.23(4)
N(5)-Ca(1)-Ca(2)	46.42(4)	N(7)-Ca(1)-Ca(2)	45.91(3)
C(1)-Ca(1)-Ca(2)	162.11(4)	C(43)-Ca(1)-Ca(2)	64.48(4)
C(64)-Ca(1)-Ca(2)	52.39(4)	N(3)-Ca(2)-N(4)	57.51(5)
N(3)-Ca(2)-N(7)	118.95(6)	N(4)-Ca(2)-N(7)	124.80(6)
N(3)-Ca(2)-N(5)	99.41(6)	N(4)-Ca(2)-N(5)	134.34(6)
N(7)-Ca(2)-N(5)	100.69(5)	N(3)-Ca(2)-N(8)	172.00(6)
N(4)-Ca(2)-N(8)	123.33(5)	N(7)-Ca(2)-N(8)	53.40(5)
N(5)-Ca(2)-N(8)	85.13(5)	N(3)-Ca(2)-C(22)	28.89(5)
N(4)-Ca(2)-C(22)	28.76(5)	N(7)-Ca(2)-C(22)	129.07(6)

N(5)-Ca(2)-C(22)	117.89(6)	N(8)-Ca(2)-C(22)	151.90(6)
N(3)-Ca(2)-C(64)	143.63(6)	N(4)-Ca(2)-C(64)	118.12(6)
N(7)-Ca(2)-C(64)	28.84(5)	N(5)-Ca(2)-C(64)	103.35(5)
N(8)-Ca(2)-C(64)	28.40(5)	C(22)-Ca(2)-C(64)	138.48(6)
N(3)-Ca(2)-Ca(1)	130.57(4)	N(4)-Ca(2)-Ca(1)	171.70(4)
N(7)-Ca(2)-Ca(1)	51.74(4)	N(5)-Ca(2)-Ca(1)	50.57(4)
N(8)-Ca(2)-Ca(1)	48.38(4)	C(22)-Ca(2)-Ca(1)	159.43(4)
C(64)-Ca(2)-Ca(1)	54.75(4)	C(1)-N(1)-C(10)	120.86(16)
C(1)-N(1)-C(1)	92.13(12)	C(10)-N(1)-Ca(1)	143.82(13)
C(1)-N(2)-C(16)	120.25(16)	C(1)-N(2)-Ca(1)	91.64(11)
C(16)-N(2)-Ca(1)	147.64(13)	C(22)-N(3)-C(31)	120.99(16)
C(22)-N(3)-Ca(2)	92.55(11)	C(31)-N(3)-Ca(2)	144.87(13)
C(22)-N(4)-C(37)	119.41(16)	C(22)-N(4)-Ca(2)	91.47(12)
C(37)-N(4)-Ca(2)	149.07(12)	C(43)-N(5)-C(52)	117.74(15)
C(43)-N(5)-Ca(2)	120.00(12)	C(52)-N(5)-Ca(2)	107.55(11)
C(43)-N(5)-Ca(1)	85.59(11)	C(52)-N(5)-Ca(1)	140.50(12)
Ca(2)-N(5)-Ca(1)	83.02(5)	C(43)-N(6)-C(58)	119.07(15)
C(43)-N(6)-Ca(1)	94.90(11)	C(58)-N(6)-Ca(1)	140.10(12)
C(64)-N(7)-C(73)	118.90(15)	C(64)-N(7)-Ca(2)	90.20(11)
C(73)-N(7)-Ca(2)	128.74(11)	C(64)-N(7)-Ca(1)	84.82(11)
C(73)-N(7)-Ca(1)	136.88(11)	Ca(2)-N(7)-Ca(1)	82.35(5)
C(64)-N(8)-C(79)	119.06(16)	C(64)-N(8)-Ca(1)	90.09(11)
C(79)-N(8)-Ca(1)	126.59(12)	C(64)-N(8)-Ca(2)	83.03(10)
C(79)-N(8)-Ca(2)	140.81(12)	Ca(1)-N(8)-Ca(2)	81.39(4)
N(2)-C(1)-N(1)	118.72(17)	N(2)-C(1)-C(2)	120.39(17)
N(1)-C(1)-C(2)	120.88(18)	N(2)-C(1)-Ca(1)	59.79(10)
N(1)-C(1)-Ca(1)	59.24(10)	C(2)-C(1)-Ca(1)	175.04(13)
C(3)-C(2)-C(1)	176.20(2)	C(2)-C(3)-C(4)	178.40(2)
C(5)-C(4)-C(9)	119.20(2)	C(5)-C(4)-C(3)	120.40(2)
C(9)-C(4)-C(3)	120.30(2)	C(4)-C(5)-C(6)	118.70(3)
C(4)-C(5)-H(5)	120.70	C(6)-C(5)-H(5)	120.70
C(7)-C(6)-C(5)	120.20(3)	C(7)-C(6)-H(6)	119.90
C(5)-C(6)-H(6)	119.90	C(8)-C(7)-C(6)	120.90(3)
C(8)-C(7)-H(7)	119.50	C(6)-C(7)-H(7)	119.50
C(7)-C(8)-C(9)	120.10(3)	C(7)-C(8)-H(8)	120.00
C(9)-C(8)-H(8)	120.00	C(8)-C(9)-C(4)	120.90(3)
C(8)-C(9)-H(9)	119.60	C(4)-C(9)-H(9)	119.60
N(1)-C(10)-C(11)	109.44(17)	N(1)-C(10)-C(15)	109.77(17)
C(11)-C(10)-H(10)	110.29(18)	N(1)-C(10)-H(10)	109.10
C(11)-C(10)-H(10)	109.10	C(15)-C(10)-H(10)	109.10
C(10)-C(11)-C(12)	112.60(2)	C(10)-C(11)-H(11A)	109.10
C(12)-C(11)-H(11A)	109.10	C(10)-C(11)-H(11B)	109.10
C(12)-C(11)-H(11B)	109.10	H(11A)-C(11)-H(11B)	107.80
C(13)-C(12)-C(11)	110.70(2)	C(13)-C(12)-H(12A)	109.50
C(11)-C(12)-H(12A)	109.50	C(13)-C(12)-H(12B)	109.50
C(11)-C(12)-H(12B)	109.50	H(12A)-C(12)-H(12B)	108.10
C(12)-C(13)-C(14)	111.30(2)	C(12)-C(13)-H(13A)	109.40
C(14)-C(13)-H(13A)	109.40	C(12)-C(13)-H(13B)	109.40
C(14)-C(13)-H(13B)	109.40	H(13A)-C(13)-H(13B)	108.00
C(15)-C(14)-C(13)	111.00(2)	C(15)-C(14)-H(14A)	109.40
C(13)-C(14)-H(14A)	109.40	C(15)-C(14)-H(14B)	109.40
C(13)-C(14)-H(14A)	109.40	H(14A)-C(14)-H(14B)	108.00
C(14)-C(15)-C(10)	114.20(2)	C(14)-C(15)-H(15A)	108.70

C(10)-C(15)-H(15A)	108.70	C(14)-C(15)-H(15B)	108.70
C(10)-C(15)-H(15B)	108.70	H(15A)-C(15)-H(15B)	107.60
N(2)-C(16)-C(17)	111.38(17)	N(2)-C(16)-C(21)	109.69(15)
C(17)-C(16)-C(21)	110.28(18)	N(2)-C(16)-H(16)	108.50
C(17)-C(16)-H(16)	108.50	C(21)-C(16)-H(16)	108.50
C(16)-C(17)-C(18)	111.59(19)	C(16)-C(17)-H(17A)	109.30
C(18)-C(17)-H(17A)	109.30	C(16)-C(17)-H(17B)	109.30
C(18)-C(17)-H(17B)	109.30	H(17A)-C(17)-H(17B)	108.00
C(19)-C(18)-C(17)	110.90(2)	C(19)-C(18)-H(18A)	109.50
C(17)-C(18)-H(18A)	109.50	C(19)-C(18)-H(18B)	109.50
C(17)-C(18)-H(18B)	109.50	H(18A)-C(18)-H(18B)	108.00
C(18)-C(19)-C(20)	110.40(2)	C(18)-C(19)-H(19A)	109.60
C(20)-C(19)-H(19A)	109.60	C(18)-C(19)-H(19B)	109.60
C(20)-C(19)-H(19B)	109.60	H(19A)-C(19)-H(19A)	108.10
C(19)-C(20)-C(21)	111.57(19)	C(19)-C(20)-H(20A)	109.30
C(21)-C(20)-H(20A)	109.30	C(19)-C(20)-H(20B)	109.30
C(21)-C(20)-H(20B)	109.30	H(20A)-C(20)-H(20B)	108.00
C(16)-C(21)-C(20)	112.49(17)	C(16)-C(21)-H(21A)	109.10
C(20)-C(21)-H(21A)	109.10	C(16)-C(21)-H(20B)	109.10
C(20)-C(21)-H(21B)	109.10	H(21A)-C(21)-H(21B)	107.80
N(4)-C(22)-N(3)	117.91(17)	N(4)-C(22)-C(23)	122.95(18)
N(3)-C(22)-C(23)	119.21(17)	N(4)-C(22)-Ca(2)	59.77(10)
N(3)-C(22)-Ca(2)	58.56(10)	C(23)-C(22)-Ca(2)	171.79(14)
C(24)-C(23)-C(22)	169.60(2)	C(23)-C(24)-C(25)	175.20(2)
C(30)-C(25)-C(26)	119.00(2)	C(30)-C(25)-C(24)	121.58(19)
C(26)-C(25)-C(24)	119.30(2)	C(27)-C(26)-C(25)	120.40(2)
C(27)-C(26)-H(26)	119.80	C(25)-C(26)-H(26)	119.80
C(28)-C(27)-C(26)	120.40(2)	C(28)-C(27)-H(27)	119.80
C(26)-C(27)-H(27)	119.80	C(27)-C(28)-C(29)	119.50(2)
C(27)-C(28)-H(28)	120.30	C(29)-C(28)-H(28)	120.30
C(28)-C(29)-C(30)	120.70(2)	C(28)-C(29)-H(29)	119.60
C(30)-C(29)-H(29)	119.60	C(25)-C(30)-C(29)	120.00(2)
C(25)-C(30)-H(30)	120.00	C(29)-C(30)-H(30)	120.00
N(3)-C(31)-C(32)	108.54(16)	N(3)-C(31)-C(36)	112.44(16)
C(32)-C(31)-C(36)	110.25(17)	N(3)-C(31)-H(31)	108.50
C(32)-C(31)-H(31)	108.50	C(36)-C(31)-H(31)	108.50
C(31)-C(32)-C(33)	112.50(18)	C(31)-C(32)-H(32A)	109.20
C(33)-C(32)-H(32A)	109.20	C(31)-C(32)-H(32B)	109.20
C(33)-C(32)-H(32B)	109.20	H(32A)-C(32)-H(32B)	107.90
C(34)-C(33)-C(32)	111.80(2)	C(34)-C(33)-H(33A)	109.30
C(32)-C(33)-H(33A)	109.30	C(34)-C(33)-H(33B)	109.30
C(32)-C(33)-H(33B)	109.30	H(33A)-C(33)-H(33B)	107.90
C(35)-C(34)-C(33)	111.20(2)	C(35)-C(34)-H(34A)	109.40
C(33)-C(34)-H(34A)	109.40	C(35)-C(34)-H(34B)	109.40
C(33)-C(34)-H(34B)	109.40	H(34A)-C(34)-H(34B)	108.00
C(34)-C(35)-C(36)	111.50(2)	C(34)-C(35)-H(35A)	109.30
C(36)-C(35)-H(35A)	109.30	C(34)-C(35)-H(35B)	109.30
C(36)-C(35)-H(35B)	109.30	H(35A)-C(35)-H(35B)	108.00
C(31)-C(36)-C(35)	111.40(18)	C(31)-C(36)-H(36A)	109.30
C(35)-C(36)-H(36A)	109.30	C(31)-C(36)-H(36B)	109.30
C(35)-C(36)-H(36B)	109.30	H(36A)-C(36)-H(36B)	108.00
N(4)-C(37)-C(42)	109.26(16)	N(4)-C(37)-C(38)	111.10(16)
C(42)-C(37)-C(38)	110.12(17)	N(4)-C(37)-H(37)	108.80

C(42)-C(37)-H(37)	108.80	C(38)-C(37)-H(37)	108.80
C(39)-C(38)-C(37)	112.92(17)	C(39)-C(38)-H(38A)	109.00
C(37)-C(38)-H(38A)	109.00	C(39)-C(38)-H(38B)	109.00
C(37)-C(38)-H(38B)	109.00	H(38A)-C(38)-H(38B)	107.80
C(40)-C(39)-C(38)	111.62(18)	C(40)-C(39)-H(39A)	109.30
C(38)-C(39)-H(39A)	109.30	C(40)-C(39)-H(39B)	109.30
C(38)-C(39)-H(39B)	109.30	H(39A)-C(39)-H(39B)	108.00
C(39)-C(40)-C(41)	110.75(19)	C(39)-C(40)-H(40A)	109.50
C(41)-C(40)-H(40A)	109.50	C(39)-C(40)-H(40B)	109.50
C(41)-C(40)-H(40A)	109.50	H(40A)-C(40)-H(40B)	108.10
C(40)-C(41)-C(42)	111.06(18)	C(40)-C(41)-H(41A)	109.40
C(42)-C(41)-H(41A)	109.40	C(40)-C(41)-H(41B)	109.40
C(42)-C(41)-H(41B)	109.40	H(41A)-C(41)-H(41B)	108.00
C(37)-C(42)-C(41)	112.73(18)	C(37)-C(42)-H(42A)	109.00
C(41)-C(42)-H(42A)	109.00	C(37)-C(42)-H(42B)	109.00
C(41)-C(42)-H(42B)	109.00	H(42A)-C(42)-H(42A)	107.80
N(6)-C(43)-N(5)	119.01(16)	N(6)-C(43)-C(44)	120.39(17)
N(5)-C(43)-C(44)	120.60(17)	N(6)-C(43)-Ca(1)	57.51(9)
N(6)-C(43)-C(1)	66.17(10)	C(44)-C(43)-Ca(1)	158.32(13)
C(45)-C(44)-C(43)	175.30(2)	C(44)-C(45)-C(46)	178.60(2)
C(47)-C(46)-C(51)	119.28(19)	C(47)-C(46)-C(45)	119.90(19)
C(51)-C(46)-C(45)	120.82(19)	C(48)-C(47)-C(46)	120.10(2)
C(48)-C(47)-H(47)	120.00	C(46)-C(47)-H(47)	120.00
C(49)-C(48)-H(47)	120.30(2)	C(49)-C(48)-H(48)	119.90
C(47)-C(48)-H(48)	119.90	C(48)-C(49)-C(50)	120.30(2)
C(48)-C(49)-H(49)	119.90	C(50)-C(49)-H(49)	119.90
C(49)-C(50)-C(51)	120.00(2)	C(49)-C(50)-H(50)	120.00
C(51)-C(50)-H(50)	120.00	C(50)-C(51)-C(46)	120.10(2)
C(50)-C(51)-H(51)	119.90	C(46)-C(51)-H(51)	119.90
N(5)-C(52)-C(53)	109.72(16)	N(5)-C(52)-C(57)	112.18(16)
C(53)-C(52)-C(57)	110.32(17)	N(5)-C(52)-H(52)	108.20
C(53)-C(52)-H(52)	108.20	C(57)-C(52)-H(52)	108.20
C(52)-C(53)-C(54)	112.89(18)	C(52)-C(53)-H(53A)	109.00
C(54)-C(53)-H(53A)	109.00	C(52)-C(53)-H(53B)	109.00
C(54)C(53)-H(53B)	109.00	H(53A)-C(53)-H(53B)	107.80
C(55)-C(54)-C(53)	111.60(2)	C(55)-C(54)-H(54A)	109.30
C(53)-C(54)-H(54A)	109.30	C(55)-C(54)-H(54B)	109.30
C(53)-C(54)-H(54B)	109.30	H(54A)-C(54)-H(54B)	108.00
C(54)-C(55)-C(56)	110.80(2)	C(54)-C(55)-H(55A)	109.50
C(56)-C(55)-H(55A)	109.50	C(54)-C(55)-H(55B)	109.50
C(56)-C(55)-H(55B)	109.50	H(55A)-C(55)-H(55B)	108.10
C(55)-C(56)-C(57)	111.00(2)	C(55)-C(56)-H(56A)	109.40
C(57)-C(56)-H(56A)	109.40	C(55)-C(56)-H(56B)	109.40
C(57)-C(56)-H(56B)	109.40	H(56A)-C(56)-H(56B)	108.00
C(56)-C(57)-C(52)	112.64(19)	C(56)-C(57)-H(57A)	109.10
C(52)-C(57)-H(57A)	109.10	C(56)-C(57)-H(57B)	109.10
C(52)-C(57)-H(57B)	109.10	H(57A)-C(57)-H(57B)	107.80
N(6)-C(58)-C(59)	110.77(15)	N(6)-C(58)-C(63)	111.57(15)
C(59)-C(58)-C(63)	109.71(17)	N(6)-C(58)-H(58)	108.20
C(59)-C(58)-H(58)	108.20	C(63)-C(58)-H(58)	108.20
C(58)-C(59)-C(60)	110.82(16)	C(58)-C(59)-H(59A)	109.50
C(60)-C(59)-H(59A)	109.50	C(58)-C(59)-H(59B)	109.50
C(60)-C(59)-H(59B)	109.50	H(59A)-C(59)-H(55B)	108.10

C(61)-C(60)-C(59)	111.39(17)	C(61)-C(60)-H(60A)	109.30
C(59)-C(60)-H(60A)	109.30	C(61)-C(60)-H(60B)	109.30
C(59)-C(60)-H(60B)	109.30	H(60A)-C(60)-H(60B)	108.00
C(60)-C(61)-C(62)	111.14(19)	C(60)-C(61)-H(61A)	109.40
C(62)-C(61)-H(61A)	109.40	C(60)-C(61)-H(61B)	109.40
C(62)-C(61)-H(61B)	109.40	H(61A)-C(61)-H(61B)	108.00
C(61)-C(62)-C(63)	111.98(19)	C(61)-C(62)-H(62A)	109.20
C(63)-C(62)-H(62A)	109.20	C(61)-C(62)-H(62B)	109.20
C(63)-C(62)-H(62B)	109.20	H(62A)-C(62)-H(62B)	107.90
C(58)-C(63)-C(62)	111.06(17)	C(58)-C(63)-H(63A)	109.40
C(62)-C(63)-H(63A)	109.40	C(58)-C(63)-H(63B)	109.40
C(62)-C(63)-H(63B)	109.40	H(63A)-C(63)-H(63B)	108.00
N(8)-C(64)-N(7)	116.17(16)	N(8)-C(64)-C(65)	121.52(17)
N(7)-C(64)-C(65)	122.31(17)	N(8)-C(64)-Ca(2)	68.57(10)
N(7)-C(64)-Ca(2)	60.96(10)	C(65)-C(64)-Ca(2)	143.29(13)
N(8)-C(64)-Ca(1)	62.22(10)	N(7)-C(64)-Ca(1)	67.40(10)
C(65)-C(64)-Ca(1)	143.84(13)	Ca(2)-C(64)-Ca(1)	72.86(5)
C(66)-C(65)-C(64)	177.00(2)	C(65)-C(66)-C(67)	179.20(2)
C(68)-C(67)-C(72)	118.30(2)	C(68)-C(67)-C(66)	120.51(18)
C(72)-C(67)-C(66)	121.21(19)	C(69)-C(68)-C(67)	121.30(2)
C(69)-C(68)-H(68)	119.40	C(67)-C(68)-H(68)	119.40
C(70)-C(69)-C(68)	120.10(2)	C(70)-C(69)-H(69)	119.90
C(68)-C(69)-H(69)	119.90	C(69)-C(70)-C(71)	119.90(2)
C(69)-C(70)-H(70)	120.10	C(71)-C(70)-H(70)	120.10
C(70)-C(71)-C(72)	120.60(2)	C(70)-C(71)-H(71)	119.70
C(72)-C(71)-H(71)	119.70	C(67)-C(72)-C(71)	119.90(2)
C(67)-C(72)-H(72)	120.10	C(71)-C(72)-H(72)	120.10
N(7)-C(73)-C(74)	109.20(15)	N(7)-C(73)-C(78)	111.65(16)
C(74)-C(73)-C(78)	110.13(16)	N(7)-C(73)-H(73)	108.60
C(74)-C(73)-H(73)	108.60	C(78)-C(73)-H(73)	108.60
C(73)-C(74)-C(75)	111.70(17)	C(73)-C(74)-H(74A)	109.30
C(75)-C(74)-H(74A)	109.30	C(73)-C(74)-H(74B)	109.30
C(75)-C(74)-H(74B)	109.30	H(4A3)-C(74)-H(74B)	107.90
C(76)-C(75)-C(74)	111.28(19)	C(76)-C(75)-H(75A)	109.40
C(74)-C(75)-H(75A)	109.40	C(76)-C(75)-H(75B)	109.40
C(74)-C(75)-H(75B)	109.40	H(75A)-C(75)-H(75B)	108.00
C(77)-C(76)-C(75)	110.86(18)	C(77)-C(76)-H(76A)	109.50
C(75)-C(76)-H(76A)	109.50	C(77)-C(76)-H(76B)	109.50
C(75)-C(76)-H(76)	109.50	H(76A)-C(76)-H(76B)	108.10
C(76)-C(77)-C(78)	110.75(18)	C(76)-C(77)-H(77A)	109.50
C(78)-C(77)-H(77A)	109.50	C(76)-C(77)-H(77B)	109.50
C(78)-C(77)-H(77B)	109.50	H(77A)-C(77)-H(77B)	108.10
C(73)-C(78)-C(77)	110.67(17)	C(73)-C(78)-H(78A)	109.50
C(77)-C(78)-H(78A)	109.50	C(73)-C(78)-H(78B)	109.50
C(77)-C(78)-H(78B)	109.50	H(78A)-C(78)-H(78B)	108.10
N(8)-C(79)-C(84)	109.45(16)	N(8)-C(79)-C(80)	112.24(16)
C(84)-C(79)-C(80)	110.98(18)	N(8)-C(79)-H(79)	108.00
C(84)-C(79)-H(79)	108.00	C(80)-C(79)-H(79)	108.00
C(79)-C(80)-C(81)	110.97(19)	C(79)-C(80)-H(80A)	109.40
C(81)-C(80)-H(80A)	109.40	C(79)-C(80)-H(80)	109.40
C(81)-C(80)-H(80B)	109.40	H(80A)-C(80)-H(80B)	108.00
C(82)-C(81)-C(80)	111.10(2)	C(82)-C(81)-H(81A)	109.40
C(80)-C(81)-H(81A)	109.40	C(82)-C(81)-H(81B)	109.40

C(80)-C(81)-H(81B)	109.40	H(81A)-C(81)-H(81B)	108.00
C(83)-C(82)-C(81)	111.30(2)	C(83)-C(82)-H(82A)	109.40
C(81)-C(82)-H(82A)	109.40	C(83)-C(82)-H(82A)	109.40
C(81)-C(82)-H(82B)	109.40	H(82A)-C(82)-H(82B)	108.00
C(82)-C(83)-C(84)	110.90(2)	C(82)-C(83)-H(83A)	109.50
C(84)-C(83)-H(83A)	109.50	C(82)-C(83)-H(83B)	109.50
C(84)-C(83)-H(83B)	109.50	H(83A)-C(83)-H(83B)	108.00
C(79)-C(84)-C(83)	110.86(18)	C(79)-C(84)-H(84A)	109.50
C(83)-C(84)-H(84A)	109.50	C(79)-C(84)-H(84A)	109.50
C(83)-C(84)-H(84B)	109.50	H(84A)-C(84)-H(84B)	108.10
C(86)-C(85)-H(85A)	109.50	C(86)-C(85)-H(85B)	109.50
H(85A)-C(85)-H(85B)	109.50	C(86)-C(85)-H(85C)	109.50
H(85A)-C(85)-H(85C)	109.50	H(85B)-C(85)-H(85C)	109.50
C(91)-C(86)-C(87)	119.10(4)	C(91)-C(86)-C(85)	120.50(4)
C(87)-C(87)-C(85)	120.40(4)	C(88)-C(87)-C(86)	119.30(4)
C(88)-C(87)-H(87)	120.40	C(86)-C(87)-H(87)	120.40
C(89)-C(88)-C(87)	119.80(4)	C(89)-C(88)-H(88)	120.10
C(87)-C(88)-H(88)	120.10	C(90)-C(89)-C(88)	121.90(4)
C(90)-C(89)-H(89)	119.00	C(88)-C(89)-H(89)	119.00
C(89)-C(90)-C(91)	118.20(4)	C(89)-C(90)-H(90)	120.90
C(91)-C(90)-H(90)	120.90	C(86)-C(91)-C(90)	121.70(4)
C(86)-C(91)-H(91)	119.20	C(90)-C(91)-H(91)	119.20

Table A19. Anisotropic displacement parameters (A^2 x 10^3) for **19**.

The anisotropic displacement factor exponent takes the form: -2 pi^2 [h^2 a^{*2} U11 + ... + 2 h k a* b* U12].

Atom	U11	U22	U33	U23	U13	U12
Ca(1)	27(1)	26(1)	23(1)	6(1)	-5(1)	14(1)
Ca(2)	28(1)	29(1)	24(1)	5(1)	-4(1)	15(1)
N(1)	38(1)	35(1)	27(1)	3(1)	-1(1)	23(1)
N(2)	37(1)	33(1)	28(1)	3(1)	-5(1)	23(1)
N(3)	26(1)	29(1)	36(1)	7(1)	-5(1)	12(1)
N(4)	25(1)	30(1)	35(1)	6(1)	-5(1)	12(1)
N(5)	24(1)	30(1)	19(1)	4(1)	-2(1)	10(1)
N(6)	24(1)	24(1)	24(1)	5(1)	-5(1)	9(1)
N(7)	27(1)	26(1)	23(1)	4(1)	-4(1)	11(1)
N(8)	28(1)	25(1)	24(1)	4(1)	-6(1)	9(1)
C(1)	24(1)	25(1)	33(1)	5(1)	-6(1)	11(1)
C(2)	26(1)	27(1)	30(1)	3(1)	-4(1)	13(1)
C(3)	28(1)	27(1)	31(1)	5(1)	-6(1)	11(1)
C(4)	32(1)	35(1)	38(1)	14(1)	-12(1)	19(1)
C(5)	50(2)	62(2)	67(2)	6(1)	5(1)	33(1)
C(6)	55(2)	96(2)	87(2)	22(2)	6(2)	48(2)
C(7)	56(2)	51 (2)	105(3)	32(2)	-25(2)	36(1)
C(8)	65(2)	44(2)	114(3)	2(2)	-7(2)	35(1)
C(9)	56(2)	41(1)	79(2)	-5(1)	3(1)	30(1)
C(10)	39(1)	36(1)	28(1)	3(1)	0(1)	24(1)
C(11)	56(2)	48(1)	39(1)	-3(1)	7(1)	30(1)

C(12)	65(2)	77(2)	37(1)	-13(1)	12(1)	46(2)
C(13)	67(2)	130(3)	25(1)	-4(2)	4(1)	64(2)
C(14)	52(2)	101(2)	40(2)	29(2)	-12(1)	40(2)
C(15)	41(1)	50(1)	35(1)	10(1)	-4(1)	25(1)
C(16)	37(1)	34(1)	29(1)	3(1)	-6(1)	22(1)
C(17)	56(2)	29(1)	45(1)	4(1)	-18(1)	14(1)
C(18)	72(2)	34(1)	58(2)	-7(1)	-14(1)	18(1)
C(19)	64(2)	56(2)	42(2)	-15(1)	0(1)	30(1)
C(20)	57(2)	53(1)	33(1)	4(1)	-12(1)	29(1)
C(21)	39(1)	34(1)	32(1)	5(1)	-10(1)	17(1)
C(22)	31(1)	29(1)	25(1)	0(1)	-2(1)	15(1)
C(23)	26(1)	31(1)	30(1)	2(1)	-3(1)	12(1)
C(24)	27(1)	34(1)	29(1)	2(1)	-3(1)	14(1)
C(25)	32(1)	36(1)	31(1)	7(1)	-7(1)	20(1)
C(26)	57(2)	39(1)	48(2)	3(1)	9(1)	21(1)
C(27)	80(2)	36(1)	70(2)	10(1)	7(2)	25(1)
C(28)	78(2)	56(2)	55(2)	22(1)	-6(2)	43(2)
C(29)	78(2)	68(2)	41(2)	4(1)	12(1)	47(2)
C(30)	51(2)	42(1)	45(1)	-2(1)	9(1)	27(1)
C(31)	30(1)	27(1)	34(1)	8(1)	-6(1)	14(1)
C(32)	29(1)	34(1)	47(1)	10(1)	-5(1)	13(1)
C(33)	35(1)	36(1)	70(2)	14(1)	-10(1)	9(1)
C(34)	55(2)	44(1)	68(2)	19(1)	-31(1)	15(1)
C(35)	69(2)	49(1)	38(1)	14(1)	-18(1)	25(1)
C(36)	41(1)	41(1)	35(1)	6(1)	-7(1)	19(1)
C(37)	24(1)	33(1)	28(1)	4(1)	-3(1)	12(1)
C(38)	34(1)	31(1)	35(1)	0(1)	-7(1)	11(1)
C(39)	40(1)	41(1)	45(1)	-1(1)	-14(1)	17(1)
C(40)	37(1)	43(1)	40(1)	3(1)	-13(1)	13(1)
C(41)	35(1)	35(1)	47(1)	-1(1)	-11(1)	3(1)
C(42)	37(1)	32(1)	44(1)	-3(1)	-10(1)	10(1)
C(43)	30(1)	26(1)	23(1)	5(1)	-7(1)	16(1)
C(44)	31(1)	29(1)	26(1)	2(1)	-4(1)	13(1)
C(45)	32(1)	31(1)	26(1)	2(1)	-5(1)	13(1)
C(46)	41(1)	26(1)	22(1)	1(1)	-6(1)	13(1)
C(47)	41(1)	40(1)	28(1)	5(1)	-8(1)	16(1)
C(48)	49(1)	45(1)	35(1)	7(1)	-18(1)	13(1)
C(49)	69(2)	43(1)	24(1)	11(1)	-18(1)	21(1)
C(50)	66(2)	50(1)	26(1)	7(1)	-5(1)	32(1)
C(51)	48(1)	43(1)	27(1)	6(1)	-7(1)	22(1)
C(52)	31(1)	32(1)	23(1)	3(1)	0(1)	13(1)
C(53)	29(1)	41(1)	34(1)	-6(1)	1(1)	16(1)
C(54)	36(1)	69(2)	50(2)	-20(1)	12(1)	24(1)
C(55)	45(2)	59(2)	56(2)	-27(1)	11(1)	15(1)
C(56)	51(2)	56(2)	46(2)	-19(1)	6(1)	26(1)
C(57)	40(1)	45(1)	35(1)	-5(1)	-1(1)	22(1)
C(58)	27(1)	26(1)	26(1)	6(1)	-6(1)	11(1)
C(59)	31(1)	31(1)	33(1)	-1(1)	-6(1)	12(1)
C(60)	31(1)	28(1)	40(1)	-2(1)	-3(1)	8(1)
C(61)	28(1)	34(1)	61(2)	-4(1)	-6(1)	8(1)
C(62)	32(1)	39(1)	63(2)	-8(1)	-17(1)	11(1)
C(63)	30(1)	31(1)	47(1)	-5(1)	-8(1)	11(1)
C(64)	26(1)	32(1)	24(1)	7(1)	-6(1)	18(1)

C(65)	28(1)	26(1)	27(1)	3(1)	-4(1)	13(1)
C(66)	27(1)	27(1)	28(1)	3(1)	-5(1)	12(1)
C(67)	27(1)	28(1)	29(1)	6(1)	-8(1)	11(1)
C(68)	53(2)	39(1)	30(1)	0(1)	-7(1)	5(1)
C(69)	73(2)	59(2)	27(1)	0(1)	-12(1)	19(1)
C(70)	74(2)	55(2)	42(2)	20(1)	-33(1)	31(1)
C(71)	81(2)	39(1)	71(2)	18(1)	-47(1)	9(1)
C(72)	63(2)	33(1)	49(2)	-2(1)	-27(1)	6(1)
C(73)	30(1)	27(1)	23(1)	4(1)	-6(1)	14(1)
C(74)	32(1)	31(1)	29(1)	4(1)	-6(1)	12(1)
C(75)	40(1)	35(1)	39(1)	0(1)	-4(1)	8(1)
C(76)	61(2)	34(1)	39(1)	-5(1)	-1(1)	20(1)
C(77)	54(2)	41(1)	35(1)	1(1)	-10(1)	29(1)
C(78)	34(1)	34(1)	35(1)	4(1)	-8(1)	18(1)
C(79)	31(1)	28(1)	28(1)	5(1)	-7(1)	10(1)
C(80)	33(1)	40(1)	50(2)	13(1)	-10(1)	13(1)
C(81)	37(1)	46(1)	67(2)	15(1)	-12(1)	1(1)
C(82)	62(2)	36(1)	76(2)	-4(1)	-8(1)	4(1)
C(83)	68(2)	29(1)	69(2)	-2(1)	-19(1)	13(1)
C(84)	39(1)	31(1)	45(1)	0(1)	-10(1)	11(1)
C(85)	108(3)	135(4)	158(5)	-26(3)	-21(3)	74(3)
C(86)	50(2)	75(2)	98(3)	-14(2)	-16(2)	19(2)
C(87)	55(2)	121(3)	94(3)	35(3)	-5(2)	9(2)
C(88)	65(2)	84(3)	145(5)	20(3)	43(3)	3(2)
C(89)	71(2)	72(2)	150(4)	-15(3)	50(3)	23(2)
C(90)	69(2)	61(2)	107(3)	-1(2)	17(2)	21(2)
C(91)	52(2)	64(2)	86(2)	1(2)	-8(2)	12(2)

Table A20. Hydrogen coordinates (x 10^4) and isotropic displacement parameters (A^2 x 10^3) for **19**.

Atom	x	y	z	U(eq)
H(5)	5608	3226	5558	69
H(6)	6351	5030	5342	90
H(7)	5706	6511	5911	78
H(8)	4326	6951	6668	84
H(9)	3568	5893	6893	68
H(10)	3767	2758	5550	38
H(11A)	3236	1155	5407	55
H(11B)	4393	1058	5395	55
H(12A)	4242	1831	4416	67
H(12B)	3990	906	4349	67
H(13A)	2197	1945	4467	81
H(13B)	2742	2299	3893	81
H(14A)	2695	3579	4533	74
H(14B)	1539	3664	4566	74
H(15A)	1681	2971	5548	49
H(15B)	2007	3850	5589	49
H(16)	3624	3672	7645	37

H(17A)	1460	4313	8069	53
H(17B)	1906	4841	7552	53
H(18A)	2708	5292	8328	67
H(18B)	1487	5704	8550	67
H(19A)	1819	4387	9226	64
H(19B)	2486	4950	9397	64
H(20A)	3527	3210	9337	54
H(20B)	3992	3742	8834	54
H(21A)	4013	2366	8324	41
H(21B)	2802	2719	8550	41
H(26)	-329	-3374	8086	59
H(27)	-586	4561	8676	76
H(28)	-1755	-4102	9583	70
H(29)	-2696	-2447	9889	70
H(30)	-2500	-1243	9283	53
H(31)	934	-1957	7983	35
H(32A)	2525	-1296	7806	45
H(32B)	2345	-1989	7314	45
H(33A)	2861	-3286	8009	59
H(33B)	3757	-2922	7916	59
H(34A)	3369	-3165	9001	67
H(34B)	3196	-2057	8890	67
H(35A)	1768	-2000	9545	62
H(35B)	1580	-2683	9050	62
H(36A)	326	-1036	8948	46
H(36B)	1278	-702	8842	46
H(37)	-2441	583	7661	34
H(38A)	-1675	382	6345	41
H(38B)	-1783	-463	6756	41
H(39A)	-3156	252	6089	50
H(39B)	-3604	364	6819	50
H(40A)	-4494	1872	6353	49
H(40B)	-3417	1891	6096	49
H(41A)	-4209	2057	7404	52
H(41B)	-4134	2932	7008	52
H(42A)	-2305	2118	6919	47
H(42B)	-2736	2230	7652	47
H(47)	4703	-657	9726	44
H(48)	5245	-1340	10690	54
H(49)	4094	-1588	11430	55
H(50)	2389	-1156	11216	54
H(51)	1826	-453	10259	46
H(52)	790	1315	9006	35
H(53A)	-550	1497	8402	42
H(53B)	-623	2519	8146	42
H(54A)	-2003	2867	8934	63
H(54B)	-1219	2203	9421	63
H(55A)	-1693	3862	9670	69
H(55B)	-1339	4028	8959	69
H(56A)	42	2819	9837	61
H(56B)	-19	3846	9594	61
H(57A)	1433	2486	9050	47
H(57B)	650	3162	8567	47

H(58)	4044	-829	8144	32
H(59A)	4654	-715	6832	38
H(59B)	4122	-1397	7094	38
H(60A)	5583	-2340	7637	42
H(60B)	5963	-2341	6904	42
H(61A)	6546	-1161	7107	52
H(61B)	7058	-2048	7570	52
H(62A)	6373	-471	8117	54
H(62B)	5863	-1146	8421	54
H(63A)	4522	446	8336	44
H(63B)	4884	441	7598	44
H(68)	492	1490	4053	55
H(69)	-185	1999	3097	67
H(70)	-1396	3606	2999	65
H(71)	-1990	4696	3867	81
H(72)	-1327	4197	4837	63
H(73)	1910	514	5425	31
H(74A)	2801	-927	6347	38
H(74B)	3367	-341	5980	38
H(75A)	3465	-1145	5015	49
H(75B)	3973	-1966	5520	49
H(76A)	2825	-2318	4937	55
H(76B)	2457	-2195	5681	55
H(77A)	996	-1304	5133	49
H(77B)	1567	-708	4782	49
H(78A)	382	287	5633	39
H(78B)	940	-551	6119	39
H(80A)	-1556	3589	7272	51
H(80B)	-1634	3357	6550	51
H(81A)	-2092	5007	6298	67
H(81B)	-2878	5003	6886	67
H(82A)	-2261	6197	7057	80
H(82B)	-1956	5400	7594	69
H(83A)	-498	5653	7255	69
H(83B)	-575	5411	6534	69
H(84A)	741	4005	6937	48
H(84B)	-62	4007	7516	48
H(85A)	6359	6782	8781	188
H(85B)	5878	6714	9480	188
H(85C)	5122	7223	8944	188
H(87)	5911	5206	9741	122
H(88)	5900	3724	9444	138
H(89)	5840	3380	8393	127
H(90)	5784	4476	7624	101
H(91)	5810	5955	7917	86

Compound **42**

Table A21. Crystal data and structure refinement for **42**.

Empirical formula	$C_{103}\ H_{103}\ Ca_2\ N_6\ O_2$
Formula weight	1564.29
Temperature	150(2) K
Wavelength	0.71073 Å
Crystal system	Triclinic
Space group	P-1
Unit cell dimensions	a = 13.38640(10) Å α = 84.7020(10)°
	b = 14.3150(2) Å β = 80.8480(10)°
	c = 26.8614(4) Å γ = 62.9200(10)°
Volume	4523.55(10) A^3
Z	2
Density (calculated)	1.148 Mg/m^3
Absorption coefficient	0.178 mm^{-1}
F(000)	1692
Crystal size	0.25 x 0.15 x 0.15 mm
Theta range for data collection	3.27 to 27.45°
Index ranges	-17<=h<=17,-18<=k<=18,-34<=l<=34
Reflections collected	83417
Independent reflections	20489[R(int)= 0.0863]
Reflections observed (>2σ)	27.45
Data Completeness	99.0 %
Absorption correction	Semi-empirical from equivalents
Max. and min. transmission	0.9738 and 0.9568
Refinement method	Full-matrix least-squares on F^2
Data / restraints / parameters	20489 / 1 / 1136
Goodness-of-fit on F^2	1.031
Final R indices [I>2σ(I)]	R1 = 0.0591, wR2 = 0.1133
R indices (all data)	R1 = 0.1133, wR2 = 0.1329
Largest diff. peak and hole	0.514 and -0.319 $e.A^{-3}$

Table A22. Atomic coordinates (x 10^4) and equivalent isotropic displacement parameters (A^2 x 10^3) for **42**. U(eq) is defined as one third of the trace of the orthogonalized Uij tensor.

Atom	x	y	z	U(eq)
Ca(1)	4174(1)	1378(1)	237(1)	28(1)
Ca(2)	9404(1)	1459(1)	4993(1)	30(1)
N(1)	4159(1)	2647(1)	742(1)	28(1)
N(2)	2179(1)	2271(1)	495(1)	31(1)
N(3)	4333(2)	2042(1)	-665(1)	32(1)
N(4)	8205(1)	3007(1)	5437(1)	32(1)
N(5)	10481(1)	2406(1)	4704(1)	32(1)
N(6)	8534(2)	1505(1)	4217(1)	36(1)
O(1)	4815(1)	328(1)	-501(1)	34(1)
O(2)	9873(1)	-20(1)	4480(1)	37(1)
C(1)	3614(2)	4541(2)	740(1)	42(1)
C(2)	3364(2)	3627(2)	684(1)	30(1)
C(3)	2270(2)	3902(2)	577(1)	32(1)
C(4)	1690(2)	3295(2)	564(1)	33(1)
C(5)	411(2)	3916(2)	650(1)	51(1)
C(6)	5122(2)	2497(2)	970(1)	32(1)
C(7)	6182(2)	2219(2)	670(1)	36(1)
C(8)	7121(2)	2006(2)	908(1)	48(1)
C(9)	7033(2)	2064(2)	1422(1)	55(1)
C(10)	5995(2)	2354(2)	1711(1)	50(1)
C(11)	5024(2)	2584(2)	1496(1)	38(1)
C(12)	6297(2)	2173(2)	103(1)	39(1)
C(13)	6900(2)	1047(2)	-81(1)	56(1)
C(14)	6895(2)	2807(2)	-164(1)	63(1)
C(15)	3892(2)	2912(2)	1828(1)	44(1)
C (16)	3707(3)	3645(3)	2242(1)	78(1)
C(17)	3755(3)	1966(3)	2060(2)	88(1)
C(18)	1465(2)	1753(2)	545(1)	34(1)
C(19)	1235(2)	1327(2)	1019(1)	47(1)
C(20)	571(2)	799(2)	1062(1)	54(1)
C(21)	136(2)	683(2)	657(1)	51(1)
C(22)	346(2)	1115(2)	195(1)	44(1)
C(23)	1014(2)	1639(2)	127(1)	38(1)
C(24)	1672(3)	1443(3)	1483(1)	64(1)
C(25)	2443(3)	395(3)	1699(2)	83(1)
C(26)	613(8)	2006(7)	1904(2)	100(3)
C(26A)	1160(20)	2239(16)	1782(10)	74(7)
C(27)	1212(2)	2103(2)	-389(1)	49(1)
C(28)	1724(3)	1297(2)	-799(1)	63(1)
C(29)	107(3)	2998(3)	-536(1)	94(1)
C(30)	4552(2)	1136(2)	-821(1)	32(1)
C(31)	4478(2)	911(2)	-1329(1)	36(1)
C(32)	4350(2)	749(2)	-1735(1)	38(1)
C(33)	4189(2)	600(2)	-2234(1)	41(1)

C(34)	3520(2)	130(3)	-2294(1)	67(1)
C(35)	3392(3)	-30(4)	-2777(2)	102(2)
C(36)	3925(3)	275(4)	-3190(1)	104(2)
C(37)	4591(3)	732(3)	-3132(1)	78(1)
C(38)	4733(2)	900(2)	-2654(1)	53(1)
C(39)	4056(2)	2992(2)	-1000(1)	32(1)
C(40)	3979(2)	3868(2)	-685(1)	43(1)
C(41)	3696(2)	4890(2)	-998(1)	43(1)
C(42)	2563(2)	5243(2)	-1188(1)	54(1)
C(43)	2631(2)	4388(2)	-1510(1)	49(1)
C(44)	2905(2)	3370(2)	-1190(1)	41(1)
C(45)	4985(2)	2822(2)	-1448(1)	36(1)
C(46)	4690(2)	3842(2)	-1764(1)	41(1)
C(47)	3564(2)	4176(2)	-1957(1)	50(1)
C(48)	4613(2)	4702(2)	-1446(1)	44(1)
C(49)	6849(2)	4849(2)	5271(1)	46(1)
C(50)	7997(2)	3896(2)	5170(1)	34(1)
C(51)	8767(2)	4054(2)	4794(1)	35(1)
C(52)	9938(2)	3437(2)	4644(1)	34(1)
C(53)	10550(2)	4078(2)	4419(1)	48(1)
C(54)	7434(2)	3073(2)	5889(1)	34(1)
C(55)	7486(2)	3524(2)	6321(1)	39(1)
C(56)	6738(2)	3564(2)	6754(1)	47(1)
C(57)	5983(2)	3158(2)	6767(1)	52(1)
C(58)	5946(2)	2705(2)	6343(1)	47(1)
C(59)	6659(2)	2659(2)	5898(1)	38(1)
C(60)	8346(2)	3941(2)	6330(1)	43(1)
C(61)	7878(3)	4954(3)	6606(2)	90(1)
C(62)	9383(3)	3119(3)	6546(2)	95(1)
C(63)	6568(2)	2195(2)	5431(1)	43(1)
C(64)	5347(2)	2643(3)	5323(1)	74(1)
C(65)	7094(3)	1001(2)	5462(1)	61(1)
C(66)	11694(2)	1932(2)	4568(1)	35(1)
C(67)	12183(2)	1621(2)	4069(1)	41(1)
C(68)	13344(2)	1248(2)	3949(1)	52(1)
C(69)	14020(2)	1142(3)	4310(1)	66(1)
C(70)	13544(2)	1395(2)	4798(1)	61(1)
C(71)	12380(2)	1796(2)	4940(1)	44(1)
C(72)	11475(2)	1697(2)	3663(1)	47(1)
C(73)	11246(3)	2638(3)	3317(1)	85(1)
C(74)	11968(3)	715(2)	3352(1)	62(1)
C(75)	11877(2)	2078(2)	5484(1)	46(1)
C(76)	12440(6)	2645(7)	5728(3)	61(2)
C(77)	12044(7)	1092(5)	5768(3)	56(2)
C(76A)	11780(20)	3058(11)	5617(5)	86(7)
C(77A)	12392(14)	1186(12)	5897(6)	62(4)
C(78)	9292(2)	565(2)	4117(1)	35(1)
C(79)	9628(2)	68(2)	3628(1)	39(1)
C(80)	9967(2)	-322(2)	3221(1)	40(1)
C(81)	10370(2)	-774(2)	2731(1)	45(1)
C(82)	11500(3)	-1434(2)	2597(1)	67(1)
C(83)	11855(4)	-1890(3)	2128(2)	102(2)
C(84)	11129(6)	-1689(4)	1790(2)	112(2)

C(85)	10013(5)	-1029(4)	1916(1)	99(1)
C(86)	9622(3)	-555(3)	2383(1)	71(1)
C(87)	7801(2)	2232(2)	3848(1)	36(1)
C(88)	8482(2)	2548(2)	3408(1)	41(1)
C(89)	7678(2)	3345(2)	3055(1)	44(1)
C(90)	6856(2)	4332(2)	3346(1)	50(1)
C(91)	6161(2)	4042(2)	3785(1)	45(1)
C(92)	6963(2)	3229(2)	4131(1)	44(1)
C(93)	7110(2)	1777(2)	3646(1)	40(1)
C(94)	6317(2)	2584(2)	3291(1)	47(1)
C(95)	7023(2)	2864(2)	2852(1)	50(1)
C(96)	5494(2)	3572(2)	3580(1)	50(1)
C(97)	1130(7)	5646(7)	1785(2)	91(3)
C(98)	109(5)	5792(6)	2160(3)	58(2)
C(99)	-804(11)	6785(12)	2211(7)	61(3)
C(100)	-1712(6)	6963(6)	2592(4)	73(2)
C(101)	-1740(8)	6110(8)	2886(4)	75(3)
C(102)	-834(12)	5152(10)	2811(4)	74(3)
C(103)	58(10)	4986(7)	2453(4)	72(2)
C(197)	-2270(20)	6616(17)	3043(9)	157(10)
C(198)	-1259(19)	6137(17)	2617(7)	103(6)
C(199)	-660(30)	5030(20)	2550(10)	115(12)
C(200)	290(20)	4609(17)	2168(13)	142(10)
C(201)	539(15)	5264(15)	1869(7)	103(5)
C(202)	-80(20)	6310(17)	1932(7)	116(6)
C(203)	-910(40)	6720(30)	2338(13)	120(15)

Table A23. Bond lengths [Å] and angles [^{o}] for **42**.

Ca(1)-O(1)#1	2.2968(14)	Ca(1)-N(1)	2.3569(18)
Ca(1)-N(2)	2.3905(17)	Ca(1)-O(1)	2.4011(15)
Ca(1)-N(3)	2.5317(17)	Ca(1)-C(30)	2.833(2)
Ca(1)-C(2)	3.178(2)	Ca(1)-Ca(1)#1	3.7636(8)
Ca(2)-O(2)#2	2.2954(14)	Ca(2)-N(4)	2.3566(18)
Ca(2)-N(5)	2.3968(19)	Ca(2)-O(2)	2.4153(16)
Ca(2)-N(6)	2.5270(18)	Ca(2)-C(78)	2.835(2)
Ca(2)-C(50)	3.159(2)	Ca(2)-Ca(2)#2	3.7312(8)
N(1)-C(2)	1.333(3)	N(1)-C(6)	1.434(3)
N(2)-C(4)	1.323(3)	N(2)-C(18)	1.437(3)
N(3)-C(30)	1.290(3)	N(3)-C(39)	1.489(3)
N(4)-C(50)	1.335(3)	N(4)-C(54)	1.441(3)
N(5)-C(52)	1.323(3)	N(5)-C(66)	1.445(3)
N(6)-C(78)	1.284(3)	N(6)-C(87)	1.489(3)
O(1)-C(30)	1.320(2)	O(1)-Ca(1)#1	2.2968(14)
O(2)-C(78)	1.323(3)	O(2)-Ca(2)#2	2.2954(14)
C(1)-C(2)	1.516(3)	C(1)-H(1A)	0.9800
C(1)-H(1B)	0.9800	C(1)-H(1C)	0.9800
C(2)-C(3)	1.403(3)	C(3)-C(4)	1.410(3)
C(3)-H(3)	0.9500	C(4)-C(5)	1.517(3)
C(5)-H(5A)	0.9800	C(5)-H(5B)	0.9800
C(5)-H(5C)	0.9800	C(6)-C(11)	1.409(3)

C(6)-C(7)	1.415(3)	C(7)-C(8)	1.397(3)
C(7)-C(12)	1.512(3)	C(8)-C(9)	1.374(4)
C(8)-H(8)	0.9500	C(9)-C(10)	1.378(4)
C(9)-H(9)	0.9500	C(10)-C(11)	1.395(3)
C(10)-H(10)	0.9500	C(11)-C(15)	1.520(3)
C(12)-C(13)	1.525(3)	C(12)-C(14)	1.528(3)
C(12)-H(12)	1.0000	C(13)-H(13A)	0.9800
C(13)-H(13B)	0.9800	C(13)-H(13C)	0.9800
C(14)-H(14A)	0.9800	C(14)-H(14B)	0.9800
C(14)-H(14C)	0.9800	C(15)-C(17)	1.513(4)
C(15)-C(16)	1.514(4)	C(15)-H(15)	1.0000
C(16)-H(16A)	0.9800	C(16)-H(16B)	0.9800
C(16)-H(16C)	0.9800	C(17)-H(17A)	0.9800
C(17)-H(17B)	0.9800	C(17)-H(17C)	0.9800
C(18)-C(19)	1.411(3)	C(18)-C(23)	1.413(3)
C(19)-C(20)	1.392(4)	C(19)-C(24)	1.509(4)
C(20)-C(21)	1.370(4)	C(20)-H(20)	0.9500
C(21)-C(22)	1.380(4)	C(21)-H(21)	0.9500
C(22)-C(23)	1.388(3)	C(22)-H(22)	0.9500
C(23)-C(27)	1.519(3)	C(24)-C(26A)	1.30(2)
C(24)-C(25)	1.509(4)	C(24)-C(26)	1.598(8)
C(24)-H(24)	1.0000	C(24)-H(24A)	1.0000
C(25)-H(25A)	0.9800	C(25)-H(25B)	0.9800
C(25)-H(25C)	0.9800	C(26)-H(26A)	0.9800
C(26)-H(26B)	0.9800	C(26)-H(26C)	0.9800
C(26A)-H(26D)	0.9800	C(26A)-H(26E)	0.9800
C(26A)-H(26F)	0.9800	C(27)-C(28)	1.511(4)
C(27)-C(29)	1.534(4)	C(27)-H(27)	1.0000
C(28)-H(28A)	0.9800	C(28)-H(28B)	0.9800
C(28)-H(28C)	0.9800	C(29)-H(29A)	0.9800
C(29)-H(29B)	0.9800	C(29)-H(29C)	0.9800
C(30)-C(31)	1.457(3)	C(31)-C(32)	1.190(3)
C(32)-C(33)	1.440(3)	C(33)-C(34)	1.377(4)
C(33)-C(38)	1.387(4)	C(34)-C(35)	1.388(4)
C(34)-H(34)	0.9500	C(35)-C(36)	1.367(6)
C(35)-H(35)	0.9500	C(36)-C(37)	1.356(6)
C(36)-H(36)	0.9500	C(37)-C(38)	1.385(4)
C(37)-H(37)	0.9500	C(38)-H(38)	0.9500
C(39)-C(40)	1.531(3)	C(39)-C(45)	1.536(3)
C(39)-C(44)	1.539(3)	C(40)-C(41)	1.536(3)
C(40)-H(40A)	0.9900	C(40)-H(40B)	0.9900
C(41)-C(42)	1.522(4)	C(41)-C(48)	1.522(3)
C(41)-H(41)	1.0000	C(42)-C(43)	1.525(4)
C(42)-H(42A)	0.9900	C(42)-H(42B)	0.9900
C(43)-C(47)	1.530(4)	C(43)-C(44)	1.542(3)
C(43)-H(43)	1.0000	C(44)-H(44A)	0.9900
C(44)-H(44B)	0.9900	C(45)-C(46)	1.536(3)
C(45)-H(45A)	0.9900	C(45)-H(45B)	0.9900
C(46)-C(48)	1.518(3)	C(46)-C(47)	1.524(3)
C(46)-H(46)	1.0000	C(47)-H(47A)	0.9900
C(47)-H(47B)	0.9900	C(48)-H(48A)	0.9900
C(48)-H(48B)	0.9900	C(49)-C(50)	1.524(3)
C(49)-H(49A)	0.9800	C(49)-H(49B)	0.9800

C(49)-H(49C)	0.9800	C(50)-C(51)	1.404(3)
C(51)-C(52)	1.417(3)	C(51)-H(51)	0.9500
C(52)-C(53)	1.518(3)	C(53)-H(53A)	0.9800
C(53)-H(53B)	0.9800	C(53)-H(53C)	0.9800
C(54)-C(55)	1.405(3)	C(54)-C(59)	1.407(3)
C(55)-C(56)	1.395(3)	C(55)-C(60)	1.524(3)
C(56)-C(57)	1.372(4)	C(56)-H(56)	0.9500
C(57)-C(58)	1.380(4)	C(57)-H(57)	0.9500
C(58)-C(59)	1.392(3)	C(58)-H(58)	0.9500
C(59)-C(63)	1.519(3)	C(60)-C(61)	1.506(4)
C(60)-C(62)	1.514(4)	C(60)-H(60)	1.0000
C(61)-H(61A)	0.9800	C(61)-H(61B)	0.9800
C(61)-H(61C)	0.9800	C(62)-H(62A)	0.9800
C(62)-H(62B)	0.9800	C(62)-H(62C)	0.9800
C(63)-C(65)	1.522(4)	C(63)-C(64)	1.527(3)
C(63)-H(63)	1.0000	C(64)-H(64A)	0.9800
C(64)-H(64B)	0.9800	C(64)-H(64C)	0.9800
C(65)-H(65A)	0.9800	C(65)-H(65B)	0.9800
C(65)-H(65C)	0.9800	C(66)-C(71)	1.406(3)
C(66)-C(67)	1.409(3)	C(67)-C(68)	1.387(3)
C(67)-C(72)	1.522(3)	C(68)-C(69)	1.380(4)
C(68)-H(68)	0.9500	C(69)-C(70)	1.368(4)
C(69)-H(69)	0.9500	C(70)-C(71)	1.392(3)
C(70)-H(70)	0.9500	C(71)-C(75)	1.516(3)
C(72)-C(73)	1.502(4)	C(72)-C(74)	1.518(4)
C(72)-H(72)	1.0000	C(73)-H(73A)	0.9800
C(73)-H(73B)	0.9800	C(73)-H(73C)	0.9800
C(74)-H(74A)	0.9800	C(74)-H(74B)	0.9800
C(74)-H(74C)	0.9800	C(75)-C(76A)	1.423(13)
C(75)-C(77)	1.480(7)	C(75)-C(76)	1.571(6)
C(75)-C(77A)	1.585(12)	C(75)-H(75)	1.0000
C(75)-H(75A)	1.0000	C(76)-H(76A)	0.9800
C(76)-H(76B)	0.9800	C(76)-H(76C)	0.9800
C(77)-H(77A)	0.9800	C(77)-H(77B)	0.9800
C(77)-H(77C)	0.9800	C(76A)-H(76D)	0.9800
C(76A)-H(76E)	0.9800	C(76A)-H(76F)	0.9800
C(77A)-H(77D)	0.9800	C(77A)-H(77E)	0.9800
C(77A)-H(77F)	0.9800	C(78)-C(79)	1.458(3)
C(79)-C(80)	1.199(3)	C(80)-C(81)	1.436(3)
C(81)-C(82)	1.378(4)	C(81)-C(86)	1.390(4)
C(82)-C(83)	1.385(5)	C(82)-H(82)	0.9500
C(83)-C(84)	1.353(6)	C(83)-H(83)	0.9500
C(84)-C(85)	1.361(6)	C(84)-H(84)	0.9500
C(85)-C(86)	1.390(5)	C(85)-H(85)	0.9500
C(86)-H(86)	0.9500	C(87)-C(92)	1.531(3)
C(87)-C(93)	1.532(3)	C(87)-C(88)	1.537(3)
C(88)-C(89)	1.539(3)	C(88)-H(88A)	0.9900
C(88)-H(88B)	0.9900	C(89)-C(95)	1.520(4)
C(89)-C(90)	1.528(3)	C(89)-H(89)	1.0000
C(90)-C(91)	1.531(4)	C(90)-H(90A)	0.9900
C(90)-H(90B)	0.9900	C(91)-C(96)	1.524(4)
C(91)-C(92)	1.532(3)	C(91)-H(91)	1.0000
C(92)-H(92A)	0.9900	C(92)-H(92B)	0.9900

C(93)-C(94)	1.539(3)	C(93)-H(93A)	0.9900
C(93)-H(93B)	0.9900	C(94)-C(96)	1.526(4)
C(94)-C(95)	1.533(4)	C(94)-H(94)	1.0000
C(95)-H(95A)	0.9900	C(95)-H(95B)	0.9900
C(96)-H(96A)	0.9900	C(96)-H(96B)	0.9900
C(97)-C(98)	1.506(13)	C(97)-H(97A)	0.9800
C(97)-H(97B)	0.9800	C(97)-H(97C)	0.9800
C(98)-C(103)	1.357(14)	C(98)-C(99)	1.391(16)
C(99)-C(100)	1.40(2)	C(99)-H(99)	0.9500
C(100)-C(101)	1.405(16)	C(100)-H(100)	0.9500
C(101)-C(102)	1.360(17)	C(101)-H(101)	0.9500
C(102)-C(103)	1.35(2)	C(102)-H(102)	0.9500
C(103)-H(103)	0.9500	C(197)-C(198)	1.56(4)
C(197)-H(19A)	0.9800	C(197)-H(19B)	0.9800
C(197)-H(19C)	0.9800	C(198)-C(203)	1.27(4)
C(198)-C(199)	1.43(3)	C(199)-C(200)	1.43(4)
C(199)-H(199)	0.9500	C(200)-C(201)	1.30(3)
C(200)-H(200)	0.9500	C(201)-C(202)	1.35(2)
C(201)-H(201)	0.9500	C(202)-C(203)	1.38(4)
C(202)-H(202)	0.9500	C(203)-H(203)	0.9500
O(1)#1-Ca(1)-N(1)	114.64(6)	O(1)#1-Ca(1)-N(2)	119.60(6)
N(1)-Ca(1)-N(2)	81.93(6)	O(1)#1-Ca(1)-O(1)	73.54(5)
N(1)-Ca(1)-O(1)	153.06(6)	N(2)-Ca(1)-O(1)	117.51(6)
O(1)#1-Ca(1)-N(3)	124.50(5)	N(1)-Ca(1)-N(3)	105.85(6)
N(2)-Ca(1)-N(3)	101.75(6)	O(1)-Ca(1)-N(3)	54.29(5)
O(1)#1-Ca(1)-C(30)	100.62(6)	N(1)-Ca(1)-C(30)	132.13(6)
N(2)-Ca(1)-C(30)	108.41(6)	O(1)-Ca(1)-C(30)	27.66(5)
N(3)-Ca(1)-C(30)	27.07(6)	O(1)#1-Ca(1)-C(2)	135.57(5)
N(1)-Ca(1)-C(2)	22.12(5)	N(2)-Ca(1)-C(2)	66.64(6)
O(1)-Ca(1)-C(2)	147.00(5)	N(3)-Ca(1)-C(2)	92.78(6)
C(30)-Ca(1)-C(2)	119.70(6)	O(1)#1-Ca(1)-Ca(1)#1	37.72(4)
N(1)-Ca(1)-Ca(1)#1	145.40(4)	N(2)-Ca(1)-Ca(1)#1	126.59(5)
O(1)-Ca(1)-Ca(1)#1	35.82(3)	N(3)-Ca(1)-Ca(1)#1	88.47(4)
C(30)-Ca(1)-Ca(1)#1	63.09(4)	C(2)-Ca(1)-Ca(1)#1	166.12(4)
O(2)#2-Ca(2)-N(4)	112.41(6)	O(2)#2-Ca(2)-N(5)	119.66(6)
N(4)-Ca(2)-N(5)	83.00(6)	O(2)#2-Ca(2)-O(2)	75.27(6)
N(4)-Ca(2)-O(2)	156.25(6)	N(5)-Ca(2)-O(2)	113.53(6)
O(2)#2-Ca(2)-N(6)	124.33(6)	N(4)-Ca(2)-N(6)	107.62(6)
N(5)-Ca(2)-N(6)	101.88(6)	O(2)-Ca(2)-N(6)	53.93(5)
O(2)#2-Ca(2)-C(78)	102.22(6)	N(4)-Ca(2)-C(78)	134.33(6)
N(5)-Ca(2)-C(78)	105.19(6)	O(2)-Ca(2)-C(78)	27.74(5)
N(6)-Ca(2)-C(78)	26.94(6)	O(2)#2-Ca(2)-C(50)	133.78(6)
N(4)-Ca(2)-C(50)	22.55(6)	N(5)-Ca(2)-C(50)	67.31(6)
O(2)-Ca(2)-C(50)	148.26(5)	N(6)-Ca(2)-C(50)	94.36(6)
C(78)-Ca(2)-C(50)	120.63(6)	O(2)#2-Ca(2)-Ca(2)#2	38.76(4)
N(4)-Ca(2)-Ca(2)#2	145.80(5)	N(5)-Ca(2)-Ca(2)#2	124.25(5)
O(2)-Ca(2)-Ca(2)#2	36.51(3)	N(6)-Ca(2)-Ca(2)#2	88.05(4)
C(78)-Ca(2)-Ca(2)#2	63.72(5)	C(50)-Ca(2)-Ca(2)#2	167.45(5)
C(2)-N(1)-C(6)	117.91(18)	C(2)-N(1)-Ca(1)	116.14(13)
C(6)-N(1)-Ca(1)	122.87(13)	C(4)-N(2)-C(18)	117.93(17)
C(4)-N(2)-Ca(1)	119.36(14)	C(18)-N(2)-Ca(1)	122.58(13)
C(30)-N(3)-C(39)	123.35(18)	C(30)-N(3)-Ca(1)	89.60(12)

C(39)-N(3)-Ca(1)	145.15(13)	C(50)-N(4)-C(54)	116.95(17)
C(50)-N(4)-Ca(2)	114.86(13)	C(54)-N(4)-Ca(2)	125.15(14)
C(52)-N(5)-C(66)	116.24(18)	C(52)-N(5)-Ca(2)	118.80(14)
C(66)-N(5)-Ca(2)	124.91(13)	C(78)-N(6)-C(87)	124.00(19)
C(78)-N(6)-Ca(2)	90.02(13)	C(87)-N(6)-Ca(2)	142.88(14)
C(30)-O(1)-Ca(1)#1	155.66(13)	C(30)-O(1)-Ca(1)	94.71(12)
Ca(1)#1-O(1)-Ca(1)	106.46(5)	C(78)-O(2)-Ca(2)#2	156.63(15)
C(78)-O(2)-Ca(2)	94.08(12)	Ca(2)#2-O(2)-Ca(2)	104.73(6)
C(2)-C(1)-H(1A)	109.5	C(2)-C(1)-H(1B)	109.5
H(1A)-C(1)-H(1B)	109.5	C(2)-C(1)-H(1C)	109.5
H(1A)-C(1)-H(1C)	109.5	H(1B)-C(1)-H(1C)	109.5
N(1)-C(2)-C(3)	125.0(2)	N(1)-C(2)-C(1)	119.72(19)
C(3)-C(2)-C(1)	115.31(19)	N(1)-C(2)-Ca(1)	41.74(10)
C(3)-C(2)-Ca(1)	88.71(13)	C(1)-C(2)-Ca(1)	148.38(15)
C(2)-C(3)-C(4)	131.42(19)	C(2)-C(3)-H(3)	114.3
C(4)-C(3)-H(3)	114.3	N(2)-C(4)-C(3)	125.06(19)
N(2)-C(4)-C(5)	120.9(2)	C(3)-C(4)-C(5)	114.0(2)
C(4)-C(5)-H(5A)	109.5	C(4)-C(5)-H(5B)	109.5
H(5A)-C(5)-H(5B)	109.5	C(4)-C(5)-H(5C)	109.5
H(5A)-C(5)-H(5C)	109.5	H(5B)-C(5)-H(5C)	109.5
C(11)-C(6)-C(7)	119.9(2)	C(11)-C(6)-N(1)	119.99(19)
C(7)-C(6)-N(1)	120.03(19)	C(8)-C(7)-C(6)	118.7(2)
C(8)-C(7)-C(12)	120.3(2)	C(6)-C(7)-C(12)	120.94(19)
C(9)-C(8)-C(7)	121.4(2)	C(9)-C(8)-H(8)	119.3
C(7)-C(8)-H(8)	119.3	C(8)-C(9)-C(10)	119.6(2)
C(8)-C(9)-H(9)	120.2	C(10)-C(9)-H(9)	120.2
C(9)-C(10)-C(11)	121.7(2)	C(9)-C(10)-H(10)	119.2
C(11)-C(10)-H(10)	119.2	C(10)-C(11)-C(6)	118.6(2)
C(10)-C(11)-C(15)	120.0(2)	C(6)-C(11)-C(15)	121.4(2)
C(7)-C(12)-C(13)	112.05(19)	C(7)-C(12)-C(14)	111.9(2)
C(13)-C(12)-C(14)	110.2(2)	C(7)-C(12)-H(12)	107.5
C(13)-C(12)-H(12)	107.5	C(14)-C(12)-H(12)	107.5
C(12)-C(13)-H(13A)	109.5	C(12)-C(13)-H(13B)	109.5
H(13A)-C(13)-H(13B)	109.5	C(12)-C(13)-H(13C)	109.5
H(13A)-C(13)-H(13C)	109.5	H(13B)-C(13)-H(13C)	109.5
C(12)-C(14)-H(14A)	109.5	C(12)-C(14)-H(14B)	109.5
H(14A)-C(14)-H(14B)	109.5	C(12)-C(14)-H(14C)	109.5
H(14A)-C(14)-H(14C)	109.5	H(14B)-C(14)-H(14C)	109.5
C(17)-C(15)-C(16)	109.2(3)	C(17)-C(15)-C(11)	111.2(2)
C(16)-C(15)-C(11)	113.5(2)	C(17)-C(15)-H(15)	107.6
C(16)-C(15)-H(15)	107.6	C(11)-C(15)-H(15)	107.6
C(15)-C(16)-H(16A)	109.5	C(15)-C(16)-H(16B)	109.5
H(16A)-C(16)-H(16B)	109.5	C(15)-C(16)-H(16C)	109.5
H(16A)-C(16)-H(16C)	109.5	H(16B)-C(16)-H(16C)	109.5
C(15)-C(17)-H(17A)	109.5	C(15)-C(17)-H(17B)	109.5
H(17A)-C(17)-H(17B)	109.5	C(15)-C(17)-H(17C)	109.5
H(17A)-C(17)-H(17C)	109.5	H(17B)-C(17)-H(17C)	109.5
C(19)-C(18)-C(23)	119.4(2)	C(19)-C(18)-N(2)	119.4(2)
C(23)-C(18)-N(2)	121.22(19)	C(20)-C(19)-C(18)	119.0(2)
C(20)-C(19)-C(24)	119.1(2)	C(18)-C(19)-C(24)	121.9(2)
C(21)-C(20)-C(19)	121.7(2)	C(21)-C(20)-H(20)	119.1
C(19)-C(20)-H(20)	119.1	C(20)-C(21)-C(22)	119.2(2)
C(20)-C(21)-H(21)	120.4	C(22)-C(21)-H(21)	120.4

C(21)-C(22)-C(23)	121.8(2)	C(21)-C(22)-H(22)	119.1
C(23)-C(22)-H(22)	119.1	C(22)-C(23)-C(18)	118.9(2)
C(22)-C(23)-C(27)	119.5(2)	C(18)-C(23)-C(27)	121.6(2)
C(26A)-C(24)-C(25)	118.2(10)	C(26A)-C(24)-C(19)	124.9(8)
C(25)-C(24)-C(19)	111.9(3)	C(25)-C(24)-C(26)	107.5(4)
C(19)-C(24)-C(26)	108.2(4)	C(26A)-C(24)-H(24)	73.8
C(25)-C(24)-H(24)	109.7	C(19)-C(24)-H(24)	109.7
C(26)-C(24)-H(24)	109.7	C(26A)-C(24)-H(24A)	97.4
C(25)-C(24)-H(24A)	97.4	C(19)-C(24)-H(24A)	97.4
C(26)-C(24)-H(24A)	133.4	C(24)-C(25)-H(25A)	109.5
C(24)-C(25)-H(25B)	109.5	H(25A)-C(25)-H(25B)	109.5
C(24)-C(25)-H(25C)	109.5	H(25A)-C(25)-H(25C)	109.5
H(25B)-C(25)-H(25C)	109.5	C(24)-C(26)-H(26A)	109.5
C(24)-C(26)-H(26B)	109.5	C(24)-C(26)-H(26C)	109.5
C(24)-C(26A)-H(26D)	109.5	C(24)-C(26A)-H(26E)	109.5
H(26D)-C(26A)-H(26E)	109.5	C(24)-C(26A)-H(26F)	109.5
H(26D)-C(26A)-H(26F)	109.5	H(26E)-C(26A)-H(26F)	109.5
C(28)-C(27)-C(23)	112.8(2)	C(28)-C(27)-C(29)	109.0(2)
C(23)-C(27)-C(29)	110.9(2)	C(28)-C(27)-H(27)	108.0
C(23)-C(27)-H(27)	108.0	C(29)-C(27)-H(27)	108.0
C(27)-C(28)-H(28A)	109.5	C(27)-C(28)-H(28B)	109.5
H(28A)-C(28)-H(28B)	109.5	C(27)-C(28)-H(28C)	109.5
H(28A)-C(28)-H(28C)	109.5	H(28B)-C(28)-H(28C)	109.5
C(27)-C(29)-H(29A)	109.5	C(27)-C(29)-H(29B)	109.5
H(29A)-C(29)-H(29B)	109.5	C(27)-C(29)-H(29C)	109.5
H(29A)-C(29)-H(29C)	109.5	H(29B)-C(29)-H(29C)	109.5
N(3)-C(30)-O(1)	119.45(19)	N(3)-C(30)-C(31)	125.74(19)
O(1)-C(30)-C(31)	114.72(19)	N(3)-C(30)-Ca(1)	63.33(11)
O(1)-C(30)-Ca(1)	57.63(10)	C(31)-C(30)-Ca(1)	162.69(16)
C(32)-C(31)-C(30)	176.1(2)	C(31)-C(32)-C(33)	177.4(3)
C(34)-C(33)-C(38)	119.8(2)	C(34)-C(33)-C(32)	120.0(2)
C(38)-C(33)-C(32)	120.1(2)	C(33)-C(34)-C(35)	119.4(3)
C(33)-C(34)-H(34)	120.3	C(35)-C(34)-H(34)	120.3
C(36)-C(35)-C(34)	120.4(4)	C(36)-C(35)-H(35)	119.8
C(34)-C(35)-H(35)	119.8	C(37)-C(36)-C(35)	120.4(3)
C(37)-C(36)-H(36)	119.8	C(35)-C(36)-H(36)	119.8
C(36)-C(37)-C(38)	120.3(3)	C(36)-C(37)-H(37)	119.8
C(38)-C(37)-H(37)	119.8	C(37)-C(38)-C(33)	119.6(3)
C(37)-C(38)-H(38)	120.2	C(33)-C(38)-H(38)	120.2
N(3)-C(39)-C(40)	107.21(17)	N(3)-C(39)-C(45)	112.23(17)
C(40)-C(39)-C(45)	107.34(19)	N(3)-C(39)-C(44)	112.14(18)
C(40)-C(39)-C(44)	107.67(18)	C(45)-C(39)-C(44)	110.00(18)
C(39)-C(40)-C(41)	111.48(19)	C(39)-C(40)-H(40A)	109.3
C(41)-C(40)-H(40A)	109.3	C(39)-C(40)-H(40B)	109.3
C(41)-C(40)-H(40B)	109.3	H(40A)-C(40)-H(40B)	108.0
C(42)-C(41)-C(48)	109.3(2)	C(42)-C(41)-C(40)	109.2(2)
C(48)-C(41)-C(40)	109.50(19)	C(42)-C(41)-H(41)	109.6
C(48)-C(41)-H(41)	109.6	C(40)-C(41)-H(41)	109.6
C(41)-C(42)-C(43)	109.4(2)	C(41)-C(42)-H(42A)	109.8
C(43)-C(42)-H(42A)	109.8	C(41)-C(42)-H(42B)	109.8
C(43)-C(42)-H(42B)	109.8	H(42A)-C(42)-H(42B)	108.2
C(42)-C(43)-C(47)	109.7(2)	C(42)-C(43)-C(44)	109.6(2)
C(47)-C(43)-C(44)	109.1(2)	C(42)-C(43)-H(43)	109.4

C(47)-C(43)-H(43)	109.4	C(44)-C(43)-H(43)	109.4
C(39)-C(44)-C(43)	109.93(19)	C(39)-C(44)-H(44A)	109.7
C(43)-C(44)-H(44A)	109.7	C(39)-C(44)-H(44B)	109.7
C(43)-C(44)-H(44B)	109.7	H(44A)-C(44)-H(44B)	108.2
C(39)-C(45)-C(46)	110.07(18)	C(39)-C(45)-H(45A)	109.6
C(46)-C(45)-H(45A)	109.6	C(39)-C(45)-H(45B)	109.6
C(46)-C(45)-H(45B)	109.6	H(45A)-C(45)-H(45B)	108.2
C(48)-C(46)-C(47)	109.9(2)	C(48)-C(46)-C(45)	110.19(19)
C(47)-C(46)-C(45)	109.28(19)	C(48)-C(46)-H(46)	109.2
C(47)-C(46)-H(46)	109.2	C(45)-C(46)-H(46)	109.2
C(46)-C(47)-C(43)	109.43(19)	C(46)-C(47)-H(47A)	109.8
C(43)-C(47)-H(47A)	109.8	C(46)-C(47)-H(47B)	109.8
C(43)-C(47)-H(47B)	109.8	H(47A)-C(47)-H(47B)	108.2
C(46)-C(48)-C(41)	109.1(2)	C(46)-C(48)-H(48A)	109.9
C(41)-C(48)-H(48A)	109.9	C(46)-C(48)-H(48B)	109.9
C(41)-C(48)-H(48B)	109.9	H(48A)-C(48)-H(48B)	108.3
C(50)-C(49)-H(49A)	109.5	C(50)-C(49)-H(49B)	109.5
H(49A)-C(49)-H(49B)	109.5	C(50)-C(49)-H(49C)	109.5
H(49A)-C(49)-H(49C)	109.5	H(49B)-C(49)-H(49C)	109.5
N(4)-C(50)-C(51)	125.45(19)	N(4)-C(50)-C(49)	119.7(2)
C(51)-C(50)-C(49)	114.81(19)	N(4)-C(50)-Ca(2)	42.59(10)
C(51)-C(50)-Ca(2)	88.37(13)	C(49)-C(50)-Ca(2)	148.86(16)
C(50)-C(51)-C(52)	131.9(2)	C(50)-C(51)-H(51)	114.1
C(52)-C(51)-H(51)	114.1	N(5)-C(52)-C(51)	124.7(2)
N(5)-C(52)-C(53)	121.8(2)	C(51)-C(52)-C(53)	113.5(2)
C(52)-C(53)-H(53A)	109.5	C(52)-C(53)-H(53B)	109.5
H(53A)-C(53)-H(53B)	109.5	C(52)-C(53)-H(53C)	109.5
H(53A)-C(53)-H(53C)	109.5	H(53B)-C(53)-H(53C)	109.5
C(55)-C(54)-C(59)	120.4(2)	C(55)-C(54)-N(4)	119.7(2)
C(59)-C(54)-N(4)	119.9(2)	C(56)-C(55)-C(54)	118.3(2)
C(56)-C(55)-C(60)	119.9(2)	C(54)-C(55)-C(60)	121.8(2)
C(57)-C(56)-C(55)	121.6(2)	C(57)-C(56)-H(56)	119.2
C(55)-C(56)-H(56)	119.2	C(56)-C(57)-C(58)	119.8(2)
C(56)-C(57)-H(57)	120.1	C(58)-C(57)-H(57)	120.1
C(57)-C(58)-C(59)	121.1(2)	C(57)-C(58)-H(58)	119.5
C(59)-C(58)-H(58)	119.5	C(58)-C(59)-C(54)	118.8(2)
C(58)-C(59)-C(63)	120.0(2)	C(54)-C(59)-C(63)	121.2(2)
C(61)-C(60)-C(62)	110.3(3)	C(61)-C(60)-C(55)	113.9(2)
C(62)-C(60)-C(55)	110.6(2)	C(61)-C(60)-H(60)	107.2
C(62)-C(60)-H(60)	107.2	C(55)-C(60)-H(60)	107.2
C(60)-C(61)-H(61A)	109.5	C(60)-C(61)-H(61B)	109.5
H(61A)-C(61)-H(61B)	109.5	C(60)-C(61)-H(61C)	109.5
H(61A)-C(61)-H(61C)	109.5	H(61B)-C(61)-H(61C)	109.5
C(60)-C(62)-H(62A)	109.5	C(60)-C(62)-H(62B)	109.5
H(62A)-C(62)-H(62B)	109.5	C(60)-C(62)-H(62C)	109.5
H(62A)-C(62)-H(62C)	109.5	H(62B)-C(62)-H(62C)	109.5
C(59)-C(63)-C(65)	112.4(2)	C(59)-C(63)-C(64)	112.1(2)
C(65)-C(63)-C(64)	110.0(2)	C(59)-C(63)-H(63)	107.4
C(65)-C(63)-H(63)	107.4	C(64)-C(63)-H(63)	107.4
C(63)-C(64)-H(64A)	109.5	C(63)-C(64)-H(64B)	109.5
H(64A)-C(64)-H(64B)	109.5	C(63)-C(64)-H(64C)	109.5
H(64A)-C(64)-H(64C)	109.5	H(64B)-C(64)-H(64C)	109.5
C(63)-C(65)-H(65A)	109.5	C(63)-C(65)-H(65B)	109.5

H(65A)-C(65)-H(65B)	109.5	C(63)-C(65)-H(65C)	109.5
H(65A)-C(65)-H(65C)	109.5	H(65B)-C(65)-H(65C)	109.5
C(71)-C(66)-C(67)	120.6(2)	C(71)-C(66)-N(5)	118.8(2)
C(67)-C(66)-N(5)	120.7(2)	C(68)-C(67)-C(66)	118.3(2)
C(68)-C(67)-C(72)	119.6(2)	C(66)-C(67)-C(72)	122.1(2)
C(69)-C(68)-C(67)	121.5(3)	C(69)-C(68)-H(68)	119.3
C(67)-C(68)-H(68)	119.3	C(70)-C(69)-C(68)	119.7(3)
C(70)-C(69)-H(69)	120.1	C(68)-C(69)-H(69)	120.1
C(69)-C(70)-C(71)	121.6(3)	C(69)-C(70)-H(70)	119.2
C(71)-C(70)-H(70)	119.2	C(70)-C(71)-C(66)	118.3(2)
C(70)-C(71)-C(75)	120.3(2)	C(66)-C(71)-C(75)	121.4(2)
C(73)-C(72)-C(74)	109.5(2)	C(73)-C(72)-C(67)	113.3(2)
C(74)-C(72)-C(67)	113.3(2)	C(73)-C(72)-H(72)	106.8
C(74)-C(72)-H(72)	106.8	C(67)-C(72)-H(72)	106.8
C(72)-C(73)-H(73A)	109.5	C(72)-C(73)-H(73B)	109.5
H(73A)-C(73)-H(73B)	109.5	C(72)-C(73)-H(73C)	109.5
H(73A)-C(73)-H(73C)	109.5	H(73B)-C(73)-H(73C)	109.5
C(72)-C(74)-H(74A)	109.5	C(72)-C(74)-H(74B)	109.5
H(74A)-C(74)-H(74B)	109.5	C(72)-C(74)-H(74C)	109.5
H(74A)-C(74)-H(74C)	109.5	H(74B)-C(74)-H(74C)	109.5
C(76A)-C(75)-C(77)	134.0(6)	C(76A)-C(75)-C(71)	113.3(6)
C(77)-C(75)-C(71)	107.6(3)	C(77)-C(75)-C(76)	109.9(3)
C(71)-C(75)-C(76)	112.3(3)	C(76A)-C(75)-C(77A)	112.2(7)
C(71)-C(75)-C(77A)	116.4(7)	C(76)-C(75)-C(77A)	84.6(7)
C(76A)-C(75)-H(75)	77.0	C(77)-C(75)-H(75)	109.0
C(71)-C(75)-H(75)	109.0	C(76)-C(75)-H(75)	109.0
C(77A)-C(75)-H(75)	122.7	C(76A)-C(75)-H(75A)	104.5
C(77)-C(75)-H(75A)	84.4	C(71)-C(75)-H(75A)	104.5
C(76)-C(75)-H(75A)	133.1	C(77A)-C(75)-H(75A)	104.5
C(75)-C(76)-H(76A)	109.5	C(75)-C(76)-H(76B)	109.5
C(75)-C(76)-H(76C)	109.5	C(75)-C(77)-H(77A)	109.5
C(75)-C(77)-H(77B)	109.5	C(75)-C(77)-H(77C)	109.5
C(75)-C(76A)-H(76D)	109.5	C(75)-C(76A)-H(76E)	109.5
H(76D)-C(76A)-H(76E)	109.5	C(75)-C(76A)-H(76F)	109.5
H(76D)-C(76A)-H(76F)	109.5	H(76E)-C(76A)-H(76F)	109.5
C(75)-C(77A)-H(77D)	109.5	C(75)-C(77A)-H(77E)	109.5
H(77D)-C(77A)-H(77E)	109.5	C(75)-C(77A)-H(77F)	109.5
H(77D)-C(77A)-H(77F)	109.5	H(77E)-C(77A)-H(77F)	109.5
N(6)-C(78)-O(2)	118.7(2)	N(6)-C(78)-C(79)	126.4(2)
O(2)-C(78)-C(79)	114.87(19)	N(6)-C(78)-Ca(2)	63.04(12)
O(2)-C(78)-Ca(2)	58.19(11)	C(79)-C(78)-Ca(2)	160.28(16)
C(80)-C(79)-C(78)	175.3(3)	C(79)-C(80)-C(81)	179.2(3)
C(82)-C(81)-C(86)	118.9(3)	C(82)-C(81)-C(80)	120.8(3)
C(86)-C(81)-C(80)	120.3(2)	C(81)-C(82)-C(83)	119.4(4)
C(81)-C(82)-H(82)	120.3	C(83)-C(82)-H(82)	120.3
C(84)-C(83)-C(82)	122.0(4)	C(84)-C(83)-H(83)	119.0
C(82)-C(83)-H(83)	119.0	C(83)-C(84)-C(85)	119.1(4)
C(83)-C(84)-H(84)	120.4	C(85)-C(84)-H(84)	120.4
C(84)-C(85)-C(86)	120.7(4)	C(84)-C(85)-H(85)	119.7
C(86)-C(85)-H(85)	119.7	C(85)-C(86)-C(81)	119.9(4)
C(85)-C(86)-H(86)	120.0	C(81)-C(86)-H(86)	120.0
N(6)-C(87)-C(92)	106.92(17)	N(6)-C(87)-C(93)	112.13(18)
C(92)-C(87)-C(93)	107.52(19)	N(6)-C(87)-C(88)	112.13(18)

C(92)-C(87)-C(88)	107.7(2)	C(93)-C(87)-C(88)	110.20(19)
C(87)-C(88)-C(89)	110.00(19)	C(87)-C(88)-H(88A)	109.7
C(89)-C(88)-H(88A)	109.7	C(87)-C(88)-H(88B)	109.7
C(89)-C(88)-H(88B)	109.7	H(88A)-C(88)-H(88B)	108.2
C(95)-C(89)-C(90)	109.8(2)	C(95)-C(89)-C(88)	109.6(2)
C(90)-C(89)-C(88)	109.4(2)	C(95)-C(89)-H(89)	109.3
C(90)-C(89)-H(89)	109.3	C(88)-C(89)-H(89)	109.3
C(89)-C(90)-C(91)	109.2(2)	C(89)-C(90)-H(90A)	109.8
C(91)-C(90)-H(90A)	109.8	C(89)-C(90)-H(90B)	109.8
C(91)-C(90)-H(90B)	109.8	H(90A)-C(90)-H(90B)	108.3
C(96)-C(91)-C(90)	109.4(2)	C(96)-C(91)-C(92)	109.2(2)
C(90)-C(91)-C(92)	109.2(2)	C(96)-C(91)-H(91)	109.7
C(90)-C(91)-H(91)	109.7	C(92)-C(91)-H(91)	109.7
C(87)-C(92)-C(91)	111.58(19)	C(87)-C(92)-H(92A)	109.3
C(91)-C(92)-H(92A)	109.3	C(87)-C(92)-H(92B)	109.3
C(91)-C(92)-H(92B)	109.3	H(92A)-C(92)-H(92B)	108.0
C(87)-C(93)-C(94)	110.0(2)	C(87)-C(93)-H(93A)	109.7
C(94)-C(93)-H(93A)	109.7	C(87)-C(93)-H(93B)	109.7
C(94)-C(93)-H(93B)	109.7	H(93A)-C(93)-H(93B)	108.2
C(96)-C(94)-C(95)	109.6(2)	C(96)-C(94)-C(93)	109.8(2)
C(95)-C(94)-C(93)	109.4(2)	C(96)-C(94)-H(94)	109.4
C(95)-C(94)-H(94)	109.4	C(93)-C(94)-H(94)	109.4
C(89)-C(95)-C(94)	109.6(2)	C(89)-C(95)-H(95A)	109.8
C(94)-C(95)-H(95A)	109.8	C(89)-C(95)-H(95B)	109.8
C(94)-C(95)-H(95B)	109.8	H(95A)-C(95)-H(95B)	108.2
C(91)-C(96)-C(94)	109.3(2)	C(91)-C(96)-H(96A)	109.8
C(94)-C(96)-H(96A)	109.8	C(91)-C(96)-H(96B)	109.8
C(94)-C(96)-H(96B)	109.8	H(96A)-C(96)-H(96B)	108.3
C(103)-C(98)-C(99)	119.0(11)	C(103)-C(98)-C(97)	122.0(8)
C(99)-C(98)-C(97)	119.0(12)	C(98)-C(99)-C(100)	120.0(14)
C(98)-C(99)-H(99)	120.0	C(100)-C(99)-H(99)	120.0
C(99)-C(100)-C(101)	119.2(9)	C(99)-C(100)-H(100)	120.4
C(101)-C(100)-H(100)	120.4	C(102)-C(101)-C(100)	118.0(10)
C(102)-C(101)-H(101)	121.0	C(100)-C(101)-H(101)	121.0
C(103)-C(102)-C(101)	122.7(11)	C(103)-C(102)-H(102)	118.7
C(101)-C(102)-H(102)	118.7	C(102)-C(103)-C(98)	120.8(9)
C(102)-C(103)-H(103)	119.6	C(98)-C(103)-H(103)	119.6
C(198)-C(197)-H(19A)	109.5	C(198)-C(197)-H(19B)	109.5
H(19A)-C(197)-H(19B)	109.5	C(198)-C(197)-H(19C)	109.5
H(19A)-C(197)-H(19C)	109.5	H(19B)-C(197)-H(19C)	109.5
C(203)-C(198)-C(199)	118(3)	C(203)-C(198)-C(197)	120(3)
C(199)-C(198)-C(197)	121(2)	C(200)-C(199)-C(198)	120(3)
C(200)-C(199)-H(199)	120.2	C(198)-C(199)-H(199)	120.1
C(201)-C(200)-C(199)	118(2)	C(201)-C(200)-H(200)	120.9
C(199)-C(200)-H(200)	120.9	C(200)-C(201)-C(202)	120(3)
C(200)-C(201)-H(201)	120.0	C(202)-C(201)-H(201)	120.0
C(201)-C(202)-C(203)	122(3)	C(201)-C(202)-H(202)	118.9
C(203)-C(202)-H(202)	118.9	C(198)-C(203)-C(202)	120(4)
C(198)-C(203)-H(203)	119.9	C(202)-C(203)-H(203)	119.9

Symmetry transformations used to generate equivalent atoms:

#1 -x+1,-y,-z #2 -x+2,-y,-z+1

Table A24. Anisotropic displacement parameters (A^2 x 10^3) for **42**. The anisotropic displacement factor exponent takes the form: -2 pi^2 [h^2 a^{*2} U11 + ... + 2 h k a* b* U12]

Atom	U11	U22	U33	U23	U13	U12
Ca(1)	30(1)	24(1)	25(1)	-2(1)	-5(1)	-9(1)
Ca(2)	31(1)	27(1)	29(1)	-1(1)	-6(1)	-8(1)
N(1)	27(1)	29(1)	28(1)	-2(1)	-3(1)	-13(1)
N(2)	31(1)	31(1)	32(1)	1(1)	-8(1)	-13(1)
N(3)	38(1)	28(1)	26(1)	2(1)	-5(1)	-11(1)
N(4)	30(1)	32(1)	29(1)	-2(1)	-5(1)	-10(1)
N(5)	30(1)	33(1)	29(1)	0(1)	-6(1)	-11(1)
N(6)	39(1)	34(1)	30(1)	1(1)	-11(1)	-11(1)
O(1)	44(1)	26(1)	27(1)	1(1)	-8(1)	-11(1)
O(2)	44(1)	32(1)	32(1)	2(1)	-15(1)	-11(1)
C(1)	45(1)	33(1)	52(2)	-2(1)	-10(1)	-19(1)
C(2)	35(1)	28(1)	25(1)	-3(1)	-1(1)	-13(1)
C(3)	33(1)	24(1)	35(2)	1(1)	-8(1)	-8(1)
C(4)	29(1)	32(1)	35(1)	1(1)	-9(1)	-10(1)
C(5)	32(1)	39(1)	76(2)	-8(1)	-12(1)	-8(1)
C(6)	35(1)	26(1)	38(1)	-1(1)	-8(1)	-16(1)
C(7)	32(1)	31(1)	44(1)	4(1)	-6(1)	-14(1)
C(8)	34(1)	47(2)	65(2)	11(1)	-13(1)	-18(1)
C(9)	52(2)	65(2)	62(2)	11(2)	-28(1)	-33(1)
C(10)	57(2)	59(2)	44(2)	2(1)	-20(1)	-31(1)
C(11)	42(1)	40(1)	37(1)	-3(1)	-10(1)	-20(1)
C(12)	30(1)	36(1)	43(1)	3(1)	-1(1)	-11(1)
C(13)	49(2)	50(2)	56(2)	-6(1)	-3(1)	-10(1)
C(14)	63(2)	71(2)	58(2)	14(2)	0(1)	-39(2)
C(15)	48(2)	48(2)	36(1)	-8(1)	-8(1)	-19(1)
C(16)	94(2)	98(3)	56(2)	-39(2)	14(2)	-55(2)
C(17)	64(2)	66(2)	126(3)	-12(2)	33(2)	-33(2)
C(18)	28(1)	28(1)	44(1)	0(1)	-5(1)	-10(1)
C(19)	56(2)	45(1)	43(1)	-2(1)	0(1)	-28(1)
C(20)	62(2)	53(2)	52(2)	-3(1)	8(1)	-34(1)
C(21)	39(1)	43(2)	74(2)	-5(1)	5(1)	-24(1)
C(22)	31(1)	37(1)	65(2)	-3(1)	-13(1)	-13(1)
C(23)	30(1)	32(1)	52(1)	3(1)	-12(1)	-13(1)
C(24)	100(2)	73(2)	38(2)	8(2)	-12(2)	-57(2)
C(25)	84(2)	84(2)	103(3)	16(2)	-44(2)	-49(2)
C(26)	100(5)	145(6)	48(3)	-28(3)	0(3)	-49(5)
C(26A)	57(14)	73(11)	84(13)	1(10)	-20(11)	-20(9)
C(27)	63(2)	55(2)	52(2)	15(1)	-31(1)	-42(1)
C(28)	70(2)	71(2)	53(2)	13(2)	-14(1)	-38(2)
C(29)	118(3)	56(2)	77(2)	21(2)	-43(2)	-8(2)
C(30)	35(1)	32(1)	25(1)	-1(1)	-5(1)	-11(1)

C(31)	45(1)	30(1)	32(1)	1(1)	-8(1)	-14(1)
C(32)	47(1)	33(1)	35(1)	-1(1)	-10(1)	-16(1)
C(33)	47(1)	40(1)	34(1)	-8(1)	-12(1)	-14(1)
C(34)	56(2)	86(2)	67(2)	-39(2)	4(1)	-37(2)
C(35)	55(2)	154(4)	105(3)	-90(3)	-1(2)	-41(2)
C(36)	63(2)	154(4)	62(2)	-63(3)	-16(2)	-7(2)
C(37)	84(2)	88(2)	33(2)	-11(2)	-3(2)	-13(2)
C(38)	60(2)	54(2)	37(1)	-5(1)	-5(1)	-19(1)
C(39)	35(1)	28(1)	28(1)	3(1)	-6(1)	-11(1)
C(40)	60(2)	31(1)	32(1)	0(1)	-7(1)	-17(1)
C(41)	61(2)	30(1)	38(1)	1(1)	-10(1)	-18(1)
C(42)	47(2)	33(1)	69(2)	16(1)	-1(1)	-11(1)
C(43)	42(1)	45(2)	66(2)	25(1)	-27(1)	-22(1)
C(44)	35(1)	36(1)	51(2)	10(1)	-8(1)	-16(1)
C(45)	36(1)	38(1)	34(1)	-1(1)	-3(1)	-17(1)
C(46)	47(1)	45(1)	34(1)	2(1)	-1(1)	-26(1)
C(47)	74(2)	51(2)	39(1)	19(1)	-25(1)	-39(1)
C(48)	50(2)	42(1)	47(1)	10(1)	-14(1)	-26(1)
C(49)	39(1)	37(1)	46(1)	4(1)	-4(1)	-4(1)
C(50)	34(1)	32(1)	32(1)	-3(1)	-9(1)	-11(1)
C(51)	38(1)	31(1)	31(1)	1(1)	-9(1)	-11(1)
C(52)	38(1)	38(1)	27(1)	-1(1)	-6(1)	-16(1)
C(53)	47(2)	41(1)	56(2)	0(1)	1(1)	-21(1)
C(54)	30(1)	30(1)	31(1)	0(1)	-3(1)	-6(1)
C(55)	41(1)	34(1)	33(1)	-4(1)	-1(1)	-11(1)
C(56)	51(2)	47(2)	35(1)	-7(1)	1(1)	-15(1)
C(57)	49(2)	57(2)	40(2)	1(1)	6(1)	-19(1)
C(58)	38(1)	54(2)	45(2)	4(1)	-3(1)	-20(1)
C(59)	33(1)	36(1)	38 (1)	4(1)	-8(1)	-8(1)
C(60)	54(2)	45(1)	32(1)	-6(1)	-1(1)	-24(1)
C(61)	89(3)	88(3)	102(3)	-54(2)	24(2)	-51(2)
C(62)	65(2)	85(3)	150(4)	41(3)	-43(2)	-46(2)
C(63)	38(1)	53(2)	39(1)	7(1)	-12(1)	-21(1)
C(64)	50(2)	104(3)	69(2)	5(2)	-26(2)	-32(2)
C(65)	76(2)	53(2)	52(2)	-5(1)	-9(1)	-26(2)
C(66)	32(1)	35(1)	38(1)	1(1)	-5(1)	-14(1)
C(67)	35(1)	43(1)	39(1)	1(1)	-3(1)	-14(1)
C(68)	39(1)	63(2)	51(2)	-10(1)	6(1)	-22(1)
C(69)	33(2)	83(2)	77(2)	-23(2)	0(1)	-21(1)
C(70)	39(2)	76(2)	65(2)	-13(2)	-17(1)	-18(1)
C(71)	36(1)	48(2)	47(2)	-4(1)	-11(1)	-15(1)
C(72)	39(1)	60(2)	31(1)	-2(1)	-2(1)	-13(1)
C(73)	133(3)	66(2)	58(2)	6(2)	-35(2)	-40(2)
C(74)	65(2)	62(2)	63(2)	0(2)	-20(2)	-28(2)
C(75)	44(1)	53(2)	41(1)	-1(1)	-18(1)	-17(1)
C(76)	82(4)	64(4)	53(3)	-5(3)	-17(3)	-43(3)
C(77)	66(4)	71(3)	44(3)	6(2)	-17(2)	-40(3)
C(76A)	153(19)	48(7)	41(6)	3(5)	-16(8)	-31(9)
C(77A)	68(9)	56(7)	62(9)	14(6)	-26(6)	-25(6)
C(78)	39(1)	35(1)	32(1)	-1(1)	-11(1)	-15(1)
C(79)	39(1)	34(1)	36(1)	0(1)	-11(1)	-9(1)
C(80)	42(1)	36(1)	39(1)	0(1)	-10(1)	-14(1)
C(81)	57(2)	41(1)	37(1)	-7(1)	3(1)	-24(1)

C(82)	64(2)	49(2)	63(2)	-1(1)	17(2)	-11(1)
C(83)	119(3)	57(2)	81(3)	-11(2)	54(3)	-15(2)
C(84)	198(6)	87(3)	55(2)	-30(2)	52(3)	-85(4)
C(85)	165(4)	141(4)	42(2)	-20(2)	3(2)	-114(4)
C(86)	82(2)	104(3)	43(2)	-17(2)	-2(2)	-55(2)
C(87)	34(1)	37(1)	31(1)	2(1)	-13(1)	-10(1)
C(88)	41(1)	38(1)	40(1)	4(1)	-12(1)	-14(1)
C(89)	48(2)	44(1)	35(1)	8(1)	-11(1)	-15(1)
C(90)	58(2)	40(1)	48(2)	10(1)	-23(1)	-15(1)
C(91)	47(1)	36(1)	38(1)	-1(1)	-13(1)	-5(1)
C(92)	48(1)	39(1)	36(1)	0(1)	-14(1)	-10(1)
C(93)	40(1)	40(1)	41(1)	2(1)	-14(1)	-17(1)
C(94)	45(1)	49(2)	49(2)	2(1)	-23(1)	-19(1)
C(95)	57(2)	50(2)	35(1)	4(1)	-23(1)	-12(1)
C(96)	43(1)	47(2)	52(2)	6(1)	-18(1)	-10(1)
C(97)	85(6)	88(5)	68(4)	-11(3)	-12(4)	-8(4)
C(98)	65(4)	52(4)	47(4)	1(4)	-23(3)	-14(3)
C(99)	79(6)	43(5)	49(8)	12(4)	-17(5)	-15(4)
C(100)	60(4)	54(4)	92(6)	7(4)	-11(4)	-15(3)
C(101)	65(5)	81(6)	87(6)	4(5)	-16(4)	-38(5)
C(102)	72(5)	56(4)	104(8)	17(5)	-38(6)	-31(4)
C(103)	69(5)	42(4)	111(7)	6(4)	-41(5)	-22(4)
C(197)	190(20)	119(16)	170(20)	-5(13)	-104(19)	-52(15)
C(198)	126(15)	112(17)	93(12)	20(12)	-75(11)	-58(15)
C(199)	150(20)	110(20)	140(30)	54(19)	-90(30)	-90(20)
C(200)	129(18)	87(13)	240(30)	42(16)	-112(19)	-54(12)
C(201)	104(11)	110(13)	107(11)	-19(10)	-35(9)	-49(10)
C(202)	200(20)	100(13)	67(9)	-1(10)	-11(12)	-83(14)
C(203)	210(30)	81(17)	56(17)	11(12)	-23(14)	-57(18)

Table A25. Hydrogen coordinates (x 10^4) and isotropic displacement parameters (A^2 x 10^3) for **42**.

Atom	x	y	z	U(eq)
H(1A)	3685	4587	1093	63
H(1B)	2995	5194	634	63
H(1C)	4323	4434	528	63
H(3)	1845	4626	499	39
H(5A)	70	3555	497	76
H(5B)	187	4619	496	76
H(5C)	149	3976	1013	76
H(8)	7837	1817	709	58
H(9)	7685	1905	1577	66
H(10)	5939	2399	2066	60
H(12)	5519	2496	5	46
H13A)	7693	730	-21	85
H(13B)	6866	1047	-442	85
H(13C)	6530	641	104	85
H14A)	6493	3531	-48	94

H(14B)	6900	2804	-529	94
H(14C)	7675	2491	-87	94
H(15)	3284	3293	1608	53
H(16A)	2947	3864	2428	118
H(16B)	3784	4264	2093	118
H(16C)	4272	3281	2474	118
H(17A)	4325	1590	2287	133
H(17B)	3855	1498	1792	133
H(17C)	2997	2197	2249	133
H(20)	415	512	1381	65
H(21)	-305	310	693	61
H(22)	25	1053	-84	52
H(24)	2084	1882	1398	76
H(24A)	2274	1630	1306	76
H(25A)	2023	-17	1801	125
H(25B)	2723	503	1994	125
H(25C)	3084	16	1443	25
H(26A)	868	2175	2191	149
H(26B)	270	1534	2018	149
H(26C)	53	2653	1761	149
H(26D)	1111	2877	1594	111
H(26E)	1593	2116	2064	111
H(26F)	399	2325	1911	111
H(27)	1751	2401	-371	59
H(28A)	2454	743	-717	94
H(28B)	1839	1635	-1122	94
H(28C)	1213	989	-822	94
H(29A)	-404	2711	-593	141
H(29B)	272	3351	-845	141
H(29C)	-254	3503	-263	141
H(34)	3150	-84	-2008	80
H(35)	2931	-353	-2822	123
H(36)	3829	166	-3519	125
H(37)	4962	937	-3421	93
H(38)	5201	1219	-2614	63
H(40A)	4710	3643	-557	51
H(40B)	3388	3995	-392	51
H(41)	3651	5446	-782	52
H(42A)	2375	5901	-1391	65
H(42B)	1960	5382	-898	65
H(43)	1889	4622	-1637	59
H(44A)	2306	3500	-899	49
H(44B)	2927	2821	-1396	49
H(45A)	5057	2260	-1661	43
H(45B)	5719	2598	-1323	43
H(46)	5295	3716	-2057	49
H(47A)	3615	3615	-2164	60
H(47B)	3382	4818	-2172	60
H(48A)	4429	5356	-1651	53
H(48B)	5350	4490	-1325	53
H(49A)	6247	4646	5258	69
H(49B)	6797	5397	5015	69
H(49C)	6766	5115	5606	69

H(51)	8441	4692	4606	42
H(53A)	10759	4339	4691	72
H(53B)	10052	4674	4223	72
H(53C)	11235	3637	4198	72
H(56)	6753	3880	7047	57
H(57)	5487	3188	7068	63
H(58)	5425	2420	6355	56
H(60)	8596	4082	5972	52
H(61A)	7239	5493	6448	135
H(61B)	8470	5183	6591	135
H(61C)	7619	4846	6959	135
H(62A)	9953	3377	6522	142
H(62B)	9694	2472	6356	142
H(62C)	9172	2976	6901	142
H(63)	7002	2393	5138	51
H(64A)	4813	2407	5588	111
H(64B)	5335	2397	4996	111
H(64C)	5007	3411	5314	111
H(65A)	7866	722	5545	91
H(65B)	7114	733	5135	91
H(65C)	6640	781	5723	91
H(68)	13682	1061	3612	63
H(69)	14812	894	4219	79
H(70)	14018	1294	5046	73
H(72)	10724	1780	3840	57
H(73A)	11965	2640	3171	128
H(73B)	10775	3279	3508	128
H(73C)	10850	2610	3046	128
H(74A)	11445	788	3117	93
H(74B)	12082	105	3577	93
H(74C)	12696	617	3162	93
H(75)	11047	2550	5498	55
H(75A)	11077	2193	5502	55
H(76A)	12458	3218	5503	92
H(76B)	13215	2141	5779	92
H(76C)	12000	2930	6053	92
H(77A)	12852	604	5735	84
H(77B)	11634	774	5633	84
H(77C)	11755	1245	6125	84
H(76D)	11409	3216	5965	129
H(76E)	11327	3612	5389	129
H(76F)	12535	3023	5587	129
H(77D)	13151	1088	5933	93
H(77E)	12439	528	5792	93
H(77F)	11905	1391	6221	93
H(82)	12031	-1575	2824	81
H(83)	12632	-2359	2041	123
H(84)	11395	-2004	1469	134
H(85)	9496	-891	1682	119
H(86)	8844	-83	2464	85
H(88A)	9034	1918	3218	49
H(88B)	8906	2862	3542	49
H(89)	8131	3534	2767	53

H(90A)	6345	4854	3119	60
H(90B)	7282	4648	3476	60
H(91)	5627	4683	3980	54
H(92A)	7387	3537	4269	53
H(92B)	6515	3047	4417	53
H(93A)	6658	1595	3931	48
H(93B)	7627	1128	3460	48
H(94)	5881	2275	3156	56
H(95A)	7557	2225	2663	60
H(95B)	6519	3369	2618	60
H(96A)	4679	4088	3353	61
H(96B)	5031	3395	3862	61
H(97A)	937	6259	1556	137
H(97B)	1371	5016	1590	137
H(97C)	1747	5569	1964	137
H(99)	-811	7343	1988	74
H(100)	-2302	7653	2651	88
H(101)	-2372	6198	3130	90
H(102)	-827	4576	3020	89
H(103)	657	4297	2405	87
H(19A)	-2389	7320	3116	235
H(19B)	-2103	6170	3348	235
H(19C)	-2955	6660	2934	235
H(199)	-889	4568	2759	138
H(200)	737	3873	2134	171
H(201)	1154	5008	1605	123
H(202)	58	6777	1689	139
H(203)	-1226	7447	2408	144